Optimisation of Functional Magnetic Resonance Imaging Protocols for Investigation of Subregional Amygdala Functional Connectivity in Major Depressive Disorder

---

A thesis submitted in fulfilment of the requirements of the degree of

Doctor of Philosophy

Sheryl L. Foster

Supervisors:

Associate Professor Mayuresh Korgaonkar

Professor Sarah Lewis

Associate Professor Ramon Landin-Romero

Faculty of Medicine and Health, The University of Sydney

February 2026

Abstract

Amygdala dysfunction is strongly implicated in emotion dysregulation across multiple psychiatric conditions and represents a key mechanism underlying symptoms of Major Depressive Disorder (MDD). Functional Magnetic Resonance Imaging (fMRI) at 3 Tesla (3T) is widely used to investigate the neural correlates of the amygdala, a small structure that has traditionally been considered as a single entity in data acquisition and analysis. However, its composition of nine functionally heterogeneous subnuclei that form three main subregions makes this approach challenging in the context of spatial specificity and accuracy of findings.

The aims of this thesis were: (1) to review the fMRI landscape regarding protocols in use for imaging the amygdala at 3T, (2) to explore the potential for optimised high resolution fMRI data and a subregional functional connectivity (FC) analysis approach to advance our understanding of amygdala neurobiology in depression, and assess the potential of 3T in relation to FC network findings reported at 7T, (3) to compare results of whole versus subregional amygdala analysis findings, and (4) to investigate whether imaging of this structure and its FC to other subcortical regions could benefit from newer optimised fMRI techniques.

The overarching results highlighted several compelling findings: i) Of 192 studies comprising the review, only 11% reported amygdala findings at a subregional level, whilst only 2% used high spatial resolution data exclusively, ii) optimised 2D data acquisitions at 3T can achieve sufficient levels of spatial resolution to identify alterations in FC at a subregional rather than whole amygdala level, allowing differentiation of treatment resistant and treatment responsive depression cohorts as well as closely mirroring network FC findings reported at 7T, iii) FC results are less sensitive when the amygdala is considered as a single structure rather than three individual subregions, and iv) newer techniques have the potential to reveal FC information in subcortical regions that are technically challenging to image well.

In the setting of limited access to higher spatial resolution imaging afforded by 7T systems, these results not only shine a spotlight on the underutilised capability of currently available MRI hardware, acquisition and analysis techniques, but taken together, the thesis findings illustrate that current fMRI protocols on 3T MRI systems can be optimised effectively to achieve more granular interrogation of amygdala function. This work highlights a feasible path forward, leading to an enhanced understanding of subregional amygdala dysfunction in MDD and other psychiatric conditions.

Statement of Original Authorship

I, Sheryl Foster, certify that the content of this thesis is my own work. This thesis has not been submitted for any other degree or purpose. I certify that the intellectual content of this thesis is the product of my own work, and that all assistance received in preparing this thesis and all sources have been acknowledged.

No content produced by generative AI tools has been used in the preparation of this thesis.

Sheryl L. Foster

September 2025

Acknowledgements

Aesop tells us that ‘no act of kindness, no matter how small, is ever wasted’ and I have found this to be true over and over again during the course of my life. If it weren’t, there would be no thesis by S. Foster. I have been on the receiving end of innumerable acts of kindness, and I want to gratefully acknowledge the generosity of all who have contributed to this work.

Let’s start with my extraordinary supervision team – Mayuresh and Sarah, you have been such wonderful colleagues and friends over many years before this fun began. To have your guidance and mentorship to rely on filled me with the confidence to just get it done. Mayuresh, your well of calm and patience is legendary and I thank you for sharing it with me during this undertaking. I have learned so much from you. Sarah, you are the most amazing role model for we women of MIS and beyond; kind and funny and smart. No wonder your fanbase is ever-expanding. I hope you realise how meaningful it was for me to have you on my team. And Ramon, you cheerfully joined the team when I may or may not have been in a lull…and brought more kindness and yet another perspective to my work. I am so very glad to have met you and have you in my orbit now, and I thank you also for bringing the awesome Sophie into that orbit too. I want to thank you all from deep in my heart for everything you have done to support me in getting this thesis over the line and for every kindness you have shown me along the way.

One of the great joys of my working life at Westmead is my team of colleagues. In fact, the term ‘colleagues’ doesn’t do these relationships justice – it’s really a team of friends. I’m almost afraid to name names because there have been so many amazing people over the years, each leaving a subtle yet distinct mark, but here goes. Our MRI research team of Nick, Anthea, Art, Dennis, Rachelle, Trang and Vien; Nick, you have steered the ship so capably in my absence, allowing me to focus on this production, and I cannot speak highly enough of the incredible job you all do together...thank you. Gloria and Tony, as well as being supportive friends, you found ways to carve out the time for me to complete this thesis…thank you. Megan and Kylie, although you have checked out of Westmead, you can never leave, as the song goes. Thank you for your enduring and supportive friendships, as well as the editing services. Dr Cromer, yes, I know I made you suffer, but in a good way…and now you have payback.

Another Westmead bonus has been working alongside colleagues from other disciplines such as Medical Physics. Lucy, your love of numbers possibly exceeds my own, and I am very grateful for your expertise in wrangling ImageJ and Excel like a boss. Mayuresh, your team at

BDC is exceptional. Issy, you always have time to dispense cheerful, well-constructed advice, and Rita and Liz, you have been amazingly supportive fellow travellers on this PhD path. I have appreciated your help and friendship, perhaps more than you know.

And then there is my other fabulous work team at USyd. Thank you all so much for the help, advice, encouragement and friendship you have shown me along the way, especially Peter and Laura. You have motivated and supported me during this endeavour and for that, I am truly grateful. I want to acknowledge my very good fortune in being part of not just one, but two magnificent work teams - a far, far better life outcome than winning the lottery.

I want to thank my prodigiously talented friend, David. David, you are so generous with your time, your skills, your knowledge and your kindness. It would be an impossible task to list all the ways in which you have helped me, but it is a given that I would not be at this end of my thesis without you in my corner. I salute you!

To my darling sisters and nieces…Robbie, your quiet love and support in so many ways can never be repaid (those spectacular feasts you conjure up at a moment's notice, not to mention the ongoing hair taming services). Gracie, you are a beacon of kindness and light in our family full of (wonderful) boys, as are you, Erinn Kyla. Thank you so much for your support and formatting expertise, Erinn, and yes, you did get there before me! Hellie, another remarkable role model – thank you for bringing Erinn into our lives. You are all amazing women, and I feel very blessed that you are my family.

To my dad and mum – although you were born into a different life, your minds have always been open to opportunity, and I am so grateful for that positivity mixed together with enormous quantities of love. Mum, you have gone along with every single notion I have ever entertained, including this one, with a mix of deep loyalty and immense trust. What a gift! I couldn't love you more.

To my beautiful boys, Julian and Xavier - from across the world you have loved and encouraged me every step of the way, perhaps without realising the power of the message you were sending. 'It's never too late!' they said. 'It'll be fun!' they said. No, it wasn't…and yes, it was! The fact that you are both exceptional humans will always be my proudest achievement.

And then there is Si. What is left to say? Your love and support are relentless, and it has ever been thus. Thank you. I dedicate this work to you.

Author Attribution Statement

Chapter Three of this thesis has been published as **Foster, S. L.,** Breukelaar, I. A., Ekanayake, K., Lewis, S., & Korgaonkar, M. S. (2023). Functional Magnetic Resonance Imaging of the Amygdala and Subregions at 3 Tesla: A Scoping Review. *Journal of Magnetic Resonance Imaging*. https://doi.org/https://doi.org/10.1002/jmri.28836. I designed the study, analysed the data and wrote the drafts of the manuscript. Co-authors contributed either to design of the study, data collection, and/or by reviewing the manuscript.

Chapter Four of this thesis has been published as **Foster, S. L.,** Landin-Romero, R., Lewis, S., Barreiros, A. R., Matis, S., Harris, A., & Korgaonkar, M. S. (2025). Amygdala subregional functional connectivity in treatment-resistant depression. *Journal of Affective Disorders Reports*, *21*, 100932. https://doi.org/https://doi.org/10.1016/j.jadr.2025.100932. I designed the study, analysed the data and wrote the drafts of the manuscript. Co-authors contributed either to design of the study, data collection, and/or by reviewing the manuscript.

Chapter Six of this thesis is under review as **Foster, S.L.**, Landin-Romero, R., Lewis, S., and Korgaonkar, M.S. (2025). Subregional Amygdala Functional Connectivity at 3T: Comparison of high-resolution 2D and 3D fMRI acquisitions in the *Journal of Neuroimaging.* I designed the study, analysed the data and wrote the drafts of the manuscript. Co-authors contributed either to design of the study, data collection, and/or by reviewing the manuscript.

Sheryl L. Foster September 2025

As Lead Supervisor for the candidature upon which this thesis is based, I can confirm that the authorship attribution statements are correct.

Associate Professor September 2025
Mayuresh Korgaonkar

Declaration of Funding Sources

This work was supported by an Australian Government Research Training Program (RTP) Fee Offset Scholarship. It was also supported by a generous grant from the Westmead Charitable Trust, the Career Development Award, administered by the Western Sydney Local Health District Research and Education Network. The University of Sydney Postgraduate Research Support Scheme (PRSS) funding also supported attendance to present this work at national and international conferences. Collection of the data used in this study (Chapter Four) was funded by Takeda Pharmaceutical Company Limited COCKPI-T (Co-Create Knowledge for Pharma Innovation with Takeda) Research Grant and a National Health and Medical Research Council (NHMRC) Grant (Grant No. APP1087560), awarded to my primary supervisor.

The author very gratefully acknowledges these contributions.

The work in Chapters Five and Six was also supported in kind by Siemens Healthineers with whom Westmead Hospital Radiology Department has an MRI research agreement. The author gratefully acknowledges the support of Dr Kieran O'Brien, Head of Collaborations and Research for ANZ, in facilitating use of the novel 3D sequence. The author would also like to thank Dr Jin Jin, Senior Scientist, for outstanding and ongoing scientific support and many interesting discussions on alternative k-space travels.

The author has no conflicts of interest to declare in relation to funding sources for any part of this work.

Publications Supporting Thesis

Foster, S.L., Landin-Romero, R., Lewis, S. & Korgaonkar, M. (2025). Subregional amygdala functional connectivity at 3T: 2D vs 3D GRE-EPI Acquisitions**.** *Journal of Neuroimaging, 35,6.* https://onlinelibrary.wiley.com/doi/10.1111/jon.70110. Chapter Six.

Foster, S. L., Landin-Romero, R., Lewis, S., Barreiros, A. R., Matis, S., Harris, A., & Korgaonkar, M. S. (2025). Amygdala subregional functional connectivity in treatment-resistant depression. *Journal of Affective Disorders Reports*, *21*, 100932. https://doi.org/10.1016/j.jadr.2025.100932. Chapter Four.

Foster, S. L., Breukelaar, I. A., Ekanayake, K., Lewis, S., & Korgaonkar, M. S. (2023). Functional Magnetic Resonance Imaging of the Amygdala and Subregions at 3 Tesla: A Scoping Review. *Journal of Magnetic Resonance Imaging*. https://doi.org/10.1002/jmri.28836. Chapter Three.

Non-Peer Reviewed Articles and Registrations Supporting Thesis

Foster, S. L., Breukelaar, I., Ekanayake, K., Lewis, S. & Korgaonkar, M.S. (2022). *Functional Magnetic Resonance Imaging of the amygdala and subregions at 3 Tesla: A scoping review protocol.* medRxiv, Available at https://doi.org/10.1101/2022.04.14.22273332. Chapter Three.

Foster, S. L. Review Protocol registered on Open Science Framework; fMRI of the Amygdala and subregions: current clinical research protocols at 3T (2022). Available at https://osf.io/kw58p. Chapter Three.

Oral Presentations Supporting Thesis

2024 **Foster, S.**, Landin-Romero, R., Lewis, S. & Korgaonkar, M. *fMRI Functional Connectivity of the Amygdala in Depression; Are we missing something?* Westmead Hospital Allied Health Research Symposium, Westmead Hospital, Australia. 23 August.

2024 **Foster, S.**, Landin-Romero, R., Lewis, S. & Korgaonkar, M. *fMRI of the Amygdala.* The University of Sydney, Faculty of Medicine and Health HDR Conference. 24-25 July.

2022 **Foster, S.**, Lewis, S., & Korgaonkar, M. *fMRI of the Amygdala: Shouldn't we all be more in harmony?* European Society for Magnetic Resonance in Medicine and Biology; 'MRI Together' Global Workshop (online); December 4-9, Video presentation. Available at: https://www.youtube.com/watch?v=c1Lzqg4gjak

2022 **Foster, S.,** Barreiros, A.R., Rai, S., Lewis, S., & Korgaonkar, M. *Imaging Diagnoses in Mental Health: How close are we?* Royal Australian and New Zealand College of Radiologists 72nd Annual Meeting; Adelaide, Australia. 27-30 October.

2022 **Foster, S.**, Lewis, S., & Korgaonkar, M. *Optimisation of Functional Magnetic Resonance Imaging protocols to further our understanding of the amygdala and its multiple functional connectivities in neuropsychiatric conditions*. Westmead Institute for Medical Research (WIMR), WIMR Research Forum, Westmead. 8 July.

Conference Proceedings and Posters Supporting Thesis

2025 **Foster, S.**, Landin-Romero, R., Lewis, S. & Korgaonkar, M. *Optimising fMRI data acquisition to investigate amygdala subregional Functional Connectivity in Depression;* International Society for Magnetic Resonance in Medicine; 2025 Annual Scientific Meeting, Honolulu, Hawai'i. 9-12 May. (Abstract accepted but unable to attend).

2024 **Foster, S.**, Landin-Romero, R., Lewis, S. & Korgaonkar, M. *Whole amygdala masks vs subregional masks in resting-state fMRI Functional Connectivity Analyses;* European Society for Magnetic Resonance in Medicine and Biology; 2024 Scientific Meeting, Barcelona, Spain. 2-5 October. Page S612 in Book of Abstracts ESMRMB 2024 Online 40th Annual Scientific Meeting 2–5 October 2024. *Magn Reson Mater Phy* **37** (Suppl 1), 1–781 (2024). https://doi.org/10.1007/s10334-024-01191-6.

Available at https://www.esmrmb2024.org/abstracts-form/posters-e/abstract-data/9c37653e5c7f18a598a19fdb3fba1fa9

2023 **Foster, S.**, Breukelaar, I., Ekanayake, K., Lewis, S., & Korgaonkar, M. *3T fMRI of the Amygdala: How are we all doing it? An overview of 3T functional magnetic resonance imaging protocols of the amygdala and subregions.* European Society for Magnetic Resonance in Medicine and Biology; 2023 Scientific Meeting, Basel, Switzerland. 4-7 October. P177 in Book of Abstracts ESMRMB 2023 Online 39th Annual Scientific Meeting 4–7 October 2023. *Magn Reson Mater Phy* **36** (Suppl 1), 1–328 (2023). Available at https://doi.org/10.1007/s10334-023-01108-9

Additional Publications During Thesis

2025 Deshmukh, T., Hume, R.D., Chen, S. Igoor, S., **Foster S.,** *et al.* Platelet derived growth factor-AB modulates post-infarct myocardium leading to extended improvement in cardiac function. *npj Regen Med* **10**, 46 (2025). https://doi.org/10.1038/s41536-025-00433-y

Barreiros, A.R., Breukelaar, I., Mayur, P., Andepalli, J., Tomimatsu, Y., Funayama, K., **Foster, S.** *et al.* Role of the rostral anterior cingulate cortex in emotion processing in Treatment Resistant Depression. *Transl Psychiatry* **15**, 378 (2025). https://doi.org/10.1038/s41398-025-03600-3

Walpola, I. C., Mohan, A., **Foster, S.,** & Kozlowska, K. (2025). Altered self-processing brain networks in paediatric functional neurological disorder. *Neuroimage Clin*, *47*, 103811. https://doi.org/10.1016/j.nicl.2025.103811

Lan, Z., **Foster, S.,** Charney, M., van Grinsven, M., Breedlove, K., Kozlowska, K., & Lin, A. (2025). Neurometabolic network (NMetNet) for functional neurological disorder in children and adolescents. *NeuroImage: Clinical*, *46*, 103767. https://doi.org/10.1016/j.nicl.2025.103767

2024 Selvakumar, D., Clayton, Z. E., Prowse, A., Dingwall, S., Kim, S. K., Reyes, L., George, J., Shah, H., Chen, S., Leung, H. H. L., Hume, R. D., Tjahjadi, L., Igoor, S., Skelton, R. J. P., Hing, A., Paterson, H., **Foster, S. L.,** Pearson, L., Wilkie, E., . . . Chong, J. J. H. (2024). Cellular heterogeneity of pluripotent stem cell-derived cardiomyocyte grafts is mechanistically linked to treatable arrhythmias. *Nature Cardiovascular Research*, *3*(2), 145-165. https://doi.org/10.1038/s44161-023-00419-3

Barreiros, A. R., Breukelaar, I. A., Prentice, A., Mayur, P., Tomimatsu, Y., Funayama, K., **Foster, S.,** Malhi, G. S., Arns, M., Harris, A., & Korgaonkar, M. S. (2024). Intra- and Inter-Network connectivity of the default mode network differentiates Treatment-Resistant depression from Treatment-Sensitive depression. *NeuroImage: Clinical*, *43*, 103656. https://doi.org/10.1016/j.nicl.2024.103656

Charney, M., **Foster, S.,** Shukla, V., Zhao, W., Jiang, S. H., Kozlowska, K., & Lin, A. (2024). Neurometabolic alterations in children and adolescents with functional neurological disorder. *NeuroImage: Clinical*, *41*, 103557. https://doi.org/10.1016/j.nicl.2023.103557

Griffiths, K. R., Breukelaar, I. A., Harvie, G., Yang, J., **Foster, S. L.,** Harris, A. W., Clarke, S., Hay, P. J., Touyz, S., Korgaonkar, M. S., & Kohn, M. R. (2024). Functional Connectivity Mechanisms Underlying Symptom Reduction Following Lisdexamfetamine Treatment in Binge-Eating Disorder: A Clinical Trial. *Biol Psychiatry Glob Open Sci*, *4*(1), 317-325. https://doi.org/10.1016/j.bpsgos.2023.08.016

2023 Amin, S., Sangadi, I., Allman-Farinelli, M., Badve, S. V., Boudville, N., Coolican, H., Coulshed, S., **Foster, S.,** Fernando, M., Haloob, I., Harris, D. C. H., Hawley, C. M., Holt, J., Howell, M., Kumar, K., Johnson, D. W., Lee, V. W., Mai, J., Rangan, A., . . . Rangan, G. K. (2023). Participant Perceptions in a Long-term Clinical Trial of Autosomal Dominant Polycystic Kidney Disease. *Kidney Medicine*, *5*(9). https://doi.org/10.1016/j.xkme.2023.100691

Peek, A. L., Rebbeck, T. J., Leaver, A. M., **Foster, S. L.,** Refshauge, K. M., Puts, N. A., Oeltzschner, G., Andronesi, O. C., Barker, P. B., Bogner, W., Cecil, K. M., Choi, I.-Y., Deelchand, D. K., de Graaf, R. A., Dydak, U., Edden, R. A. E., Emir, U. E., Harris, A. D., Lin, A. P., . . . Wilson, M. (2023). A comprehensive guide to MEGA-PRESS for GABA measurement. *Analytical Biochemistry*, *669*, 115113. https://doi.org/10.1016/j.ab.2023.115113

2022 Selvakumar, D., Deshmukh, T., **Foster, S.,** Sanaei, N., Min, A., Grieve, S., Pathan, F., & Chong, J. (2022). Comparative Assessment of Motion Averaged Free-Breathing or Breath-Held Cardiac Magnetic Resonance Imaging Protocols in a Porcine Myocardial

Infarction Model. *Heart, Lung and Circulation*, *31*, S153-S154. https://doi.org/10.1016/j.hlc.2022.06.236

Rai, S., Griffiths, K. R., Breukelaar, I. A., Barreiros, A. R., Boyce, P., Hazell, P., **Foster, S.L.,** Malhi, G. S., Harris, A. W. F., & Korgaonkar, M. S. (2022). Common and differential neural mechanisms underlying mood disorders. *Bipolar Disorders*, *24*(8), 795-805. https://doi.org/10.1111/bdi.13248

Rai, S., **Foster, S.,** Griffiths, K. R., Breukelaar, I. A., Kozlowska, K., & Korgaonkar, M. S. (2022). Altered resting-state neural networks in children and adolescents with functional neurological disorder. *NeuroImage: Clinical*, *35*, 103110. https://doi.org/10.1016/j.nicl.2022.103110

Barreiros, A. R., Breukelaar, I., Mayur, P., Andepalli, J., Tomimatsu, Y., Funayama, K., **Foster, S.,** Boyce, P., Malhi, G. S., Harris, A., & Korgaonkar, M. S. (2022). Abnormal habenula functional connectivity characterizes treatment-resistant depression. *Neuroimage Clin*, *34*, 102990. https://doi.org/10.1016/j.nicl.2022.102990

Rangan, G. K., Wong, A. T. Y., Munt, A., Zhang, J. Q. J., Saravanabavan, S., Louw, S., Allman-Farinelli, M., Badve, S. V., Boudville, N., Chan, J., Coolican, H., Coulshed, S., Edwards, M. E., Erickson, B. J., Fernando, M., **Foster, S.,** Gregory, A. V., Haloob, I., Hawley, C. M., . . . Harris, D. C. H. (2022). Prescribed Water Intake in Autosomal Dominant Polycystic Kidney Disease. *NEJM Evidence*, *1*(1), EVIDoa2100021. https://doi.org/doi:10.1056/EVIDoa2100021

2021 Peek, A. L., Leaver, A. M., **Foster, S.,** Puts, N. A., Oeltzschner, G., Henderson, L., Galloway, G., Ng, K., Refshauge, K., & Rebbeck, T. (2021). Increase in ACC GABA+ levels correlate with decrease in migraine frequency, intensity and disability over time. *J Headache Pain*, *22*(1), 150. https://doi.org/10.1186/s10194-021-01352-1

Rai, S., Griffiths, K. R., Breukelaar, I. A., Barreiros, A. R., Chen, W., Boyce, P., Hazell, P., **Foster, S. L.,** Malhi, G. S., Harris, A. W. F., & Korgaonkar, M. S. (2021). Default-mode and fronto-parietal network connectivity during rest distinguishes asymptomatic patients with bipolar disorder and major depressive disorder. *Translational psychiatry*, *11*(1), 547. https://doi.org/10.1038/s41398-021-01660-9

Table of Contents

Structure of Thesis

In addition to three fundamental chapters (introductory, general methods and summary) the final format of this thesis combines three published manuscripts (Chapters Three, Four and Six), and an unpublished manuscript (Chapter Five). As such, there is redundancy in the introductions and methods of some chapters.

Ethical approvals related to this thesis (2019/ETH02223, 2023/ETH02153) were granted by Western Sydney Local Health District Human Research Ethics Committee.

List of Figures

List of Tables

List of Acronyms

1.5T, 3T, 7T – 1.5 Tesla, 3 Tesla, 7 Tesla

2D, 3D – two-dimensional, three dimensional

AC – PC – Anterior Commissure to Posterior Commissure

A – P – Anterior to Posterior

BOLD – Blood Oxygen Level Dependent

CM – centromedial

CNR – Contrast-to-Noise Ratio

CSF – Cerebrospinal Fluid

DMN – Default Mode Network

DWI – Diffusion Weighted Imaging

FC – Functional Connectivity

FID – Free Induction Decay

fMRI – functional Magnetic Resonance Imaging

FOV – Field-of-View

FSL – FMRIB Software Library

GLM – General Linear Model

GRE-EPI – Gradient Recalled Echo – Echo Planar Imaging

HC – healthy control/s

HCP – Human Connectome Project

HRF – Haemodynamic Response Function

LB – laterobasal

MDD – Major Depressive Disorder

MNI – Montreal Neurological Institute

RF - radiofrequency

ROI – Region-of-Interest

rs-fMRI – resting state functional Magnetic Resonance Imaging

SAR – Specific Absorption Rate

SC – Structural Connectivity

SE – Spin Echo

SF - superficial

SNR – Signal-to-Noise Ratio

SPM – Statistical Parametric Mapping

T1-W, T2*-W – T1-weighted, T2 star-weighted

TE – echo time

TR – repetition time

TRD – Treatment Resistant Depression

TSD – Treatment Sensitive Depression

tSNR – temporal Signal-to-Noise Ratio

VV – voxel volume

Chapter 1: Overview of Imaging the Amygdala in Depression

The introduction of Magnetic Resonance Imaging has led to its widespread use in investigation of neuropsychiatric conditions such as depression. This chapter discusses current diagnostic methods of diagnosing depression and the role of MR imaging in depression. The amygdala is highlighted as a critical structure, as its dysfunction is implicated in depression. The work of previous studies points to the need for improved imaging of the amygdala at a more granular level to increase our understanding of its role in depression. In the setting of lack of access to higher field strength 7 Tesla MRI systems, the case is made for the use of 3 Tesla systems for this purpose. The overarching goal is to move away from subjective symptom-based diagnoses to more objective imaging-based diagnoses in depression cohorts.

1.1 Introduction

The field of neuropsychiatry has an interesting history following its germination in France and Germany in the 1800s. Prior to that time, mental illness and brain diseases were considered two very separate fields until several scientists including Wilhelm Griesinger, a professor of both neurology and psychiatry in Berlin, promulgated the view that "mental illnesses are diseases of the brain" (Arzy & Danziger, 2014; Griesinger, 1845). Since then, there has been at different times, a divergence of the two specialties followed by 'coming together' at various points based on views of prominent clinicians such as Sigmund Freud, as well as global events such as World War II (Taslim et al., 2024). More recently, the focus of neuropsychiatry is considered to be "…the assessment and treatment of the cognitive, behavioural, and mood symptoms of patients with neurological disorders" (Yudofsky & Hales, 2002). The marriage between the two fields was cemented in the early 1990's with the advent of functional Magnetic Resonance Imaging (fMRI), a technique allowing non-invasive, image-based investigation of brain function as well as structure (Roalf & Gur, 2017; Sutterer & Tranel, 2017). Wider access to fMRI has allowed researchers to utilise neuroimaging to investigate brain function in fields such as neuroscience, psychology and psychiatry and has led to a large number of publications since that time (Glover, 2011).

1.2 Depression – Current Diagnostic Methods

Neuropsychiatric illnesses such as unipolar depression (known as Major Depressive Disorder (MDD) or depression), anxiety and bipolar disorder impose a considerable financial burden on society, in addition to the significant cost to health and lifestyle imposed on the individual (McCallum et al., 2019). The latest World Health Organisation figures for 2023 showed that around 5% of adults globally are affected by unipolar depression or MDD (World Health Organisation, 2023). MDD is notable for its heterogeneity, and at patient presentation there is a raft of diagnostic criteria, symptoms and specifiers that clinicians must consider in order to make a diagnosis, as outlined in Table 1.1. In brief, patients are diagnosed with a depressive episode after experiencing a persistent negative mood with symptoms such as sadness, irritability, poor concentration, feelings of hopelessness and sleep and appetite disturbances for most days during a two-week period. The symptoms, ranging from mild to severe, can be extremely debilitating at the latter end of the scale and impact heavily on all aspects of a person's life (Coryell, 2023; Mitterschiffthaler et al., 2006). Adequate response to antidepressant medication occurs in approximately 50% of cases (Gaynes et al., 2008);

however, upwards of 30% of patients are diagnosed with treatment-resistant depression (TRD) after an initial trial of a first-line antidepressant plus another pharmaceutical treatment or alternative therapy has failed to resolve their symptoms (Ionescu et al., 2015; Voineskos et al., 2020).

Table 1.1: Major Depressive Disorder – adult diagnostic criteria, symptoms and specifiers

Diagnostic Criteria	Symptoms
• 5 or more depressive **symptoms** for ≥ 2 weeks that are a change from previous functioning • Depressed mood and/or loss of interest or pleasure must be present • Symptoms must cause significant distress or impairment in functioning • Episode not attributable to psychological effects of substance abuse or another medical condition • Episode not better explained by schizoaffective disorder, schizophrenia, or other schizophrenia spectrum and other psychotic disorders • No history of manic or hypomanic episodes	1. Depressed Mood 2. Markedly diminished interest or pleasure in most or all activities 3. Significant weight loss (or poor appetite) or weight gain 4. Insomnia or hypersomnia 5. Psychomotor agitation or retardation 6. Fatigue or loss of energy 7. Feelings of worthlessness or excessive or inappropriate guilt 8. Decreased concentration or indecisiveness 9. Recurrent thoughts of death (not just fear of dying), or suicidal ideation, plan, or attempt
Specify: • Single or Recurrent episode • Severity a. Mild b. Moderate c. Severe d. With psychotic features e. In partial remission f. In full remission g. Unspecified	Specify: With anxious distress • With mixed features • With melancholic features • With atypical features • With mood-congruent psychotic features • With mood-incongruent psychotic features • With catatonia • With peripartum onset • With seasonal pattern

Note: Adapted from (Diagnostic and Statistical Manual of Mental Disorders, 2013)

A more nuanced understanding of the neurobiological features that distinguish TRD from MDD would be valuable for treating clinicians in terms of prescribing the most suitable treatment from the outset, particularly in the context of ongoing debate regarding the question of TRD being a different depression subtype versus a consequence of inappropriate treatment (Malhi et al., 2019). Aside from the benefits of stratification within a notably heterogenous condition, differentiating between different conditions can also be problematic for the clinician for similar reasons. Some conditions have a raft of overlapping symptoms and, as an example, it is well-documented that many symptoms of unipolar depression are shared with bipolar disorder. With diagnosis being dependent on behavioural observations and patient self-reporting of symptoms, misdiagnosis has been reported in over 60% of bipolar cases at initial presentation (Singh & Rajput, 2006). Inappropriate treatment of bipolar disorder with antidepressants can result in development of manias, and delays in receiving the correct mood-stabilising treatment can lead to increases in hospital attendance and suicide rates (Siegel-Ramsay et al., 2022).

There is wide recognition in the field of neuroscience that current diagnostic tools based on clinical presentation, diagnostic categories and symptom classification lack precision. Further confounding this picture are the presence of comorbidities leading to broad heterogeneity within and across patient populations (García-Gutiérrez et al., 2020). Clinicians have shown particular interest in the field of functional neuroimaging with its capacity to focus on identification of potential differences in neural substrates underlying neuropsychiatric conditions. As the field has evolved and research into the identification of so-called biomarkers has matured, the hope is that the emergence of fMRI as an investigative tool signals a shift away from 'subjective' diagnoses towards the use of diagnostic biomarkers, objective measures of biological processes capable of differentiating psychiatric conditions and subtypes (García-Gutiérrez et al., 2020; Sechidis et al., 2018). The 'holy grail' for clinicians is the development of predictive biomarkers, already in use in oncology, that aid in identification of potential treatment-responders. Objective alternatives to the current trial-and-error approach to medication use that are likely to result in improvements in patient outcomes and take us a step closer to personalised medicine would be widely welcomed (Evers, 2009). Notwithstanding that fMRI has proven itself to be an excellent mechanistic tool in increasing our understanding of the heterogenous nature of depression in both diagnosis and treatment response, there is

further work to be done in addressing the potential reasons for inconsistencies across study results, particularly in relation to amygdala (Varkevisser et al., 2024).

1.3 The Role of Imaging in Depression

The introduction of fMRI was well-received by researchers who looked to use this technology to investigate the neural correlates underlying psychiatric conditions with a view to identifying potential biomarkers not only specific to a particular disorder, but also for stratification within a disorder. This imaging innovation was seen as a pathway to increased accuracy in diagnosis and a future in which condition-specific treatments might be developed for improved outcomes for patients (Zhan & Yu, 2015).

For those reasons previously mentioned, differentiation of unipolar depression from bipolar disorder became a neuroimaging focus, and many authors comparing results between groups have reported both structural and functional differences using MRI. These neuroimaging findings are well-summarised in the meta-analysis by Han and colleagues who have noted the contribution of the amygdala to the collective differences seen in neural circuits involved in reward, emotion and cognition-processing in distinguishing unipolar depression and bipolar disorder (Han et al., 2019). Previous work done by our own group has also described activation and connectivity differences between unipolar depression and bipolar disorder, particularly in relation to the amygdala (Korgaonkar et al., 2019).

Similarly, fMRI has been utilised to classify patients with a diagnosis of depression into subgroups. Previous work has identified neural differences in structure and function between unipolar depression patients who respond to initial treatment and those who are treatment-resistant (Barreiros et al., 2022; Lui et al., 2011; Wu et al., 2011; Zhang et al., 2022).

A recent review of over twenty fMRI studies focussing on TRD noted that the amygdala and striatal areas, regions primarily linked to emotion and reward processing, showed altered structure, activation and connectivity in TRD cohorts compared to both treatment responders and healthy individuals (Kotoula et al., 2023).

1.4 Depression and the Amygdala

The amygdala has long been identified as having major significance in affective disorders including depression due to its role in emotion regulation and processing (Davidson, 2003; LeDoux, 2000). Studies have also evidenced amygdala links to neural processes such as social

cognition, memory formation, reward processing and visual recognition and it has been reported to act as a hub to integrate sensory information (Brabec et al., 2010; Bzdok et al., 2013)

Abnormalities in both structure and function of the amygdala have been widely implicated in neuropsychiatric and neurodevelopmental disorders (Davidson, 2003; Schumann et al., 2011). Previous studies have associated amygdala dysfunction with a range of neuropsychiatric conditions, notably depression and anxiety (Ferri et al., 2017; Hamilton et al., 2012; Leppänen, 2006; Sah et al., 2003). Ineffectual emotion regulation is known to be implicated in the development of depressive symptoms, with sufferers experiencing rumination, a dysfunctional emotion regulation strategy characterised by persistent negative thought patterns. For sufferers, higher levels of repetitive focus on negative memories and experiences is associated with more severe bouts of depression (Compare et al., 2014; Eliot et al., 2021; Leppänen, 2006). Results such as these have driven research interest in imaging of the amygdala in depression cohorts.

1.5 What is the Amygdala?

There are two amygdalae in the brain; they are a pair of small almond-shaped structures located deep in the anterior medial temporal lobes in each hemisphere where they form part of the limbic system (Kim et al., 2012). Although the volume of each amygdala is very small, reportedly between 1000-2000mm^3 (Amunts et al., 2005; Brabec et al., 2010) each has multiple afferent and efferent connections to other brain regions (Davidson, 2003; LeDoux, 2000). In essence, each amygdala is heterogeneous both functionally and structurally and contains highly differentiated groups of cells belonging to various functional brain systems including the main and accessory olfactory, autonomic and frontotemporal systems (Swanson & Petrovich, 1998).

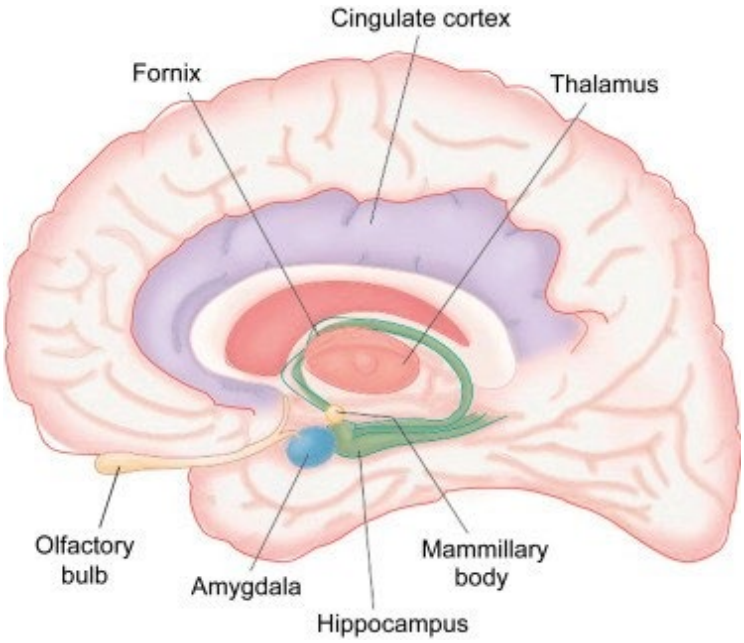

Figure 1.1: Location of the amygdala and other structures forming the brain's limbic system

Note: From (Moini et al., 2021)

The so-called 'classic amygdala' as defined by pioneering texts and papers based on human histological samples is composed of ten 'structures' (Crosby & Humphrey, 1941; Sims & Williams, 1990).

The seminal work by Crosby and Humphrey published in 1941 identifies the amygdaloid complex as consisting of two groups (each comprising four sub-groups) and two areas. The two groups were named the baso-lateral group (lateral amygdaloid complex, basal amygdaloid nucleus, accessory basal nucleus, intercalated cell masses) and the cortico-medial group (cortical amygdaloid nucleus, medial amygdaloid nucleus, nucleus of the lateral olfactory tract, central amygdaloid nucleus). The two areas are the anterior amygdaloid area and cortico-amygdaloid transition area (Crosby & Humphrey, 1941).

It is now universally acknowledged that the amygdala is a collection of nine nuclei that can be grouped into three main subregions, the laterobasal (LB), centromedial (CM) and superficial (SF), each of which has its own unique structural and functional connections with other parts of the brain (Amaral, 1992; De Olmos et al., 1990; Haris et al., 2023; McDonald, 2009; Nieuwenhuys et al., 2008). Advances have been made in identifying and defining the amygdala subnuclei and subregional borders using cytoarchitectonic parcellations as seen in Figure 1.2

below, resulting in the development of probability maps for subregional localisation in the data analysis phase.

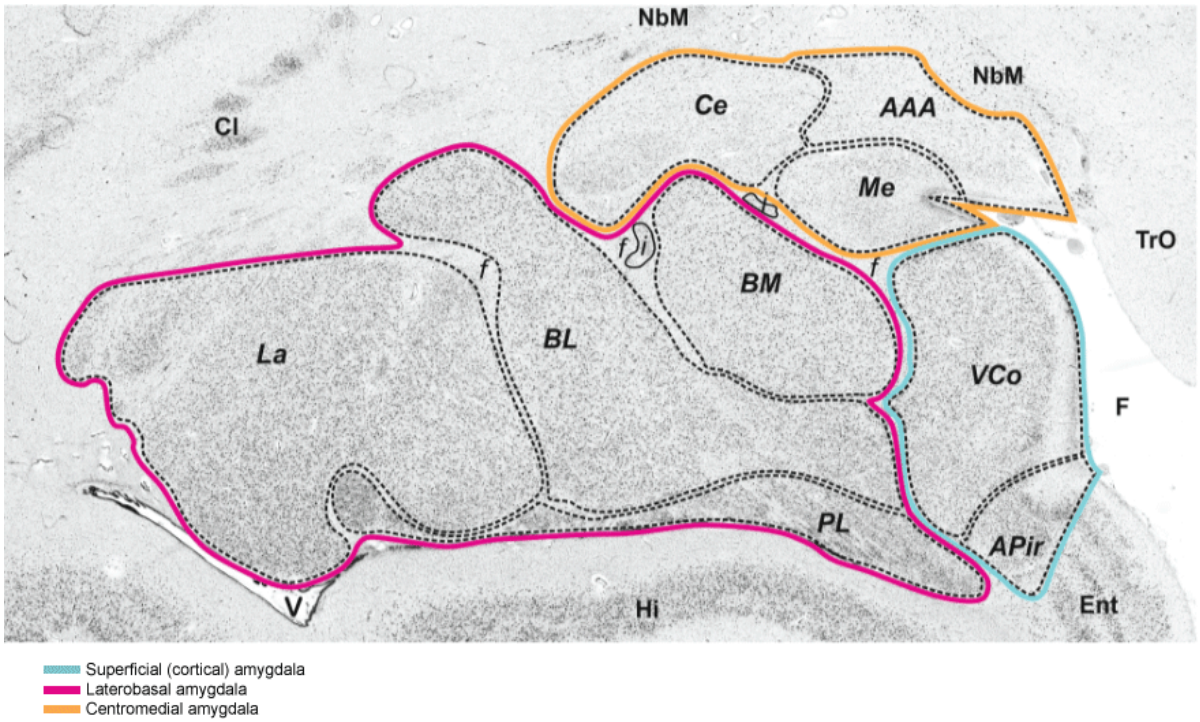

Figure 1.2: Cytoarchitecture of the amygdala in the coronal plane

Note: Subnuclei encompassed in red outline form the basolateral subregion (La = lateral nucleus; BL = basolateral nucleus; BM = basomedial nucleus; PL = paralaminar nucleus). Subnuclei encompassed in orange outline form the centromedial subregion (Ce = central nucleus; Me = medial nucleus; AAA = anterior amygdaloid area). Subnuclei encompassed in blue outline form the superficial subregion (VCo = ventral cortical nucleus; APir = amygdalopiriform transition area) (Kedo et al., 2016).

The groundbreaking work of Bzdok and colleagues in investigating structural, 'connectional' and functional specialisations of amygdala subregions, showed that the amygdala demonstrated three discrete clusters, each having a different pattern of activational connectivity as well as each cluster corresponding well to those structural subregions mapped cytoarchitectonically by Amunts and colleagues (Amunts et al., 2005; Bzdok et al., 2013). The SF subregions selectively coactivate with brain areas associated with affective and autonomic processing, olfaction and reward prediction whilst the CM subregions connect to brain regions associated with visceral and somatosensory processing, perceptual modulation and motor behaviour. The LB

subregions connect to areas of the early visual cortex and areas associated with visual and auditory input processing (Bzdok et al., 2013). These authors also found that the right LB selectively coactivated with the Default Mode Network areas of prefrontal cortex, precuneus and inferior parietal cortex. Brain regions selectively coactivated by the individual left and right subregions are listed in Table 1.2.

Investigation of the amygdala and its subregions with MRI (depicted in Figure 1.3) has become widely accepted as a method of furthering our understanding of its structure and complexity and, more recently, the function of the subregions has come under increased scrutiny as researchers hope to learn more about the role of the amygdala in depression (Ball et al., 2007; Kerestes et al., 2017; Kim et al., 2003; Roy et al., 2009). The need for greater understanding of the individual roles of the subregions has also been noted in other neurological conditions such as frontotemporal dementia (Huang et al., 2024) and epilepsy, with one study reporting subregional amygdala differences linked to the side of the epileptic focus (Doucet et al., 2013). Given published reports of between 40-60% of epilepsy patients displaying symptoms of depression (Grabowska-Grzyb et al., 2006), these results lend further weight to the necessity for expanding our knowledge and understanding of the amygdala subregions and their connections to other parts of the brain.

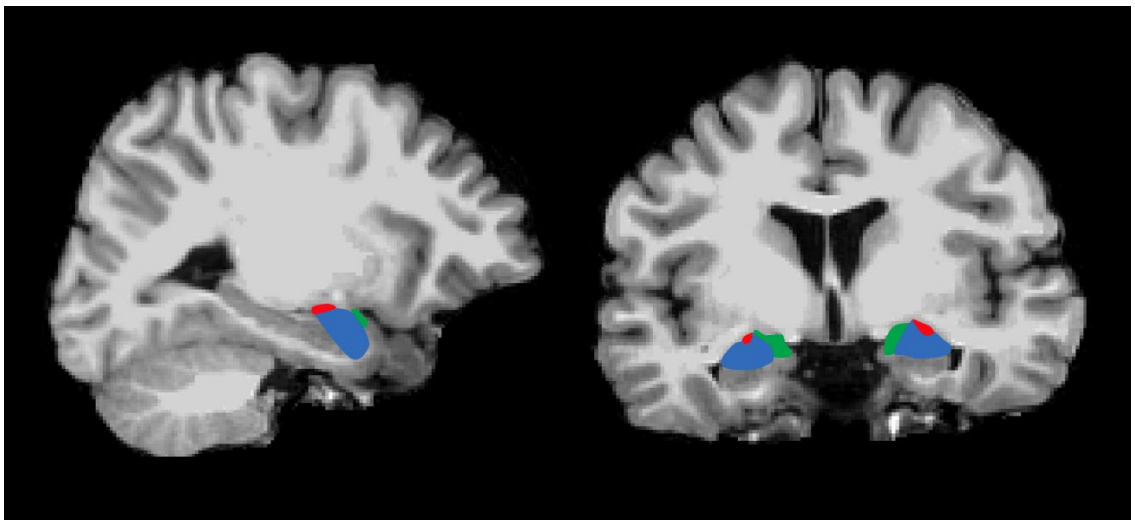

Figure 1.3: T1-weighted sagittal (left), and coronal (right) images showing location of the amygdala and three main subregions *(SF = green, LB = blue, CM = red)*

Table 1.2: Individual left and right amygdala subregions and their selective connections to different brain regions, and bilateral subregional roles

Subregion	Selectively Connected Brain Region
Left LB	precuneus, inferior occipital gyrus, cerebellum, superior temporal gyrus/associative auditory cortex, middle frontal gyrus/frontal eye field all on left. Bilateral temporal poles, right inferior parietal cortex
Right LB	dorsomedial prefrontal cortex, temporal pole, precuneus, inferior parietal cortex bilaterally, ventromedial prefrontal cortex, superior temporal gyrus/associative auditory cortex, middle frontal gyrus/frontal eye field, hippocampus, and posterior superior temporal sulcus all on the left side Selectively coactivated with Default Mode Network
LB role	Higher-level visual and auditory input processing
Left CM	supplementary motor cortex, pallidum, putamen, cerebellum, insula, thalamus bilaterally. Left posterior mid-cingulate cortex, left primary somatosensory cortex, right occipital lobe
Right CM	primary motor cortex, supplementary motor cortex, pallidum, putamen, primary somatosensory cortex, inferior frontal gyrus bilaterally. Right thalamus, left insula
CM role	Motor behaviour, perceptual modulation, visceral & somatosensory processing
Left SF	ventral striatum/nucleus accumbens and olfactory tubercle bilaterally. Right anterior insula
Right SF	left anterior mid-cingulate cortex, bilateral anterior insula extending into the inferior frontal gyrus
SF role	Reward prediction, olfaction, affective & vegetative processing

Note: LB = laterobasal; CM = centromedial; SF = superficial. Adapted from Bzdok et al. (Bzdok et al., 2013).

1.6 Investigating the Amygdala with MRI – A Narrative Overview

Continued advancements have been made in MRI technology relating to increased field strengths as well as innovations in radiofrequency coil technology, the combination of which has resulted in higher signal-to-noise ratio (SNR) levels and the capability for higher resolution imaging. Earlier studies were performed on 1.5T systems prior to the mid-2000s, after which 3T systems became available for clinical research. Dedicated 7T research systems became available in the 2010s but it was not until 2017 that these systems were cleared for clinical use (Platt et al., 2021). In order to provide clarity for the coming discussions, it is timely to provide a definition of what is considered high, standard and low-resolution imaging; however, this topic will be covered in greater detail in Chapter Two. High resolution fMRI data acquired in the brain is composed of imaging voxels with a volume of $20mm^3$ or lower whilst standard resolution voxels have a volume of between $20mm^3$ and $50mm^3$ (Olman & Yacoub, 2011). Imaging is considered low resolution at voxel volumes in excess of $50mm^3$. It should also be noted here that higher spatial resolution can be achieved in structural imaging than is possible in functional imaging at the same field strength, a concept which will also be covered in greater depth in Chapter Two.

In the years following the introduction of 3T systems, researchers sought to take advantage of this innovation in MRI technology to further explore the subregions and their potential individual roles. Following on from the work of Solano-Castiella and colleagues who recognised the importance of investigating not only the structural subdivisions of the amygdala but also their potentially different functional connectivity (Solano-Castiella et al., 2010), other researchers also showed that it was possible to demonstrate in-vivo, differences in volumes, white matter tracts and tissue properties between subregions in the amygdala (Bach et al., 2011; Roddy et al., 2021; Saygin et al., 2011). Bzdok and colleagues took this further by using a data-driven approach to investigate the potential for differentiation of the subregions on the basis of not only their structural properties but their functional and connectional properties as well (Bzdok et al., 2013). The following sections take a closer look at the evolution of methods of investigating both amygdala structure and function.

1.6.1 Amygdala Structure – Volume, Asymmetry, Gender Disparity and White Matter Connections

In the early 1990s Watson and colleagues, having recognised an opportunity in the still relatively new technology to fill a knowledge gap, undertook the task of reporting reliable measurements of amygdala and hippocampal volumes using a structural MR imaging protocol they had developed on a 1.5T MRI system (Watson et al., 1992). This group was the first to report standardised measurements of amygdala volumes in-vivo in the early days when many were striving for what was then considered high-resolution imaging, with voxel volumes of 2.86mm^3 providing a previously unachievable level of accuracy in a small cohort of eleven participants. In their seminal paper, the authors reported amygdala volumes of around 3400mm^3. They also noted asymmetry, with the left amygdala reportedly smaller than the right (Watson et al., 1992).

Ten years later, Brierley and colleagues carried out a meta-analysis of amygdala volumes derived from data also acquired on a 1.5T MRI system in 1491 healthy individuals in order to establish a normal range. They reported much smaller average volumes than Watson *et al*, with figures of approximately 1700mm^3 (range 1050 mm^3 to 3880 mm^3) and, unlike the previous study, found the left amygdala to be larger than the right, although the difference was not statistically significant (Brierley et al., 2002). Interestingly, these authors noted the disparity in data quality across studies and concluded that those studies to which they had assigned higher quality scores, reflective of superior spatial resolution equating to a higher degree of measurement accuracy, exhibited overall smaller amygdala volumes in keeping with 'gold standard' post-mortem estimates being reported at that time (Brierley et al., 2002).

Size disparity related to gender has also been reported, with amygdala volumes found to be significantly larger in males (Goldstein et al., 2001; Lotze et al., 2019; Ritchie et al., 2018) However, in a meta-analysis of 46 MRI studies published in 2017, the authors noted that the 10% larger size of the male amygdala was comparable to the differences in overall intracranial volumes between the genders. After correction, they found no significant differences and concluded that the human amygdala could not be considered 'sexually dimorphic' (Marwha et al., 2017). These authors also noted that evolving technology including higher field strengths and more nuanced analysis methods have played a role in the increasing accuracy of MRI-related measurements, so it is interesting to pause and note here that between 2010 and 2020,

the bulk of studies were still reporting whole rather than subregional amygdala volumes despite the fact that data acquisition and analysis methods had matured significantly.

It was inevitable that researchers would look to MRI to identify potential differences in amygdala size in patients with depression. A meta-analysis by Hamilton and colleagues concluded that unmedicated depression is associated with reduced amygdala size, whereas increased size was found in medicated cohorts (Hamilton et al., 2008). Zhuo and colleagues undertook a very comprehensive assessment of the literature pertaining to fMRI studies of MDD compared to a healthy control cohort (HC) published between 1995 and 2018 (Zhuo et al., 2019). Among the findings of the many studies included was that amygdala sizes were significantly smaller in females with MDD compared to HC, but not in males (Hastings et al., 2004). The authors noted that the clinical impact of the findings in these studies was limited in part by heterogeneity of the imaging data, potentially manifesting in inconsistency of results across studies (Zhuo et al., 2019).

More recent work by Tesen and colleagues in an MDD cohort has attempted to improve our understanding of the contribution of variations in amygdala volumes at a subregional level by acquiring high spatial resolution structural data at 3T with a voxel volume of only $1mm^3$ combined with segmentation of nine amygdala subnuclei based on a probabilistic atlas. Whilst they found no significant volume differences between first episode MDD and HC, they showed an inverse linear relationship between depression severity and size of the right lateral nucleus and anterior-amygdaloid regions in the MDD group (Tesen et al., 2022).

Imaging of structural white matter tracts using a combination of Diffusion-weighted imaging and probabilistic tractography has also been done, with prior work investigating white matter connections of the subregions at both 3T and 7T (Bach et al., 2011) (Saygin et al., 2011). In their investigation of an MDD cohort compared to HC, Brown and colleagues acquired ultra-high resolution ($1.1mm^3$) data at 7T and showed right-sided white matter hyperconnectivity in MDD vs HC as well as differential alterations in connection density between amygdala nuclei, supporting the necessity for moving beyond viewing the amygdala as a single structure in imaging (Brown et al., 2020).

1.6.2 *Amygdala Function – Task-based Activation*

Aside from reported structural disparities in amygdala size between left and right sides, between males and females, and between medicated and unmedicated depression cohorts, there

has also been mounting imaging evidence of functional differences related to amygdala activation although, once again, there are mixed results. As with the amygdala volume work, many of the earlier task-based fMRI studies were performed on 1.5T systems, with more recent meta-analyses such as those from Filkowski *et al*. combining studies with both 1.5T and 3T data (Filkowski et al., 2017), a further potential source of results inconsistency.

Initially, both emotion processing and cognitive function were a focus in depression patients in whom sustained amygdala activation was widely reported during tasks designed to interrogate emotional and cognitive responses (Mitterschiffthaler et al., 2006). Many early studies were based on investigation of whole amygdala responses to visual emotional stimuli, such as the work done by Gläscher and Adolphus, who reported the right amygdala as having a role in our initial and purely emotional or subconscious response to a stimulus whereas the left plays more of a role in the subsequent conscious cognitive assessment of the stimulus (Gläscher & Adolphs, 2003). Another study noted gender differences in amygdala lateralisation in response to visual stimuli, with males exhibiting increased activation, particularly in the left amygdala (Hamann et al., 2004) whilst a larger meta-analysis investigating emotion processing found no amygdala activation differences between genders (Sergerie et al., 2008). Other researchers sought to investigate lateralisation differences more broadly. In their meta-analysis of 54 fMRI studies investigating the amygdala and emotion processing in HC, Baas and colleagues reported that the left amygdala was activated significantly more than the right across all studies (Baas et al., 2004). More recently, reports of asymmetry of functional connectivity between left and right subregions have been published, raising the possibility of not only functional subregional specialisation but fluctuations in connectivity related to task demand (Kerestes et al., 2017; Zhang et al., 2018).

In a meta-analysis of 20 studies investigating facial emotion processing in MDD vs HC, whole amygdala activation patterns were significantly different between the two groups in only half the studies (Stuhrmann et al., 2011). These authors noted the lack of standardisation across tasks or paradigms presented to the participants as a likely contributor to these inconsistent results and suggested that factorial design, a cognitive comparison task strategy (Amaro & Barker, 2006), needs to become a greater consideration in task-based investigations. Further to this, they recommended FC analyses as a more precise method of investigating relationships between the amygdala and the rest of the brain (Stuhrmann et al., 2011). It has also been noted that resting state investigations require no prior assumptions regarding activation; the

fundamental association between task-related activation and underlying brain activity involves a complex set of interactions which are still not well understood (Canario et al., 2021).

With an increasing focus on amygdala subregional morphology, researchers sought to identify individual subregional activation patterns by employing subregional analysis methods, although spatial resolution of data used in some of these studies was potentially not adequate to probe the diminutive amygdala subregions (Ball et al., 2007; Michely et al., 2020; Morris et al., 2001).

Others began to utilise high resolution data to investigate subregional activation, including Frühholz and Grandjean, who reported sensitivity to vocal emotional cues in the LB and SF subregions in HC (Frühholz & Grandjean, 2013). Further to this, Balderston and colleagues used high resolution fMRI data to investigate potential differences in engagement of amygdala subregions in response to emotional vs non-emotional tasks. These authors advanced a 'three-stage information processing model' in which the LB subregion perceives environmental input, distils it within intrinsic amygdala circuits, with the CM subregion then responsible for modifying behaviour in response (Balderston et al., 2015). Interestingly, one study investigating the effects of oxytocin on the subregions and its utility as a potential treatment in neuropsychiatric disorders used high resolution data with voxel volumes of only $8mm^3$, noting the benefits of high resolution data in imaging these very small structures (Gamer et al., 2010).

1.6.3 *Amygdala Function – Connectivity*

Coinciding with the introduction of 3T systems in the mid-2000s, increasing interest in brain functional connectivity profiles at rest, that is, resting-state fMRI, was engendered by its versatility and simplicity of acquisition (Chen et al., 2020). Researchers recognised the possibilities of this technique in characterising neural circuitry, particularly in neuropsychiatric conditions (Etkin et al., 2009; Lv et al., 2018), resulting in a numerous studies focusing on amygdala functional connectivity in depression. In their meta-analysis of 19 studies published between 2009 and 2017, Tang *et al.* reported that adult MDD patients show affective network anomalies that are potentially related to the emotional dysfunction evident in these patients. A key component of this network is the amygdala, and FC abnormalities have been shown to be specific to its functional connections with the hippocampus, insular cortex and prefrontal regions (Tang et al., 2018). Decreased FC between the amygdala and medial prefrontal cortex has also been reported in MDD adolescents and adults compared with HC (Kim et al., 2016;

Tang et al., 2013). These studies all reported FC measures related to the amygdala as a single structure.

In a large study of 336 MDD patients and 350 HC investigating FC variations in depression, Cheng and colleagues parcellated the amygdala into three 'subdivisions' and reported decreased 'subdivisional' FC with a number of regions including the medial and lateral orbitofrontal cortices, parahippocampal and fusiform gyri, insula, striatum and pre-and post-central gyri (Cheng et al., 2018). Their findings were based on standard resolution fMRI data, as is the case with numerous other studies reporting subregional amygdala FC findings in neuropsychiatric conditions (Ambrosi et al., 2017; Etkin et al., 2009; Fateh et al., 2020; Geng et al., 2016; Jiang et al., 2021; Qin et al., 2014; Roy et al., 2013; Zhang et al., 2020). Interestingly, several relatively recent studies have reported their findings based on low resolution data (Liu et al., 2021; Qiao et al., 2020; Tu et al., 2025; Wang et al., 2021) whilst a few have reported use of high resolution data (Hofmann & Straube, 2019; Kwon et al., 2024; Li et al., 2021; Nair et al., 2024; Rausch et al., 2016).

1.6.4 *Whole vs Subregional Amygdala Analyses*

As scientific interest in amygdala and subregional morphology grew, so too did interest in its functional role which began to escalate in the early 2000s; however, there were two main roadblocks to advancement. Firstly, the absence of MR imaging techniques with sufficient resolution and image contrast to identify and resolve the amygdala subregions in-vivo became evident; however, this issue would soon be addressed by the introduction of 3T systems. The second issue was the lack of user-friendly analysis software that could localise the subregions in a standardised format for researchers. This led to the development of cytoarchitectonically-verified probabilistic maps such as those created by Amunts and colleagues using post-mortem brain images acquired on a 1.5T system, the highest field strength system in use for clinical research at that time. They demonstrated that the true borders of the structure are not accurately delineated by macroanatomical landmarks (Amunts et al., 2005). Together with the hippocampal-amygdaloid transition area, Amunts and colleagues were able to identify and label the other three main groups or subregions previously defined by neuroanatomists Heimer and colleagues and Crosby and Humphrey in their earlier works (Crosby & Humphrey, 1941; Heimer et al., 1999). As previously noted, these subregions were labelled as superficial (SF), centromedial (CM) and laterobasal (LB) (Amunts et al., 2005).

The introduction of these probabilistic maps into more user-friendly analysis software enabled researchers to input both anatomical and functional data into a common reference space and perform integrated analyses (Eickhoff et al., 2005). Unfortunately, these updated subregional analysis methods were slow to be adopted and more than a decade later, many studies were still reporting whole amygdala activation as demonstrated by Filkowski and colleagues in their meta-analysis of 56 studies focusing on emotional perception. They reported increased bilateral whole amygdala activation in HC females compared to males, a finding at odds with previous results (Baas et al., 2004; Filkowski et al., 2017; Sergerie et al., 2008). Regrettably, there is very little consensus in results across studies investigating the amygdala after 25 years of fMRI investigation, with paradigm selection, data analysis variations and, crucially, technical factors such as MRI protocol parameter choices likely contributing to this quandary (Elliott et al., 2021; Hartling et al., 2021; Poldrack et al., 2017). Further, there are still few studies reporting subregional amygdala findings and this, together with the issue of variations in data acquisition protocols, led to the scoping review that forms Chapter Three. This Chapter reports on variations in fMRI protocols in use by researchers to investigate FC of the amygdala in neuropsychiatric conditions with a focus on spatial resolution. It also outlines the percentage of studies reporting subregional versus whole amygdala findings.

1.7 The Choice of 3T MRI Systems for Clinical Research

Since its introduction in the late 1980s, MRI has made many advances in both hardware and software, especially radiofrequency (RF) coil technology and pulse sequence design, meaning that images acquired at the same field strength and spatial resolution on current systems provide superior SNR for increased spatial and/or temporal resolution (Edelman, 2014). With their arrival on the market in the mid-2000s, 3T systems have been become popular, displacing 1.5T systems in research settings due to their inherently higher SNR.

In Australia, 3T systems are in place at specialist research sites such as The Florey, Hunter Research Medical Institute, Herston Imaging Research Facility, University of Queensland Centre for Advanced Imaging, Monash Biomedical Imaging and NeuRa, to name just a few (National Imaging Facility, 2024). Very high field MR systems such as 7 Tesla (7T) and above provide much higher SNR and concomitant increased spatial resolution, but are limited in numbers globally, thereby restricting access to primarily pure research work (Iranpour et al., 2015). In Australia at this time, there are currently only two 7T systems, one each in Brisbane (Centre for Advanced Imaging, The University of Queensland) and Melbourne (Melbourne

Brain Centre Imaging Unit, The University of Melbourne); therefore, the ability to access a very high field strength magnet system for brain research is limited to very few groups nationally (National Imaging Facility, 2024).

In comparison to data acquired at 7T, fMRI acquisition methods at 3T have, in the main, provided suboptimal spatial resolution for adequately demonstrating FC variations in deep brain regions such as the amygdala and its subregions (Sladky et al., 2018). However, meaningful improvements in FC imaging protocols can potentially be made at 3T by optimising existing sequences or employing novel data acquisition sequences to provide improved spatial resolution and image quality for the amygdala and its subregions. These improved techniques may hold the promise of furthering our understanding of the clinical implications of amygdala FC variations in neuropsychiatric conditions such as depression.

1.8 Summary and Study Rationale

This chapter has outlined the history of how neuroimaging, and particularly functional neuroimaging, has been used as a tool for furthering our knowledge of the neural correlates underlying depression. With the amygdala being identified early on as a prime target for researchers, we have seen the field progress from comparisons of structural amygdala volume measurements, then on to task-based fMRI studies designed to elicit neural 'activation' and measure potential differences through to the use of the resting-state technique, a simple acquisition strategy easily implemented. We have also noted that, almost without exception, these early MR imaging data were acquired on 1.5T MRI systems with lower SNR and spatial resolution. 3T MRI systems possessing higher inherent SNR coupled with improved radiofrequency coil technology came into use in clinical research in the mid-2000s, meaning data acquired after that time was potentially of higher quality; however, the increased SNR was not necessarily invested in achieving higher spatial resolution data, an important consideration when investigating the amygdala subregions.

It is also noteworthy that, although there has been a shift towards discussion of the differential contributions of the subregions, there is still limited consensus across study findings, and it is also of note that the amygdala has continued to be considered, in the main, as a single structure for imaging and analysis purposes.

A strong, emerging theme across all this imaging work relating to the amygdala is that, whilst fMRI has been instrumental in investigating the core characteristics of depression including

negative emotion processing, cognitive impairment and excessive rumination, there is a general acknowledgement that results inconsistency and data heterogeneity are overarching limitations to progress, further exacerbated by the outdated practice of regarding the amygdala as a single homogenous structure. In addition, there is currently no standardisation across tasks or paradigms investigating emotion processing, even in studies investigating the same or similar hypotheses, with reports of varying profiles of neural activity across four commonly used emotion processing paradigms (Hartling et al., 2021). Taken together, these inconsistencies are an obstacle to meaningful comparisons of study findings (Hartling et al., 2021; Mitterschiffthaler et al., 2006; Poldrack et al., 2020) and, in addition, serve to diminish the quality of meta-analytic reporting (*Cochrane Handbook for Systematic Reviews of Interventions*, 2024).

To recap, the following key points underscore the rationale for this work. Although it is accepted that amygdala dysfunction plays a significant role in the development of depression, there remains a lack of understanding of the functional differences in amygdala subregions in the context of depression. A pivotal study by Klein-Flügge and colleagues provides a compelling incentive for mental health researchers to move beyond symptom-based diagnoses. Their research demonstrated that alterations in FC values of specific amygdala subnuclei with other brain regions more accurately predicted variations in social and general life satisfaction, negative emotions, and issues with anger and rejection than traditional aggregate depression scores, such as the DSM-oriented "Depressive Problems" score and the Achenbach Adult Self-Report 'anxious/depressed' (AnxD) score (Klein-Flügge et al., 2022). Additionally, they found that behavioural predictions in mental health were more precise when considering FC variations of individual subnuclei rather than treating the amygdala as a single entity. They attributed their findings to access to high-resolution data and more accurate analysis methods made available by the Human Connectome Project, a National Institutes of Health initiative to map the structural and functional connectivity, or connectome, of the human brain using high resolution imaging (Elam et al., 2021).

Moreover, a recent appraisal of the literature highlighted the ongoing debate and challenges surrounding the utility of amygdala fMRI and the inconsistency of findings across studies. This appraisal emphasised the importance of optimising scanning protocols in fMRI data acquisition of the amygdala (Varkevisser et al., 2024). These insights collectively reinforce the rationale for this work, aiming to advance our understanding of the role of the amygdala subregions and

their functional connections in depression using 3T MRI systems that are widely accessible for clinical research.

1.9 Aims and Significance of Thesis

Current 3T MRI systems are capable of providing much-improved data quality for researchers than the first generation of 3T systems that made their debut 20 years ago. It is evident that functional imaging protocols in use for many studies have not kept pace with these innovations. In demonstrating underutilised potential in current imaging systems, this research aims to improve our understanding of the individual roles of the amygdala subregions and their contributions to brain networks in the context of depression. The following steps outline the general structural pathway to achieving the research aims:

- Review of the literature and collation of technical information on existing fMRI protocols used in reporting amygdala findings at 3T
- Use of an existing 3T fMRI technique (2D) and assessment of its capability, when optimised, to investigate subregional FC of the amygdala to other brain regions
- Introduction of a novel technique (3D). Qualitative comparison of both existing and new techniques in mirroring previously published 7T findings (Elvira et al., 2022) reporting amygdala FC to resting state networks that are implicated in depression and commonly investigated using existing 2D techniques
- Direct comparison between existing and novel techniques at 3T in investigating amygdala subregional FC, specifically to subcortical brain regions which are problematic to image well using existing 2D techniques

Secondary to these aims, subregional functional connectivity findings using both whole and subregional amygdala ROI analysis methods will be directly compared. Several authors have noted the potential for conflicting results but there are very few reports of comparative results in the literature.

In demonstrating the validity of using high spatial resolution fMRI data acquired at 3T to show potential functional connectivity alterations in the amygdala subregions, this work also aims to highlight to researchers the benefits of utilising optimised acquisition techniques and matching the imaging and analysis protocols to the research question. In addition, the work demonstrates

the value-add of the inclusion of a specialist in MRI protocol optimisation to collaborative research groups.

Therefore, the overarching goal of this thesis was to investigate the capabilities of fMRI sequences optimised for higher spatial resolution in demonstrating functional connectivity patterns of the amygdala subregions using a 3T MRI system, the most widely accessible field strength for clinical researchers. The MRI system used for all data acquisition in this work is a 3T Prisma system with VE11C software in conjunction with a 64-channel head and neck array radiofrequency coil (Siemens Healthineers, Erlangen, Germany).

Aim 1

- Review the literature and collate information on functional MRI protocols used at 3T for investigating activation and functional connectivity in studies reporting amygdala findings, with a focus on spatial resolution values of data acquisition sequences
- Formulate recommendations regarding equipment, sequence type and parameter selections at 3T with a focus on fMRI of the amygdala subregions

Chapter Three is composed of two parts of a formal scoping review of the literature:

a. The first part is the proposed formal Scoping Review protocol registered on the Open Science Framework and published on the medRxiv Preprint Server for Health Sciences
https://www.medrxiv.org/content/10.1101/2022.04.14.22273332v1.full-text.
This protocol is located in Appendix C

b. The main part of the chapter comprising the full Scoping Review including recommendations for imaging the amygdala subregions at 3T, is published in the Journal of Magnetic Resonance Imaging
https://onlinelibrary.wiley.com/doi/full/10.1002/jmri.28836

Novelty - The published scoping review forming part of Chapter Three represents the first comprehensive summary of the current landscape in relation to the technical data acquisition aspects of fMRI of the amygdala at 3T and concludes with recommendations for imaging the amygdala subregions

Aim 2

- Test the capability of an optimised 3T version of the existing 2D fMRI sequence (2.5mm isotropic high resolution) to detect subregional amygdala (rather than whole

amygdala) functional connectivity alterations between two depression cohortsand a healthy control cohort

Chapter Four investigates subregional FC in a TRD cohort and compares these findings to healthy controls and treatment-sensitive depression (TSD) patients. It also includes a comparison of FC differences using a subregional versus whole amygdala analysis approach.

Novelty - This published study was the first to use both high resolution data and a subregional data analysis approach to locate and report FC alterations of the amygdala subregions in a TRD cohort compared to a TSD cohort. The study also highlighted the differences in functional connectivity results when using a subregional versus whole amygdala analysis approach, an issue about which there are only a handful of reports in the literature.

The findings from Chapter Four are published in the Journal of Affective Disorders Reports.

Aim 3

- Commission and optimise a novel higher(er) resolution 3D Works-in-Progress 2mm isotropic sequence.
- Acquire pilot data at 3T using previously optimised 2D sequence and novel 3D sequence and qualitatively compare amygdala subregional FC findings against previously published 7T findings of amygdala subnuclei FC to resting state networks to validate the use of data acquired at 3T in identifying amygdala FC at a subregional level.

Chapter Five is a pilot study in which data is acquired with both 2D and 3D sequences in ten healthy individuals. The study investigates amygdala subregional FC using the widely used 2D sequence optimised for high spatial resolution described in Chapter Four and the novel 3D sequence, both acquired at 3T. The capabilities of each sequence are assessed in identifying functional connections of the amygdala at a subregional level to three resting state networks. Due to lack of access to 7T for data acquisition, qualitative comparisons are made against results of a study published by authors using 2D data acquired at 7T, the gold standard, to report amygdala connectivity findings at the more granular subnuclei (rather than subregional) level.

Novelty - To our knowledge, this is the first study to qualitatively assess the capabilities of fMRI data acquired at 3T against data acquired at 7T in demonstrating functional connectivity of the amygdala on a more granular subregional level to resting state networks.

Aim 4

- Investigate the potential for high-resolution 2D and novel 3D data acquired at 3T to reveal subregional amygdala functional connections to other deep subcortical brain regions

Based on the same pilot data, Chapter Six investigates subcortical FC. In a head-to-head comparison, the widely used 2D and novel 3D sequences are tested in relation to their capabilities in identifying subregional amygdala functional connections to other deep subcortical brain regions that are difficult to image well due to their central location. It also includes a comparison of FC differences using a subregional versus whole amygdala analysis approach.

Novelty – this is the first published study to directly compare the performance of widely used 2D and novel 3D fMRI high resolution data acquired at 3T in identifying subregional amygdala functional connections to deep subcortical structures such as the brainstem and contralateral amygdala

The findings from Chapter Six are published in the Journal of Neuroimaging.

The results from all chapters will be synthesized for discussion in the final chapter which will provide an overview of the utility of high resolution imaging for interrogating functional connections of the amygdala at a subregional level to other brain regions, noting the comparative results when treating the amygdala as a single structure. The comparison between the widely used 2D and novel 3D versions of the sequence will provide us with some insights as to the current and future capabilities of fMRI in providing data with sufficient resolution at 3T to probe amygdala FC at a more granular level than is the current practice. Given the importance of the amygdala in MDD, it is essential that our imaging results are truly representative of the individuality of its underlying functions. The results of this work could lead to widespread changes in practice regarding image acquisition and analysis protocols for investigating the amygdala to ensure that this is the case.

1.10 References

Amaral, D. G. (1992). The amygdale : Neurobiological aspects emotion memory and mental dysfunction. *Anatomical organization of the primate amygdaloid complex*. https://ci.nii.ac.jp/naid/10019626517/en/

Amaro, E., & Barker, G. J. (2006). Study design in fMRI: Basic principles. *Brain and Cognition*, *60*(3), 220-232. https://doi.org/10.1016/j.bandc.2005.11.009

Ambrosi, E., Arciniegas, D. B., Madan, A., Curtis, K. N., Patriquin, M. A., Jorge, R. E., Spalletta, G., Fowler, J. C., Frueh, B. C., & Salas, R. (2017). Insula and amygdala resting-state functional connectivity differentiate bipolar from unipolar depression. *Acta Psychiatrica Scandinavica*, *136*(1), 129-139. https://doi.org/10.1111/acps.12724

Amunts, K., Kedo, O., Kindler, M., Pieperhoff, P., Mohlberg, H., Shah, N. J., Habel, U., Schneider, F., & Zilles, K. (2005). Cytoarchitectonic mapping of the human amygdala, hippocampal region and entorhinal cortex: intersubject variability and probability maps. *Anatomy and Embryology*, *210*(5), 343-352. https://doi.org/10.1007/s00429-005-0025-5

Arzy, S., & Danziger, S. (2014). The Science of Neuropsychiatry: Past, Present, and Future. *The Journal of Neuropsychiatry and Clinical Neurosciences*, *26*(4), 392-395. https://doi.org/10.1176/appi.neuropsych.13120371

Baas, D., Aleman, A., & Kahn, R. S. (2004). Lateralization of amygdala activation: a systematic review of functional neuroimaging studies. *Brain Research Reviews*, *45*(2), 96-103. https://doi.org/j.brainresrev.2004.02.004

Bach, D. R., Behrens, T. E., Garrido, L., Weiskopf, N., & Dolan, R. J. (2011). Deep and Superficial Amygdala Nuclei Projections Revealed In Vivo by Probabilistic Tractography. *The Journal of Neuroscience*, *31*(2), 618. https://doi.org/10.1523/JNEUROSCI.2744-10.2011

Balderston, N. L., Schultz, D. H., Hopkins, L., & Helmstetter, F. J. (2015). Functionally distinct amygdala subregions identified using DTI and high-resolution fMRI. *Soc Cogn Affect Neurosci*, *10*(12), 1615-1622. https://doi.org/10.1093/scan/nsv055

Ball, T., Rahm, B., Eickhoff, S. B., Schulze-Bonhage, A., Speck, O., & Mutschler, I. (2007). Response Properties of Human Amygdala Subregions: Evidence Based on Functional MRI Combined with Probabilistic Anatomical Maps. *PLOS ONE*, *2*(3), e307. https://doi.org/10.1371/journal.pone.0000307

Barreiros, A. R., Breukelaar, I., Mayur, P., Andepalli, J., Tomimatsu, Y., Funayama, K., Foster, S., Boyce, P., Malhi, G. S., Harris, A., & Korgaonkar, M. S. (2022). Abnormal habenula functional connectivity characterizes treatment-resistant depression. *Neuroimage Clin*, *34*, 102990. https://doi.org/10.1016/j.nicl.2022.102990

Brabec, J., Rulseh, A., Hoyt, B., Vizek, M., Horinek, D., Hort, J., & Petrovicky, P. (2010). Volumetry of the human amygdala — An anatomical study. *Psychiatry Research: Neuroimaging*, *182*(1), 67-72. https://doi.org/10.1016/j.pscychresns.2009.11.005

Brierley, B., Shaw, P., & David, A. S. (2002). The human amygdala: a systematic review and meta-analysis of volumetric magnetic resonance imaging. *Brain Research Reviews*, *39*(1), 84-105. https://doi.org/10.1016/S0165-0173(02)00160-1

Brown, S. S. G., Rutland, J. W., Verma, G., Feldman, R. E., Schneider, M., Delman, B. N., Murrough, J. M., & Balchandani, P. (2020). Ultra-High-Resolution Imaging of Amygdala Subnuclei Structural Connectivity in Major Depressive Disorder. *Biological Psychiatry: Cognitive Neuroscience and Neuroimaging*, *5*(2), 184-193. https://doi.org/https://doi.org/10.1016/j.bpsc.2019.07.010

Bzdok, D., Laird, A. R., Zilles, K., Fox, P. T., & Eickhoff, S. B. (2013). An investigation of the structural, connectional, and functional subspecialization in the human amygdala. *Human Brain Mapping*, *34*(12), 3247-3266. https://doi.org/10.1002/hbm.22138

Canario, E., Chen, D., & Biswal, B. (2021). A review of resting-state fMRI and its use to examine psychiatric disorders. *Psychoradiology*, *1*(1), 42-53. https://doi.org/10.1093/psyrad/kkab003

Chen, J. J., Herman, P., Keilholz, S., & Thompson, G. J. (2020). Editorial: Origins of the Resting-State fMRI Signal [Editorial]. *Frontiers in Neuroscience*, *14*. https://doi.org/10.3389/fnins.2020.594990

Cheng, W., Rolls, E. T., Qiu, J., Xie, X., Lyu, W., Li, Y., Huang, C.-C., Yang, A. C., Tsai, S.-J., & Lyu, F. (2018). Functional connectivity of the human amygdala in health and in depression. *Social cognitive and affective neuroscience*, *13*(6), 557-568. https://doi.org/10.1093/scan/nsy032

Cochrane Handbook for Systematic Reviews of Interventions. (2024). (J. T. Higgins, J; Chandler, J; Cumpston, M; Li, T; Page, MJ; Welch, VA, Ed.). Cochrane. www.training.cochrane.org/handbook.

Compare, A., Zarbo, C., Shonin, E., Van Gordon, W., & Marconi, C. (2014). Emotional Regulation and Depression: A Potential Mediator between Heart and Mind. *Cardiovasc Psychiatry Neurol*, *2014*, 324374. https://doi.org/10.1155/2014/324374

Coryell, W. (2023, 2023/10). *Depressive Disorders*. MSD Manual. https://www.msdmanuals.com/professional/psychiatric-disorders/mood-disorders/depressive-disorders

Crosby, E. C., & Humphrey, T. (1941). Studies of the vertebrate telencephalon. II. The nuclear pattern of the anterior olfactory nucleus, tuberculum olfactorium and the amygdaloid complex in adult man. *Journal of Comparative Neurology*, *74*(2), 309-352. https://doi.org/10.1002/cne.900740209

Davidson, R. J. (2003). Darwin and the neural bases of emotion and affective style. *Ann N Y Acad Sci*, *1000*, 316-336. https://doi.org/10.1196/annals.1280.014

De Olmos, J., Paxinos, G., & Mai, J. (1990). The human nervous system. In. *Diagnostic and Statistical Manual of Mental Disorders*. (2013). American Psychiatric Association.

Doucet, G. E., Skidmore, C., Sharan, A. D., Sperling, M. R., & Tracy, J. I. (2013). Functional connectivity abnormalities vary by amygdala subdivision and are associated with psychiatric symptoms in unilateral temporal epilepsy. *Brain and Cognition*, *83*(2), 171-182. https://doi.org/10.1016/j.bandc.2013.08.001

Edelman, R. R. (2014). The History of MR Imaging as Seen through the Pages of Radiology. *Radiology*, *273*(2S), S181-S200. https://doi.org/10.1148/radiol.14140706

Eickhoff, S. B., Stephan, K. E., Mohlberg, H., Grefkes, C., Fink, G. R., Amunts, K., & Zilles, K. (2005). A new SPM toolbox for combining probabilistic cytoarchitectonic maps and functional imaging data. *Neuroimage*, *25*(4), 1325-1335. https://doi.org/10.1016/j.neuroimage.2004.12.034

Elam, J. S., Glasser, M. F., Harms, M. P., Sotiropoulos, S. N., Andersson, J. L. R., Burgess, G. C., Curtiss, S. W., Oostenveld, R., Larson-Prior, L. J., Schoffelen, J.-M., Hodge, M. R., Cler, E. A., Marcus, D. M., Barch, D. M., Yacoub, E., Smith, S. M., Ugurbil, K., & Van Essen, D. C. (2021). The Human Connectome Project: A retrospective. *Neuroimage*, *244*, 118543. https://doi.org/10.1016/j.neuroimage.2021.118543

Eliot, L., Ahmed, A., Khan, H., & Patel, J. (2021). Dump the "dimorphism": Comprehensive synthesis of human brain studies reveals few male-female differences beyond size. *Neuroscience & Biobehavioral Reviews*, *125*, 667-697. https://doi.org/10.1016/j.neubiorev.2021.02.026

Elliott, M. L., Knodt, A. R., & Hariri, A. R. (2021). Striving toward translation: strategies for reliable fMRI measurement. *Trends Cogn Sci*, *25*(9), 776-787. https://doi.org/10.1016/j.tics.2021.05.008

Elvira, U. K. A., Seoane, S., Janssen, J., & Janssen, N. (2022). Contributions of human amygdala nuclei to resting-state networks. *PLOS ONE*, *17*(12), e0278962. https://doi.org/10.1371/journal.pone.0278962

Etkin, A., Prater, K. E., Schatzberg, A. F., Menon, V., & Greicius, M. D. (2009). Disrupted amygdalar subregion functional connectivity and evidence of a compensatory network in generalized anxiety disorder. *Arch Gen Psychiatry*, *66*(12), 1361-1372. https://doi.org/10.1001/archgenpsychiatry.2009.104

Evers, K. (2009). Personalized medicine in psychiatry: ethical challenges and opportunities. *Dialogues Clin Neurosci*, *11*(4), 427-434. https://doi.org/10.31887/DCNS.2009.11.4/kevers

Fateh, A. A., Cui, Q., Duan, X., Yang, Y., Chen, Y., Li, D., He, Z., & Chen, H. (2020). Disrupted dynamic functional connectivity in right amygdalar subregions differentiates bipolar disorder from major depressive disorder. *Psychiatry Research: Neuroimaging*, *304*, 111149. https://doi.org/10.1016/j.pscychresns.2020.111149

Ferri, J., Eisendrath, S. J., Fryer, S. L., Gillung, E., Roach, B. J., & Mathalon, D. H. (2017). Blunted amygdala activity is associated with depression severity in treatment-resistant depression. *Cogn Affect Behav Neurosci*, *17*(6), 1221-1231. https://doi.org/10.3758/s13415-017-0544-6

Filkowski, M. M., Olsen, R. M., Duda, B., Wanger, T. J., & Sabatinelli, D. (2017). Sex differences in emotional perception: Meta analysis of divergent activation. *Neuroimage*, *147*, 925-933. https://doi.org/10.1016/j.neuroimage.2016.12.016

Frühholz, S., & Grandjean, D. (2013). Amygdala subregions differentially respond and rapidly adapt to threatening voices. *Cortex*, *49*(5), 1394-1403. https://doi.org/10.1016/j.cortex.2012.08.003

Gamer, M., Zurowski, B., & Büchel, C. (2010). Different amygdala subregions mediate valence-related and attentional effects of oxytocin in humans. *Proceedings of the National Academy of Sciences*, *107*(20), 9400-9405. https://doi.org/10.1073/pnas.1000985107

García-Gutiérrez, M. S., Navarrete, F., Sala, F., Gasparyan, A., Austrich-Olivares, A., & Manzanares, J. (2020). Biomarkers in Psychiatry: Concept, Definition, Types and Relevance to the Clinical Reality. *Front Psychiatry*, *11*, 432. https://doi.org/10.3389/fpsyt.2020.00432

Gaynes, B. N., Rush, A. J., Trivedi, M. H., Wisniewski, S. R., Spencer, D., & Fava, M. (2008). The STAR*D study: Treating depression in the real world. *Cleveland Clinic Journal of Medicine*, *75*(1), 57. http://www.ccjm.org/content/75/1/57.abstract

Geng, H., Li, X., Chen, J., Li, X., & Gu, R. (2016). Decreased intra-and inter-salience network functional connectivity is related to trait anxiety in adolescents. *Frontiers in Behavioral Neuroscience*, *9*, 350.

Gläscher, J., & Adolphs, R. (2003). Processing of the Arousal of Subliminal and Supraliminal Emotional Stimuli by the Human Amygdala. *The Journal of Neuroscience*, *23*(32), 10274. https://doi.org/10.1523/JNEUROSCI.23-32-10274.2003

Glover, G. H. (2011). Overview of functional magnetic resonance imaging. *Neurosurgery clinics of North America*, *22*(2), 133-vii. https://doi.org/10.1016/j.nec.2010.11.001

Goldstein, J. M., Seidman, L. J., Horton, N. J., Makris, N., Kennedy, D. N., Caviness, V. S., Jr, Faraone, S. V., & Tsuang, M. T. (2001). Normal Sexual Dimorphism of the Adult Human Brain Assessed by In Vivo Magnetic Resonance Imaging. *Cerebral Cortex*, *11*(6), 490-497. https://doi.org/10.1093/cercor/11.6.490

Grabowska-Grzyb, A., Jędrzejczak, J., Nagańska, E., & Fiszer, U. (2006). Risk factors for depression in patients with epilepsy. *Epilepsy & Behavior*, *8*(2), 411-417. https://doi.org/10.1016/j.yebeh.2005.12.005

Griesinger, W. (1845). The Pathology and Therapy of Mental Illnesses, for Physicians and Students. In *German Text Archive* (1st ed.). Stuttgart: Crab.

Hamann, S., Herman, R. A., Nolan, C. L., & Wallen, K. (2004). Men and women differ in amygdala response to visual sexual stimuli. *Nat Neurosci*, *7*(4), 411-416. https://doi.org/10.1038/nn1208

Hamilton, J. P., Etkin, A., Furman, D. J., Lemus, M. G., Johnson, R. F. a., & Gotlib, I. H. (2012). Functional Neuroimaging of Major Depressive Disorder: A Meta-Analysis and New Integration of Baseline Activation and Neural Response Data. *American Journal of Psychiatry*, *169*(7), 693-703. https://doi.org/10.1176/appi.ajp.2012.11071105

Hamilton, J. P., Siemer, M., & Gotlib, I. H. (2008). Amygdala volume in major depressive disorder: a meta-analysis of magnetic resonance imaging studies. *Mol Psychiatry*, *13*(11), 993-1000. https://doi.org/10.1038/mp.2008.57

Han, K.-M., De Berardis, D., Fornaro, M., & Kim, Y.-K. (2019). Differentiating between bipolar and unipolar depression in functional and structural MRI studies. *Progress in Neuro-Psychopharmacology and Biological Psychiatry*, *91*, 20-27. https://doi.org/10.1016/j.pnpbp.2018.03.022

Haris, E. M., Bryant, R. A., Williamson, T., & Korgaonkar, M. S. (2023). Functional connectivity of amygdala subnuclei in PTSD: a narrative review. *Molecular Psychiatry*, *28*(9), 3581-3594. https://doi.org/10.1038/s41380-023-02291-w

Hartling, C., Metz, S., Pehrs, C., Scheidegger, M., Gruzman, R., Keicher, C., Wunder, A., Weigand, A., & Grimm, S. (2021). Comparison of Four fMRI Paradigms Probing Emotion Processing. *Brain Sciences*, *11*(5), 525. https://www.mdpi.com/2076-3425/11/5/525

Hastings, R. S., Parsey, R. V., Oquendo, M. A., Arango, V., & Mann, J. J. (2004). Volumetric Analysis of the Prefrontal Cortex, Amygdala, and Hippocampus in Major Depression. *Neuropsychopharmacology*, *29*(5), 952-959. https://doi.org/10.1038/sj.npp.1300371

Heimer, L., de Olmos, J. S., Alheid, G. F., Pearson, J., Sakamoto, N., Shinoda, K., Marksteiner, J., & Switzer, R. C. (1999). Chapter II - The human basal forebrain. Part II. In F. E. Bloom, A. Björklund, & T. Hökfelt (Eds.), *Handbook of Chemical Neuroanatomy* (Vol. 15, pp. 57-226). Elsevier. https://doi.org/10.1016/S0924-8196(99)80024-4

Hofmann, D., & Straube, T. (2019). Resting-state fMRI effective connectivity between the bed nucleus of the stria terminalis and amygdala nuclei. *Hum Brain Mapp*, *40*(9), 2723-2735. https://doi.org/10.1002/hbm.24555

Huang, M., Landin-Romero, R., Matis, S., Dalton, M. A., & Piguet, O. (2024). Longitudinal volumetric changes in amygdala subregions in frontotemporal dementia. *J Neurol*, *271*(5), 2509-2520. https://doi.org/10.1007/s00415-023-12172-5

Ionescu, D. F., Rosenbaum, J. F., & Alpert, J. E. (2015). Pharmacological approaches to the challenge of treatment-resistant depression. *Dialogues Clin Neurosci*, *17*(2), 111-126. https://doi.org/10.31887/DCNS.2015.17.2/dionescu

Iranpour, J., Morrot, G., Claise, B., Jean, B., & Bonny, J.-M. (2015). Using high spatial resolution to improve BOLD fMRI detection at 3T. *PLOS ONE*, *10*(11), e0141358. https://doi.org/10.1371/journal.pone.0141358

Jiang, X., Ma, X., Geng, Y., Zhao, Z., Zhou, F., Zhao, W., Yao, S., Yang, S., Zhao, Z., Becker, B., & Kendrick, K. M. (2021). Intrinsic, dynamic and effective connectivity among large-scale brain networks modulated by oxytocin. *Neuroimage*, *227*, 117668. https://doi.org/10.1016/j.neuroimage.2020.117668

Kedo, O., Zilles, K., & Amunts, K. (2016). Advances in Cytoarchitectonic Mapping of the Human Amygdala and the Hippocampus. *2*(3).

Kerestes, R., Chase, H. W., Phillips, M. L., Ladouceur, C. D., & Eickhoff, S. B. (2017). Multimodal evaluation of the amygdala's functional connectivity. *Neuroimage*, *148*, 219-229. https://doi.org/10.1016/j.neuroimage.2016.12.023

Kim, H., Kim, N., Kim, S., Hong, S., Park, K., Lim, S., Park, J. M., Na, B., Chae, Y., Lee, J., Yeo, S., Choe, I. H., Cho, S. Y., & Cho, G. (2012). Sex differences in amygdala subregions: evidence from subregional shape analysis. *Neuroimage*, *60*(4), 2054-2061. https://doi.org/10.1016/j.neuroimage.2012.02.025

Kim, H., Somerville, L. H., Johnstone, T., Alexander, A. L., & Whalen, P. J. (2003). Inverse amygdala and medial prefrontal cortex responses to surprised faces. *Neuroreport*, *14*(18), 2317-2322. https://doi.org/10.1097/00001756-200312190-00006

Kim, S., Park, S., Kim, Y., Son, Y., Chung, U., Min, K., & Han, D. (2016). Affective network and default mode network in depressive adolescents with disruptive behaviors. *Neuropsychiatric Disease & Treatment*, *12*, 49-56. https://doi.org/10.2147/NDT.S95541

Korgaonkar, M. S., Erlinger, M., Breukelaar, I. A., Boyce, P., Hazell, P., Antees, C., Foster, S., Grieve, S. M., Gomes, L., Williams, L. M., Harris, A. W. F., & Malhi, G. S. (2019). Amygdala Activation and Connectivity to Emotional Processing Distinguishes Asymptomatic Patients With Bipolar Disorders and Unipolar Depression. *Biological Psychiatry: Cognitive Neuroscience and Neuroimaging*, *4*(4), 361-370. https://doi.org/10.1016/j.bpsc.2018.08.012

Kotoula, V., Evans, J. W., Punturieri, C., Johnson, S. C., & Zarate, C. A. (2023). Chapter 5 - Functional MRI markers for treatment-resistant depression: Insights and challenges. In C.-T. Li & C.-M. Cheng (Eds.), *Progress in Brain Research* (Vol. 278, pp. 117-148). Elsevier. https://doi.org/10.1016/bs.pbr.2023.04.001

Kwon, H., Ha, M., Choi, S., Park, S., Jang, M., Kim, M., & Kwon, J. S. (2024). Resting-state functional connectivity of amygdala subregions across different symptom subtypes of obsessive–compulsive disorder patients. *NeuroImage: Clinical*, *43*, 103644. https://doi.org/10.1016/j.nicl.2024.103644

LeDoux, J. E. (2000). Emotion Circuits in the Brain. *Annual Review of Neuroscience*, *23*(1), 155-184. https://doi.org/10.1146/annurev.neuro.23.1.155

Leppänen, J. M. (2006). Emotional information processing in mood disorders: a review of behavioral and neuroimaging findings. *Current Opinion in Psychiatry*, *19*(1). https://journals.lww.com/co-psychiatry/Fulltext/2006/01000/Emotional_information_processing_in_mood.7.aspx

Li, Y. Y., Ni, X. K., You, Y. F., Qing, Y. H., Wang, P. R., Yao, J. S., Ren, K. M., Zhang, L., Liu, Z. W., Song, T. J., Wang, J., Zang, Y. F., Shen, Y. D., & Chen, W. (2021). Common and Specific Alterations of Amygdala Subregions in Major Depressive Disorder With and Without Anxiety: A Combined Structural and Resting-State Functional MRI Study. *Front Hum Neurosci*, *15*, 634113. https://doi.org/10.3389/fnhum.2021.634113

Liu, T., Ke, J., Qi, R., Zhang, L., Zhang, Z., Xu, Q., Zhong, Y., Lu, G., & Chen, F. (2021). Altered functional connectivity of the amygdala and its subregions in typhoon-related post-traumatic stress disorder. *Brain and Behavior*, *11*(1), e01952. https://doi.org/10.1002/brb3.1952

Lotze, M., Domin, M., Gerlach, F. H., Gaser, C., Lueders, E., Schmidt, C. O., & Neumann, N. (2019). Novel findings from 2,838 Adult Brains on Sex Differences in Gray Matter Brain Volume. *Sci Rep*, *9*(1), 1671. https://doi.org/10.1038/s41598-018-38239-2

Lui, S., Wu, Q., Qiu, L., Yang, X., Kuang, W., Chan, R. C. K., Huang, X., Kemp, G. J., Mechelli, A. a., & Gong, Q. (2011). Resting-State Functional Connectivity in Treatment-Resistant Depression. *American Journal of Psychiatry*, *168*(6), 642-648. https://doi.org/10.1176/appi.ajp.2010.10101419

Lv, H., Wang, Z., Tong, E., Williams, L. M., Zaharchuk, G., Zeineh, M., Goldstein-Piekarski, A. N., Ball, T. M., Liao, C., & Wintermark, M. (2018). Resting-State Functional MRI: Everything That Nonexperts Have Always Wanted to Know. *AJNR Am J Neuroradiol*, *39*(8), 1390-1399. https://doi.org/10.3174/ajnr.A5527

Malhi, G. S., Das, P., Mannie, Z., & Irwin, L. (2019). Treatment-resistant depression: problematic illness or a problem in our approach? *British Journal of Psychiatry*, *214*(1), 1-3. https://doi.org/10.1192/bjp.2018.246

Marwha, D., Halari, M., & Eliot, L. (2017). Meta-analysis reveals a lack of sexual dimorphism in human amygdala volume. *Neuroimage*, *147*, 282-294. https://doi.org/10.1016/j.neuroimage.2016.12.021

McCallum, S. M., Batterham, P. J., Calear, A. L., Sunderland, M., & Carragher, N. (2019). Reductions in quality of life and increased economic burden associated with mental disorders in an Australian adult sample. *Australian Health Review*, *43*(6), 644-652. https://doi.org/10.1071/AH16276

McDonald, A. J. (2009). Amygdala. In M. D. Binder, N. Hirokawa, & U. Windhorst (Eds.), *Encyclopedia of Neuroscience* (pp. 100-104). Springer Berlin Heidelberg. https://doi.org/10.1007/978-3-540-29678-2_201

Michely, J., Rigoli, F., Rutledge, R. B., Hauser, T. U., & Dolan, R. J. (2020). Distinct processing of aversive experience in amygdala subregions. *Biological Psychiatry: Cognitive Neuroscience and Neuroimaging*, *5*(3), 291-300. https://doi.org/10.1016/j.bpsc.2019.07.008

Mitterschiffthaler, M. T., Ettinger, U., Mehta, M. A., Mataix-Cols, D., & Williams, S. C. R. (2006). Applications of functional magnetic resonance imaging in psychiatry. *Journal of Magnetic Resonance Imaging*, *23*(6), 851-861. https://doi.org/10.1002/jmri.20590

Moini, J., Avgeropoulos, N. G., & Samsam, M. (2021). Chapter 1 - Anatomy and physiology. In J. Moini, N. G. Avgeropoulos, & M. Samsam (Eds.), *Epidemiology of Brain and Spinal Tumors* (pp. 3-40). Academic Press. https://doi.org/10.1016/B978-0-12-821736-8.00002-9

Morris, J. S., Buchel, C., & Dolan, R. J. (2001). Parallel neural responses in amygdala subregions and sensory cortex during implicit fear conditioning. *Neuroimage*, *13*(6 Pt 1), 1044-1052. https://doi.org/10.1006/nimg.2000.0721

Nair, A. U., Klimes-Dougan, B., Silamongkol, T., Başgöze, Z., Roediger, D. J., Mueller, B. A., Albott, C. S., Croarkin, P. E., Lim, K. O., Widge, A. S., Nahas, Z., Eberly, L. E., Cullen, K. R., & Thai, M. E. (2024). Deep transcranial magnetic stimulation for adolescents with treatment-resistant depression: Behavioral and neural correlates of clinical improvement. *J Affect Disord*, *372*, 665-675. https://doi.org/10.1016/j.jad.2024.12.057

National Imaging Facility. (2024, 2024). *Instruments and Infrastructure*. https://anif.org.au/what-we-do/our-capabilities/capabilities/

Nieuwenhuys, R., Voogd, J., & van Huijzen, C. (2008). Telencephalon: Amygdala and Claustrum. In *The human central nervous system* (Fourth ed., pp. 401-426). Springer Berlin Heidelberg. https://doi.org/10.1007/978-3-540-34686-9_1310.1007/978-3-540-34686-9_1310

Olman, C. A., & Yacoub, E. (2011). High-field FMRI for human applications: an overview of spatial resolution and signal specificity. *Open Neuroimag J*, *5*, 74-89. https://doi.org/10.2174/1874440001105010074

Platt, T., Ladd, M. E., & Paech, D. (2021). 7 Tesla and Beyond: Advanced Methods and Clinical Applications in Magnetic Resonance Imaging. *Invest Radiol*, *56*(11), 705-725. https://doi.org/10.1097/rli.0000000000000820

Poldrack, R. A., Baker, C. I., Durnez, J., Gorgolewski, K. J., Matthews, P. M., Munafò, M. R., Nichols, T. E., Poline, J. B., Vul, E., & Yarkoni, T. (2017). Scanning the horizon: towards transparent and reproducible neuroimaging research. *Nat Rev Neurosci*, *18*(2), 115-126. https://doi.org/10.1038/nrn.2016.167

Poldrack, R. A., Whitaker, K., & Kennedy, D. (2020). Introduction to the special issue on reproducibility in neuroimaging. *Neuroimage*, *218*, 116357. https://doi.org/10.1016/j.neuroimage.2019.116357

Qiao, J., Tao, S., Wang, X., Shi, J., Chen, Y., Tian, S., Yao, Z., & Lu, Q. (2020). Brain functional abnormalities in the amygdala subregions is associated with anxious depression. *Journal of Affective Disorders*, *276*, 653-659.

Qin, S., Young, C. B., Duan, X., Chen, T., Supekar, K., & Menon, V. (2014). Amygdala Subregional Structure and Intrinsic Functional Connectivity Predicts Individual Differences in Anxiety During Early Childhood. *Biological Psychiatry*, *75*(11), 892-900. https://doi.org/10.1016/j.biopsych.2013.10.006

Rausch, A., Zhang, W., Haak, K. V., Mennes, M., Hermans, E. J., van Oort, E., van Wingen, G., Beckmann, C. F., Buitelaar, J. K., & Groen, W. B. (2016). Altered functional connectivity of the amygdaloid input nuclei in adolescents and young adults with autism spectrum disorder: a resting state fMRI study. *Molecular autism*, *7*(1), 1-13. https://doi.org/10.1186/s13229-015-0060-x

Ritchie, S. J., Cox, S. R., Shen, X., Lombardo, M. V., Reus, L. M., Alloza, C., Harris, M. A., Alderson, H. L., Hunter, S., Neilson, E., Liewald, D. C. M., Auyeung, B., Whalley, H. C., Lawrie, S. M., Gale, C. R., Bastin, M. E., McIntosh, A. M., & Deary, I. J. (2018). Sex Differences in the Adult Human Brain: Evidence from 5216 UK Biobank Participants. *Cerebral Cortex*, *28*(8), 2959-2975. https://doi.org/10.1093/cercor/bhy109

Roalf, D. R., & Gur, R. C. (2017). Functional brain imaging in neuropsychology over the past 25 years. *Neuropsychology*, *31*(8), 954-971. https://doi.org/10.1037/neu0000426

Roddy, D., Kelly, J. R., Farrell, C., Doolin, K., Roman, E., Nasa, A., Frodl, T., Harkin, A., O'Mara, S., O'Hanlon, E., & O'Keane, V. (2021). Amygdala substructure volumes in Major Depressive Disorder. *Neuroimage Clin*, *31*, 102781. https://doi.org/10.1016/j.nicl.2021.102781

Roy, A. K., Fudge, J. L., Kelly, C., Perry, J. S. A., Daniele, T., Carlisi, C., Benson, B., Castellanos, F. X., Milham, M. P., & Pine, D. S. (2013). Intrinsic functional connectivity of amygdala-based networks in adolescent generalized anxiety disorder. *Journal of the American Academy of Child & Adolescent Psychiatry*, *52*(3), 290-299. https://doi.org/10.1016/j.jaac.2012.12.010

Roy, A. K., Shehzad, Z., Margulies, D. S., Kelly, A. M. C., Uddin, L. Q., Gotimer, K., Biswal, B. B., Castellanos, F. X., & Milham, M. P. (2009). Functional connectivity of the human amygdala using resting state fMRI. *Neuroimage*, *45*(2), 614-626. https://doi.org/10.1016/j.neuroimage.2008.11.030

Sah, P., Faber, E. S. L., & Lopez De Armentia, M. P., J. (2003). The Amygdaloid Complex: Anatomy and Physiology. *Physiological Reviews*, *83*(3), 803-834. https://doi.org/10.1152/physrev.00002.2003

Saygin, Z. M., Osher, D. E., Augustinack, J., Fischl, B., & Gabrieli, J. D. (2011). Connectivity-based segmentation of human amygdala nuclei using probabilistic tractography. *Neuroimage*, *56*(3), 1353-1361. https://doi.org/10.1016/j.neuroimage.2011.03.006

Schumann, C. M., Bauman, M. D., & Amaral, D. G. (2011). Abnormal structure or function of the amygdala is a common component of neurodevelopmental disorders. *Neuropsychologia*, *49*(4), 745-759. https://doi.org/10.1016/j.neuropsychologia.2010.09.028

Sechidis, K., Papangelou, K., Metcalfe, P. D., Svensson, D., Weatherall, J., & Brown, G. (2018). Distinguishing prognostic and predictive biomarkers: an information theoretic approach. *Bioinformatics*, *34*(19), 3365-3376. https://doi.org/10.1093/bioinformatics/bty357

Sergerie, K., Chochol, C., & Armony, J. L. (2008). The role of the amygdala in emotional processing: A quantitative meta-analysis of functional neuroimaging studies. *Neuroscience & Biobehavioral Reviews*, *32*(4), 811-830. https://doi.org/10.1016/j.neubiorev.2007.12.002

Siegel-Ramsay, J. E., Bertocci, M. A., Wu, B., Phillips, M. L., Strakowski, S. M., & Almeida, J. R. C. (2022). Distinguishing between depression in bipolar disorder and unipolar depression using magnetic resonance imaging: a systematic review. *Bipolar Disorders*, *24*(5), 474-498. https://doi.org/10.1111/bdi.13176

Sims, K. S., & Williams, R. S. (1990). The human amygdaloid complex: A cytologic and histochemical atlas using Nissl, myelin, acetylcholinesterase and nicotinamide adenine dinucleotide phosphate diaphorase staining. *Neuroscience*, *36*(2), 449-472. https://doi.org/10.1016/0306-4522(90)90440-F

Singh, T., & Rajput, M. (2006). Misdiagnosis of bipolar disorder. *Psychiatry (Edgmont)*, *3*(10), 57-63.

Sladky, R., Geissberger, N., Pfabigan, D. M., Kraus, C., Tik, M., Woletz, M., Paul, K., Vanicek, T., Auer, B., Kranz, G. S., Lamm, C., Lanzenberger, R., & Windischberger, C. (2018). Unsmoothed functional MRI of the human amygdala and bed nucleus of the stria terminalis during processing of emotional faces. *Neuroimage*, *168*, 383-391. https://doi.org/10.1016/j.neuroimage.2016.12.024

Solano-Castiella, E., Anwander, A., Lohmann, G., Weiss, M., Docherty, C., Geyer, S., Reimer, E., Friederici, A. D., & Turner, R. (2010). Diffusion tensor imaging segments the human amygdala in vivo. *Neuroimage*, *49*(4), 2958-2965. https://doi.org/10.1016/j.neuroimage.2009.11.027

Stuhrmann, A., Suslow, T., & Dannlowski, U. (2011). Facial emotion processing in major depression: a systematic review of neuroimaging findings. *Biology of mood & anxiety disorders*, *1*(1), 1-17. https://doi.org/10.1186/2045-5380-1-10

Sutterer, M. J., & Tranel, D. (2017). Neuropsychology and cognitive neuroscience in the fMRI era: A recapitulation of localizationist and connectionist views. *Neuropsychology*, *31*(8), 972-980. https://doi.org/10.1037/neu0000408

Swanson, L. W., & Petrovich, G. D. (1998). What is the amygdala? [Article]. *Trends in Neurosciences*, *21*(8), 323-331. https://doi.org/10.1016/S0166-2236(98)01265-X

Tang, S., Lu, L., Zhang, L., Hu, X., Bu, X., Li, H., Hu, X., Gao, Y., Zeng, Z., Gong, Q., & Huang, X. (2018). Abnormal amygdala resting-state functional connectivity in adults and adolescents with major depressive disorder: A comparative meta-analysis. *EBioMedicine*, *36*, 436-445. https://doi.org/10.1016/j.ebiom.2018.09.010

Tang, Y., Kong, L., Wu, F., Womer, F., Jiang, W., Cao, Y., Ren, L., Wang, J., Fan, G., Blumberg, H. P., Xu, K., & Wang, F. (2013). Decreased functional connectivity between the amygdala and the left ventral prefrontal cortex in treatment-naive patients with major depressive disorder: a resting-state functional magnetic resonance imaging study. *Psychological Medicine*, *43*(9), 1921-1927. https://doi.org/10.1017/S0033291712002759

Taslim, S., Shadmani, S., Saleem, A. R., Kumar, A., Brahma, F., Blank, N., Bashir, M. A., Ansari, D., Kumari, K., Tanveer, M., Varrassi, G., Kumar, S., & Raj, A. (2024). Neuropsychiatric Disorders: Bridging the Gap Between Neurology and Psychiatry. *Cureus*, *16*(1), e51655. https://doi.org/10.7759/cureus.51655

Tesen, H., Watanabe, K., Okamoto, N., Ikenouchi, A., Igata, R., Konishi, Y., Kakeda, S., & Yoshimura, R. (2022). Volume of Amygdala Subregions and Clinical Manifestations in Patients With First-Episode, Drug-Naïve Major Depression [Original Research]. *Frontiers in Human Neuroscience*, *15*. https://doi.org/10.3389/fnhum.2021.780884

Tu, P. C., Chang, W. C., Su, T. P., Lin, W. C., Li, C. T., Bai, Y. M., Tsai, S. J., & Chen, M. H. (2025). Thalamocortical functional connectivity and rapid antidepressant and antisuicidal effects of low-dose ketamine infusion among patients with treatment-

resistant depression. *Mol Psychiatry*, *30*(1), 61-68. https://doi.org/10.1038/s41380-024-02640-3

Varkevisser, T., Geuze, E., & van Honk, J. (2024). Amygdala fMRI—A Critical Appraisal of the Extant Literature. *Neuroscience Insights*, *19*, 26331055241270591. https://doi.org/10.1177/26331055241270591

Voineskos, D., Daskalakis, Z. J., & Blumberger, D. M. (2020). Management of Treatment-Resistant Depression: Challenges and Strategies. *Neuropsychiatr Dis Treat*, *16*, 221-234. https://doi.org/10.2147/ndt.S198774

Wang, M., Cao, L., Li, H., Xiao, H., Ma, Y., Liu, S., Zhu, H., Yuan, M., Qiu, C., & Huang, X. (2021). Dysfunction of Resting-State Functional Connectivity of Amygdala Subregions in Drug-Naïve Patients With Generalized Anxiety Disorder. *Front Psychiatry*, *12*, 758978. https://doi.org/10.3389/fpsyt.2021.758978

Watson, Andermann, F., Gloor, P., Jones-Gotman, M., Peters, T., Evans, A., Olivier, A., Melanson, D., & Leroux, G. (1992). Anatomic basis of amygdaloid and hippocampal volume measurement by magnetic resonance imaging. *Neurology*, *42*(9), 1743-1750. https://doi.org/10.1212/wnl.42.9.1743

Williams, L. M., Korgaonkar, M. S., Song, Y. C., Paton, R., Eagles, S., Goldstein-Piekarski, A., Grieve, S. M., Harris, A. W. F., Usherwood, T., & Etkin, A. (2015). Amygdala Reactivity to Emotional Faces in the Prediction of General and Medication-Specific Responses to Antidepressant Treatment in the Randomized iSPOT-D Trial. *Neuropsychopharmacology*, *40*(10), 2398-2408. https://doi.org/10.1038/npp.2015.89

World Health Organisation. (2023). Depressive disorder (Depression). https://www.who.int/news-room/fact-sheets/detail/depression

Wu, Q.-Z., Li, D.-M., Kuang, W.-H., Zhang, T.-J., Lui, S., Huang, X.-Q., Chan, R. C. K., Kemp, G. J., & Gong, Q.-Y. (2011). Abnormal regional spontaneous neural activity in treatment-refractory depression revealed by resting-state fMRI. *Human Brain Mapping*, *32*(8), 1290-1299. https://doi.org/10.1002/hbm.21108

Yudofsky, S. C., & Hales, R. E. (2002). Neuropsychiatry and the Future of Psychiatry and Neurology. *American Journal of Psychiatry*, *159*(8), 1261-1264. https://doi.org/10.1176/appi.ajp.159.8.1261

Zhan, X., & Yu, R. (2015). A Window into the Brain: Advances in Psychiatric fMRI. *BioMed research international*, *2015*, 542467. https://doi.org/10.1155/2015/542467

Zhang, M., Yang, F., Fan, F., Wang, Z., Hong, X., Tan, Y., Tan, S., & Hong, L. E. (2020). Abnormal amygdala subregional-sensorimotor connectivity correlates with positive symptom in schizophrenia. *NeuroImage: Clinical*, *26*, 102218. https://doi.org/10.1016/j.nicl.2020.102218

Zhang, S., Cui, J., Zhang, Z., Wang, Y., Liu, R., Chen, X., Feng, Y., Zhou, J., Zhou, Y., & Wang, G. (2022). Functional connectivity of amygdala subregions predicts vulnerability to depression following the COVID-19 pandemic. *J Affect Disord*, *297*, 421-429. https://doi.org/10.1016/j.jad.2021.09.107

Zhang, X., Cheng, H., Zuo, Z., Zhou, K., Cong, F., Wang, B., Zhuo, Y., Chen, L., Xue, R., & Fan, Y. (2018). Individualized Functional Parcellation of the Human Amygdala Using a Semi-supervised Clustering Method: A 7T Resting State fMRI Study [Original Research]. *Frontiers in Neuroscience*, *12*(270). https://doi.org/10.3389/fnins.2018.00270

Zhuo, C., Li, G., Lin, X., Jiang, D., Xu, Y., Tian, H., Wang, W., & Song, X. (2019). The rise and fall of MRI studies in major depressive disorder. *Translational psychiatry*, *9*(1), 335. https://doi.org/10.1038/s41398-019-0680-6

Chapter 2: Brain Connectivity, BOLD and fMRI

This Methods chapter describes the fundamentals of the techniques and equipment required to carry out the research reported in Chapters Four, Five and Six. It also outlines the technical selections made, including justifications for each. The chapter also includes descriptions of brain connectivity and Blood Oxygen Level Dependent contrast as well as a brief explanation as to how fMRI is performed. Novel sequences are introduced in the context of their potential for improving our functional imaging of the amygdala.

2.1 What is Brain Connectivity?

The brain has both structural and functional connections. Structural connectivity (SC), the anatomical white matter microstructural organisation in the form of fibre tracts, was first imaged by Basser and colleagues (Basser et al., 1994). Around the same time in the early 1990's the term 'functional connectivity' (FC) was defined by Karl Friston and colleagues as 'temporal correlations between spatially remote neurophysiological events' (Friston et al., 1993). The two types of connectivity differ in that SC is prefaced on anatomic connections, that is, axonal projections between cells or groups of axonal projections forming tracts between different regions whilst FC is a temporally varying statistical measure that can be determined by the temporal covariation or correlation of activity between brain regions (Fornito et al., 2016; Grafton & Volz, 2019).

In the early days of fMRI, investigations centred primarily on the sensory and motor cortices of the brain; however, interest in the functioning of the association cortex, responsible for cognitive processes, was amplified in the setting of technical advances in neuroimaging (Javed et al., 2023; Seitzman et al., 2019). Analysing previously unknown brain networks was considered pivotal in order to progress knowledge of cognitive processes, potentially leading to new therapies for developmental and acquired brain abnormalities (Greicius et al., 2003; Sporns et al., 2005). This premise was widely recognised by the scientific community and was the genesis of the Human Connectome Project undertaken in 2009 by the National Institutes of Health in the USA (Elam et al., 2021). The aim of this wide-ranging project was "...to map the neural pathways that underlie human brain function" by acquiring high resolution SC and FC data to be made available to researchers to investigate the complex connections of brain circuitry, known more simply as the brain's connectome (National Institutes of Health, 2023). The term 'connectome' was proposed to describe the potential matrix of connectivity resulting from imaging on a large scale, revealing in greater depth the network elements and interconnections of the brain. The combination of connectivity matrices based on the acquisition of Diffusion Weighting Imaging (DWI) datasets for SC assessment together with Resting State fMRI (rs-fMRI) data for FC analysis allowed researchers to explore the interplay between the two types of connectivity (Elam et al., 2021; Sporns et al., 2005).

2.1.1 Resting State Networks and the Default Mode

The term 'resting state functional connectivity' was coined by Biswal and colleagues who, in 1995, were the first to report low frequency (<0.1 Hz) temporal correlations between brain regions in the absence of a defined task, that is, during 'rest' (Biswal et al., 1995; Biswal, 2012). More than 15 years later, in their seminal work focusing on patterns of functional connectivity based on resting state data, Yeo *et al.* outlined their findings of large-scale cortical circuits organised into networks, including local motor and sensory networks, that exhibit these low-frequency fluctuations. Their work identified a network of coordinated systems of spatially disparate and temporally coherent regions that co-activated functionally, known as distributed networks (Yeo et al., 2011). Although several of the networks had been previously described by other authors (Fox, Corbetta, et al., 2006; Greicius et al., 2003; Raichle et al., 2001; Vincent et al., 2008), Yeo and colleagues' parcellation of the brain into seven primary functional resting state networks (Figure 2.1), including a more granular 17-network estimate, continues to be widely used.

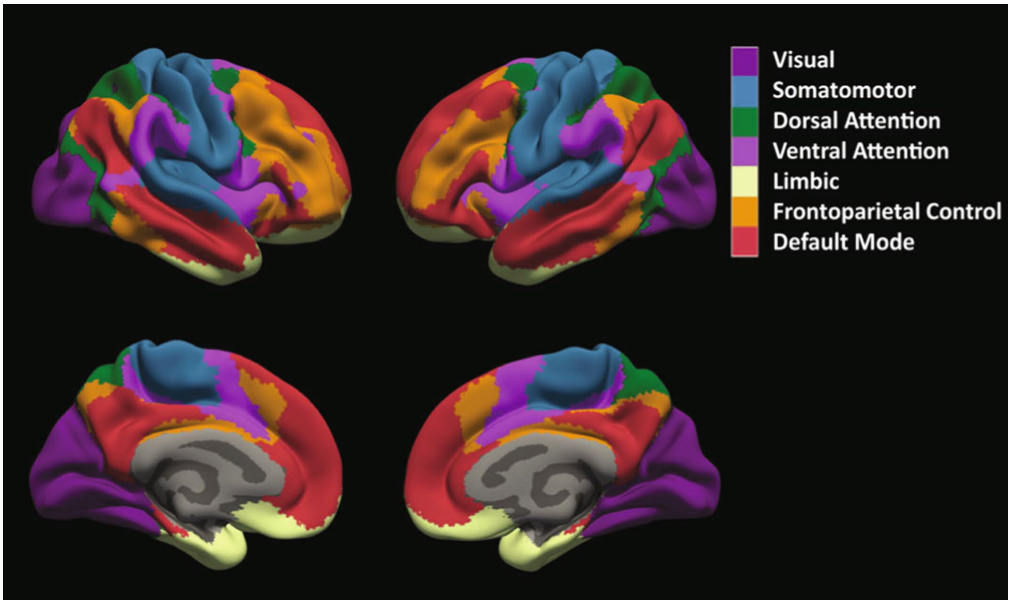

Figure 2.1: Depiction of the parcellation of seven main resting-state networks as identified by Yeo et al.

Note: The Default Mode Network (red) is the focus of investigation for Major Depressive Disorder. Adapted from (Cohen et al., 2023; Yeo et al., 2011).

The earliest of these brain networks to be identified was the Default Mode Network (DMN), depicted in red in Figure 2.1, a system of interconnected regions that are active in the absence

of external tasks or stimuli, during which time the network 'defaults' to a focus on spontaneous internal or self-referential thought processes (Menon, 2023; Raichle et al., 2001; Sheline et al., 2009). There is evidence that the DMN is comprised of two main subsystems, the dorsal medial prefrontal cortex (dMPFC) and the medial temporal lobe (MTL) along with a midline core of two main hubs, the anterior medial prefrontal cortex (aMPFC) and the posterior cingulate cortex (PCC) (Figure 2.2), with an overarching role centred on internal mentation (Andrews-Hanna, 2012; Andrews-Hanna et al., 2010)

Of the seven resting state networks identified by Yeo *et al*., the DMN has become the focal network for researchers looking to extend their understanding of the neural correlates of MDD due to its role in self-referential processing (Chen et al., 2020; Sheline et al., 2009; Yan et al., 2019). Rumination, a repetitive self-referential cycle of dwelling on negative thoughts and feelings, is a deleterious cognitive symptom experienced by those suffering from depression and is thought to be related to dysfunction in processes associated with cognitive control (Alderman et al., 2015; Hamilton et al., 2015; Tozzi et al., 2021). As such, investigations into the implications of potentially aberrant DMN function in MDD continue to be a priority for researchers in the field (Damborská et al., 2020; Dutta et al., 2019; Stoliker et al., 2024).

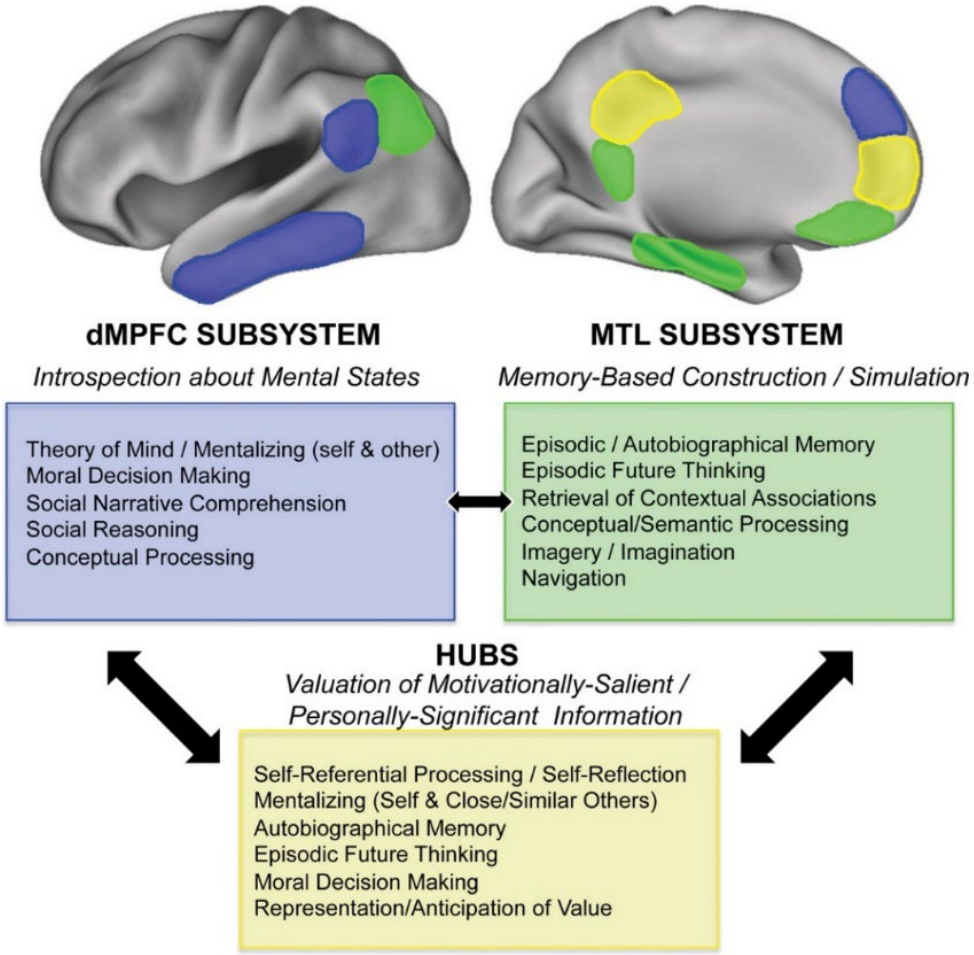

Figure 2.2: Default mode network; organisation of subsystems and hubs

Note: Two subsystems are dMPFC = dorsal Medial Prefrontal Cortex; MTL = medial temporal lobe. Two main hubs are aMPFC = anterior medial prefrontal cortex; PCC = posterior cingulate cortex. From (Andrews-Hanna, 2012).

2.1.2 *The Amygdala and the Default Mode Network*

As outlined in Chapter One, the amygdala, at a subregional level, possesses functional connections to many different brain regions including regions of the DMN (Bzdok et al., 2013; Roy et al., 2009) and its dysfunction leads to disordered emotion processing in MDD (Bakoyiannis, 2023; Ferri et al., 2017). Studies have demonstrated DMN involvement in discrete emotions such as fear, disgust and anger (Saarimäki et al., 2022; Satpute & Lindquist, 2019) and extremely negative self-referential focusing related to DMN dysfunction (Sambataro et al., 2014; Sheline et al., 2009; Whitfield-Gabrieli & Ford, 2012). In light of evidence of cognitive processes being influenced by emotional input (Sambuco et al., 2022; Stoliker et al.,

2024), these findings are supportive of a modulatory role for the amygdala in relation to the DMN (Azarias et al., 2025).

Although the DMN is not the focus of this thesis, reports of aberrant function of both the DMN and amygdala in MDD indicate that a more comprehensive understanding of the functional connections between the amygdala and DMN may shed more light on interactions between emotion processing and self-referential negative internalisation of thought processes. However, as acknowledged by Yeo and colleagues in their work identifying the seven resting-state networks, spatial resolution of current fMRI data is a recognised study limitation (Yeo et al., 2011). There is clearly a need for improved imaging data quality to progress the field of MDD research, particularly in relation to spatial resolution of small structures such as the amygdala and its subregions.

2.2 How is Functional Magnetic Resonance Imaging (fMRI) performed?

Whereas MRI is widely used clinically to investigate all parts of the body, fMRI is typically used to investigate brain function. Most clinical MRI systems can acquire fMRI data, as the sequences used for research are adaptations of clinical versions. In the MRI systems discussed in this work, the direction of the main magnetic field B_0 is horizontal, although vertical field systems are also available (Kazemivalipour et al., 2021). Whilst a comprehensive coverage of the physics of MRI is outside the scope of this thesis, a brief review is pertinent in relation to radiofrequency (RF) coil choice for fMRI as the type of coil employed significantly impacts SNR levels and consequently, achievable spatial resolution of the acquired images (Gruber et al., 2018). In most MRI examinations, the body coil intrinsic to the MRI system performs the role of RF transmitter. A time-varying RF field, B_1, is generated perpendicular to B_0, exciting protons in the field of view (FOV) to precess at the Larmor frequency, which allows an efficient energy transfer between the $B1$ field and precessing protons. The B_1 field is turned on and off at very short intervals, typically milliseconds, generating pulses that 'flip' the protons through a pre-specified number of degrees; hence the term flip angle (Gruber et al., 2018). In moving away from the longitudinal plane, protons acquire transverse magnetisation which then begins to decay after the B_1 field is switched off (Kwok, 2022). This process is shown schematically in Figure 2.3. Through the process of electromagnetic induction, an electrical current is induced and subsequently detected by the RF receive coil as the MR signal. Traditionally, fMRI data are acquired in 2D slices which are defined via the imposition of a slice-select gradient

perpendicular to the selected image plane in combination with a frequency-specific RF pulse that excites the tissue in the desired plane and location (McRobbie et al., 2017).

***Technical note**:* The MRI system used in this thesis work is a 3T Prisma system with VE 11C software (Siemens Healthineers, Erlangen, Germany).

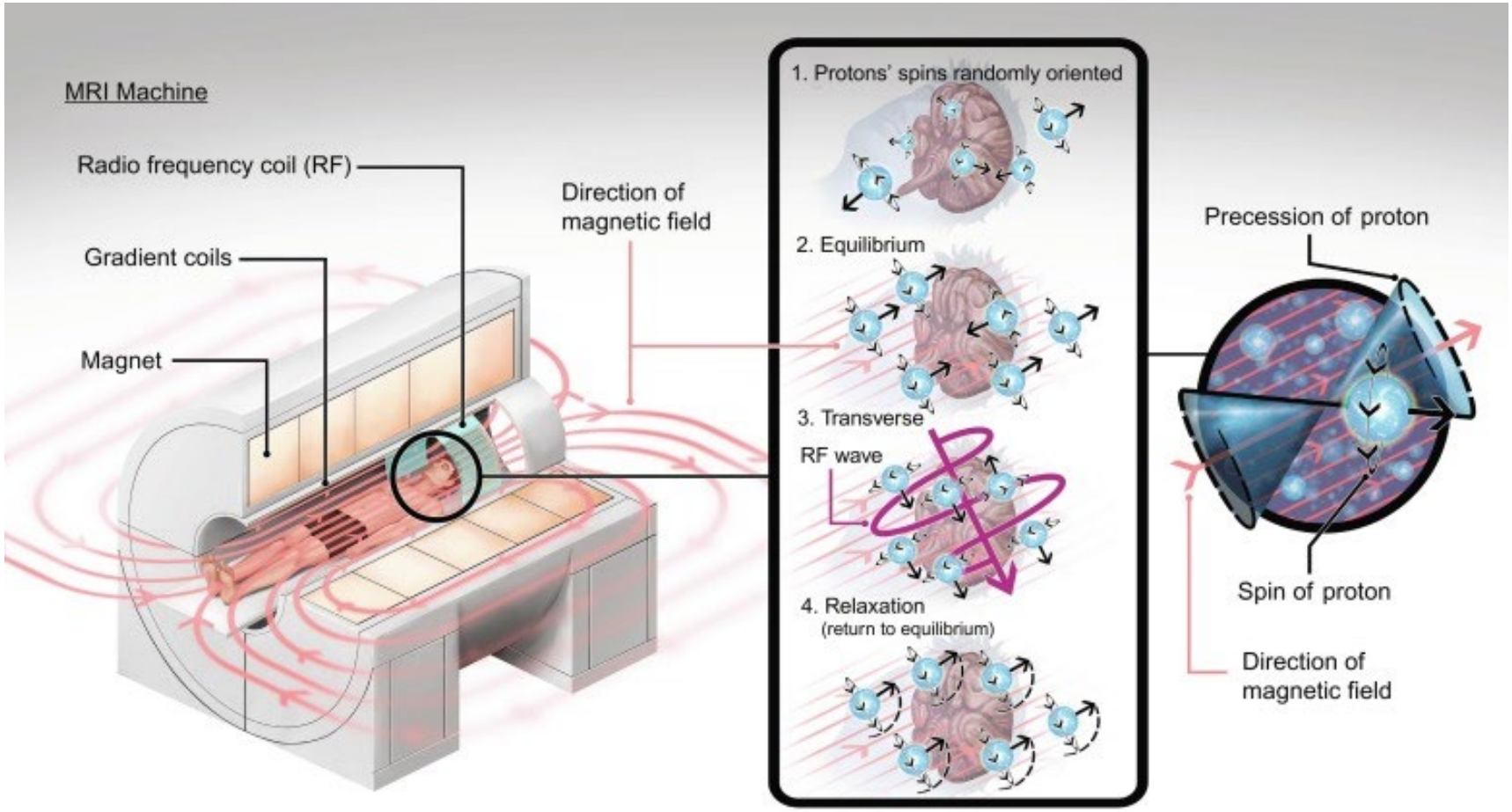

Figure 2.3: Proton precession in an applied magnetic field

Note: Left - Schematic of participant in MRI system. Body radiofrequency transmitter (RF) coil represented in green. Head receiver RF coil used in fMRI not shown. Middle panel - proton orientation at different phases of image acquisition. 1) Random orientation of proton outside of magnetic field. 2) Protons align longitudinally with magnetic field inside scanner, precessing at Larmor frequency. 3) Time-varying RF field generated by RF pulse at Larmor frequency flips protons into transverse plane. 4) Protons relax back to longitudinal plane (equilibrium) when RF pulse switched off. Right – Schematic of proton precessing around direction of magnetic field. Adapted from (Kodaverdian, 2019).

2.2.1 Contribution of Radiofrequency (RF) Receive Coils

Whilst the principal function of the body coil is RF transmission, it can also act as a receiver; however, there are few circumstances in which this approach is employed due to inefficiencies related to RF coil loading that result in poor SNR levels. In order to reduce noise levels, thereby maximising SNR levels, the RF receive coil needs to be closely coupled in size to the body part under examination (Redpath, 2014). The receive coil is tuned to the resonant or Larmor frequency of proton precession for a specific magnetic field strength, for example, around 128 MHz at 3T. Other than the intrinsic body coil, there is a subset of receive coils available that can also be used as transmitters (known as transmit/receive or T/R coils), and these are typically used when imaging at field strengths of 7T and above where issues stemming from field inhomogeneity and tissue heating are more pronounced (Gruber et al., 2018). At clinical field strengths of 1.5T and 3T, transmit/receive knee coils are widely used in musculoskeletal examinations to alleviate aliasing issues related to mismapping of tissues outside the FOV from the opposite limb that occur when the sampling rate is inadequate (McRobbie et al., 2017). Transmit/receive head coils are typically employed in the setting of a requirement for compliance with MR-conditional scanning of implants and devices where MR safety is not assured when transmitting over a larger field with the body coil (Ferreira et al., 2014). The added complexity of transmit/receive coil design together with technical issues around potential RF coupling mean that receive-only coils are predominantly used for clinical and research imaging (Gruber et al., 2018).

2.2.2 Head phased array receive-only coils

The RF coil design of choice for fMRI is the receive-only phased-array head coil composed of multiple groups of small surface coils with independent receive-channels formed into a close-fitting helmet-shape, the primary benefit of which is higher SNR due to lower local noise contributions (Gruber et al., 2018). However, a second major advantage of this technology is the innovative design which supported the introduction of firstly, parallel imaging and later, simultaneous multislice techniques which have been key to the evolution of fMRI. These techniques allow faster imaging, that is, higher temporal resolution, an important consideration in fMRI. Parallel imaging, effectively a k-space undersampling technique, is predicated on the variation in spatial sensitivities of individual arrays that make up the whole coil; signals can be spatially localised and encoded during signal reception, allowing for the acquisition of fewer phase-encoding steps for image reconstruction but with a concomitant SNR reduction which is

offset by the phased-array design (Kwok, 2022). Other advantages of parallel imaging include susceptibility-related distortion artifact reduction in echo planar imaging (EPI) sequences and reduction in Specific Absorption Rate (SAR) due to lower RF power deposition. Currently available phased array head coils have the capacity to accelerate along all three axes; however, the preferred direction of acceleration for fMRI is typically the z-direction (superior to inferior) (Keil et al., 2013). In practice, head coils such as the 64-channel head and neck phased array coil are often designed with a greater number of coil elements along the z-axis which also facilitates the use of simultaneous multislice, a technique in which multiple slices in the acquisition plane are excited simultaneously and signals spatially assigned using variations in local array sensitivities in a similar way to parallel imaging (Barth et al., 2016).

Regarding coil design, it is interesting to note that although he individual surface arrays in a 64-channel coil design are smaller with presumably less sensitivity centrally in the image as calculated using the Bio-Savart law (Haase et al., 2000) the 64-channel design, similar to that used in this work, has been shown to outperform its 32-channel counterpart in terms of SNR centrally, particularly with higher levels of acceleration (Keil et al., 2013).

Technical note: The head coil used in this thesis work is a 64-channel head and neck phased array (Siemens Healthineers, Erlangen, Germany).

2.3 Blood Oxygen Level Dependent (BOLD) Contrast

Following Kwong and colleagues' discovery in 1992 that blood could be imaged as an endogenous contrast agent in fMRI using a gradient echo imaging technique (Kwong et al., 1992), it is now well established that fMRI can provide information about neuronal activity predicated on the mechanism of Blood Oxygen Level Dependent (BOLD) contrast. MRI BOLD signals are an indirect measure of neural activity reflected in changes in regional cerebral blood flow (Hillman, 2014; Soares et al., 2016). The BOLD image contrast generated using the gradient echo imaging technique is reliant on the decay of transverse magnetisation manifesting as field inhomogeneities resulting from localised changes in blood oxygen levels resulting from neuronal activity. This process, known as T2* relaxation or T2* decay, is responsible for the signal changes due to variations in blood flow, and it differs from T2 relaxation in that it occurs at a faster rate (Chavhan et al., 2009). The sensitivity of T2*-Weighted (T2*-W) GRE sequences to localised alterations in paramagnetic deoxyhaemoglobin in the blood are the basis of BOLD signal measurement and these sensitivity levels can be

altered by manipulation of parameters including Echo Time (TE), Repetition Time (TR) and flip angle that form the basis of the EPI pulse sequence, GRE-EPI, used in 3T fMRI (Chavhan et al., 2009; Hillman, 2014).

Since its inception, fMRI has primarily been used to probe motor, sensory and cognitive processes with various tasks or paradigms. In its simplest form, the initial method of choice was a basic block-design paradigm divided into multiple task and non-task periods that were effectively subtracted to reveal signal intensities or activation related to the task (Fox & Raichle, 2007). The fundamental concepts of BOLD contrast are best explained with this simple task design in mind. Transient neuronal activity such as task performance or visual stimuli provokes an increase in oxygen consumption resulting in an increase in local blood flow to the area of activation, a mechanism known as neurovascular coupling (Huneau et al., 2015). This response to the increased demand for oxygenated blood stimulated by neuronal activity is known as the haemodynamic response and it typically lags several seconds behind the increase in activity (Menon & Goodyear, 2001). When blood is fully oxygenated it has diamagnetic or non-magnetic properties, whilst in its fully deoxygenated state it has paramagnetic properties. As deoxygenated blood causes local dephasing of protons, its T2* value is shorter resulting in MR signal attenuation (Boxerman et al., 1995). Put simply, stimulus presentation provokes neuronal firing, following which the neurons require re-oxygenation, subsequently delivered by the blood which, in turn, results in increased signal as the blood becomes less paramagnetic (Figure 2.4). In fact, early adopters of the fMRI technique, initially expecting to see a decrease in signal resulting from an increase in deoxygenated blood, noted a paradoxical increase in MR signal during neuronal activity; however, it is now understood that the BOLD changes being imaged are actually downstream from the activation site where T2* is elevated due to the inflow of fully oxygenated blood (McRobbie et al., 2017).

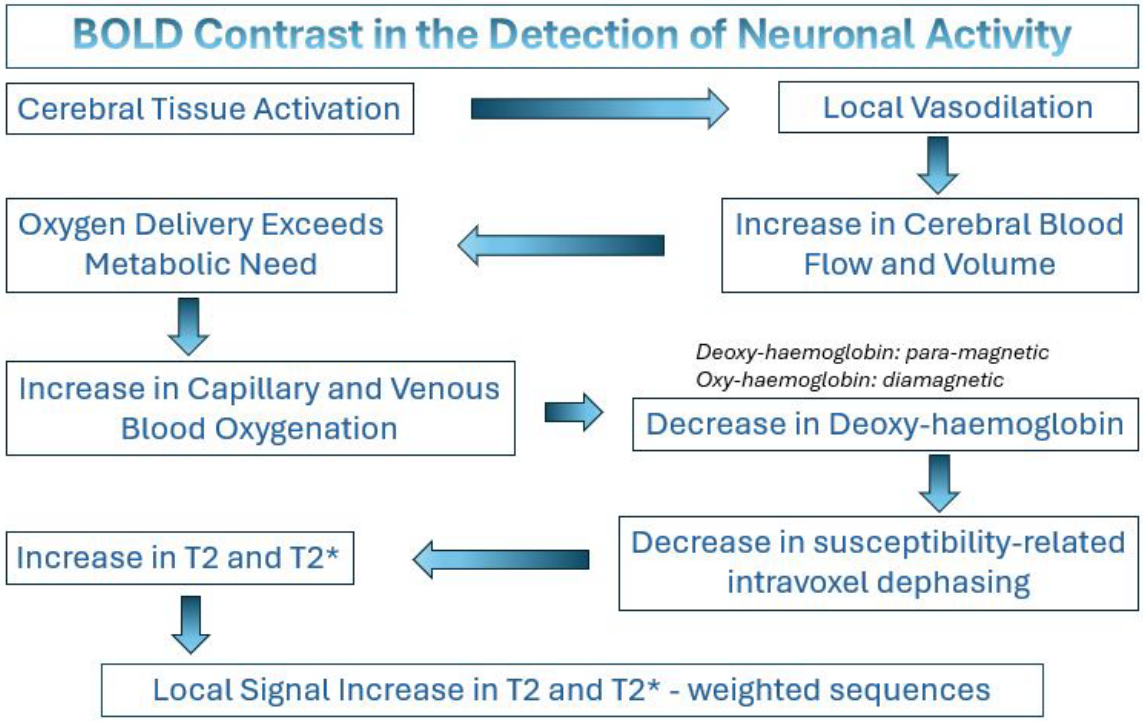

Figure 2.4: Sequence of events from neuronal activity to BOLD imaging with fMRI

Note: Image adapted from (Bandettini, 2002).

The BOLD signal, although only an indirect measure of neuronal activity, appears to have a consistent shape, peaking around five seconds after stimulus advent before undershooting and then subsequently recovering to the baseline after around 20 seconds. The so-called haemodynamic response function (HRF) is a mathematical modelling of the localised neurovascular coupling and the coincident BOLD signal (Hillman, 2014; Rangaprakash et al., 2021). There are several versions of HRF modelling available, the most common of which is known as canonical HRF (Darányi et al., 2021). Multiple brain volumes are acquired resulting in a time series as demonstrated in Figure 2.5 and, as the signal amplitudes of BOLD contrast are very small, estimated to be only 1-5% of baseline, subsequent statistical analysis is required for interpretation and creation of activation maps (McRobbie et al., 2017; Soares et al., 2016).

Task-based acquisitions also contain low frequency fluctuations when the brain is presumed to be 'at rest' during the course of the acquisition, that is, the two states, activation during a task and fluctuations during rest, do not exist in isolation. These spontaneous low frequency fluctuations were initially treated as noise contributions and subsequently minimised by averaging during task data analysis (Fox & Raichle, 2007). However, it is now well-recognised that this noise is, in part, attributable to the correlated resting state BOLD signal (Figure 2.5,

right), and resting state sequences are now typically acquired separately as a means of investigating other aspects of brain networks, often as an adjunct to task data (Lv et al., 2018). Notwithstanding, it has been shown that underlying low frequency BOLD signals can be distilled from task-based acquisitions, and that these fluctuations are commensurate with the signals from dedicated rs-fMRI data acquired in the same cohort and imaging session. This finding is important in the context of validating the use of previously acquired task-based data for retrospective FC interrogation (Korgaonkar et al., 2014). Interestingly, it has also been proposed that variations in correlations of spontaneous BOLD activity between task and rest states can be explained by layering or superimposition of the two activity states and that this is a potential explanation for inconsistencies across study results due to variability in human behaviour (Fox, Snyder, et al., 2006).

In summary, the acquisition of both task-related and resting state data to explore brain function is reliant on the mechanism of BOLD contrast; however, different methods are required for subsequent data analysis (Chang & Glover, 2009; Cole et al., 2010).

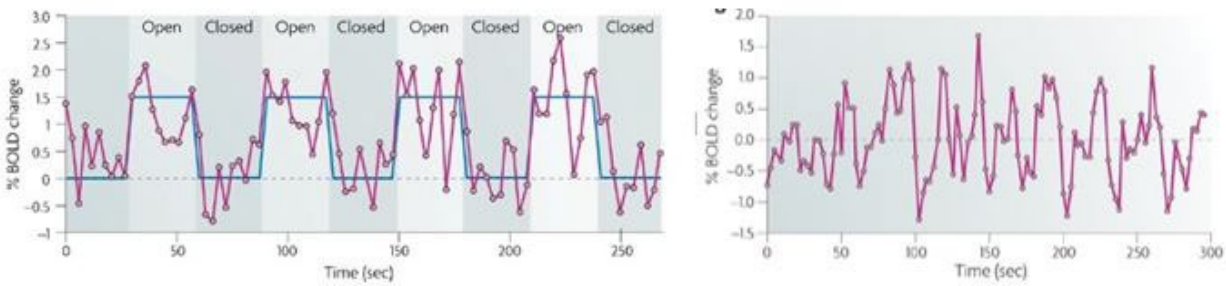

Figure 2.5: Representation of visual task-related BOLD time series with task overlaid in blue (left) and resting state BOLD time series (right)

Note: Different scales on y-axis in left and right figures. Adapted from (Fox & Raichle, 2007).

2.4 Recap of Task-Based and Resting State Methods for Investigating the Amygdala

There are two primary fMRI methods available to researchers for investigating brain function: task-based and resting-state. As noted in Chapter One, task-based studies involve recording the patient's response to the performance of a task or a type of stimulus during data acquisition in order to anatomically localise areas of 'activation' (Logothetis, 2008). These tasks, or paradigms, vary in terms of experimental design and are classified as block design, event-related or mixed block/event related. Block design is superior in identifying activation whilst

event-related tasks are more effective in distinguishing the time course of activations (Liu et al., 2001).

To examine and record amygdala activation for task-based studies, researchers have typically relied on eliciting emotional responses to different types of facial stimuli (for example, happy, sad. angry, neutral) (Varkevisser et al., 2024) and cognitive-based tasks such as working memory and attention (West et al., 2021). However, several inherently confounding issues have been noted in relation to amygdala activation results. Variations in neural responses have been revealed when comparing the nature of task instructions, that is, implicit versus explicit (Hariri et al., 2000). Additionally, flaws in reproducibility have been reported, notably the variability that may stem from the differential effects of habituation to the stimulus presentation over time (Hariri et al., 2000; Labuschagne et al., 2024). A meta-analysis of studies investigating the role of the amygdala in emotion processing reported that some studies were unable to distinguish temporal responses, suggesting that study design was the reason behind greater reporting of increased activation in the left amygdala (Sergerie et al., 2008). These findings support the model proposed by Gläscher and Adolphs in which inherent lateralised temporal differences are responsible for apparent left-sided increased activation; that is, the right amygdala response was of shorter duration in comparison to the left and thus not visible, potentially due to a more automatic emotional reaction, whilst the role of the left amygdala may be more discriminating in terms of extent of arousal (Gläscher & Adolphs, 2003; Plichta et al., 2014; Wright et al., 2001).

With advances in gradient and RF coil technology, researchers now have the capability to image at higher temporal rates (Yang & Lewis, 2021). Nevertheless, limitations on temporal resolution of data acquisition remain predicated by the timeline of the haemodynamic response function, which can be overcome to a degree by careful study design, for example, randomly varying the timing of stimulus presentation in event-related task design (Glover, 2011). Similarly, choice of HRF model and analysis method can also impact results (Darányi et al., 2021). However, a fundamental issue for task-based fMRI investigations is the inherent challenge in paradigm development and selection in attempting to answer a distinct research question (Hartling et al., 2021). As the specific functions and contributions of the three amygdala subregions within the emotional circuitry are still not well understood, the development of specific tasks to effectively interrogate each individual subregion task is problematic and, as a consequence, stimuli currently in use are of a more general nature rather

than being designed to elicit activation that can be definitively localised to specific subregions (Labuschagne et al., 2024).

Resting-state fMRI is an altogether different approach. Rather than demonstrating areas of localised brain activation as a response to a stimulus, the resting-state technique measures the synchronous low frequency fluctuations of the brain that occur spontaneously during a period of alert wakefulness, allowing identification of regions that are 'functionally connected' although they may be spatially remote and structurally discrete (Lv et al., 2018). Participants are typically instructed to keep their eyes open and think of nothing in particular, often focusing on a fixation cross during the acquisition, the result of which is the production of functional connectivity 'maps' that provide information reflective of spontaneous brain activity unprovoked by tasks or extrinsic stimuli (Roy et al., 2009; Soares et al., 2016). Simple and effective, the rs-fMRI technique requires no auxiliary equipment, meaning data acquisition across all age groups, imaging settings and most conditions is possible. rs-fMRI also provides an assessment of the whole brain, whereas task-based methods may focus on activity in selected areas based on task design (Canario et al., 2021). Interestingly, differing FC results between the states of 'eyes open' and 'eyes closed' has been reported; therefore, clear and consistent instructions to study participants is vital in experimental tasks (Patriat et al., 2013).

With growing awareness of the merits and advantages of the resting-state technique, interest has burgeoned, resulting in a six-fold increase in the number of publications from 817 in 2003 to 4985 in 2022 (Wei et al., 2024). It has been suggested that this trend may be due, in part, to the recognition that resting-state functional connectivity measures are superior as a differentiator of social cognition and neurocognition biotypes, both of which are key in depression (Viviano et al., 2018).

Technical note: The fMRI technique used in this thesis work is resting state.

2.5 Introduction to analysis methods

There are currently a number of resting state data analysis methods available to researchers, with two methods in common use due to their high levels of reproducibility (Snyder & Raichle, 2012). The first, known as Independent Component Analysis, is a data-driven multivariate statistical method that distinguishes between temporally or spatially independent resting state networks by separating out noise from low frequency network signals, and is often the method of choice for exploratory, hypothesis-free investigations (Canario et al., 2021). Independent

Component Analysis has successfully been used in investigating the DMN in MDD cohorts (Greicius et al., 2007; Guo et al., 2014; Kakeda et al., 2020; Li et al., 2013; Manoliu et al., 2014; Sexton et al., 2012; Veer et al., 2010; Verdijk et al., 2024; Zhu et al., 2012).

The second method is a hypothesis-driven method known as seed-based connectivity analysis which has been widely used since the inception of fMRI (Cole et al., 2010). Seed-based connectivity is based on a priori selection of discrete regions-of-interest (ROIs) or seeds. FC between brain regions is revealed by averaging the time-series across all voxels in the seed or ROI and generating correlation maps of each seed to every other voxel in the brain, effectively measuring temporal correlations (Canario et al., 2021). Because of the focus of this work on the amygdala, the latter method was used and the discrete seed ROIs selected were the amygdala subregions.

Whilst a comprehensive explanation of all analysis methods is outside the scope of this work, the reader is directed to Rajamanickam's concise overview of advantages and disadvantages of current fMRI analysis methods (Rajamanickam, 2020).

***Technical note**:* The analysis technique used in this thesis work is Seed Based Connectivity.

***2.5.1** Software and Regions of Interest (ROIs)*

Various software platforms are available to researchers for resting state functional connectivity data analysis. The list, by no means exhaustive, includes Statistical Parametric Mapping (SPM), Analysis of Functional NeuroImages (AFNI), REsting State fMRI data analysis Toolkit (REST), Data Processing Assistant for Resting-State fMRI (DPARSF), FMRIB Software Library (FSL), NeuroImaging PREProcessing toolS (NiPreps) and Connectivity Toolbox (CONN). In this thesis work CONN (http://www.nitrc.org/projects/conn/) was used in conjunction with MATLAB version R2022b (The MathWorks Inc. Natick, Massachusetts) and SPM12 (Wellcome Trust Centre for Neuroimaging, London, UK).

However, there is no established convention or standard in place across software platforms for defining ROI locations in resting state analyses (Poldrack, 2007; Sohn et al., 2015). Commonly used methods include basing ROI location on activations from previous work, prior knowledge of the relevant anatomy or employing standard brain atlases such as the Talairach and Tournoux atlas (Talairach & Tournoux, 1988), a pioneering reference widely used in the early days of fMRI. This stereotactic atlas provided a reference template for 'normalising' brain data into common space, including a coordinate system for reporting results, allowing comparison of

results between research groups (Chau & McIntosh, 2005) However, a principal disadvantage of 'Talairach labels' is that they were established from a single subject postmortem dissection and are based on macroanatomical landmarks such as sulci, leading to inaccuracies in regions where cortical microanatomy and function may vary across the wider population (Amunts et al., 1999). To address these limitations, the first iteration of the Montreal Neurological Institute (MNI) template (MNI-305), based on 3D brain MR images from 305 subjects, was released in 1995; however, it was superseded by MNI-152 in 2001, which was constructed using automated image registration and higher resolution whole brain coverage including the cerebellum. MNI-152 is now included in software platforms such as SPM and FSL and is widely used as the standard template knowns as MNI space (Mandal et al., 2012).

The development and integration of the SPM plugin known as the SPM (or Jülich-Brain) Anatomy toolbox by Eickhoff and colleagues into analysis software in 2005 enabled researchers to map functional cortical activations to standardised anatomical locations in MNI space through the use of three-dimensional probabilistic cytoarchitectonic maps (Eickhoff et al., 2005). Also in 2005, Amunts and colleagues introduced stereotactic probabilistic maps for the sub-cortical subregions of the hippocampus and amygdala (CM, LB and SF) as well as the entorhinal cortex, noting the need for detailed localisation of MRI data in neuropsychiatric disorders (Amunts et al., 2005). These subregional amygdala probabilistic maps are also compatible with, and are embedded in, the SPM Anatomy Toolbox.

In recognition of the heterogeneity of the amygdala subnuclei and, by extension, the subregions, together with the requirement for increased spatial specificity, further work has been undertaken to create an atlas for differentiation of nine amygdala subnuclei with increased spatial specificity for use at 7T (Saygin et al., 2017). Additionally, individualised functional parcellation methods of the amygdala subregions based on the Jülich atlas have also been developed, with reported benefits in functional homogeneity and overall accuracy at 7T (Zhang et al., 2018). However, although these methods may have the capability of providing more accurate localisation for individual subject ROIs by accounting for individual variability of regional borders, they contribute to differences in methodology in performing the individual subject parcellations (Levi et al., 2023), resulting in an additional source of variability and potentially confounding comparison of results across studies.

In consideration of the increasing focus on reproducibility in neuroimaging (Poldrack et al., 2017) the subregional amygdala ROIs available in the SPM Anatomy Toolbox were chosen to serve as the seed ROIs in this research work were imported into CONN for use during analysis.

***Technical note**:* CONN toolbox and SPM Anatomy Toolbox were used for data analysis in this thesis work.

2.6 The Requirement for Improved fMRI Data Quality

For as long as it has been appreciated as an invaluable tool in neuroimaging, the shortcomings of fMRI data quality have also been recognised. The contrast-to-noise ratio (CNR) as well as spatial and temporal resolution of fMRI studies acquired on the available 1.5T MR systems at the time of the technique's introduction in 1990 were quite low with voxel sizes in the tens of cubic mm (Menon and Goodyear, 2001). However, as the BOLD response is quite robust when the underlying neural activation is occurring on the same spatial scale, it was possible to adequately study hemispheric and gyral organisation at a functional level with this new technique (Menon and Goodyear, 2001).

However, it has since been recognised that higher spatial resolution acquisitions can improve the detection of discrete neural activity in several ways; smaller voxels not only lead to an increase in the level of BOLD contrast detected by reducing the effects of partial voluming, but susceptibility issues resulting in signal dropout and distortion are also reduced (Glover, 2011). Iranpour and colleagues demonstrated this concept at 3T by acquiring 2D GRE-EPI data using two different voxel volumes (VV), 3.4mm^3 and 27mm^3, concluding that the smaller voxel imaging sequence was more sensitive in detecting activations during their fMRI tasks than the larger, particularly in brain regions such as the amygdala where susceptibility artifacts generally compromise data quality (Iranpour et al., 2015). Two fMRI meta-analyses of task-related studies also noted these issues in relation to amygdala imaging as study limitations, noting that unilateral activations demonstrated in some lower resolution studies were found to be bilateral in higher-resolution data sets (Tang et al., 2012; van der Laan et al., 2011).

***2.6.1** Image Resolution - Spatial Versus Temporal*

Numerous parameter options can be manipulated to alter the contrast and appearance of images produced by an MRI system. With many parameters having co-dependent relationships (see Table S1 Appendix B for parameter trade-offs), their selection is predicated on the purpose of the specific acquisition sequence in question and compromises are widely acknowledged as

inevitable (McRobbie et al., 2017) In MRI, temporal resolution is a measure of how quickly data is acquired, and in fMRI, this is a crucial aspect of the imaging sequence. Spatial resolution is a measure of the number of pixels in an image, with more pixels providing higher resolution. Spatial resolution is referenced by voxel (volume pixel) size which is dependent on matrix size, slice thickness and field-of-view (FOV). It is limited by SNR, inferred by the inverse relationship between SNR and acquisition time which underpins the oppositional nature of spatial and temporal resolution (Glover, 2011; Loued-Khenissi et al., 2019). In structural MRI, high spatial resolution images with VV of less than $1mm^3$ can be achieved by employing longer acquisition times to improve SNR. However, this strategy has traditionally not been possible in fMRI due to the requirement for rapid scanning to acquire time series data (Glover, 2011). This temporal requirement has placed a ceiling on SNR resulting in spatial resolution in fMRI acquisitions in earlier studies commonly having VV of up to $64mm^3$ and, in some cases, $100mm^3$ in order to maintain satisfactory SNR levels and adequate temporal resolution to image the whole brain quickly (Menon & Goodyear, 2001; Soares et al., 2016). To contextualise these figures, data with VV of $20mm^3$ or less is considered high resolution (Olman & Yacoub, 2011).

Temporal resolution of fMRI acquisitions requires optimisation and is dependent on the TR of the imaging sequence which is typically constrained by the number of slices in the imaging volume as well as scanner performance (Bandettini, 2002). One TR period is commonly in the order of 1.5 to 3 seconds during which time all slices are imaged; this is repeated multiple times until sufficient volumes for the individual sequence have been acquired. Temporal resolution is also restricted by the relatively slow HRF which is a consideration in paradigm design in task-based studies. Stimuli spaced too closely may result in blurring of responses as a result of not allowing adequate time for the haemodynamic response to return to baseline (Loued-Khenissi et al., 2019). A TR of several seconds has also traditionally been prefaced on the requirement for T1 signal recovery between acquisitions to ensure adequate SNR (Bandettini, 2001).

With the advent of acceleration techniques, achievable temporal sampling rates have increased, leading more recent studies including the HCP (Van Essen et al., 2012) to report use of TR values of less than one second (Liao et al., 2013; Stirnberg et al., 2017; Yang & Lewis, 2021). As previously noted, the increase in array density in RF coil design has enabled this advancement in acquisition sequence design; in general, SNR levels, although reduced per

volume as a result of the selected TR being shorter than the T1 relaxation time of the tissue, have remained comparable when taking into account increased temporal sampling resulting in a greater number of volumes acquired in a similar time frame (Jahanian et al., 2019). There are two primary advantages of high temporal resolution; firstly, HRF characterisation is more accurate, leading to increased BOLD sensitivity in task-related studies, and secondly, higher sampling rates preclude the issue of cardiac and respiratory signal aliasing overlying BOLD resting state signals (Huotari et al., 2019; Yang & Lewis, 2021).

For most fMRI studies, acquisition protocols are optimised by finding a middle ground between spatial and temporal resolution requirements, that is, taking into account the research question, preferred analysis method and study cohort. For example, paediatric studies investigating network connectivity may be better served by focusing on temporal resolution, using shorter TRs and acquiring more volumes but in a relatively short overall scan time (Liao et al., 2013). However, small structures such as the amygdala require the opposite approach. Due to the diminutive size and location of the amygdala in the temporal lobe, image quality can suffer from susceptibility artifacts, distortion and partial volume effects, all of which can be mitigated by the use of higher spatial resolution protocols with smaller voxels (Bandettini, 2002; Jahanian et al., 2019; Olman et al., 2009). According to previous work, the optimum slice thickness to maximise SNR in fMRI investigations of the amygdala using 2D GRE-EPI at 3T is between 2mm to 2.5mm (Figure 2.6), beyond which SNR levels decrease with increasing voxel size due mainly to intravoxel dephasing (Robinson et al., 2004).

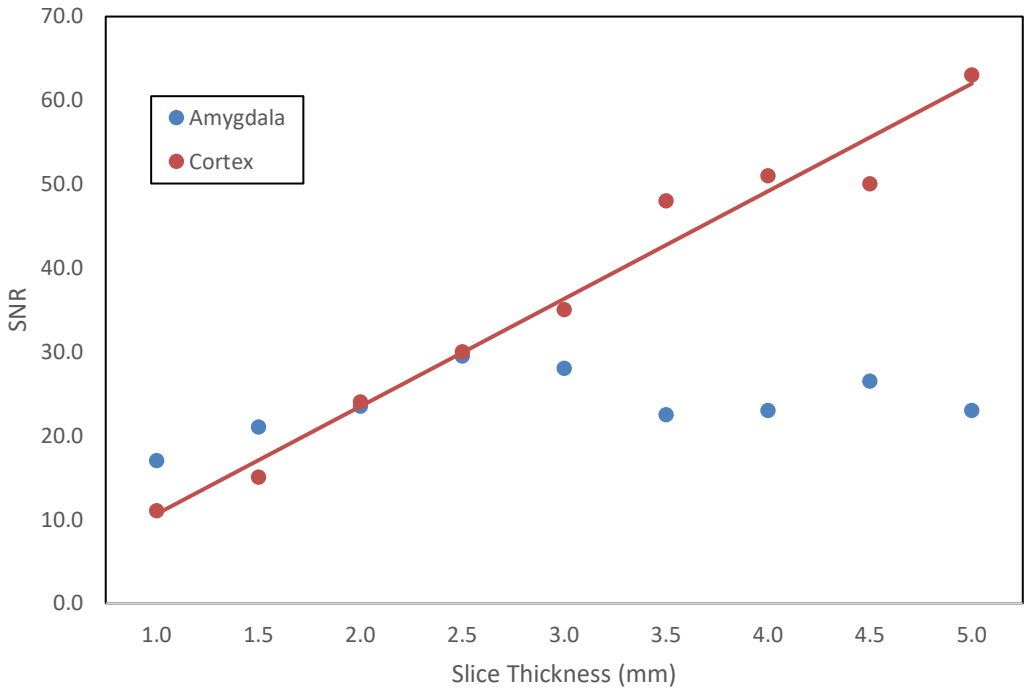

Figure 2.6: SNR variation with slice thickness in the amygdala and cortex

Note: Adapted from (Robinson et al., 2004)

In a comparison between their standard fMRI protocol with VV of 51.3mm^3 and an optimised high resolution acquisition with VV of 6.4mm^3, Robinson and colleagues demonstrated an increase of 60% in SNR in voxels in amygdala locations in the native high resolution optimised acquisition, despite the doubling of bandwidth which accounts for a SNR penalty of √2, although they resampling the data to standard voxel size during preprocessing (Robinson et al., 2004). To demonstrate the translational value of this finding, the time-series SNR maps were thresholded at a value of 50 and overlaid on T1-W axial images to show the comparative lack of SNR in the regions of the amygdala using the standard protocol with large voxels compared to the optimised high resolution protocol (Figure 2.7) (Robinson et al., 2004).

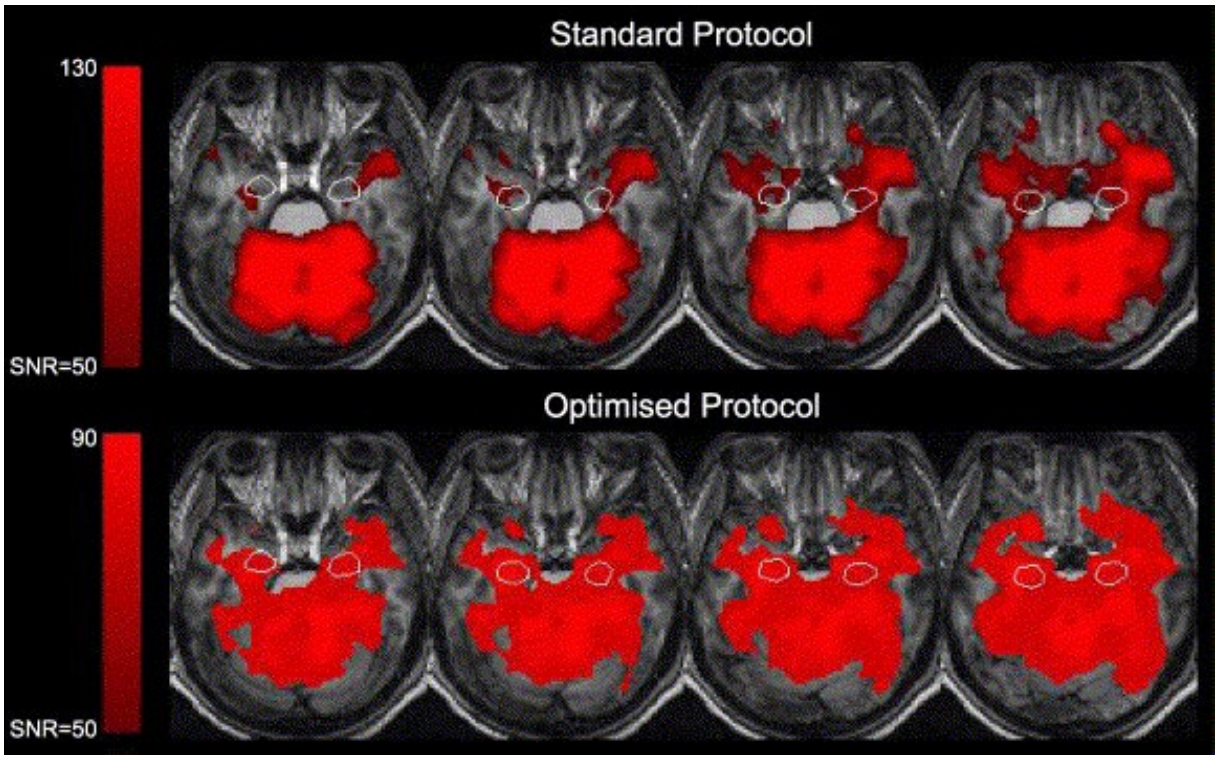

Figure 2.7: Time series SNR values thresholded at a value of 50 overlaid on axial T1-W slices in the approximate region of the amygdala (outlined)

Note: Top row: Standard protocol. Bottom row: Optimised protocol. Images from left to right represent inferior to superior slice locations (Robinson et al., 2004).

2.6.2 *Voxel Volume (VV) of Current Protocols*

At 7T, very small VV of between 1.1 mm^3 and 3.375mm^3 have been reported in use for fMRI due to the inherently higher SNR available (Geissberger et al., 2020; Murphy et al., 2020; Sladky et al., 2018; Zhang et al., 2018). At 3T, VV has been typically much larger (Foster et al., 2023). Empirically, the choice of VV was based on the requirement for adequate SNR, and at the time 3T technology arrived in the mid-2000s, coil technology was much less advanced, with lower density array head coils in widespread use (Kabasawa, 2022). Many studies reporting amygdala findings at 3T continued to utilize larger VV, for example, 27mm^3 (Baczkowski et al., 2017; Michely et al., 2020; Wackerhagen et al., 2020), 42mm^3 (Chumachenko et al., 2021; Deng et al., 2019; Reich et al., 2019), 64mm^3 (Delli Pizzi et al., 2017; Salzwedel et al., 2019; Shou et al., 2017) and up to 70mm^3 (Fan et al., 2020; Tong et al., 2019; Wang et al., 2021). Whilst these fMRI protocols resulted in high SNR levels, spatial

resolution was limited (Bandettini, 2002; Invernizzi et al., 2021), particularly in reference to Olman and Yacoub's definition (Olman & Yacoub, 2011).

To further capitalise on the advantages of 3T, more advanced higher density 32-channel arrays with higher SNR capabilities became available in the latter 2000s and early work highlighted their SNR and temporal resolution advantages (Wiggins et al., 2006). Interestingly, although the studies referenced above in relation to VV were published ten or more years after its introduction, only two noted the use of a 32-channel head coil, with others referencing use of 8-channel and 12-channel arrays or circularly polarised designs (used prior to array technology). In fact, completion of the scoping review forming Chapter Three revealed only two reports of use of the 64-channel array (Bonduelle et al., 2021; Sanz-Arigita et al., 2021) that became available for 3T systems around 2013 (Keil et al., 2013).

2.6.3 *VV in relation to the Amygdala*

As outlined in Chapter One, the amygdala is composed of nine individual heterogeneous subnuclei that form three subregions, the CM, LB and SF (Figure 2.8). The total volume of the amygdala is somewhere between 1000mm^3 and 2000mm^3 with values varying according to measurement technique; that is, ex-vivo volumes tend to be smaller at around 1240mm^3 (Saygin et al., 2017) compared with in-vivo volumes of around 1850mm^3 (Morey et al., 2020). For the purposes of the following explanation, we will consider the amygdala volume as an average of these two figures, at 1545mm^3.

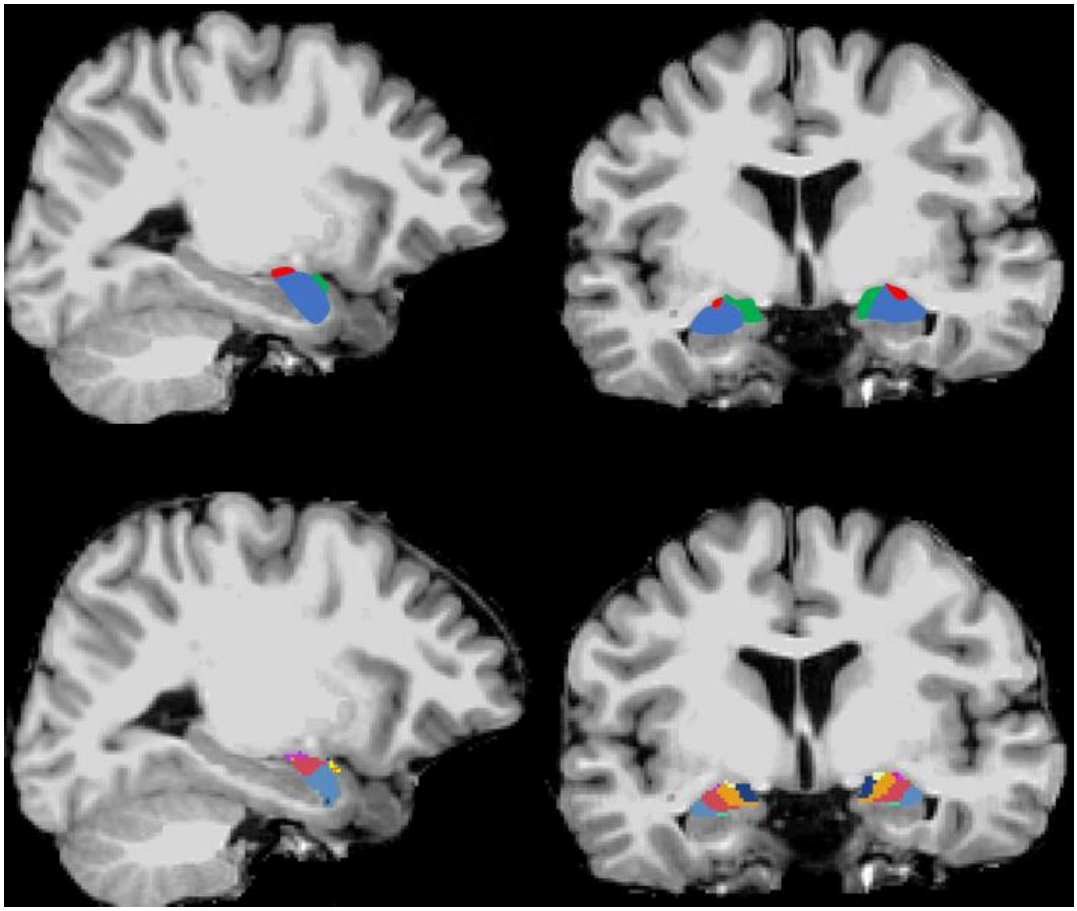

Figure 2.8: Sagittal (left) and coronal (right) T1-W images depicting the size and location of the amygdala subregions (top row) and amygdala subnuclei (bottom row)

Note: Subregion key: Centromedial = red, Laterobasal = blue, Superficial = red. Subnuclei key: Lateral = light blue, Basal = red, Accessory basal = orange, Paralaminar = aqua, Cortico-Amygdaloid transition = dark blue, Cortical = yellow, Central = purple (Medial subnucleus and Anterior Amygdaloid Area not shown).

To put the size of the amygdala as a single structure into perspective, it is helpful to consider the volume of the whole brain, which has been measured at around 1000cm^3 (1,000,000mm^3) (Cotter et al., 1999). If we consider imaging at very low resolution with VV of 1000mm^3, the whole brain will consist of approximately 1000 voxels, of which the amygdala would theoretically appear in one or two voxels. If VV is reduced to 4mm^3 the whole brain would consist of 15,625 voxels of which the amygdala would theoretically be composed of around 24 voxels. At VV of 2mm^3, the number of voxels comprising the amygdala is much higher at 193. Now to consider imaging the amygdala subregions individually; as an example, averaging of

the volume data reported by Saygin *et al* and Morey *et al* for the CM, the smallest of the three subregions, results in a volume of 68mm^3 (Morey et al., 2020; Saygin et al., 2017). Imaging with VV of 2mm^3 would result in around 8 voxels within the CM but this is reduced to only one voxel when imaging at VV of 4mm^3, a level at which it is unlikely that the heterogeneity of the structure can be resolved. The graphic representation in Figure 2.9 serves as a visual cue with respect to increasing VV and its impact on spatial resolution.

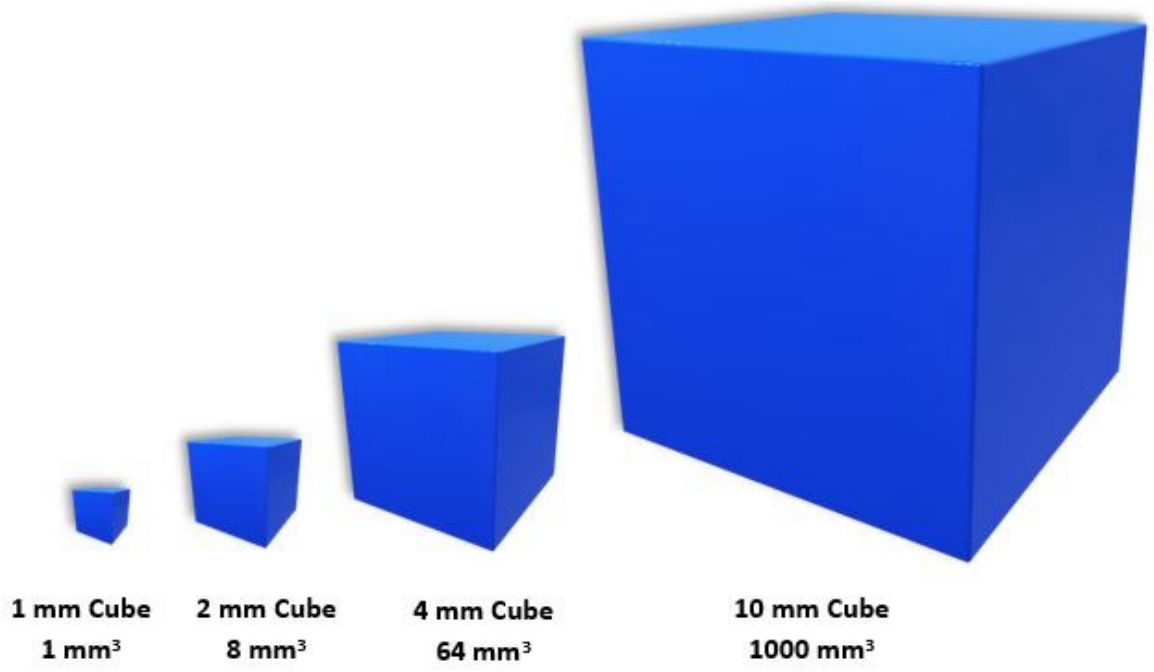

Figure 2.9: Diagrammatic representation of various voxel volumes for comparison

The results of a formal scoping review done in Chapter Three (Foster et al., 2023) support anecdotal evidence that VV used in the majority of 3T fMRI protocols to report both whole amygdala and subregional findings is well above 20mm^3, the lower limit of high resolution (Olman & Yacoub, 2011). In essence, current protocols are unlikely of sufficient spatial resolution to adequately resolve individual subregional activation and FC (Merboldt et al., 2001; Sladky et al., 2018).

Technical note: VVs of the sequences used in this thesis work were 2D GRE-EPI = 15.625mm^3 (2.5mm isotropic) and 3D GRE-EPI = 8mm^3 (2mm isotropic)

2.7 Where Are We Now With fMRI Protocols?

Different fMRI acquisition strategies are in use at different field strengths. At higher field strengths of 7T and beyond, the principal contrast mechanism is diffusion-weighted T2 relaxation, allowing the use of spin-echo (SE) sequences (Glover, 2011). Inherently high SNR allows very high spatial resolution imaging at 7T (Nasr et al., 2016; Pedersen et al., 2017; Sladky et al., 2018), but disadvantages include poorer static field homogeneity, greater RF power deposition, and increased susceptibility and B_1 inhomogeneity artifacts (Edelman, 2014; Glover, 2011; Ladd et al., 2018). For these technical reasons, combined with the lack of access to 7T, the majority of fMRI studies are performed at 3T where T2* contrast predominates over T2 contrast. Gradient refocused echo or gradient echo (GRE) T2*-W acquisition techniques are widely used to maximise CNR at this clinically available field strength (Bandettini, 2001). Elementary refinements to acquisition protocols through optimisation of spatial resolution have the potential for broad positive impact on data quality across institutions currently accessing 3T MRI systems for their neuroimaging research. The focus of this thesis is on GRE sequence use.

2.7.1 2D T2-Weighted Gradient-Echo-Echo Planar Imaging (T2*-W GRE-EPI) sequence*

In order to understand why the 2D T2*-W GRE-EPI sequence is the gold standard for fMRI at 3T, we will revisit the fundamentals. There are two pulse sequence families in MRI: spin echo (SE) and GRE. SE sequences employ a pair of RF pulses, firstly to flip and then refocus protons in the imaged slice. In their simplest form, SE sequences comprise a 90° pulse, then a 180° pulse following which the signal is sampled at the Echo Time (TE in ms). This process is then played out multiple times to form what is known as a pulse sequence, with the time between each 90° pulse known as the Repetition Time (TR in ms). GRE sequences, however, utilise a single RF pulse, following which the Free Induction Decay (FID) signal is manipulated via a dephasing and rephasing gradient reversal (Figure 2.10). Because of their inherent design, GRE sequences possess the critical advantage of speed over SE. As only one RF pulse is required, with a flip angle of much less than 90°, both the TR and TE values can effectively be reduced, resulting in a reduction in overall acquisition time (McRobbie et al., 2017).

In SE sequences, the 180° refocussing pulse effectively minimises effects of B_0 field inhomogeneities by rephasing the spins prior to signal sampling, thus producing images with predominantly T2 contrast. However, GRE sequences are far more susceptible to magnetic

field inhomogeneities, the susceptibility effects of which are not refocused by the gradient reversal process, resulting in T2* contrast (Jackson et al., 2005). Although this outcome is not desirable for all imaging purposes, it is this phenomenon of T2* contrast that forms the basis of BOLD imaging, as noted in Section 2.3.

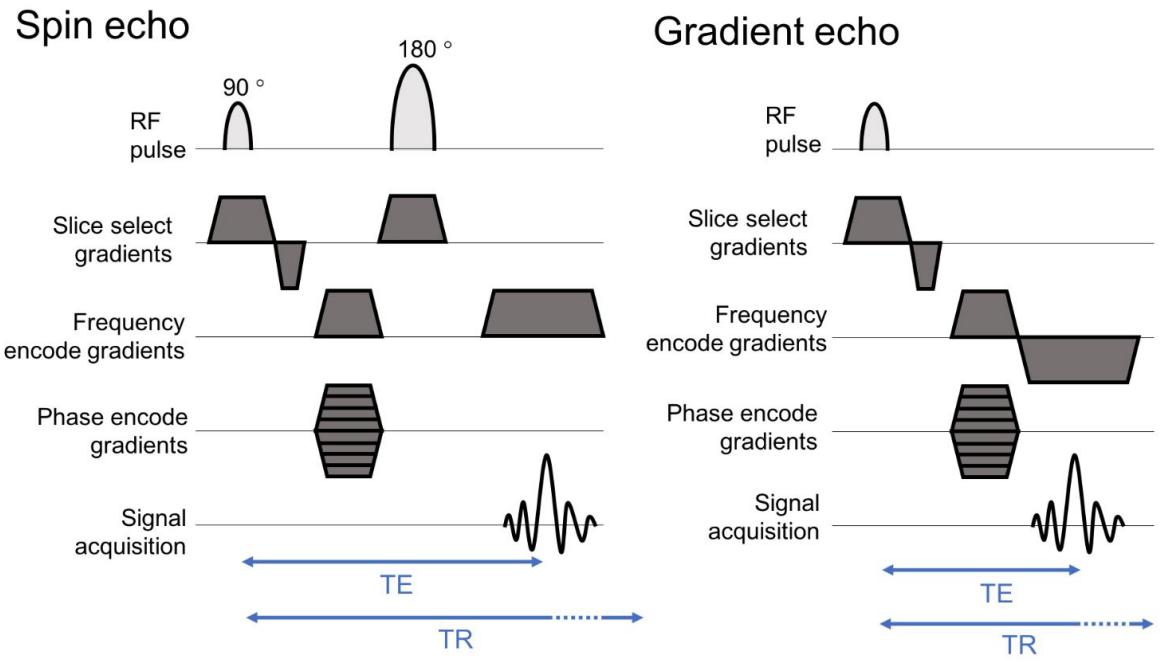

Figure 2.10: Differences between Repetition Time (TR) and Echo Time (TE) values resulting from pulse sequence design.

Note: Spin echo technique (left) requires two RF pulses whereas gradient echo technique (right) requires only a single pulse with a flip angle of less than 90°, resulting in shorter allowable TR and TE values (Campbell-Washburn, 2018).

2.7.2 *Echo Planar Imaging (EPI)*

Although the technique known as EPI was first described by Mansfield in 1977, the advanced gradient technology required to implement it for imaging on clinical whole body MRI systems did not become available until the 1990s (Huettel et al., 2004; Mansfield, 1977). Fundamentally, EPI sequences allow acquisition of a full set of k-space data following a single RF excitation pulse, that is, in one TR period. Speed is of the essence, as this must occur prior to significant T2* signal decay. When first introduced, the EPI technique effectively facilitated the acquisition of a full complement of slices covering the whole brain volume in a single TR,

or single ‘shot’, of several seconds duration and its implementation was critical to the development of fMRI (Bandettini, 2001; McRobbie et al., 2017). The significant increase in temporal resolution afforded by EPI was the foundation for fast imaging of brain activity associated with brain function and, although EPI is implementable in both SE and GRE pulse sequences, this discussion focuses on the GRE implementation used for fMRI.

The method of k-space filling is the differentiating factor responsible for speed in EPI acquisitions. EPI requires an unconventional Cartesian method whereby alternate lines are filled in opposing directions, requiring a 90° turn at the end of each completed line (Figure 2.11). This process requires the generation of a train of gradient echoes following each RF excitation pulse, typically produced by means of a bipolar oscillating readout gradient. Each echo in the echo train is differentially phase-encoded such that multiple lines of k-space are generated after a single RF pulse, each with a slightly different T2* weighting. In a single shot EPI sequence, the number of lines is dictated by the number of echoes in the train, known as the echo train length, and a wide receiver bandwidth is employed to minimise acquisition time for each echo (Bernstein et al., 2004; Huettel et al., 2004; McRobbie et al., 2017).

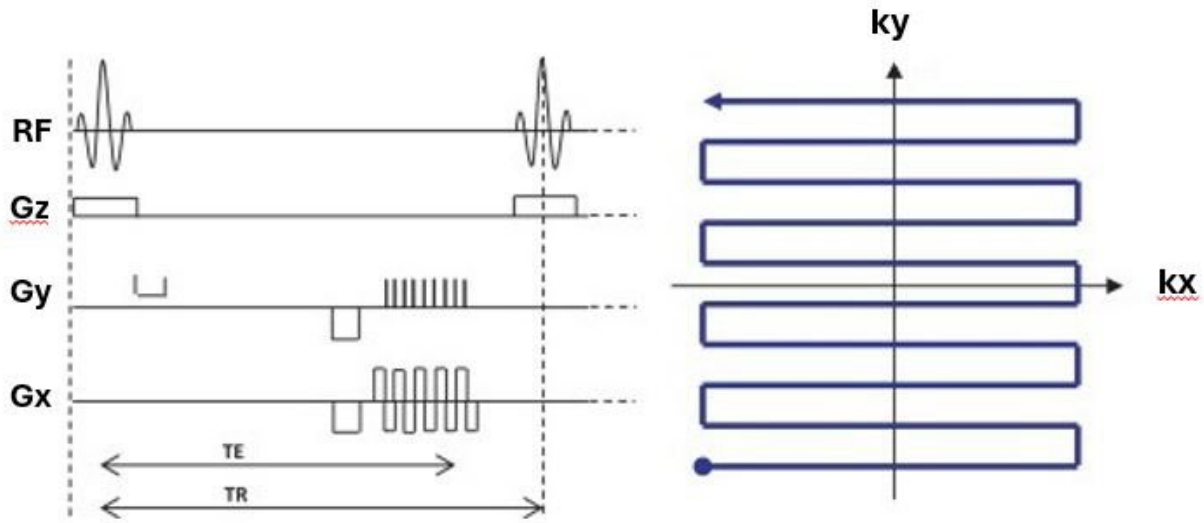

Figure 2.11: Diagrammatic representation of a single shot GRE-EPI pulse sequence (left) and corresponding Cartesian k-space trajectory (right).

Note: Figure adapted from (Kazan & Weiskopf, 2017).

The novel k-space trajectory places significant demands on the gradient and reconstruction systems; both to enable the multiple changes in direction at the end of each k-space line and in accommodating the opposing acquisition direction of adjacent lines during reconstruction. Additionally, very strong readout gradients are required to facilitate wide receiver bandwidth imaging (Bernstein et al., 2004). As a result, image quality can be impacted, particularly due to artifacts such as Nyquist ghosting resulting from phase errors which appear in the phase encoding direction as ghost images shifted by half the field-of-view (McRobbie et al., 2017). Similarly, magnetic field inhomogeneity and susceptibility-related signal losses due to off-resonance effects can result in image distortion, which can be mitigated with the use of parallel imaging (Bernstein et al., 2004; Weiskopf et al., 2006). More recently, technological imaging acceleration advancements such as simultaneous multi-slice and parallel imaging techniques (see Section 2.2.2) that can be used in conjuction with EPI have led to even higher achievable temporal resolution and a reduction in image artifacts (Bollmann & Barth, 2021).

Technical note: The 2D sequence used in this thesis work (previously optimised and currently implemented onsite) is T2*-W GRE-EPI.

2.8 Towards Improving fMRI Data Acquisition Strategies

Although T2*-W GRE-EPI sequences are the sequence of choice at 3T, providing optimal BOLD contrast sensitivity and the required speed for fMRI data collection, there is broad consensus that the technique suffers from artifacts that are detrimental to data quality, in particular, susceptibility issues resulting in signal loss close to air/tissue interfaces (Glover, 2011; Soares et al., 2016). This is a particularly salient consideration in studies focusing on the amygdala, given its location in relation to the skull base (Merboldt et al., 2001). Researchers have proposed various alterations and modifications to acquisition techniques to counter these susceptibility issues, mainly involving more efficient alternatives to the rectangular Cartesian k-space trajectory used in GRE-EPI (McRobbie et al., 2017).

2.8.1 *Spiral k-space Trajectories*

A new method of alleviating signal dropout in the parietal and orbitofrontal brain regions caused by uneven dephasing at air-tissue boundaries at 3T was proposed by Glover and Law. Utilising two versions of this sequence with ‘spiral-in’ and ‘spiral-in/out’ k-space trajectories, they acquired images with VV of 70mm^3, reporting overall increases in SNR and BOLD contrast and preservation of signal in those areas traditionally compromised by dephasing and

signal loss in conventional EPI sequences (Glover & Law, 2001). Qin and colleagues, also using a version of the sequence described by Glover and Law (Glover & Law, 2001), investigated amygdala subregional structure and FC using rs-fMRI data with VV of 39mm^3 acquired at 3T. They reported superior SNR and decreased susceptibility artifact in the temporal lobes compared with the conventional EPI k-space acquisition strategy (Qin et al., 2014).

Following the apparent success of the spiral-in/out approach, Jung and colleagues utilised a multi-shot interleaved variation of the technique to investigate its performance in acquiring high-resolution fMRI data at 3T, reporting VV as low as 2mm^3 and 3.4mm^3 for visual and memory tasks respectively. However, they noted trade-offs between spatial resolution, image artifacts and image blurring which required further work (Jung et al., 2013). Further disadvantages included very long reconstruction times and inability to utilise partial-Fourier and rectangular FOV techniques to decrease scan times due to the non-uniform k-space data sampling pattern. Additionally, although EPI can display geometric distortion and ghosting issues, spiral imaging suffers from twisting and intensity distortions caused by gradient deviations and attempts at improving reconstructed images introduced new artifacts (Block & Frahm, 2005). In summary, issues exacerbated by sensitivity to gradient imperfections and non-uniformity of the B_0 field, as well as the heavy demands placed on system reconstruction have combined to rule out routine use of spiral sequences for fMRI (Bollmann & Barth, 2021; Kasper et al., 2020).

2.8.2 *3D T2*-W GRE-EPI*

The quest for a technique capable of providing both increased temporal and spatial resolution imaging has led to the development of several 3D acquisition strategies, one of which is a version of the 2D sequence previously described. Rather than selectively exciting slices within the imaging volume, the 3D GRE-EPI technique involves exciting the entire imaging volume and employing a second phase encoding direction in which parallel imaging can also be enabled (Poser et al., 2010; van der Zwaag et al., 2012). This strategy provides a number of key advantages. Firstly, SNR (calculated by $\sqrt{N_{slices}}$) is substantially increased, predicated on the whole volume excitation effectively contributing an increased number of data points to the subsequent 3D Fourier reconstruction, meaning higher spatial resolution imaging, that is, significantly smaller VV, is achievable. Secondly, the k-space acquisition strategy allows undersampling in two planes, affording substantial increases in achievable temporal resolution

(Poser et al., 2010). Compared to the 2D approach, significant reductions in RF power deposition are also achieved with the use of lower flip angles together with the 3D undersampling strategy which precludes the need for the simultaneous multi-slice technique (Bollmann & Barth, 2021; Le Ster et al., 2019; Poser et al., 2010). In essence, the 3D version has the potential to surpass the performance of an optimised 2D sequence in regions of high susceptibility such as the amygdala.

Technical note: The 3D sequence used in this thesis work is a T2*-W 3D GRE-EPI Works-in-Progress sequence kindly provided by Siemens Healthineers, Erlangen, Germany.

2.8.3 Other Data Quality Considerations

As we have seen, the amygdala is a challenging region for fMRI data acquisition. It is very small, it is in an area prone to susceptibility-related signal loss, and it is composed of three heterogenous subregions with multiple connections to other brain regions. A fuller discussion of technical issues requiring consideration in building a protocol for fMRI studies of the amygdala, together with protocol recommendations, is located in the Discussion section of Chapter Three.

2.9 Summary

Despite the focus on mental health research over the last several decades since the introduction of fMRI as an investigative tool, the fundamental neural mechanisms of depression remain poorly understood. Broad cohort heterogeneity, current methods of diagnosis based on symptom presentation, as well as data acquisition technique and paradigm-related variations are all acknowledged contributors to the modest rate of progress. Increased precision in both patient and therapy evaluations based on differential brain FC has been heralded as a way to move the field closer to the holy grail of biomarker identification (Grogans et al., 2022; Tura & Goya-Maldonado, 2023). The imaging work of Klein-Flugge and colleagues has demonstrated the benefits to neuropsychiatric clinicians of considering the amygdala not as a single structure, but on an individual subnuclei level by identifying FC alterations to accurately predict mental health dimensions such as life satisfaction, anger and sleep (Klein-Flügge et al., 2022). Volz and colleagues have noted the benefits of resolving issues of data quality by protocol optimisation at the data acquisition phase rather than through post-processing methods (Volz et al., 2019) whilst a recent discussion of the challenges around the utility of amygdala

fMRI and inconsistency of study findings noted the importance of optimising scanning protocols in fMRI data acquisition of the amygdala (Varkevisser et al., 2024).

The overarching aim of this thesis work is to further our understanding of the amygdala subregions and their functional connections in depression using high resolution fMRI. There is clearly a need for improved data quality to accurately identify those functional connections, which can conceivably lead to a better appreciation of the implications of aberrant connectivity. This chapter has focused on the methods available to interrogate the amygdala, justifying the selection of acquisition sequences, spatial resolution values, RF receiver coil, data analysis software and post-processing tools that are utilised for the studies reported in Chapters Four and Five. Chapter Four focuses on comparing Treatment-Resistant (TSD) and Treatment Sensitive (TSD) cohorts with healthy individuals using an optimised version of the conventional 2D version of the T2*-W GRE-EPI sequence, whilst Chapters Five and Six compare the capabilities of the 2D sequence and a novel 3D sequence in healthy individuals in two different scenarios, connectivity to resting state networks and connectivity to subcortical brain regions. Resting-state data is acquired on a 3T Prisma MRI system in conjunction with a 64-channel head and neck RF coil. Data are post-processed and analysed in CONN toolbox using subregional amygdala ROIs from the JuBrain (SPM) Anatomy Toolbox and Seed Based Connectivity measures are used for comparisons.

Acknowledgements

Thank you to Simon Pullman and Elizabeth Haris for assistance with figure and table creation.

2.10 References

Alderman, B. L., Olson, R. L., Bates, M. E., Selby, E. A., Buckman, J. F., Brush, C. J., Panza, E. A., Kranzler, A., Eddie, D., & Shors, T. J. (2015). Rumination in major depressive disorder is associated with impaired neural activation during conflict monitoring. *Front Hum Neurosci*, *9*, 269. https://doi.org/10.3389/fnhum.2015.00269

Amunts, K., Kedo, O., Kindler, M., Pieperhoff, P., Mohlberg, H., Shah, N. J., Habel, U., Schneider, F., & Zilles, K. (2005). Cytoarchitectonic mapping of the human amygdala, hippocampal region and entorhinal cortex: intersubject variability and probability maps. *Anatomy and Embryology*, *210*(5), 343-352. https://doi.org/10.1007/s00429-005-0025-5

Amunts, K., Schleicher, A., Bürgel, U., Mohlberg, H., Uylings, H. B., & Zilles, K. (1999). Broca's region revisited: cytoarchitecture and intersubject variability. *J Comp Neurol*, *412*(2), 319-341. https://doi.org/10.1002/(sici)1096-9861(19990920)412:2<319::aid-cne10>3.0.co;2-7

Andrews-Hanna, J. R. (2012). The Brain's Default Network and Its Adaptive Role in Internal Mentation. *The Neuroscientist*, *18*(3), 251-270. https://doi.org/10.1177/1073858411403316

Andrews-Hanna, J. R., Reidler, J. S., Sepulcre, J., Poulin, R., & Buckner, R. L. (2010). Functional-anatomic fractionation of the brain's default network. *Neuron*, *65*(4), 550-562. https://doi.org/10.1016/j.neuron.2010.02.005

Azarias, F. R., Almeida, G. H. D. R., de Melo, L. F., Rici, R. E. G., & Maria, D. A. (2025). The Journey of the Default Mode Network: Development, Function, and Impact on Mental Health. *Biology*, *14*(4), 395. https://www.mdpi.com/2079-7737/14/4/395

Baczkowski, B. M., van Zutphen, L., Siep, N., Jacob, G. A., Domes, G., Maier, S., Sprenger, A., Senft, A., Willenborg, B., & Tüscher, O. (2017). Deficient amygdala–prefrontal intrinsic connectivity after effortful emotion regulation in borderline personality disorder. *European Archives of Psychiatry and Clinical Neuroscience*, *267*(6), 551-565.

Bakoyiannis, I. (2023). Amygdala's role in treatment-resistant depression. *Nature Mental Health*, *1*(5), 300-300. https://doi.org/10.1038/s44220-023-00069-1

Bandettini, P. A. (2001). Selection of the optimal pulse sequence for functional MRI. In P. Jezzard, P. M. Matthews, & S. M. Smith (Eds.), *Functional Magnetic Resonance Imaging: An Introduction to Methods* (pp. 123–145). Oxford University Press. https://doi.org/10.1093/acprof:oso/9780192630711.003.0006

Bandettini, P. A. (2002). The spatial, temporal and interpretive limits of functional MRI In K. L. Davis, D. Charney, J. T. Coyle, & C. B. Nemeroff (Eds.), *Neuropsychopharmacology: The Fifth Generation of Progress : An Official*

Publication of the American College of Neuropsychopharmacology (pp. 343-356). Lippincott Williams & Wilkins.

Barth, M., Breuer, F., Koopmans, P. J., Norris, D. G., & Poser, B. A. (2016). Simultaneous multislice (SMS) imaging techniques. *Magn Reson Med*, *75*(1), 63-81. https://doi.org/10.1002/mrm.25897

Basser, P. J., Mattiello, J., & LeBihan, D. (1994). MR diffusion tensor spectroscopy and imaging. *Biophysical journal*, *66*(1), 259-267. https://doi.org/10.1016/S0006-3495(94)80775-1

Bernstein, M. A., King, K. F., & Zhou, X. J. (2004). Chapter 16 – Echo Train Pulse Sequences. In M. A. Bernstein, K. F. King, & X. J. Zhou (Eds.), *Handbook of MRI Pulse Sequences* (pp. 702-801). Academic Press. https://doi.org/https://doi.org/10.1016/B978-012092861-3/50023-6

Biswal, B., Yetkin, F. Z., Haughton, V. M., & Hyde, J. S. (1995). Functional connectivity in the motor cortex of resting human brain using echo-planar MRI. *Magn Reson Med*, *34*(4), 537-541. https://doi.org/10.1002/mrm.1910340409

Biswal, B. B. (2012). Resting state fMRI: A personal history. *Neuroimage*, *62*(2), 938-944. https://doi.org/10.1016/j.neuroimage.2012.01.090

Block, K. T., & Frahm, J. (2005). Spiral imaging: A critical appraisal. *Journal of Magnetic Resonance Imaging*, *21*(6), 657-668. https://doi.org/10.1002/jmri.20320

Bollmann, S., & Barth, M. (2021). New acquisition techniques and their prospects for the achievable resolution of fMRI. *Prog Neurobiol*, *207*, 101936. https://doi.org/10.1016/j.pneurobio.2020.101936

Bonduelle, S. L. B., Chen, Q., Wu, G.-R., Braet, C., De Raedt, R., & Baeken, C. (2021). Exposure to criticism modulates left but not right amygdala functional connectivity in healthy adolescents: Individual influences of perceived and self-criticism. *Front Psychiatry*, *12*.

Boxerman, J. L., Bandettini, P. A., Kwong, K. K., Baker, J. R., Davis, T. L., Rosen, B. R., & Weisskoff, R. M. (1995). The intravascular contribution to fmri signal change: monte carlo modeling and diffusion-weighted studies in vivo. *Magnetic Resonance in Medicine*, *34*(1), 4-10. https://doi.org/10.1002/mrm.1910340103

Bzdok, D., Laird, A. R., Zilles, K., Fox, P. T., & Eickhoff, S. B. (2013). An investigation of the structural, connectional, and functional subspecialization in the human amygdala. *Human Brain Mapping*, *34*(12), 3247-3266. https://doi.org/10.1002/hbm.22138

Campbell-Washburn, A. (2018). MRI: The Classical Description. International Society for Magnetic Resonance in Medicine, Paris.

Canario, E., Chen, D., & Biswal, B. (2021). A review of resting-state fMRI and its use to examine psychiatric disorders. *Psychoradiology*, *1*(1), 42-53. https://doi.org/10.1093/psyrad/kkab003

Chang, C., & Glover, G. H. (2009). Effects of model-based physiological noise correction on default mode network anti-correlations and correlations. *Neuroimage*, *47*(4), 1448-1459. https://doi.org/10.1016/j.neuroimage.2009.05.012

Chau, W., & McIntosh, A. R. (2005). The Talairach coordinate of a point in the MNI space: how to interpret it. *Neuroimage*, *25*(2), 408-416. https://doi.org/10.1016/j.neuroimage.2004.12.007

Chavhan, G. B., Babyn, P. S., Thomas, B., Shroff, M. M., & Haacke, E. M. (2009). Principles, Techniques, and Applications of T2*-based MR Imaging and Its Special Applications. *RadioGraphics*, *29*(5), 1433-1449. https://doi.org/10.1148/rg.295095034

Chen, X., Chen, N.-X., Shen, Y.-Q., Li, H.-X., Li, L., Lu, B., Zhu, Z.-C., Fan, Z., & Yan, C.-G. (2020). The subsystem mechanism of default mode network underlying rumination: A reproducible neuroimaging study. *Neuroimage*, *221*, 117185. https://doi.org/10.1016/j.neuroimage.2020.117185

Chumachenko, S. Y., Cali, R. J., Rosal, M. C., Allison, J. J., Person, S. J., Ziedonis, D., Nephew, B. C., Moore, C. M., Zhang, N., & King, J. A. (2021). Keeping weight off: Mindfulness-Based Stress Reduction alters amygdala functional connectivity during weight loss maintenance in a randomized control trial. *PLOS ONE*, *16*(1), e0244847. https://doi.org/10.1371/journal.pone.0244847

Cohen, N. T., Chang, P., Gholipour, T., Oluigbo, C., Vezina, L. G., Xie, H., Zhang, A., & Gaillard, W. D. (2023). Limbic network co-localization predicts pharmacoresistance in dysplasia-related epilepsy. *Annals of Clinical and Translational Neurology*, *10*(11), 2161-2165. https://doi.org/10.1002/acn3.51892

Cole, D. M., Smith, S. M., & Beckmann, C. F. (2010). Advances and pitfalls in the analysis and interpretation of resting-state FMRI data. *Front Syst Neurosci*, *4*, 8. https://doi.org/10.3389/fnsys.2010.00008

Cotter, D., Miszkiel, K., Al-Sarraj, S., Wilkinson, I. D., Paley, M., Harrison, M. J. G., Hall-Craggs, M. A., & Everall, I. P. (1999). The assessment of postmortem brain volume; a comparison of stereological and planimetric methodologies. *Neuroradiology*, *41*(7), 493-496. https://doi.org/10.1007/s002340050789

Damborská, A., Honzírková, E., Barteček, R., Hořínková, J., Fedorová, S., Ondruš, Š., Michel, C. M., & Rubega, M. (2020). Altered directed functional connectivity of the right amygdala in depression: high-density EEG study. *Scientific Reports*, *10*(1), 4398. https://doi.org/10.1038/s41598-020-61264-z

Darányi, V., Hermann, P., Homolya, I., Vidnyánszky, Z., & Nagy, Z. (2021). An empirical investigation of the benefit of increasing the temporal resolution of task-evoked fMRI data with multi-band imaging. *Magnetic Resonance Materials in Physics, Biology and Medicine*, *34*(5), 667-676. https://doi.org/10.1007/s10334-021-00918-z

Delli Pizzi, S., Chiacchiaretta, P., Mantini, D., Bubbico, G., Ferretti, A., Edden, R. A., Di Giulio, C., Onofrj, M., & Bonanni, L. (2017). Functional and neurochemical interactions within the amygdala–medial prefrontal cortex circuit and their relevance to emotional processing. *Brain Structure and Function*, *222*(3), 1267-1279.

Deng, Y., Li, S., Zhou, R., & Walter, M. (2019). Neuroticism modulates the functional connectivity from amygdala to frontal networks in females when avoiding emotional negative pictures. *Frontiers in Behavioral Neuroscience*, *13*, 102.

Dutta, A., McKie, S., Downey, D., Thomas, E., Juhasz, G., Arnone, D., Elliott, R., Williams, S., Deakin, J. F. W., & Anderson, I. M. (2019). Regional default mode network connectivity in major depressive disorder: modulation by acute intravenous citalopram. *Translational psychiatry*, *9*(1), 116. https://doi.org/10.1038/s41398-019-0447-0

Edelman, R. R. (2014). The History of MR Imaging as Seen through the Pages of Radiology. *Radiology*, *273*(2S), S181-S200. https://doi.org/10.1148/radiol.14140706

Eickhoff, S. B., Stephan, K. E., Mohlberg, H., Grefkes, C., Fink, G. R., Amunts, K., & Zilles, K. (2005). A new SPM toolbox for combining probabilistic cytoarchitectonic maps and functional imaging data. *Neuroimage*, *25*(4), 1325-1335. https://doi.org/10.1016/j.neuroimage.2004.12.034

Elam, J. S., Glasser, M. F., Harms, M. P., Sotiropoulos, S. N., Andersson, J. L. R., Burgess, G. C., Curtiss, S. W., Oostenveld, R., Larson-Prior, L. J., Schoffelen, J.-M., Hodge, M. R., Cler, E. A., Marcus, D. M., Barch, D. M., Yacoub, E., Smith, S. M., Ugurbil, K., & Van Essen, D. C. (2021). The Human Connectome Project: A retrospective. *Neuroimage*, *244*, 118543. https://doi.org/10.1016/j.neuroimage.2021.118543

Fan, Y., Bao, C., Wei, Y., Wu, J., Zhao, Y., Zeng, X., Qin, W., Wu, H., & Liu, P. (2020). Altered functional connectivity of the amygdala in Crohn's disease. *Brain Imaging and Behavior*, *14*(6), 2097-2106.

Ferreira, A. M., Costa, F., Tralhão, A., Marques, H., Cardim, N., & Adragão, P. (2014). MRI-conditional pacemakers: current perspectives. *Med Devices (Auckl)*, *7*, 115-124. https://doi.org/10.2147/mder.S44063

Ferri, J., Eisendrath, S. J., Fryer, S. L., Gillung, E., Roach, B. J., & Mathalon, D. H. (2017). Blunted amygdala activity is associated with depression severity in treatment-resistant depression. *Cogn Affect Behav Neurosci*, *17*(6), 1221-1231. https://doi.org/10.3758/s13415-017-0544-6

Fornito, A., Zalesky, A., & Bullmore, E. T. (2016). An Introduction to Brain Networks. In A. Fornito, A. Zalesky, & E. T. Bullmore (Eds.), *Fundamentals of Brain Network Analysis* (pp. 1-35). Academic Press. https://doi.org/10.1016/B978-0-12-407908-3.00001-7

Foster, S. L., Breukelaar, I. A., Ekanayake, K., Lewis, S., & Korgaonkar, M. S. (2023). Functional Magnetic Resonance Imaging of the Amygdala and Subregions at 3 Tesla: A Scoping Review. *Journal of Magnetic Resonance Imaging*. https://doi.org/10.1002/jmri.28836

Fox, M. D., Corbetta, M., Snyder, A. Z., Vincent, J. L., & Raichle, M. E. (2006). Spontaneous neuronal activity distinguishes human dorsal and ventral attention systems. *Proc Natl Acad Sci U S A*, *103*(26), 10046-10051. https://doi.org/10.1073/pnas.0604187103

Fox, M. D., & Raichle, M. E. (2007). Spontaneous fluctuations in brain activity observed with functional magnetic resonance imaging. *Nature Reviews Neuroscience*, *8*(9), 700-711. https://doi.org/10.1038/nrn2201

Fox, M. D., Snyder, A. Z., Zacks, J. M., & Raichle, M. E. (2006). Coherent spontaneous activity accounts for trial-to-trial variability in human evoked brain responses. *Nat Neurosci*, *9*(1), 23-25. https://doi.org/10.1038/nn1616

Friston, K. J., Frith, C. D., Liddle, P. F., & Frackowiak, R. S. (1993). Functional connectivity: the principal-component analysis of large (PET) data sets. *J Cereb Blood Flow Metab*, *13*(1), 5-14. https://doi.org/10.1038/jcbfm.1993.4

Geissberger, N., Tik, M., Sladky, R., Woletz, M., Schuler, A.-L., Willinger, D., & Windischberger, C. (2020). Reproducibility of amygdala activation in facial emotion processing at 7T. *Neuroimage*, *211*, 116585. https://doi.org/10.1016/j.neuroimage.2020.116585

Gläscher, J., & Adolphs, R. (2003). Processing of the Arousal of Subliminal and Supraliminal Emotional Stimuli by the Human Amygdala. *The Journal of Neuroscience*, *23*(32), 10274. https://doi.org/10.1523/JNEUROSCI.23-32-10274.2003

Glover, G. H. (2011). Overview of functional magnetic resonance imaging. *Neurosurgery clinics of North America*, *22*(2), 133-vii. https://doi.org/10.1016/j.nec.2010.11.001

Glover, G. H., & Law, C. S. (2001). Spiral-in/out BOLD fMRI for increased SNR and reduced susceptibility artifacts. *Magnetic Resonance in Medicine*, *46*(3), 515-522. https://doi.org/10.1002/mrm.1222

Grafton, S. T., & Volz, L. J. (2019). Chapter 13 - From ideas to action: The prefrontal–premotor connections that shape motor behavior. In M. D'Esposito & J. H. Grafman (Eds.), *Handbook of Clinical Neurology* (Vol. 163, pp. 237-255). Elsevier. https://doi.org/10.1016/B978-0-12-804281-6.00013-6

Greicius, M. D., Flores, B. H., Menon, V., Glover, G. H., Solvason, H. B., Kenna, H., Reiss, A. L., & Schatzberg, A. F. (2007). Resting-State Functional Connectivity in Major Depression: Abnormally Increased Contributions from Subgenual Cingulate Cortex and Thalamus. *Biological Psychiatry*, *62*(5), 429-437. https://doi.org/10.1016/j.biopsych.2006.09.020

Greicius, M. D., Krasnow, B., Reiss, A. L., & Menon, V. (2003). Functional connectivity in the resting brain: a network analysis of the default mode hypothesis. *Proc Natl Acad Sci U S A*, *100*(1), 253-258. https://doi.org/10.1073/pnas.0135058100

Grogans, S. E., Fox, A. S., & Shackman, A. J. (2022). The Amygdala and Depression: A Sober Reconsideration. *American Journal of Psychiatry*, *179*(7), 454-457. https://doi.org/10.1176/appi.ajp.20220412

Gruber, B., Froeling, M., Leiner, T., & Klomp, D. W. J. (2018). RF coils: A practical guide for nonphysicists. *Journal of Magnetic Resonance Imaging*, *48*(3), 590-604. https://doi.org/10.1002/jmri.26187

Guo, W., Liu, F., Zhang, J., Zhang, Z., Yu, L., Liu, J., Chen, H., & Xiao, C. (2014). Abnormal Default-Mode Network Homogeneity in First-Episode, Drug-Naive Major Depressive Disorder. *PLOS ONE*, *9*(3), e91102. https://doi.org/10.1371/journal.pone.0091102

Haase, A., Odoj, F., Von Kienlin, M., Warnking, J., Fidler, F., Weisser, A., Nittka, M., Rommel, E., Lanz, T., Kalusche, B., & Griswold, M. (2000). NMR probeheads for in vivo applications. *Concepts in Magnetic Resonance*, *12*(6), 361-388. https://doi.org/10.1002/1099-0534(2000)12:6<361::AID-CMR1>3.0.CO;2-L

Hamilton, J. P., Farmer, M., Fogelman, P., & Gotlib, I. H. (2015). Depressive Rumination, the Default-Mode Network, and the Dark Matter of Clinical Neuroscience. *Biol Psychiatry*, *78*(4), 224-230. https://doi.org/10.1016/j.biopsych.2015.02.020

Hariri, A. R., Bookheimer, S. Y., & Mazziotta, J. C. (2000). Modulating emotional responses: effects of a neocortical network on the limbic system. *Neuroreport*, *11*(1), 43-48. https://doi.org/10.1097/00001756-200001170-00009

Hartling, C., Metz, S., Pehrs, C., Scheidegger, M., Gruzman, R., Keicher, C., Wunder, A., Weigand, A., & Grimm, S. (2021). Comparison of Four fMRI Paradigms Probing Emotion Processing. *Brain Sciences*, *11*(5), 525. https://www.mdpi.com/2076-3425/11/5/525

Hillman, E. M. (2014). Coupling mechanism and significance of the BOLD signal: a status report. *Annu Rev Neurosci*, *37*, 161-181. https://doi.org/10.1146/annurev-neuro-071013-014111

Huettel, S. A., Song, A. W., & McCarthy, G. (2004). *Functional magnetic resonance imaging* (1st ed. ed.). Sinauer Associates.

Huneau, C., Benali, H., & Chabriat, H. (2015). Investigating Human Neurovascular Coupling Using Functional Neuroimaging: A Critical Review of Dynamic Models [Review]. *Frontiers in Neuroscience*, *9*(467). https://doi.org/10.3389/fnins.2015.00467

Huotari, N., Raitamaa, L., Helakari, H., Kananen, J., Raatikainen, V., Rasila, A., Tuovinen, T., Kantola, J., Borchardt, V., Kiviniemi, V. J., & Korhonen, V. O. (2019). Sampling Rate Effects on Resting State fMRI Metrics [Original Research]. *Frontiers in Neuroscience*, *Volume 13 - 2019*. https://doi.org/10.3389/fnins.2019.00279

Invernizzi, A., Gravel, N., Haak, K. V., Renken, R. J., & Cornelissen, F. W. (2021). Assessing Uncertainty and Reliability of Connective Field Estimations From Resting State fMRI Activity at 3T [Original Research]. *Frontiers in Neuroscience*, *15*(80). https://doi.org/10.3389/fnins.2021.625309

Iranpour, J., Morrot, G., Claise, B., Jean, B., & Bonny, J.-M. (2015). Using high spatial resolution to improve BOLD fMRI detection at 3T. *PLOS ONE*, *10*(11), e0141358. https://doi.org/10.1371/journal.pone.0141358

Jackson, G. D., Kuzniecky, R. I., & Pell, G. S. (2005). CHAPTER 2 - Principles of Magnetic Resonance Imaging. In R. I. Kuzniecky & G. D. Jackson (Eds.), *Magnetic Resonance in Epilepsy (Second Edition)* (pp. 17-28). Academic Press. https://doi.org/10.1016/B978-012431152-7/50006-9

Jahanian, H., Holdsworth, S., Christen, T., Wu, H., Zhu, K., Kerr, A. B., Middione, M. J., Dougherty, R. F., Moseley, M., & Zaharchuk, G. (2019). Advantages of short repetition time resting-state functional MRI enabled by simultaneous multi-slice imaging. *Journal of neuroscience methods*, *311*, 122-132. https://doi.org/10.1016/j.jneumeth.2018.09.033

Javed, K., Reddy, V., & Lui, F. (2023, 25.07.2023). *Neuroanatomy, Cerebral Cortex*. StatPearls Publishing. Retrieved 06.05.2025 from https://www.ncbi.nlm.nih.gov/books/NBK537247/

Jung, Y., Samsonov, A. A., Liu, T. T., & Buracas, G. T. (2013). High efficiency multishot interleaved spiral-in/out: acquisition for high-resolution BOLD fMRI. *Magnetic Resonance in Medicine*, *70*(2), 420-428. https://doi.org/10.1002/mrm.24476

Kabasawa, H. (2022). MR Imaging in the 21st Century: Technical Innovation over the First Two Decades. *Magn Reson Med Sci*, *21*(1), 71-82. https://doi.org/10.2463/mrms.rev.2021-0011

Kakeda, S., Watanabe, K., Nguyen, H., Katsuki, A., Sugimoto, K., Igata, N., Abe, O., Yoshimura, R., & Korogi, Y. (2020). An independent component analysis reveals brain structural networks related to TNF-α in drug-naïve, first-episode major depressive disorder: a source-based morphometric study. *Translational psychiatry*, *10*(1), 187. https://doi.org/10.1038/s41398-020-00873-8

Kasper, L., Engel, M., Heinzle, J., Mueller-Schrader, M., Graedel, N. N., Reber, J., Schmid, T., Barmet, C., Wilm, B. J., Stephan, K. E., & Pruessmann, K. P. (2020). Advances in Spiral fMRI: A High-resolution Study with Single-shot Acquisition. *bioRxiv*, 842179. https://doi.org/10.1101/842179

Kazan, S. M., & Weiskopf, N. (2017). fMRI Methods. In J. C. Lindon, G. E. Tranter, & D. W. Koppenaal (Eds.), *Encyclopedia of Spectroscopy and Spectrometry (Third Edition)* (pp. 670-677). Academic Press. https://doi.org/10.1016/B978-0-12-409547-2.12109-2

Kazemivalipour, E., Bhusal, B., Vu, J., Lin, S., Nguyen, B. T., Kirsch, J., Nowac, E., Pilitsis, J., Rosenow, J., Atalar, E., & Golestanirad, L. (2021). Vertical open-bore MRI scanners generate significantly less radiofrequency heating around implanted leads: A study of deep brain stimulation implants in 1.2T OASIS scanners versus 1.5T horizontal systems. *Magn Reson Med*, *86*(3), 1560-1572. https://doi.org/10.1002/mrm.28818

Keil, B., Blau, J. N., Biber, S., Hoecht, P., Tountcheva, V., Setsompop, K., Triantafyllou, C., & Wald, L. L. (2013). A 64-channel 3T array coil for accelerated brain MRI. *Magnetic Resonance in Medicine*, *70*(1), 248-258. https://doi.org/10.1002/mrm.24427

Klein-Flügge, M. C., Jensen, D. E. A., Takagi, Y., Priestley, L., Verhagen, L., Smith, S. M., & Rushworth, M. F. S. (2022). Relationship between nuclei-specific amygdala connectivity and mental health dimensions in humans. *Nature Human Behaviour*, *6*(12), 1705-1722. https://doi.org/10.1038/s41562-022-01434-3

Kodaverdian, N. (2019). Chapter 3 - fMRI in Economics: What Functional Imaging of the Brain Can Add to Behavioral Economics Experiments. In G. Foster (Ed.), *Biophysical Measurement in Experimental Social Science Research* (pp. 47-83). Academic Press. https://doi.org/10.1016/B978-0-12-813092-6.00005-8

Korgaonkar, M. S., Ram, K., Williams, L. M., Gatt, J. M., & Grieve, S. M. (2014). Establishing the resting state default mode network derived from functional magnetic resonance imaging tasks as an endophenotype: A twins study. *Hum Brain Mapp*, *35*(8), 3893-3902. https://doi.org/10.1002/hbm.22446

Kwok, W. E. (2022). Basic Principles of and Practical Guide to Clinical MRI Radiofrequency Coils. *RadioGraphics*, *42*(3), 898-918. https://doi.org/10.1148/rg.210110

Kwong, K. K., Belliveau, J. W., Chesler, D. A., Goldberg, I. E., Weisskoff, R. M., Poncelet, B. P., Kennedy, D. N., Hoppel, B. E., Cohen, M. S., Turner, R., & et al. (1992). Dynamic magnetic resonance imaging of human brain activity during primary sensory stimulation. *Proc Natl Acad Sci U S A*, *89*(12), 5675-5679. https://doi.org/10.1073/pnas.89.12.5675

Labuschagne, I., Dominguez, J. F., Grace, S., Mizzi, S., Henry, J. D., Peters, C., Rabinak, C. A., Sinclair, E., Lorenzetti, V., Terrett, G., Rendell, P. G., Pedersen, M., Hocking, D.

R., & Heinrichs, M. (2024). Specialization of amygdala subregions in emotion processing. *Human Brain Mapping*, *45*(5), e26673. https://doi.org/10.1002/hbm.26673

Ladd, M. E., Bachert, P., Meyerspeer, M., Moser, E., Nagel, A. M., Norris, D. G., Schmitter, S., Speck, O., Straub, S., & Zaiss, M. (2018). Pros and cons of ultra-high-field MRI/MRS for human application. *Progress in Nuclear Magnetic Resonance Spectroscopy*, *109*, 1-50. https://doi.org/10.1016/j.pnmrs.2018.06.001

Le Ster, C., Moreno, A., Mauconduit, F., Gras, V., Stirnberg, R., Poser, B. A., Vignaud, A., Eger, E., Dehaene, S., Meyniel, F., & Boulant, N. (2019). Comparison of SMS-EPI and 3D-EPI at 7T in an fMRI localizer study with matched spatiotemporal resolution and homogenized excitation profiles. *PLOS ONE*, *14*(11), e0225286. https://doi.org/10.1371/journal.pone.0225286

Levi, P. T., Chopra, S., Pang, J. C., Holmes, A., Gajwani, M., Sassenberg, T. A., DeYoung, C. G., & Fornito, A. (2023). The effect of using group-averaged or individualized brain parcellations when investigating connectome dysfunction in psychosis. *Network Neuroscience*, *7*(4), 1228-1247. https://doi.org/10.1162/netn_a_00329

Li, B., Liu, L., Friston, K. J., Shen, H., Wang, L., Zeng, L.-L., & Hu, D. (2013). A Treatment-Resistant Default Mode Subnetwork in Major Depression. *Biological Psychiatry*, *74*(1), 48-54. https://doi.org/10.1016/j.biopsych.2012.11.007

Liao, X.-H., Xia, M.-R., Xu, T., Dai, Z.-J., Cao, X.-Y., Niu, H.-J., Zuo, X.-N., Zang, Y.-F., & He, Y. (2013). Functional brain hubs and their test–retest reliability: A multiband resting-state functional MRI study. *Neuroimage*, *83*, 969-982. https://doi.org/10.1016/j.neuroimage.2013.07.058

Liu, T. T., Frank, L. R., Wong, E. C., & Buxton, R. B. (2001). Detection Power, Estimation Efficiency, and Predictability in Event-Related fMRI. *Neuroimage*, *13*(4), 759-773. https://doi.org/10.1006/nimg.2000.0728

Logothetis, N. K. (2008). What we can do and what we cannot do with fMRI. *Nature*, *453*(7197), 869-878. https://doi.org/10.1038/nature06976

Loued-Khenissi, L., Döll, O., & Preuschoff, K. (2019). An Overview of Functional Magnetic Resonance Imaging Techniques for Organizational Research. *Organizational Research Methods*, *22*(1), 17-45. https://doi.org/10.1177/1094428118802631

Lv, H., Wang, Z., Tong, E., Williams, L. M., Zaharchuk, G., Zeineh, M., Goldstein-Piekarski, A. N., Ball, T. M., Liao, C., & Wintermark, M. (2018). Resting-State Functional MRI: Everything That Nonexperts Have Always Wanted to Know. *AJNR Am J Neuroradiol*, *39*(8), 1390-1399. https://doi.org/10.3174/ajnr.A5527

Mandal, P. K., Mahajan, R., & Dinov, I. D. (2012). Structural brain atlases: design, rationale, and applications in normal and pathological cohorts. *J Alzheimers Dis*, *31 Suppl 3*(0 3), S169-188. https://doi.org/10.3233/jad-2012-120412

Manoliu, A., Meng, C., Brandl, F., Doll, A., Tahmasian, M., Scherr, M., Schwerthöffer, D., Zimmer, C., Förstl, H., & Bäuml, J. (2014). Insular dysfunction within the salience network is associated with severity of symptoms and aberrant inter-network connectivity in major depressive disorder. *Frontiers in Human Neuroscience*, *7*, 930. https://doi.org/10.3389/fnhum.2013.00930

Mansfield, P. (1977). Multi-planar image formation using NMR spin echoes. *Journal of Physics C: Solid State Physics*, *10*(3), L55. https://doi.org/10.1088/0022-3719/10/3/004

McRobbie, D. W., Moore, E. A., Graves, M. J., & Prince, M. R. (2017). *MRI from Picture to Proton* (3 ed.). Cambridge University Press. https://doi.org/DOI: 10.1017/9781107706958

Menon, R. S., & Goodyear, B. G. (2001). Spatial and temporal resolution in fMRI. In P. Jezzard, P. M. Matthews, & S. M. Smith (Eds.), *Functional Magnetic Resonance Imaging: An Introduction to Methods* (pp. 146-158). Oxford University Press. https://doi.org/10.1093/acprof:oso/9780192630711.003.0007

Menon, V. (2023). 20 years of the default mode network: A review and synthesis. *Neuron*, *111*(16), 2469-2487. https://doi.org/10.1016/j.neuron.2023.04.023

Merboldt, K.-D., Fransson, P., Bruhn, H., & Frahm, J. (2001). Functional MRI of the Human Amygdala? *Neuroimage*, *14*(2), 253-257. https://doi.org/10.1006/nimg.2001.0802

Michely, J., Rigoli, F., Rutledge, R. B., Hauser, T. U., & Dolan, R. J. (2020). Distinct processing of aversive experience in amygdala subregions. *Biological Psychiatry: Cognitive Neuroscience and Neuroimaging*, *5*(3), 291-300. https://doi.org/10.1016/j.bpsc.2019.07.008

Morey, R. A., Clarke, E. K., Haswell, C. C., Phillips, R. D., Clausen, A. N., Mufford, M. S., Saygin, Z., Brancu, M., Beckham, J. C., Calhoun, P. S., Dedert, E., Elbogen, E. B., Fairbank, J. A., Hurley, R. A., Kilts, J. D., Kimbrel, N. A., Kirby, A., Marx, C. E., McDonald, S. D., . . . LaBar, K. S. (2020). Amygdala Nuclei Volume and Shape in Military Veterans With Posttraumatic Stress Disorder. *Biological Psychiatry: Cognitive Neuroscience and Neuroimaging*, *5*(3), 281-290. https://doi.org/10.1016/j.bpsc.2019.11.016

Murphy, J. E., Yanes, J. A., Kirby, L. A. J., Reid, M. A., & Robinson, J. L. (2020). Left, right, or bilateral amygdala activation? How effects of smoothing and motion correction on ultra-high field, high-resolution functional magnetic resonance imaging (fMRI) data alter inferences [Article]. *Neuroscience Research*, *150*, 51-59. https://doi.org/10.1016/j.neures.2019.01.009

Nasr, S., Polimeni, J. R., & Tootell, R. B. H. (2016). Interdigitated color- and disparity-selective columns within human visual cortical areas V2 and V3 [Article]. *Journal of Neuroscience*, *36*(6), 1841-1857. https://doi.org/10.1523/JNEUROSCI.3518-15.2016

National Institutes of Health. (2023, 23.06.2023). *NIH Blueprint for Neuroscience Research*. U.S. Department of Health and Human Services. Retrieved 20.10.2021 from https://neuroscienceblueprint.nih.gov/human-connectome/connectome-programs

Olman, C. A., Davachi, L., & Inati, S. (2009). Distortion and Signal Loss in Medial Temporal Lobe. *PLOS ONE*, *4*(12), e8160. https://doi.org/10.1371/journal.pone.0008160

Olman, C. A., & Yacoub, E. (2011). High-field FMRI for human applications: an overview of spatial resolution and signal specificity. *Open Neuroimag J*, *5*, 74-89. https://doi.org/10.2174/1874440001105010074

Patriat, R., Molloy, E. K., Meier, T. B., Kirk, G. R., Nair, V. A., Meyerand, M. E., Prabhakaran, V., & Birn, R. M. (2013). The effect of resting condition on resting-state fMRI reliability and consistency: a comparison between resting with eyes open, closed, and fixated. *Neuroimage*, *78*, 463-473. https://doi.org/10.1016/j.neuroimage.2013.04.013

Pedersen, W. S., Muftuler, L. T., & Larson, C. L. (2017). Disentangling the effects of novelty, valence and trait anxiety in the bed nucleus of the stria terminalis, amygdala and hippocampus with high resolution 7T fMRI. *Neuroimage*, *156*, 293-301. https://doi.org/10.1016/j.neuroimage.2017.05.009

Plichta, M. M., Grimm, O., Morgen, K., Mier, D., Sauer, C., Haddad, L., Tost, H., Esslinger, C., Kirsch, P., Schwarz, A. J., & Meyer-Lindenberg, A. (2014). Amygdala habituation: A reliable fMRI phenotype. *Neuroimage*, *103*, 383-390. https://doi.org/10.1016/j.neuroimage.2014.09.059

Poldrack, R. A. (2007). Region of interest analysis for fMRI. *Soc Cogn Affect Neurosci*, *2*(1), 67-70. https://doi.org/10.1093/scan/nsm006

Poldrack, R. A., Baker, C. I., Durnez, J., Gorgolewski, K. J., Matthews, P. M., Munafò, M. R., Nichols, T. E., Poline, J. B., Vul, E., & Yarkoni, T. (2017). Scanning the horizon: towards transparent and reproducible neuroimaging research. *Nat Rev Neurosci*, *18*(2), 115-126. https://doi.org/10.1038/nrn.2016.167

Poser, B. A., Koopmans, P. J., Witzel, T., Wald, L. L., & Barth, M. (2010). Three dimensional echo-planar imaging at 7 Tesla. *Neuroimage*, *51*(1), 261-266. https://doi.org/10.1016/j.neuroimage.2010.01.108

Qin, S., Young, C. B., Duan, X., Chen, T., Supekar, K., & Menon, V. (2014). Amygdala Subregional Structure and Intrinsic Functional Connectivity Predicts Individual Differences in Anxiety During Early Childhood. *Biological Psychiatry*, *75*(11), 892-900. https://doi.org/10.1016/j.biopsych.2013.10.006

Raichle, M. E., MacLeod, A. M., Snyder, A. Z., Powers, W. J., Gusnard, D. A., & Shulman, G. L. (2001). A default mode of brain function. *Proc Natl Acad Sci U S A*, *98*(2), 676-682. https://doi.org/10.1073/pnas.98.2.676

Rajamanickam, K. (2020). A Mini Review on Different Methods of Functional-MRI Data Analysis. *Archives of Internal Medicine Research*, *3*, 44-60. https://www.fortunejournals.com/articles/a-mini-review-on-different-methods-of-functionalmri-data-analysis.html

Rangaprakash, D., Tadayonnejad, R., Deshpande, G., O'Neill, J., & Feusner, J. D. (2021). FMRI hemodynamic response function (HRF) as a novel marker of brain function: applications for understanding obsessive-compulsive disorder pathology and treatment response. *Brain Imaging and Behavior*, *15*(3), 1622-1640. https://doi.org/10.1007/s11682-020-00358-8

Redpath, T. W. (2014). Signal-to-noise ratio in MRI. *British Journal of Radiology*, *71*(847), 704-707. https://doi.org/10.1259/bjr.71.847.9771379

Reich, D. B., Belleau, E. L., Temes, C. M., Gonenc, A., Pizzagalli, D. A., & Gruber, S. A. (2019). Amygdala Resting State Connectivity Differences between Bipolar II and Borderline Personality Disorders. *Neuropsychobiology*, *78*(4), 229-237. https://doi.org/10.1159/000502440

Robinson, S., Windischberger, C., Rauscher, A., & Moser, E. (2004). Optimized 3 T EPI of the amygdalae. *Neuroimage*, *22*(1), 203-210. https://doi.org/10.1016/j.neuroimage.2003.12.048

Roy, A. K., Shehzad, Z., Margulies, D. S., Kelly, A. M. C., Uddin, L. Q., Gotimer, K., Biswal, B. B., Castellanos, F. X., & Milham, M. P. (2009). Functional connectivity of the human amygdala using resting state fMRI. *Neuroimage*, *45*(2), 614-626. https://doi.org/10.1016/j.neuroimage.2008.11.030

Saarimäki, H., Glerean, E., Smirnov, D., Mynttinen, H., Jääskeläinen, I. P., Sams, M., & Nummenmaa, L. (2022). Classification of emotion categories based on functional connectivity patterns of the human brain. *Neuroimage*, *247*, 118800. https://doi.org/10.1016/j.neuroimage.2021.118800

Salzwedel, A. P., Stephens, R. L., Goldman, B. D., Lin, W., Gilmore, J. H., & Gao, W. (2019). Development of amygdala functional connectivity during infancy and its relationship with 4-year behavioral outcomes. *Biological Psychiatry: Cognitive Neuroscience and Neuroimaging*, *4*(1), 62-71. https://doi.org/10.1016/j.bpsc.2018.08.010

Sambataro, F., Wolf, N. D., Pennuto, M., Vasic, N., & Wolf, R. C. (2014). Revisiting default mode network function in major depression: evidence for disrupted subsystem connectivity. *Psychol Med*, *44*(10), 2041-2051. https://doi.org/10.1017/s0033291713002596

Sambuco, N., Bradley, M. M., & Lang, P. J. (2022). Narrative imagery: Emotional modulation in the default mode network. *Neuropsychologia*, *164*, 108087. https://doi.org/10.1016/j.neuropsychologia.2021.108087

Sanz-Arigita, E., Daviaux, Y., Joliot, M., Dilharreguy, B., Micoulaud-Franchi, J. A., Bioulac, S., Taillard, J., Philip, P., & Altena, E. (2021). Brain reactivity to humorous films is affected by insomnia. *Sleep*, *44*(9), zsab081. https://doi.org/10.1093/sleep/zsab081

Satpute, A. B., & Lindquist, K. A. (2019). The Default Mode Network's Role in Discrete Emotion. *Trends Cogn Sci*, *23*(10), 851-864. https://doi.org/10.1016/j.tics.2019.07.003

Saygin, Z. M., Kliemann, D., Iglesias, J. E., van der Kouwe, A. J. W., Boyd, E., Reuter, M., Stevens, A., Van Leemput, K., McKee, A., Frosch, M. P., Fischl, B., & Augustinack, J. C. (2017). High-resolution magnetic resonance imaging reveals nuclei of the human amygdala: manual segmentation to automatic atlas. *Neuroimage*, *155*, 370-382. https://doi.org/10.1016/j.neuroimage.2017.04.046

Seitzman, B. A., Snyder, A. Z., Leuthardt, E. C., & Shimony, J. S. (2019). The State of Resting State Networks. *Top Magn Reson Imaging*, *28*(4), 189-196. https://doi.org/10.1097/rmr.0000000000000214

Sergerie, K., Chochol, C., & Armony, J. L. (2008). The role of the amygdala in emotional processing: A quantitative meta-analysis of functional neuroimaging studies. *Neuroscience & Biobehavioral Reviews*, *32*(4), 811-830. https://doi.org/10.1016/j.neubiorev.2007.12.002

Sexton, C. E., Allan, C. L., Le Masurier, M., McDermott, L. M., Kalu, U. G., Herrmann, L. L., Mäurer, M., Bradley, K. M., Mackay, C. E., & Ebmeier, K. P. (2012). Magnetic resonance imaging in late-life depression: multimodal examination of network disruption. *Archives of General Psychiatry*, *69*(7), 680-689. https://doi.org/10.1001/archgenpsychiatry.2011.1862

Sheline, Y. I., Barch, D. M., Price, J. L., Rundle, M. M., Vaishnavi, S. N., Snyder, A. Z., Mintun, M. A., Wang, S., Coalson, R. S., & Raichle, M. E. (2009). The default mode network and self-referential processes in depression. *Proc Natl Acad Sci U S A*, *106*(6), 1942-1947. https://doi.org/10.1073/pnas.0812686106

Shou, H., Yang, Z., Satterthwaite, T. D., Cook, P. A., Bruce, S. E., Shinohara, R. T., Rosenberg, B., & Sheline, Y. I. (2017). Cognitive behavioral therapy increases amygdala connectivity with the cognitive control network in both MDD and PTSD. *NeuroImage: Clinical*, *14*, 464-470.

Sladky, R., Geissberger, N., Pfabigan, D. M., Kraus, C., Tik, M., Woletz, M., Paul, K., Vanicek, T., Auer, B., Kranz, G. S., Lamm, C., Lanzenberger, R., & Windischberger, C. (2018). Unsmoothed functional MRI of the human amygdala and bed nucleus of the stria terminalis during processing of emotional faces. *Neuroimage*, *168*, 383-391. https://doi.org/10.1016/j.neuroimage.2016.12.024

Snyder, A. Z., & Raichle, M. E. (2012). A brief history of the resting state: the Washington University perspective. *Neuroimage*, *62*(2), 902-910. https://doi.org/10.1016/j.neuroimage.2012.01.044

Soares, J. M., Magalhães, R., Moreira, P. S., Sousa, A., Ganz, E., Sampaio, A., Alves, V., Marques, P., & Sousa, N. (2016). A Hitchhiker's Guide to Functional Magnetic Resonance Imaging [Review]. *Frontiers in Neuroscience*, *10*(515). https://doi.org/10.3389/fnins.2016.00515

Sohn, W. S., Yoo, K., Lee, Y. B., Seo, S. W., Na, D. L., & Jeong, Y. (2015). Influence of ROI selection on resting state functional connectivity: an individualized approach for resting state fMRI analysis. *Front Neurosci*, *9*, 280. https://doi.org/10.3389/fnins.2015.00280

Sporns, O., Tononi, G., & Kötter, R. (2005). The human connectome: A structural description of the human brain. *PLoS computational biology*, *1*(4), e42-e42. https://doi.org/10.1371/journal.pcbi.0010042

Stirnberg, R., Huijbers, W., Brenner, D., Poser, B. A., Breteler, M., & Stöcker, T. (2017). Rapid whole-brain resting-state fMRI at 3 T: Efficiency-optimized three-dimensional EPI versus repetition time-matched simultaneous-multi-slice EPI. *Neuroimage*, *163*, 81-92. https://doi.org/10.1016/j.neuroimage.2017.08.031

Stoliker, D., Novelli, L., Vollenweider, F. X., Egan, G. F., Preller, K. H., & Razi, A. (2024). Neural Mechanisms of Resting-State Networks and the Amygdala Underlying the Cognitive and Emotional Effects of Psilocybin. *Biological Psychiatry*, *96*(1), 57-66. https://doi.org/10.1016/j.biopsych.2024.01.002

Talairach, J., & Tournoux, P. (1988). *Co-planar stereotaxic atlas of the human brain : 3-dimensional proportional system : an approach to cerebral imaging*. G. Thieme ; New York : Thieme Medical Publishers.

Tang, D. W., Fellows, L. K., Small, D. M., & Dagher, A. (2012). Food and drug cues activate similar brain regions: A meta-analysis of functional MRI studies. *Physiology & Behavior*, *106*(3), 317-324. https://doi.org/10.1016/j.physbeh.2012.03.009

Tong, X., An, D., Xiao, F., Lei, D., Niu, R., Li, W., Ren, J., Liu, W., Tang, Y., & Zhang, L. (2019). Real-time effects of interictal spikes on hippocampus and amygdala functional connectivity in unilateral temporal lobe epilepsy: An EEG-fMRI study. *Epilepsia*, *60*(2), 246-254. https://doi.org/10.1111/epi.14646

Tozzi, L., Zhang, X., Chesnut, M., Holt-Gosselin, B., Ramirez, C. A., & Williams, L. M. (2021). Reduced functional connectivity of default mode network subsystems in depression: Meta-analytic evidence and relationship with trait rumination. *NeuroImage: Clinical*, *30*, 102570. https://doi.org/10.1016/j.nicl.2021.102570

Tura, A., & Goya-Maldonado, R. (2023). Brain connectivity in major depressive disorder: a precision component of treatment modalities? *Translational psychiatry*, *13*(1), 196. https://doi.org/10.1038/s41398-023-02499-y

van der Laan, L. N., de Ridder, D. T. D., Viergever, M. A., & Smeets, P. A. M. (2011). The first taste is always with the eyes: A meta-analysis on the neural correlates of processing visual food cues. *Neuroimage*, *55*(1), 296-303. https://doi.org/10.1016/j.neuroimage.2010.11.055

van der Zwaag, W., Marques, J. P., Kober, T., Glover, G., Gruetter, R., & Krueger, G. (2012). Temporal SNR characteristics in segmented 3D-EPI at 7T. *Magnetic Resonance in Medicine*, *67*(2), 344-352. https://doi.org/10.1002/mrm.23007

Van Essen, D. C., Ugurbil, K., Auerbach, E., Barch, D., Behrens, T. E. J., Bucholz, R., Chang, A., Chen, L., Corbetta, M., Curtiss, S. W., Della Penna, S., Feinberg, D., Glasser, M. F., Harel, N., Heath, A. C., Larson-Prior, L., Marcus, D., Michalareas, G., Moeller, S., . . . Yacoub, E. (2012). The Human Connectome Project: A data acquisition perspective. *Neuroimage*, *62*(4), 2222-2231. https://doi.org/10.1016/j.neuroimage.2012.02.018

Varkevisser, T., Geuze, E., & van Honk, J. (2024). Amygdala fMRI—A Critical Appraisal of the Extant Literature. *Neuroscience Insights*, *19*, 26331055241270591. https://doi.org/10.1177/26331055241270591

Veer, I. M., Beckmann, C. F., van Tol, M. J., Ferrarini, L., Milles, J., Veltman, D. J., Aleman, A., van Buchem, M. A., van der Wee, N. J., & Rombouts, S. A. (2010). Whole brain resting-state analysis reveals decreased functional connectivity in major depression. *Front Syst Neurosci*, *4*. https://doi.org/10.3389/fnsys.2010.00041

Verdijk, J. P. A. J., van de Mortel, L. A., ten Doesschate, F., Pottkämper, J. C. M., Stuiver, S., Bruin, W. B., Abbott, C. C., Argyelan, M., Ousdal, O. T., Bartsch, H., Narr, K., Tendolkar, I., Calhoun, V., Lukemire, J., Guo, Y., Oltedal, L., van Wingen, G., & van Waarde, J. A. (2024). Longitudinal resting-state network connectivity changes in electroconvulsive therapy patients compared to healthy controls. *Brain Stimulation: Basic, Translational, and Clinical Research in Neuromodulation*, *17*(1), 140-147. https://doi.org/10.1016/j.brs.2023.12.005

Vincent, J. L., Kahn, I., Snyder, A. Z., Raichle, M. E., & Buckner, R. L. (2008). Evidence for a frontoparietal control system revealed by intrinsic functional connectivity. *J Neurophysiol*, *100*(6), 3328-3342. https://doi.org/10.1152/jn.90355.2008

Viviano, J. D., Buchanan, R. W., Calarco, N., Gold, J. M., Foussias, G., Bhagwat, N., Stefanik, L., Hawco, C., DeRosse, P., Argyelan, M., Turner, J., Chavez, S., Kochunov, P., Kingsley, P., Zhou, X., Malhotra, A. K., & Voineskos, A. N. (2018). Resting-State Connectivity Biomarkers of Cognitive Performance and Social Function in Individuals With Schizophrenia Spectrum Disorder and Healthy Control Subjects. *Biol Psychiatry*, *84*(9), 665-674. https://doi.org/10.1016/j.biopsych.2018.03.013

Volz, S., Callaghan, M. F., Josephs, O., & Weiskopf, N. (2019). Maximising BOLD sensitivity through automated EPI protocol optimisation. *Neuroimage*, *189*, 159-170. https://doi.org/10.1016/j.neuroimage.2018.12.052

Wackerhagen, C., Veer, I. M., Erk, S., Mohnke, S., Lett, T. A., Wüstenberg, T., Romanczuk-Seiferth, N. Y., Schwarz, K., Schweiger, J. I., Tost, H., Meyer-Lindenberg, A., Heinz, A., & Walter, H. (2020). Amygdala functional connectivity in major depression – disentangling markers of pathology, risk and resilience. *Psychological Medicine*, *50*(16), 2740-2750. https://doi.org/10.1017/S0033291719002885

Wang, M., Cao, L., Li, H., Xiao, H., Ma, Y., Liu, S., Zhu, H., Yuan, M., Qiu, C., & Huang, X. (2021). Dysfunction of Resting-State Functional Connectivity of Amygdala Subregions in Drug-Naïve Patients With Generalized Anxiety Disorder. *Front Psychiatry*, *12*, 758978. https://doi.org/10.3389/fpsyt.2021.758978

Wei, W., Zhang, K., Chang, J., Zhang, S., Ma, L., Wang, H., Zhang, M., Zu, Z., Yang, L., Chen, F., Fan, C., & Li, X. (2024). Analyzing 20 years of Resting-State fMRI Research: Trends and collaborative networks revealed. *Brain research*, *1822*, 148634. https://doi.org/10.1016/j.brainres.2023.148634

Weiskopf, N., Hutton, C., Josephs, O., & Deichmann, R. (2006). Optimal EPI parameters for reduction of susceptibility-induced BOLD sensitivity losses: A whole-brain analysis at 3 T and 1.5 T. *Neuroimage*, *33*(2), 493-504. https://doi.org/10.1016/j.neuroimage.2006.07.029

West, H. V., Burgess, G. C., Dust, J., Kandala, S., & Barch, D. M. (2021). Amygdala Activation in Cognitive Task fMRI Varies with Individual Differences in Cognitive Traits. *Cogn Affect Behav Neurosci*, *21*(1), 254-264. https://doi.org/10.3758/s13415-021-00863-3

Whitfield-Gabrieli, S., & Ford, J. M. (2012). Default mode network activity and connectivity in psychopathology. *Annu Rev Clin Psychol*, *8*, 49-76. https://doi.org/10.1146/annurev-clinpsy-032511-143049

Wiggins, G. C., Triantafyllou, C., Potthast, A., Reykowski, A., Nittka, M., & Wald, L. L. (2006). 32-channel 3 Tesla receive-only phased-array head coil with soccer-ball element geometry. *Magnetic Resonance in Medicine*, *56*(1), 216-223. https://doi.org/10.1002/mrm.20925

Wright, C. I., Fischer, H., Whalen, P. J., McInerney, S. C., Shin, L. M., & Rauch, S. L. (2001). Differential prefrontal cortex and amygdala habituation to repeatedly presented emotional stimuli. *Neuroreport*, *12*(2), 379-383. https://doi.org/10.1097/00001756-200102120-00039

Yan, C. G., Chen, X., Li, L., Castellanos, F. X., Bai, T. J., Bo, Q. J., Cao, J., Chen, G. M., Chen, N. X., Chen, W., Cheng, C., Cheng, Y. Q., Cui, X. L., Duan, J., Fang, Y. R., Gong, Q. Y., Guo, W. B., Hou, Z. H., Hu, L., . . . Zang, Y. F. (2019). Reduced default

mode network functional connectivity in patients with recurrent major depressive disorder. *Proc Natl Acad Sci U S A*, *116*(18), 9078-9083. https://doi.org/10.1073/pnas.1900390116

Yang, Z., & Lewis, L. D. (2021). Imaging the temporal dynamics of brain states with highly sampled fMRI. *Curr Opin Behav Sci*, *40*, 87-95. https://doi.org/10.1016/j.cobeha.2021.02.005

Yeo, B. T., Krienen, F. M., Sepulcre, J., Sabuncu, M. R., Lashkari, D., Hollinshead, M., Roffman, J. L., Smoller, J. W., Zöllei, L., Polimeni, J. R., Fischl, B., Liu, H., & Buckner, R. L. (2011). The organization of the human cerebral cortex estimated by intrinsic functional connectivity. *J Neurophysiol*, *106*(3), 1125-1165. https://doi.org/10.1152/jn.00338.2011

Zhang, X., Cheng, H., Zuo, Z., Zhou, K., Cong, F., Wang, B., Zhuo, Y., Chen, L., Xue, R., & Fan, Y. (2018). Individualized Functional Parcellation of the Human Amygdala Using a Semi-supervised Clustering Method: A 7T Resting State fMRI Study [Original Research]. *Frontiers in Neuroscience*, *12*(270). https://doi.org/10.3389/fnins.2018.00270

Zhu, Z., Lu, Q., Meng, X., Jiang, Q., Peng, L., & Wang, Q. (2012). Spatial patterns of intrinsic neural activity in depressed patients with vascular risk factors as revealed by the amplitude of low-frequency fluctuation. *Brain research*, *1483*, 82-88. https://doi.org/10.1016/j.brainres.2012.07.015

Chapter 3: Functional Magnetic Resonance Imaging of the Amygdala and Subregions at 3 Tesla: A Scoping Review

---

This chapter is composed of two parts. The scoping review protocol, registered with the Open Science Framework and published on the medRxiv preprint server for Health Sciences, is located in Appendix C. The formal scoping review in the following pages was undertaken to provide a broad overview of current practices in relation to spatial resolution of fMRI acquisitions used in studies reporting on amygdala activation and functional connectivity at 3T.

The review identified considerable disparity in fMRI acquisition protocols across imaging sites, resulting in broad data heterogeneity, particularly in relation to studies focusing on the amygdala subregions. Of the 192 studies included, only 16% used high resolution data exclusively and almost 90% of studies reported findings relating to the amygdala as a single structure. To mitigate this issue, recommendations were made for optimization of sequences for imaging the amygdala and its subregions at 3T. Protocol optimization and harmonization across sites performing similar research studies was also recommended as a simple yet effective way to progress the field.

The formal scoping review in this chapter is published in the Journal of Magnetic Resonance Imaging.

Functional Magnetic Resonance Imaging of the Amygdala and Subregions at 3 Tesla: A Scoping Review

Sheryl L. Foster, MHlthSc (MRS)(MRI),[1,2*] Isabella A. Breukelaar, PhD,[3] Kanchana Ekanayake, BA(Special)-LIS,[4] Sarah Lewis, PhD,[1] and Mayuresh S. Korgaonkar, PhD[3]

The amygdalae are a pair of small brain structures, each of which is composed of three main subregions and whose function is implicated in neuropsychiatric conditions. Functional Magnetic Resonance Imaging (fMRI) has been utilized extensively in investigation of amygdala activation and functional connectivity (FC) with most clinical research sites now utilizing 3 Tesla (3T) MR systems. However, accurate imaging and analysis remains challenging not just due to the small size of the amygdala, but also its location deep in the temporal lobe. Selection of imaging parameters can significantly impact data quality with implications for the accuracy of study results and validity of conclusions. Wide variation exists in acquisition protocols with spatial resolution of some protocols suboptimal for accurate assessment of the amygdala as a whole, and for measuring activation and FC of the three main subregions, each of which contains multiple nuclei with specialized roles. The primary objective of this scoping review is to provide a broad overview of 3T fMRI protocols in use to image the activation and FC of the amygdala with particular reference to spatial resolution. The secondary objective is to provide context for a discussion culminating in recommendations for a standardized protocol for imaging activation of the amygdala and its subregions. As the advantages of big data and protocol harmonization in imaging become more apparent so, too, do the disadvantages of data heterogeneity.
Evidence Level: 3
Technical Efficacy: Stage 2

J. MAGN. RESON. IMAGING 2024;59:361–375.

Functional Magnetic Resonance Imaging (fMRI) has become one of the most powerful tools in the investigation of functional organization of the brain since its inception in the early 1990s.[1] Continuous technical developments in this noninvasive technique have led to its broad adoption for investigating neural activation and functional connectivity (FC) within the brain,[2,3] particularly by neuropsychiatric researchers investigating potential neural alterations in mental health conditions.[4]

From a neuroimaging standpoint, FC has been defined by Friston et al, as "…the temporal correlations between spatially remote neurophysiological events."[5] Put simply, different areas of the brain are considered to be part of the same functional network, demonstrated through a statistical relationship, if they are "active" at the same time.[6]

One region that has been identified in structural and fMRI studies as being broadly implicated in many mental health conditions is the amygdala.[7] The amygdalae are key

View this article online at wileyonlinelibrary.com. DOI: 10.1002/jmri.28836

Received Mar 5, 2023, Accepted for publication May 18, 2023.

*Address reprint requests to: S.L.F., Discipline of Medical Imaging Science, Level 7, Susan Wakil Health Building (D18), Camperdown Campus, Sydney, NSW 2006, Australia.
E-mail: sheryl.foster@sydney.edu.au
Sarah Lewis and Mayuresh S. Korgaonkar are co-senior authors.

From the [1]Sydney School of Health Sciences, Faculty of Medicine and Health, The University of Sydney, Sydney, New South Wales, Australia; [2]Department of Radiology, Westmead Hospital, Westmead, New South Wales, Australia; [3]Brain Dynamics Centre, The Westmead Institute for Medical Research, Westmead, New South Wales, Australia; and [4]University Library, The University of Sydney, Sydney, New South Wales, Australia

Additional supporting information may be found in the online version of this article

components of the brain's emotion circuitry[8] and comprise a pair of very small almond-like structures located in the temporal lobes.[9] fMRI using both task and resting-state techniques has facilitated investigation of the functional role of the amygdala and how it is connected to the rest of the brain in mental health conditions.[7,10] This is important as it has been posited that changes in the organization of functional brain connections are responsible for mental health conditions rather than their causes being attributed to local or regional structural abnormalities.[11] Despite being the subject of much investigation, the role of the amygdala and its functional connections with other brain regions remains poorly understood.[12] This is due, in part, to its diminutive size with average volumes reportedly around 1240 mm^3 (1.24 cm^3).[13] A further barrier to greater understanding is that the amygdala comprises nine functionally different nuclei which are grouped into three discrete subregions, the laterobasal (LB), centromedial (CM), and superficial (SF) (Fig. 1). It has been previously shown that each subregion has a specialized role and displays differential connections to the rest of the brain.[14–17]

Blood Oxygenation Level Dependent (BOLD) contrast, based on an intrinsic sensitivity to local alterations in oxygen consumption driven by neural activation, is the primary mechanism used in fMRI to detect activation in the brain.[18] BOLD signal changes detected on 1.5 Tesla (1.5T) and 3 Tesla (3T) systems are very small, being only 1%–5%[19,20] and Contrast-to-Noise ratio (CNR) provides a measure of these relatively small BOLD signal fluctuations compared to the noise. Aside from the modest BOLD signal changes achieved, a limitation to its use in investigation of the amygdala is the conflicting requirement for high resolution in both space (spatial resolution) and time (temporal resolution).[21] Signal-to-noise ratio (SNR) is the "currency" of MRI and is a major determinant of the levels of spatial and temporal resolution achievable. Typically, imaging sequences provide high spatial or high temporal resolution with each outcome being compromised by the other. As SNR and field strength are directly proportional, ultra-high field strength systems such as 7 Tesla (7T) and above possess inherently higher SNR and can produce images with higher spatial resolution and larger activation-related signal changes.[22,23] However, the bulk of fMRI clinical research is currently performed on 3T systems due to their relatively wider availability and, although the SNR levels are proportionally lower than 7T, there are fewer issues with problematic susceptibility and dephasing artifacts which are a function of ultra-high field strength systems.[22] 3T is now considered as the standard field strength for fMRI studies[24]; however, acquisition protocols appear to be variable, particularly in relation to spatial resolution, resulting in data that is potentially suboptimal in the investigation of very small structures.[25–27]

High spatial resolution, indicated by voxel volume (VV) in mm^3, is required in order to accurately image very small structures such as the amygdala and its subregions[28] and this level of resolution is easily achievable in structural MRI with VV of less than 1 mm^3 (0.001 cm^3) currently in common use.[29] However, for fMRI protocols, data is acquired at much lower spatial resolution, with larger VVs of 20–50 mm^3 considered as "standard"[24] and up to 100 mm^3 commonly in use.[30] This is due to additional temporal constraints on the acquisition of task and resting state fMRI data such as task design, adequate sampling of the brain's haemodynamic response and sufficient SNR and CNR for desired brain coverage. Slices covering the whole brain (one volume) are acquired within one repetition time (TR) period of typically 2–3 seconds which is long enough to account for the brain's relatively slow haemodynamic response[21] and multiple volumes form a time series dataset which can be used to estimate the haemodynamic response function for each task condition. Due to the direct proportionality between SNR and VV the combination of temporal requirements results in parameter selection compromises, making it more challenging to achieve higher spatial resolution.[30] Published fMRI studies reveal wide data heterogeneity with VV in use for reporting on amygdala activation and connectivity ranging from 8 mm^3 (0.008 cm^3) to 64 mm^3 (0.064 cm^3).[26,27]

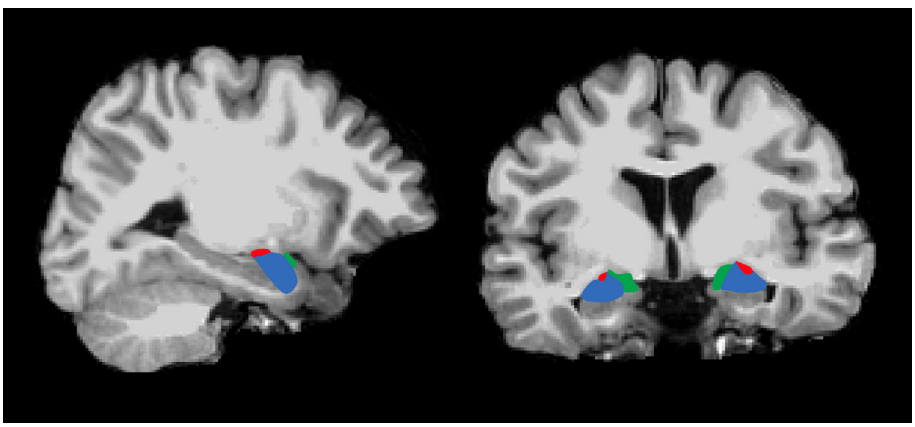

FIGURE 1: T1-weighted sagittal (left), and coronal (right) images showing location of the amygdala and three main subregions (SF = green, LB = blue, CM = red).

Given reports of additional activation and FC patterns being differentiated in many brain regions using high spatial resolution fMRI at both 3T and 7T,[22,23] optimization and wider implementation of a high-resolution technique at 3T is overdue, particularly for the amygdala and its significantly smaller subregions. Other aspects of the data collection process also deserve scrutiny. Appropriate selection of acquisition plane can potentially reduce through-plane signal dephasing and improve SNR levels.[31,32] Similarly, the choice of radiofrequency (RF) coil design is an important consideration which can impact significantly on SNR levels and achievable spatial resolution.[33]

Many technical choices are made in the establishment of fMRI protocols, with sites having differing access to hardware and software options and varying levels of expertise. However, selection of optimal VV is an important aspect that can be easily implemented with positive consequences for data quality.[34] The focus of this scoping review is on the spatial resolution values achieved in a wide range of published fMRI protocols used for reporting amygdala activation and FC. Its objective is to provide a broad overview for the purpose of stimulating discussion in three key areas:

1. Variations in VV used in studies evaluating activation and FC in the amygdala and its subregions.
2. Potential advantages of protocol optimization such as improvements in data quality and reproducibility with an emphasis on the amygdala subregions.
3. Value of protocol harmonization in addressing the challenges of data heterogeneity in big data collaborations.

Methods

This review protocol follows the Preferred Reporting Items for Systematic reviews and Meta-Analyses extension for Scoping Reviews (PRISMA-ScR) methodology[35] as well as the 5-step methodological framework of Arksey and O'Malley.[36] The scoping review protocol is registered at the Open Science Framework (osf.io/e3c28) and published as a preprint online.[37]

Adhering to the recommendations of Bramer and colleagues[38] for achieving maximum recall rate, the following databases were searched on February 9th and 11th, 2022; Medline, Embase, Web of Science, Google Scholar and Scopus. Medical Subject Headings terms for the search, which excluded nonhuman studies, encompassed the following terms:

1. Functional Magnetic Resonance Imaging OR functional MRI OR fMRI
2. Amygdal* OR amygdal* nucleus
3. Functional connect* OR FC (functional connectivity)
4. 3 Tesla OR 3T

The database searches yielded a total of 572 publications which were then imported into Covidence software.[39] Of these, 186 were automatically identified as duplicates leaving 386 for screening and data extraction. Two authors (SF and IB) independently performed all screening; 75 records were excluded during abstract and title screening while a further 119 were excluded at full-text review resulting in a total of 192 articles for inclusion. The mean number of participants per study was 69. A PRISMA flowchart outlining the search, screening and selection strategy along with reasons for exclusion is shown at Fig. 2.

Given that fMRI data quality and inherent image resolution is a complex topic, six sub-questions were investigated and data were extracted for discussion:

1. What sequence type was used for data acquisition?
2. What spatial resolution values were achieved (VV in mm^3)
3. What imaging plane was utilized?
4. Was whole brain coverage achieved?
5. What was the sequence acquisition time?
6. What type of radiofrequency (RF) coil was utilized for signal reception?

Results

As this review captured a large number of publications, the full data extraction table and reference list is provided in the Supplementary materials. Table 1 provides an overall data summary and Table 2 provides a summary of studies with subregional findings. Figure 3 illustrates the results at-a-glance.

Sequence Type

The T2*-weighted two-dimensional (2D) Gradient Echo-Echo Planar Imaging (GE-EPI) sequence was the most common acquisition sequence with 85% of studies (n = 164) reporting its use exclusively and a further 6% (n = 11) of authors not specifically naming their sequence but reporting parameter selections in keeping with GE-EPI. A total of 11 studies used spiral sequences, three of which also used GE-EPI and combined the data from both sequences. Two studies used Spin Echo-Echo Planar Imaging (SE-EPI), one used dual-echo EPI, one used a gradient spin echo technique and one used the Arterial Spin Labeling (ASL) technique. One study acquired data with both GE-EPI and ASL techniques.

A majority of studies (56%, n = 108) focused on acquisition of resting state fMRI (rs-fMRI) data while 35% (n = 68) focused on task-based fMRI, where participants are asked to view images or actively engage in a task during the scan. Sixteen studies reported both task and rs-fMRI acquisitions, while two studies by the same group reported using task data for intrinsic resting state data analysis,[40,41] an approach that has been previously validated.[42]

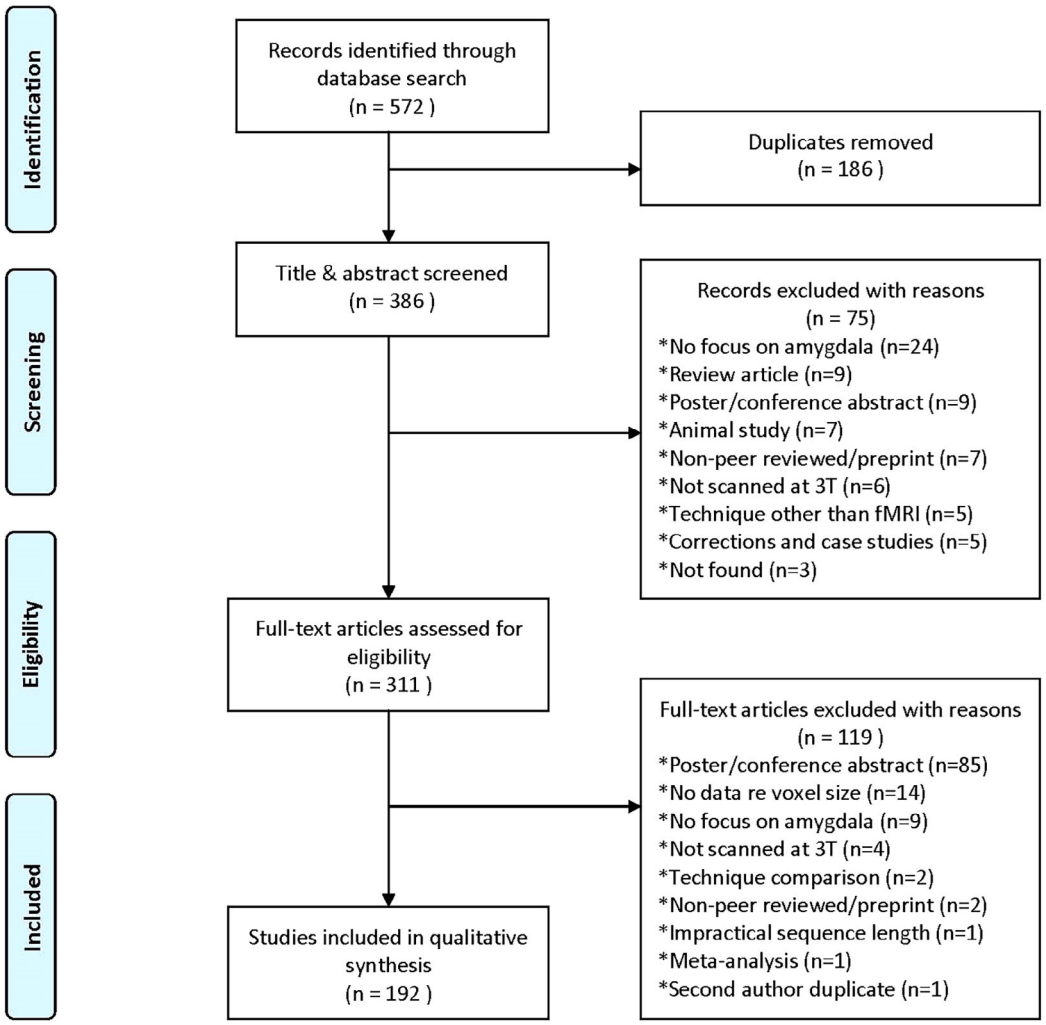

FIGURE 2: PRISMA flowchart outlining inclusion and exclusion process.

Spatial Resolution

VV ranged widely from 7.3 mm^3 (pixel size = 2.44 mm^2 × slice thickness = 3 mm) to 100 mm^3 (pixel size = 25 mm^2 × slice thickness = 4 mm). Fourteen of the 192 studies aggregated data from multiple protocols and scanners, only one of which used the same VV across protocols. To facilitate presentation and discussion of our results, we used Olman and Yacoub's proposal of VV ranges. From 1 to 20 mm^3 was considered high resolution and greater than 20 mm to 50 mm^3 was considered standard resolution.[24] All studies with VV greater than 50 mm^3 were considered to be low resolution.

Of the 192 studies reviewed, only 16% (n = 30) acquired high-resolution data exclusively with a further four combining high and standard resolution data. All data acquired in 66% of studies (n = 126) was standard resolution with a further three combining standard and low-resolution data. Of the remaining studies, 15% (n = 30) reported use of low-resolution data exclusively and a further three combined low and standard resolution data. Of the low-resolution studies, the data from all but one fell into the range of 50–70.3 mm^3 with a single study reporting a VV of 100 mm^3.

Slice thickness or through-plane resolution ranged from 2 to 5 mm with 66% of studies (n = 127) exclusively using data with the median slice thickness of 3.5 mm or less. The protocol in 74% of studies (n = 143) did not use a slice gap technique. Studies not specifically reporting a slice gap were presumed to have none. Of the remaining 49 studies reporting a slice gap, four combined data using both techniques.

Slice gaps, commonly referenced as a percentage of slice thickness, ranged from 0% to 33.4% of slice thickness in 88% of the 49 studies using this technique. Of the remainder, two studies employed a gap of 50% (4 mm/2 mm, 2 mm/1 mm), two used a gap of 53.8% (2.6 mm/1.4 mm), one used a gap of 100% (3 mm/3 mm) while one reported a gap of 125% (3.4 mm/4.25 mm).

Imaging Plane

Axial or axial oblique acquisition planes were by far the most popular choice, with 97% of studies (n = 186) utilizing this

TABLE 1. Data Summary of All Studies (n = 192)

Sequence Type		Spatial Resolution, VV Range = 7.3–100 mm^3		Imaging Plane		Full Brain Coverage		Acquisition Time (TA), Range = 2 Minutes 44 Seconds–24 Minutes		RF Coil Type	
GE-EPI	175	High res 1–20 mm^3	30	Axial/axial oblique	186	Yes	185	<6 minutes	23	8 Ch	35
Spiral version	8	Std res >20–50 mm^3	126	Coronal/coronal oblique	2	No	7	6–8 minutes	52	12 Ch	21
GE-EPI & Spiral	3	Low res >50 mm^3	29	Sagittal	4			>8–10 minutes	21	16 Ch	1
SE-EPI	2	Mixed resolution	7					>10 minutes	13	20 Ch	1
DE-EPI	1	Slice thickness (ST) range = 2–5 mm						Mixed TA	4	24 Ch	1
Gradient SE	1	ST ≤3.5 mm	127					Not stated	79	32 Ch	42
ASL	1	ST >3.5 mm	65							64 Ch	3
GE-EPI & ASL	1	No slice gap	143							Mixed	3
		Slice gap	45							Other	17
		Mixed gap/no gap	4							Not stated	68

TABLE 2. Data Summary of Subregional Studies (n = 21)

Sequence Type		Spatial Resolution, VV Range = 8–70.3 mm^3		Imaging Plane		Full Brain Coverage		Acquisition Time (TA), Range = 4 Minutes 48 Seconds–15 Minutes		RF Coil Type	
GE-EPI	18	High res 1–20 mm3	4	Axial/axial oblique	20	Yes	21	<6 minutes	2	8 Ch	1
Spiral version	1	Std res >20–50 mm^3	10	Axial oblique (−30°)	1	No	0	6–8 minutes	8	12 Ch	2
DE-EPI	1	Low res >50 mm^3	4	Coronal/coronal oblique	0			>8–10 minutes	2	32 Ch	7
GE-EPI & ASL	1	Mixed resolution	3	Sagittal	0			>10 minutes	4	Mixed 12 & 16ch	1
		Slice thickness (ST), range = 2–5 mm						Not stated	5	Other	3
		ST ≤3.5 mm	11							Not stated	7
		ST >3.5 mm	8								
		Mixed slice thickness	2								
		No slice gap	17								
		Slice gap	2								
		Mixed gap/no gap	2								

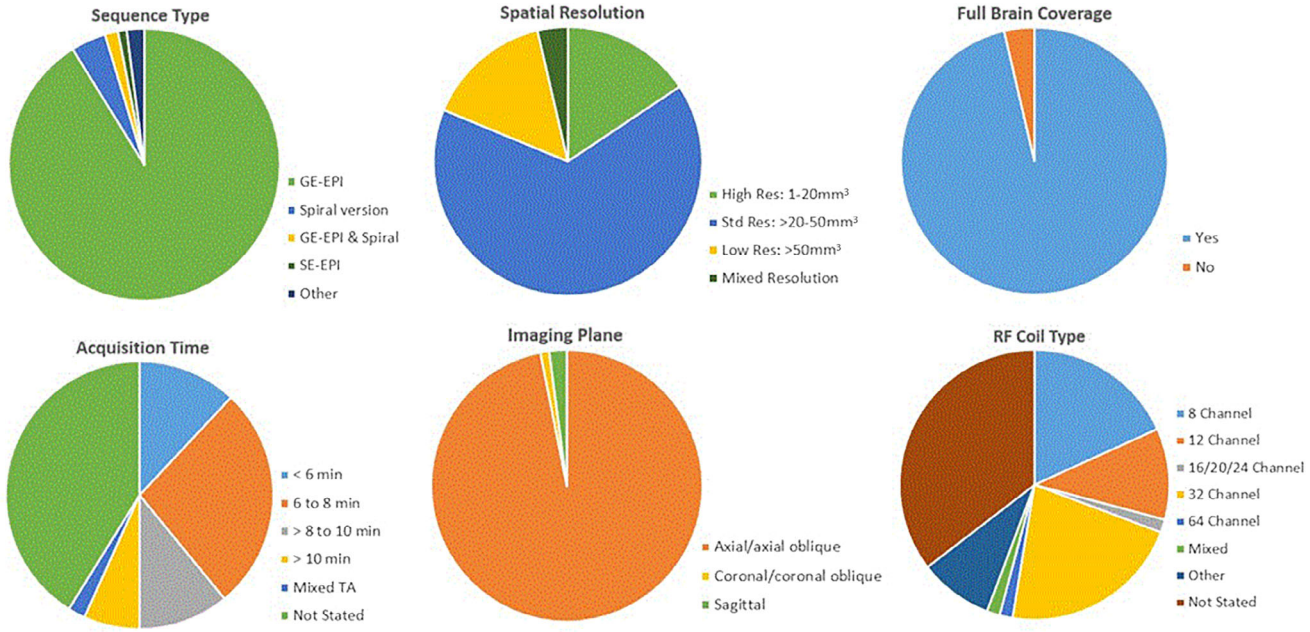

FIGURE 3: Results at-a-glance.

plane. Of the remaining six studies, four used sagittal and two used coronal or coronal oblique planes. Studies not directly reporting an acquisition plane (n = 68) were presumed to have acquired axial or oblique axial slices due to this being the most commonly used plane.[43]

Whole Brain Coverage

Whole brain coverage was obtained in 96% of studies (n = 185), with all but six of these also utilizing the axial or oblique axial plane. Of the seven studies acquiring limited brain coverage, only five acquired high-resolution data and all used axial or oblique axial planes as well.

Sequence Acquisition Times

There was a wide variation in acquisition times (TA) with the shortest sequence being reported at 2 minutes 44 seconds and the longest single TA at 24 minutes. TA was unreported in 41% of studies (n = 79) and, of the remaining 113 studies, 20% (n = 23) used TA of less than 6 minutes only, 46% (n = 52) used a TA of 6 to 8 minutes only, 19% (n = 21) used a TA of more than 8 to 10 minutes only and 12% (n = 13) used a TA greater than 10 minutes only. Four studies reported TAs from two different TA groups, due to either the use of different TA for task and rs-fMRI acquisitions or the combination of data from different sites and/or MRI systems. Two studies combined four separate 15 minute acquisitions for a total of 1 hour of data.

Radiofrequency Coils

As expected, most studies used data acquired on a single coil type with the most commonly used being the 32-channel phased array in 22% (n = 42) of studies. This was followed by the 8-channel phased array with 18% (n = 35) and 12 channel phased array with 11% (n = 21). Three studies utilized the newer technology 64 channel head/neck phased array while one used the 16-channel phased array, and one each used 20 and 24 channel phased arrays. Three studies combined data acquired on different coil types, two of which used data from both 8 and 32 channel phased arrays while one combined data from 12 and 16 channel phased arrays. The remaining 9% (n = 17) reported use of birdcage, quadrature, custom-designed or other ambiguously-named coil types. In approximately 35% of studies (n = 68), the authors reported no information on RF coil type.

Results for Studies Reporting Subregional Findings

Twenty-one studies reported subregional activation in the amygdala.[17,44–63] A summary of the data relating to these studies is reported in Table 2. Of these, 18 used the GE-EPI sequence and one each used the spiral and DE-EPI techniques, with one combining data acquired with both GE-EPI and ASL techniques. Only four studies used high-resolution data exclusively[17,45,46,62] while two other studies used a combination of high and standard resolution data.[44,59] Ten studies used standard resolution data.[47–49,53–56,58,61,63] Four studies used low-resolution data[51,52,57,60] and one combined standard and low-resolution data.[50] Interestingly, four studies reported subregional findings using low-resolution data with VV larger than 50 mm^3,[51,57] two of which used VV of 70.3 mm^3.[52,60] Four of the studies used a slice gap technique, two of which used a gap of 33.3%,[54,55] one used a gap of 25%,[50] and one used a gap of 12.5%.[56]

All 21 studies acquired whole brain data in the axial oblique plane with one study reporting use of a "—30°" slice

tilt to minimize signal loss.[63] TA ranged from 4 minutes 48 seconds in a study using VV of 42.9 mm^3[47] to 15 minutes per sequence in two studies that utilized Human Connectome Project[64] data with VV of 8 mm^3. These groups combined data from four 15-minute acquisitions for analysis.[17,45] Five studies did not report their TA but of the 16 that did, 50% used a TA from 6 to 8 minutes. Seven studies did not report on their RF coil type, but of the remaining 14, 50% used a 32-channel phased array.

Discussion

In providing an overview of the acquisition protocols in use at a large number of imaging sites, this review has revealed the disparity in spatial resolution of fMRI data acquired to investigate the amygdala and its subregions. While the same sequence type and imaging plane was used in a large majority of studies, spatial resolution values and acquisition times were found to vary widely. This was particularly notable in the studies reporting subregional activation in the amygdala, with results in 81% of these studies relying on standard, low or mixed resolution data. This use of suboptimal techniques to image the amygdala together with significant variation in scanning parameters may be contributing to incongruent findings across studies as well as lack of success in study replication.

The T2*-weighted Gradient Recalled Echo (GRE) or Gradient Echo (GE) pulse sequence is inherently sensitive to BOLD-related susceptibility effects and is the mainstay in use at 3T due to the predominance of T2* contrast over T2 contrast.[3] The 2D version of the GE Echo Planar Imaging (GE-EPI) sequence, with its high BOLD sensitivity, is considered the gold standard.[43] In addition, its ease of implementation and wide availability in both research and clinical environments has rendered it the sequence of choice for fMRI of the brain[24] and this was evident in our review with over 90% of studies employing this technique. The primary difference between spiral and GE-EPI sequences is the k-space trajectories; spiral sequences traverse k-space from the center to the periphery while GE-EPI employs a Cartesian trajectory of line-by-line acquisition.[65] Spiral k-space trajectory techniques have been shown to be superior to GE-EPI techniques in recovering signal in areas typically affected by susceptibility-induced field gradients such as frontal and medio-temporal areas, with the difference in magnetic susceptibility values at air/tissue interfaces typically being around eight parts per million (ppm).[66] However, the use of these techniques is not widespread, as evidenced in our review, partly due to the requirement for lengthy non-standard offline image reconstruction which many clinical research sites cannot support.[67] The use of alternative acquisition techniques was also minimal due to their shortcomings. Arterial spin labeling is limited in fMRI due to its relatively poor functional contrast and temporal resolution, despite its high spatial accuracy.[68] Gradient spin echo techniques are also not commonly used due to their lower sensitivity, reduced brain coverage and greater heat deposition into the patient reported as Specific Absorption Rate (SAR) in watts per kilogram.[43]

Data Quality—SNR, CNR, and Spatial Resolution Considerations

Both SNR and CNR are used as measures in assessment of overall data quality in fMRI. As data provides information about signal fluctuations and stability over a time course SNR is referenced as temporal SNR (tSNR), or mean signal intensity over time.[25,69] As previously outlined, SNR and VV are directly proportional.[19] In theory, the use of smaller VV to achieve higher resolution fMRI data results in reduced tSNR per individual voxel which seems intuitively undesirable. Therefore, in the compromise between tSNR and achievable spatial resolution when selecting VV, often spatial resolution suffers.

However, there are several other issues to consider in relation to overall data quality when choosing VV. Of primary concern is the location of the amygdala itself. tSNR is diminished by localized main magnetic field (B0) inhomogeneity which results in signal loss and image distortion at air/tissue interfaces. Intravoxel dephasing or signal drop-out occurs when B0 is inhomogeneous within an individual voxel, effectively reducing its SNR contribution.[70] Areas particularly impacted are the inferior temporal regions and sphenoid sinuses adjacent to the amygdala where protons are effectively spinning at different frequencies.[71] Also, with Cartesian k-space trajectories such as that used in GE-EPI sequences, distortion results from voxels being mismapped due to phase errors. In these scenarios, increasing spatial resolution by reducing VV has been shown to improve data quality[21] and potential increases in BOLD signal can be obtained by acquiring smaller voxels in areas such as air/bone interfaces that are traditionally difficult to shim well.[19] Similarly, Olman and colleagues reported that although tSNR was reduced when using smaller VV there was less signal variability across the Medial Temporal Lobe, resulting in more consistent BOLD sensitivity across the region of interest.[70] Further, Robinson et al focusing their measurements on the amygdala, showed that the SNR penalty incurred in halving the VV by reducing the slice thickness to 2 mm was offset by a notable decrease in intravoxel dephasing.[72]

Partial volume averaging occurs with larger voxels that encompass a mix of tissue types and its effects can be reduced by matching the VV or spatial resolution to the size of the potential activation during the acquisition in order to maximize functional CNR.[73] Partial volume averaging effects have also been shown to be particularly significant in imaging the amygdala, not only due to its small size but its location adjacent to the Basal Vein of Rosenthal which has been shown to

give rise to confounding vascular signals when it is partially contained when using larger voxels.[32]

As BOLD signal changes are effectively the signal of interest, CNR has been suggested as the primary indicator of data quality.[20] CNR is maximized by reducing noise contributions which have a greater negative impact in fMRI. Unlike background noise in MRI images, noise in fMRI time series data is a blend of physiological noise such as respiratory and cardiac pulsation and thermal noise being emitted by the MR system components as well as from the patient's body.[20,74] Maximal CNR has been shown to be achievable with higher spatial resolution imaging in conjunction with mitigation of noise contributed by artifactual and physiological signal fluctuations.[19] Physiological noise contributions also reduce tSNR levels and can be addressed during data post-processing and analysis.[75]

Taken together, these technical points provide justification for utilizing smaller VV in fMRI focusing on the amygdala, even though only 16% of studies in this review utilized high-resolution data in reporting their findings.

Selection of Slice Orientation and Acquisition Method

Data acquisition can be performed sequentially or in an interleaved fashion. Researchers typically use an interleaved slice acquisition technique which is advantageous as it precludes the use of a slice gap.[76] Using a sequential slice acquisition method without a slice gap can result in slice excitation leakage or adjacent slice saturation leading to reduced tSNR[77]; however, MR system manufacturers have developed and implemented methods to mitigate these effects.[78] Of the studies reporting use of a slice gap technique it is unknown whether an interleaved or sequential slice acquisition technique was used as this data was not extracted for the current review.

A general disadvantage of using a gap technique is that spin-history artifacts can occur with through-plane head motion which is more severe with increasing gap size. On the other hand, the gap technique can be advantageous as it allows increased brain coverage while keeping within a defined TR and slice envelope. However, when imaging the amygdala, use of a gap technique could result in missing potential activation occurring in tissue in between the imaged slices.[79–81] As the almond-shaped amygdala is very small at only around 10 mm in width[32] with an average volume of approximately 1240 mm^3,[13] the acquisition of interleaved contiguous axial 3 mm slices would likely result in amygdala tissue appearing in only 3–4 slices, and even fewer if thicker slices or a slice gap technique was used. This highlights the importance of considering the size of the structure of interest when making protocol decisions about spatial resolution and slice acquisition techniques. Of the studies in this review reporting on the subregions 20% used some or all data acquired with slice gaps, two of which used standard resolution data with 3 mm slices and a 33% gap while another used combined standard and low-resolution data with 5 mm slices and a 25% gap.

Slice orientation has the potential to contribute to signal loss in T2*-weighted imaging and selection of acquisition plane should be also considered in relation to the particular brain regions under investigation. The plane introduced by Talairach and commonly referred to as the AC-PC (Anterior Commissure—Posterior Commissure) line is reportedly the most widely used and has been broadly adopted as a standard reference angulation in fMRI acquisitions[43,82] and this was evident in our review with 97% of studies reporting its use. Acquisition of whole brain data parallel to the AC-PC line is more time-efficient as it requires around 30% less slices compared to the coronal plane.[72,82] The use of axial slices angled at approximately −30° (i.e., with the anterior edge of the slice tilted cranially) has been reported to improve BOLD sensitivity in the region of the amygdala as well as decreasing susceptibility-related signal loss; however, this angulation may be suboptimal for imaging other regions when acquiring whole brain data that is a requirement for FC studies.[63,83] Only one study in our review utilized this slice angulation and they reported subregional findings using standard resolution data. Although the study was based on task activation rather than investigation of FC, whole brain coverage was acquired with this angulation.[63] Selection of imaging plane in relation to orientation of the structure of interest, especially when using rectangular or anisotropic voxels, is also an important consideration. The use of large voxels that are also anisotropic has been shown to provide inaccurate data on volume and shape of small nuclei as well as a reduction in signal sampling accuracy which is based on the largest voxel dimension. Therefore, small isotropic voxels are preferred because of their cubic nature.[84,85]

Earlier studies on 1.5T systems have explored the use of other slice orientations for improved imaging of the amygdala. Merboldt et al found that optimal BOLD imaging for investigation of the amygdala required data acquisition in the coronal plane.[86] Chen and colleagues also reported that, for the amygdala, the largest susceptibility field gradients occur in the superior–inferior (SI) direction and higher BOLD sensitivity was demonstrated in oblique coronal images in conjunction with frequency-encoding in the SI direction.[87] This was in agreement with Bandettini who noted the use of coronal and sagittal slice acquisitions in many studies for the same reason.[19] However, along with the arrival in the mid-2000s of 3T systems with more powerful gradients, came a number of additional technical considerations. While superior gradient performance has many advantages, use of stronger gradients was restricted when using a coronal orientation in conjunction with SI phase encoding. This was due to reports of peripheral nerve stimulation and potential signal aliasing

using this configuration, thereby limiting its use.[34,87] A further consideration following the primary selection of phase encoding direction is the secondary choice, for example, SI or inferior–superior (IS). In areas affected by susceptibility artifacts this choice has been shown to impact on the accuracy of data analysis. Depending on the direction selected, images can be either distorted by distraction or compression; choosing the direction resulting in signal distraction is preferred as signal within regions of interest that have been compressed cannot be recovered during analysis.[70] In our review only, four studies used the sagittal plane and two used coronal or coronal oblique planes. None of the six reported subregional findings and all acquired whole brain coverage with standard or low resolution VV, a protocol decision potentially driven by the conflicting need to acquire more slices for high-resolution data when scanning in these orientations.

Whole Brain Coverage vs. a Targeted Approach

To accommodate the need for high spatial resolution data acquisition, multi-resolution approaches have been proposed in which a lower-resolution whole brain dataset is acquired to identify the site of activation, following which a targeted high-resolution dataset is acquired at that site.[73] In cases where the location of the target is known, it can be time-saving to focus only on the desired area of activation rather than acquiring high-resolution data over the whole brain. The latter approach necessitates an increased number of slices for coverage resulting in increased TR and reduced temporal resolution. These issues present a conundrum when considering the optimal acquisition strategy for the amygdala as both high spatial and temporal resolution are required. If the purpose of the study is to investigate FC, whole brain coverage is necessary as activation needs to be interpreted within the context of amygdala connections with other spatially remote brain regions, rendering a reduced-coverage approach impractical.[34,88] Seven studies in our review used a targeted approach with all acquiring task rather than resting-state data. Of these, five acquired high-resolution data and two acquired standard resolution data. Only 1 of the 21 studies reporting on the amygdala subregions used a targeted approach and this group acquired high-resolution data.[62]

Optimal Sequence Acquisition Time

Choice of TA can involve compromise for a variety of reasons, with participant population being a major consideration. TA can also differ between task and resting state acquisitions with longer TAs of 15–25 minutes being recommended for FC studies with greater reproducibility.[89] However, Van Dijk and colleagues showed that fMRI with TA of around 6 minutes was satisfactory for demonstrating FC patterns in the brain and that performing more runs reflected only marginally on data reliability.[90] Of the 113 studies in our review that reported their TA, only 15 used a TA of less than 6 minutes to acquire FC data and 40 studies used a TA of 6 to 8 minutes. Acquiring more data over a longer TA allows the possibility of discarding portions of motion-affected data while still retaining enough temporal measurements for analysis. However, as extended scan times can result in patient movement, TAs of 6 to 8 minutes provide a reasonable compromise.

In the absence of acceleration techniques (discussed below) TA is a relatively simple calculation of the product of TR and number of volumes acquired. Temporal resolution in fMRI, effectively the time taken to acquire all slices once (i.e. one TR) is negatively impacted when acquiring higher spatial resolution data as more slices are required for whole brain coverage. Maintaining the same TA could be achieved by a reduction in the number of volumes acquired.[77] However, the very small signal changes of only around 1%–5% make BOLD imaging extremely challenging and decreasing both the number of volumes and the VV in order to maintain the TA would significantly reduce tSNR.[25] In fact, one method used to improve tSNR when seeking to image at higher resolution is to acquire a greater number of time points or volumes by scanning for longer, thus reaping the benefits of signal averaging; however, a doubling of scan time only increases SNR by a factor of $\sqrt{2}$.[33]

The critical nature of the relationship between TA and tSNR in detection of fMRI effect size has been demonstrated by Murphy et al, whose work outlined the value to researchers of prospectively determining the required effect size to a specific *P*-value. Using this information together with tSNR values they demonstrated that the TA appropriate to each fMRI experiment can be calculated and that an increase in tSNR can significantly reduce TA for a given effect size.[25]

Radiofrequency Coil Technology

The evolution of RF coil technology and, in particular, the introduction of phased array coils has positively impacted SNR levels and data quality.[33] This review revealed use of a wide range of coil types, including traditional volume transmit/receive types through to a variety of multi-channel phased array receivers ranging from 8 to 64 channels. Multi-channel phased arrays have been shown to provide SNR benefits over traditional volume coils, in part due to their improved filling-factor which relates to coil fit with regard to the region of interest.[33] Of the studies in this review reporting their coil type, 84% used a multi-channel phased array for signal reception.

An early demonstration of the superiority of multi-channel coil technology in the anterior Middle Temporal Lobe was reported by Bellgowan et al in a comparison between higher and standard resolution slices (2 and 4 mm) acquired with both an older style transmit/receive volume coil and a 16-channel array receiver. They reported significant

improvements in tSNR and CNR when acquiring high-resolution data but noted this was only possible with the use of the multi-channel array coil.[91]

Since their introduction, multi-channel coils have been adapted to accommodate increasing numbers of individual elements and 64 channel phased array coils are now available. A less desirable function of coils with very high numbers of elements is a reduction in depth penetration in line with decreasing element size. Higher SNR is evident peripherally due to the close proximity of the arrays to the anatomy while signal drop-off may be seen centrally, resulting in signal non-uniformity across the FOV.[33] Correction algorithms to compensate for this are widely available on commercial MRI systems, the use of which is recommended in studies focusing on deeper sub-cortical structures such as the amygdala.[92]

The most commonly used coil type in this review was a 32-channel phased array which is intuitively a good compromise between high SNR and adequate depth penetration for improved signal uniformity, an important consideration as the amygdala is a relatively deep brain structure. Interestingly, in a direct comparison between 32 and 64 channel phased arrays, a study by Keil et al[93] found that the 64-channel phased array outperformed the 32-channel phased array centrally as well as peripherally in SNR terms when acceleration factors of 3 or more were used. This was due to g-factor (noise amplification) improvements attributed to the reduced element size allowing better spatial distinction of the variation in signal intensities and this was also the case when the Simultaneous Multi Slice (SMS) technique was employed. As the 64-channel head/neck array is relatively new technology, its use may become more widespread as sites look to upgrade their head coils in the future.

Phased array coils possess several advantages over earlier coil designs. Along with the capability for imaging larger fields-of-view with inherently higher SNR, their use allows spatial localization of signals. This provides opportunities for reducing TA by employing in-plane (parallel imaging) and through-plane (SMS) acceleration techniques. In general, differing coil sensitivity profiles in these arrays allow signals to be spatially localized, thus enabling data undersampling with a concomitant reduction in TA. Data can then be fully reconstructed based on individual coil sensitivity profiles. However, although in-plane acceleration is used in fMRI, its main advantage is not reduced TA but improved data quality. This results from reduced signal dephasing due to shorter achievable echo train lengths, inter-echo spacing and optimal echo time (TE) selection. The primary disadvantage of its use is the accompanying SNR penalty as a result of undersampling.[77,94] Even so, Schmidt and colleagues recommended its use in the Medial Temporal Lobes, prioritizing the marked decrease in image distortion in this location over the potential loss of SNR and BOLD sensitivity.[95]

Conversely, the primary advantage of the through-plane SMS technique is a reduction in temporal resolution. In this case, the variations in coil sensitivity profiles enable spatial differentiation of multiple slices which can be excited simultaneously. This allows the use of shorter TRs, meaning that either TA can be reduced or statistical significance improved by acquiring more data points.[96] While the SMS technique does not attract a SNR penalty, its implementation may result in higher SAR levels.[76]

Further Considerations

There are many other aspects relating to fMRI data acquisition and quality that are outside the scope of this review. First, the choice of echo times (TE) is an important consideration. Shorter TEs may result in improved data quality due to a decrease in susceptibility-related signal loss due to dephasing. However, the penalty is reduced BOLD sensitivity which is optimized when the effective TE value approximates the T2* of the tissue being imaged (around 40–50 msec at 3T).[95] T2* values also increase with improved spatial resolution.[19] Robinson and colleagues, in a comparison between high and standard resolution VV, showed that the measured T2* value in the amygdala doubled from 22 to 43 msec in the high-resolution data set, approaching the cortical value of 52 msec which was similar at both resolutions.[72] This has obvious implications for researchers using shorter TEs based on T2* values calculated from standard or lower resolution data acquired in the amygdala.

Second, the use of SMS allows significant reductions in TR, speeding up the acquisition but also resulting in lower SNR if the TR is lower than the T1 of the brain tissue being imaged. TR values of lower than 500 msec reportedly result in a marked reduction in functional contrast levels.[19] This was confirmed by McDowell and Carmichael in their 3T investigation of event-related tasks in which they showed there was little advantage to using TR values below 800 msec.[97] However, the potential benefits in rs-fMRI may outweigh the primary disadvantage of using typical TRs of 2–3 seconds used in task acquisitions, this being aliasing of respiratory and cardiac signal fluctuations into the lower frequency range associated with resting state fluctuations, confounding the data.[96,98] However, when using short TRs that could result in tissue saturation, the flip angle should be optimized to the Ernst angle to maximize SNR, and this may also have the added benefit of lower SAR.[76] Further, it has been shown that consideration needs to be given to choice of multiband (MB) factor (the number of slices acquired simultaneously) when using SMS. To prevent saturation artifacts, a simple calculation must be made in which the total number of slices divided by the MB factor should result in an odd number.[76]

Although data processing and analysis techniques are integral to this topic, their discussion is also outside the scope of this review. However, it should be noted that, as improvements are made in spatial resolution of acquisitions,

consideration should be given to suitability of data pre-processing steps and analysis techniques in current use. For high spatial resolution datasets, tSNR and detectability of BOLD signal changes have been shown to be increased by spatial smoothing.[99] However, other aspects of the data processing and analysis pipeline may detrimentally affect the spatial resolution of the acquired data and researchers have called for an awareness to look beyond the use of conventional parameters when pre-processing high-resolution data in order to avoid nullifying any benefits derived from its acquisition.[25,100]

Our Recommendations

We conclude with a list of our hardware and protocol recommendations for fMRI of the amygdala and its subregions that may be easily implemented in clinical and research sites. Having compiled evidence during the review process of best practice for individual aspects of image acquisition protocols relating to our topic, we established that this information may be useful to other researchers.

1. 3 Tesla MRI system and 32 or 64 channel phased array coil to accommodate parallel imaging and SMS techniques
2. T2*-W 2D GE-EPI high resolution sequence with VVs of 20 mm^3 or less (preferably 2–2.5 mm isotropic)
3. Contiguous interleaved axial oblique images parallel to the AC-PC line
4. Whole brain coverage to facilitate FC analysis
5. TA of 6–8 minutes (or prior determination of effect size at given p-value to calculate required TA)
6. MR system-specific non-uniformity correction algorithm
7. TR value optimized for study objective (task vs. resting state)
8. TE value optimized for spatial resolution of acquired data

Further to these recommendations and in the interests of promoting protocol harmonization and reproducibility, we recommend the development and use by researchers of a checklist for reporting key aspects of hardware and fMRI data acquisition, comparable to that developed recently by Lin and colleagues for use in reporting Magnetic Resonance Spectroscopy (MRS) studies for publication.[101] In 2008, Poldrack et al included a list of data acquisition recommendations for fMRI in their publication "Guidelines for reporting an fMRI study".[102] Taking into account technological advances since that time and noting that key imaging parameters such as acceleration factors are often not reported, we have proposed a checklist template for fMRI data acquisition. This template can assist researchers in two ways; first, as a means of ensuring protocol harmonization and reproducibility for multicenter studies as well as serving as a draft providing an accurate description of data acquisition for reporting of methods for publication. A copy of the checklist template is located in the Supplementary Materials.

Limitations

The field of fMRI is broad with many variations in data acquisition techniques in use. Our purpose was to map out an overview of current techniques with a focus on spatial resolution. The narrow confines of the review are a major limitation due to the interrelatedness of multiple aspects of the data acquisition and analysis process, outlined above, that fell outside its scope. However, it focuses on one nontrivial aspect of the acquisition process that can be easily manipulated by researchers looking to optimize their data to answer specific questions.

A further limitation is that articles in-press or published after our literature search are not included. However, our selection of databases and search strategy was designed to maximize the number of publications identified for inclusion.

Last, we have not attempted to compare SNR levels between studies as there are many complex factors determining these values for individual studies. Due to lack of consensus among researchers, both SNR and CNR values can be calculated using different methods resulting in different scales, rendering any comparisons meaningless.[20]

Conclusion

This scoping review provides an overview of the fMRI protocols in use for investigation of amygdala activation and connectivity. Data quality in fMRI is contingent on a complex amalgamation of components which includes both CNR and SNR and, by extension, spatial resolution. While researchers are locked into their site's field strength and scanner capability and, to a lesser extent, RF coil and sequence availability, decisions relating to parameter selections such as VV, acquisition time, slice orientation and coverage should be carefully scrutinized by researchers in the context of their study objectives. This review has identified considerable disparity in fMRI acquisition protocols across imaging sites, resulting in broad data heterogeneity, particularly in relation to studies focusing on the subregions. To counter this, we provide recommendations for optimization of imaging the amygdala and its subregions at 3T. The continued focus on biomarker identification at an individual level in many health conditions, the advent of machine learning in large datasets and fewer funding opportunities for research has resulted in renewed interest in collaborative consortium-style approaches as demonstrated by groups such as Enhanced Neuroimaging and Genetics through Meta-Analysis and International Consortium for Brain Mapping. Protocol optimization and harmonization across sites performing similar research studies would be a simple yet effective way to progress the field.

Acknowledgments

The authors would like to thank Elizabeth Haris for creation of T1-W images and Simon Pullman for assistance with

graphic results. This work was supported by the Westmead Charitable Trust Career Development Grant, Westmead Hospital. Open access publishing facilitated by The University of Sydney, as part of the Wiley - The University of Sydney agreement via the Council of Australian University Librarians.

Conflict of Interest

The authors declare no relevant conflicts of interest.

Data Availability Statement

The data are available from the corresponding author upon reasonable request.

References

1. Bandettini PA, Wong EC, Hinks RS, Tikovsky RS, Hyde JS. Time course EPI of human brain function during task activation. Magn Reson Med 1992;25(2):390-397.
2. Lang EW, Tomé AM, Keck IR, Górriz-Sáez JM, Puntonet CG. Brain connectivity analysis: A short survey. Comput Intell Neurosci 2012; 2012:412512.
3. Glover GH. Overview of functional magnetic resonance imaging. Neurosurg Clin N Am 2011;22(2):133-vii.
4. Zhan X, Yu R. A window into the brain: Advances in psychiatric fMRI. Biomed Res Int 2015;2015:542467.
5. Friston KJ, Frith CD, Liddle PF, Frackowiak RS. Functional connectivity: The principal-component analysis of large (PET) data sets. J Cereb Blood Flow Metab 1993;13(1):5-14.
6. Eickhoff SB, Müller VI. Functional connectivity. In: Toga AW, editor. *Brain Mapping*. Waltham: Academic Press; 2015. p 187-201.
7. Schumann CM, Bauman MD, Amaral DG. Abnormal structure or function of the amygdala is a common component of neurodevelopmental disorders. Neuropsychologia 2011;49(4):745-759.
8. LeDoux JE. Emotion circuits in the brain. Annu Rev Neurosci 2000; 23(1):155-184.
9. Amunts K, Kedo O, Kindler M, et al. Cytoarchitectonic mapping of the human amygdala, hippocampal region and entorhinal cortex: Intersubject variability and probability maps. Anat Embryol 2005;210(5): 343-352.
10. Leppänen JM. Emotional information processing in mood disorders: A review of behavioral and neuroimaging findings. Curr Opin Psychiatry 2006;19(1):34-39.
11. Fornito A, Harrison B. Brain connectivity and mental illness. Front Psychiatry 2012;3:72.
12. Mohanty R, Sethares W, Nair V, Prabhakaran V. Rethinking measures of functional connectivity via feature extraction. Sci Rep 2020;10(1): 1298.
13. Brabec J, Rulseh A, Hoyt B, et al. Volumetry of the human amygdala—An anatomical study. Psychiatry Res 2010;182(1):67-72.
14. Nieuwenhuys R, Voogd J, van Huijzen C. Telencephalon: Amygdala and claustrum. In: *The human central nervous system* (4th ed.). Berlin, Heidelberg: Springer Berlin Heidelberg; 2008. p. 401-426.
15. Bzdok D, Laird A, Zilles K, Fox P, Eickhoff S. An investigation of the structural, connectional, and functional subspecialization in the human amygdala. Hum Brain Mapp 2013;34(12):3247-3266.
16. Swanson LW, Petrovich GD. What is the amygdala? Trends Neurosci 1998;21(8):323-331.
17. Hofmann D, Straube T. Resting-state fMRI effective connectivity between the bed nucleus of the stria terminalis and amygdala nuclei. Hum Brain Mapp 2019;40(9):2723-2735.
18. Matthews PM. An introduction to functional magnetic resonance imaging of the brain. In: Jezzard P, Matthews PM, Smith SM, editors. *Functional magnetic resonance imaging: An introduction to methods*. Oxford: Oxford University Press; 2001. p 4-34.
19. Bandettini PA. Selection of the optimal pulse sequence for functional MRI. In: Jezzard P, Matthews PM, Smith SM, editors. *Functional magnetic resonance imaging: An introduction to methods*. Oxford: Oxford University Press; 2001. p 123-145.
20. Welvaert M, Rosseel Y. On the definition of signal-to-noise ratio and contrast-to-noise ratio for fMRI data. PLoS One 2013;8(11):e77089.
21. Bandettini PA. The spatial, temporal and interpretive limits of functional MRI. In: Davis KL et al., editors. *Neuropsychopharmacology: The fifth generation of progress: An official publication of the American College of Neuropsychopharmacology*. Philadelphia: Lippincott Williams & Wilkins; 2002. p 343-356.
22. Iranpour J, Morrot G, Claise B, Jean B, Bonny J-M. Using high spatial resolution to improve BOLD fMRI detection at 3T. PLoS One 2015; 10(11):e0141358.
23. Sladky R, Geissberger N, Pfabigan D, et al. Unsmoothed functional MRI of the human amygdala and bed nucleus of the stria terminalis during processing of emotional faces. Neuroimage 2018;168:383-391.
24. Olman CA, Yacoub E. High-field FMRI for human applications: An overview of spatial resolution and signal specificity. Open Neuroimag J 2011;5:74-89.
25. Murphy K, Bodurka J, Bandettini PA. How long to scan? The relationship between fMRI temporal signal to noise ratio and necessary scan duration. Neuroimage 2007;34(2):565-574.
26. Salzwedel AP, Stephens R, Goldman B, Lin W, Gilmore JH, Gao W. Development of amygdala functional connectivity during infancy and its relationship with 4-year behavioral outcomes. Biol Psychiatry Cogn Neurosci Neuroimaging 2019;4(1):62-71.
27. Westlund Schreiner M, Klimes-Dougan B, Mueller B, et al. Multimodal neuroimaging of adolescents with non-suicidal self-injury: Amygdala functional connectivity. J Affect Disord 2017;221:47-55.
28. Roy AK, Shehzad Z, Margulies D, et al. Functional connectivity of the human amygdala using resting state fMRI. Neuroimage 2009;45(2): 614-626.
29. Kolesar TA, Bilevicius E, Wilson A, Kornelsen J. Systematic review and meta-analyses of neural structural and functional differences in generalized anxiety disorder and healthy controls using magnetic resonance imaging. Neuroimage Clin 2019;24:102016.
30. Menon RS, Goodyear BG. Spatial and temporal resolution in fMRI. In: Jezzard P, Matthews PM, Smith SM, editors. *Functional magnetic resonance imaging: An introduction to methods*. Oxford: Oxford University Press; 2001. p 146-158.
31. Kim H, Somerville L, Johnstone T, Alexander A, Whalen P. Inverse amygdala and medial prefrontal cortex responses to surprised faces. Neuroreport 2003;14(18):2317-2322.
32. Boubela RN, Kalcher K, Huf W, et al. fMRI measurements of amygdala activation are confounded by stimulus correlated signal fluctuation in nearby veins draining distant brain regions. Sci Rep 2015;5(1):10499.
33. Gruber B, Froeling M, Leiner T, Klomp D. RF coils: A practical guide for nonphysicists. J Magn Reson Imaging 2018;48(3):590-604.
34. Volz S, Callaghan M, Josephs O, Weiskopf N. Maximising BOLD sensitivity through automated EPI protocol optimisation. Neuroimage 2019;189:159-170.
35. Tricco AC, Lillie E, Zarin W, et al. PRISMA extension for scoping reviews (PRISMA-ScR): Checklist and explanation. Ann Intern Med 2018;169(7):467-473.
36. Arksey H, O'Malley L. Scoping studies: Towards a methodological framework. Int J Soc Res Methodol 2005;8(1):19-32.
37. Foster SL, Breukelaar I, Ekanayake K, Lewis S, Korgaonkar M. Functional magnetic resonance imaging of the amygdala and subregions at 3 tesla: A scoping review protocol. medRxiv 2022. https://doi.org/10.1101/2022.04.14.22273332

38. Bramer WM, Rethlefsen M, Kleijnen J, Franco O. Optimal database combinations for literature searches in systematic reviews: A prospective exploratory study. Syst Rev 2017;6(1):245.

39. Covidence. *Covidence systematic review software*. Melbourne, Australia: Veritas Health Innovation; 2022.

40. Kemmotsu N, Kucukboyaci N, Cheng C, et al. Alterations in functional connectivity between the hippocampus and prefrontal cortex as a correlate of depressive symptoms in temporal lobe epilepsy. Epilepsy Behav 2013;29(3):552-559.

41. Kemmotsu N, Kucukboyaci N, Leyden K, et al. Frontolimbic brain networks predict depressive symptoms in temporal lobe epilepsy. Epilepsy Res 2014;108(9):1554-1563.

42. Korgaonkar MS, Ram K, Williams L, Gatt J, Grieve S. Establishing the resting state default mode network derived from functional magnetic resonance imaging tasks as an endophenotype: A twins study. Hum Brain Mapp 2014;35(8):3893-3902.

43. Norris DG. Pulse sequences for fMRI. In: Uludag K, Ugurbil K, Berliner L, editors. *fMRI: From nuclear spins to brain functions*. Boston, MA: Springer US; 2015. p 131-162.

44. Bielski K, Adamus S, Kolada E, Rączaszek-Leonardi J, Szatkowska I. Parcellation of the human amygdala using recurrence quantification analysis. Neuroimage 2021;227:117644.

45. Hansen HA, Li J, Saygin ZM. Adults vs. neonates: Differentiation of functional connectivity between the basolateral amygdala and occipitotemporal cortex. PLoS One 2020;15(10):e0237204.

46. Rausch A, Zhang W, Haak K, et al. Altered functional connectivity of the amygdaloid input nuclei in adolescents and young adults with autism spectrum disorder: A resting state fMRI study. Mol Autism 2016;7(1):1-13.

47. Terburg D, Morgan B, Montoya E, et al. Hypervigilance for fear after basolateral amygdala damage in humans. Transl Psychiatry 2012;2(5):e115.

48. Ambrosi E, Arciniegas D, Madan A, et al. Insula and amygdala resting-state functional connectivity differentiate bipolar from unipolar depression. Acta Psychiatr Scand 2017;136(1):129-139.

49. Roy AK, Fudge J, Kelly C, et al. Intrinsic functional connectivity of amygdala-based networks in adolescent generalized anxiety disorder. J Am Acad Child Adolesc Psychiatry 2013;52(3):290-299.

50. Coombs G III, Loggia M, Greve D, Holt D. Amygdala perfusion is predicted by its functional connectivity with the ventromedial prefrontal cortex and negative affect. PLoS One 2014;9(5):e97466.

51. Qiao J, Tao S, Wang X, et al. Brain functional abnormalities in the amygdala subregions is associated with anxious depression. J Affect Disord 2020;276:653-659.

52. Wang Z, Zhu H, Yuan M, et al. The resting-state functional connectivity of amygdala subregions associated with post-traumatic stress symptom and sleep quality in trauma survivors. Eur Arch Psychiatry Clin Neurosci 2021;271(6):1053-1064.

53. Zhang M, Yang F, Fan F, et al. Abnormal amygdala subregional-sensorimotor connectivity correlates with positive symptom in schizophrenia. Neuroimage Clin 2020;26:102218.

54. Geng H, Li X, Chen J, Li X, Gu R. Decreased intra-and inter-salience network functional connectivity is related to trait anxiety in adolescents. Front Behav Neurosci 2016;9:350.

55. Cheng W, Rolls E, Qiu J, et al. Functional connectivity of the human amygdala in health and in depression. Soc Cogn Affect Neurosci 2018;13(6):557-568.

56. Qin S, Young C, Duan X, et al. Amygdala subregional structure and intrinsic functional connectivity predicts individual differences in anxiety during early childhood. Biol Psychiatry 2014;75(11):892-900.

57. Liu T, Ke J, Qi R, et al. Altered functional connectivity of the amygdala and its subregions in typhoon-related post-traumatic stress disorder. Brain Behav 2021;11(1):e01952.

58. Jiang X, Ma X, Geng Y, et al. Intrinsic, dynamic and effective connectivity among large-scale brain networks modulated by oxytocin. Neuroimage 2021;227:117668.

59. Bickart KC, Hollenbeck M, Barrett L, Dickerson B. Intrinsic amygdala–cortical functional connectivity predicts social network size in humans. J Neurosci 2012;32(42):14729-14741.

60. Cao L, Li H, Hu X, et al. Distinct alterations of amygdala subregional functional connectivity in early-and late-onset obsessive-compulsive disorder. J Affect Disord 2022;298(Pt A):421-430.

61. Fateh AA, Cui Q, Duan X, et al. Disrupted dynamic functional connectivity in right amygdalar subregions differentiates bipolar disorder from major depressive disorder. Psychiatry Res Neuroimaging 2020;304:111149.

62. Gamer M, Zurowski B, Büchel C. Different amygdala subregions mediate valence-related and attentional effects of oxytocin in humans. Proc Natl Acad Sci USA 2010;107(20):9400-9405.

63. Michely J, Rigoly F, Rutledge R, Hauser T, Dolan R. Distinct processing of aversive experience in amygdala subregions. Biological Psychiatry Cogn Neurosci Neuroimaging 2020;5(3):291-300.

64. National Institutes of Health. The NIH Human Connectome Project [Website]. 2023.

65. Kasper L, Engel M, Heinzle J, Mueller-Schrader M, Graedel NN, Reber J, et al. Advances in spiral fMRI: A high-resolution study with single-shot acquisition. NeuroImage 2022;246:118738. https://doi.org/10.1016/j.neuroimage.2021.118738

66. Glover GH, Law CS. Spiral-in/out BOLD fMRI for increased SNR and reduced susceptibility artifacts. Magn Reson Med 2001;46(3):515-522.

67. Kasper L, Engel M, Heinzle J, et al. Advances in spiral fMRI: A high-resolution study with single-shot acquisition. Neuroimage 2022;246:118738.

68. Borogovac A, Asllani I. Arterial spin labeling (ASL) fMRI: Advantages, theoretical constrains and experimental challenges in neurosciences. Int J Biomed Imaging 2012;2012:818456.

69. Triantafyllou C, Polimeni JR, Wald LL. Physiological noise and signal-to-noise ratio in fMRI with multi-channel array coils. Neuroimage 2011;55(2):597-606.

70. Olman CA, Davachi L, Inati S. Distortion and signal loss in medial temporal lobe. PLoS One 2009;4(12):e8160.

71. Andersson JLR. Chapter 9 – Diffusion MRI artifact correction. In: Choi I-Y, Jezzard P, editors. *Advances in magnetic resonance technology and applications*. Cambridge: Academic Press; 2021. p 123-146.

72. Robinson S, Windischberger C, Rauscher A, Moser E. Optimized 3 T EPI of the amygdalae. Neuroimage 2004;22(1):203-210.

73. Yoo S-S, Guttmann C, Panych L. Multiresolution data acquisition and detection in functional MRI. Neuroimage 2001;14(6):1476-1485.

74. Wald LL, Polimeni JR. Impacting the effect of fMRI noise through hardware and acquisition choices – Implications for controlling false positive rates. Neuroimage 2017;154:15-22.

75. Li Y-T, Chang C-Y, Hsu Y-C, et al. Impact of physiological noise in characterizing the functional MRI default-mode network in Alzheimer's disease. J Cereb Blood Flow Metab 2021;41(1):166-181.

76. Barth M, Breuer F, Koopmans P, Norris D, Poser B. Simultaneous multislice (SMS) imaging techniques. Magn Reson Med 2016;75(1):63-81.

77. Todd N, Moeller S, Auerbach E, Yacoub E, Flandin G, Weiskopf N. Evaluation of 2D multiband EPI imaging for high-resolution, whole-brain, task-based fMRI studies at 3T: Sensitivity and slice leakage artifacts. Neuroimage 2016;124(Pt A):32-42.

78. Stirnberg R, Huijbers W, Brenner D, Poser BA, Breteler M, Stöcker T. Rapid whole-brain resting-state fMRI at 3 T: Efficiency-optimized three-dimensional EPI versus repetition time-matched simultaneous-multi-slice EPI. Neuroimage 2017;163:81-92.

79. Parker D, Rotival G, Laine A, Razlighi Q. Retrospective detection of interleaved slice acquisition parameters from fMRI data. In *2014 IEEE 11th International Symposium on Biomedical Imaging* (*ISBI*). 2014.

80. Yancey SE, Rotenberg D, Tam F, et al. Spin-history artifact during functional MRI: Potential for adaptive correction. Med Phys 2011; 38(8):4634-4646.

81. Muresan L, Renken R, Roerdink J, Duifhuis H. Automated correction of spin-history related motion artefacts in fMRI: Simulated and phantom data. IEEE Trans Biomed Eng 2005;52(8):1450-1460.

82. Weiss KL, Pan H, Storrs J, et al. Clinical brain MR imaging prescriptions in Talairach space: Technologist- and computer-driven methods. AJNR Am J Neuroradiol 2003;24(5):922-929.

83. Weiskopf N, Hutton C, Josephs O, Deichmann R. Optimal EPI parameters for reduction of susceptibility-induced BOLD sensitivity losses: A whole-brain analysis at 3 T and 1.5 T. Neuroimage 2006;33(2): 493-504.

84. Mulder MJ, Keuken M, Bazin P, Alkemade A, Forstmann B. Size and shape matter: The impact of voxel geometry on the identification of small nuclei. PLoS One 2019;14(4):e0215382.

85. Smith SM, Beckmann C, Andersson J, et al. Resting-state fMRI in the Human Connectome Project. Neuroimage 2013;80:144-168.

86. Merboldt K-D, Fransson P, Bruhn H, Frahm J. Functional MRI of the human amygdala? Neuroimage 2001;14(2):253-257.

87. Chen N-K, Dickey C, Yoo S-S, Guttmann C, Panych L. Selection of voxel size and slice orientation for fMRI in the presence of susceptibility field gradients: Application to imaging of the amygdala. Neuroimage 2003;19(3):817-825.

88. Stöcker T, Kellermann T, Schneider F, et al. Dependence of amygdala activation on echo time: Results from olfactory fMRI experiments. Neuroimage 2006;30(1):151-159.

89. Anderson JS, Ferguson M, Lopez-Larson M, Yurgelun-Todd D. Reproducibility of single-subject functional connectivity measurements. AJNR Am J Neuroradiol 2011;32(3):548-555.

90. Van Dijk KR, Hedden T, Venkataraman A, Evans K, Lazar S, Buckner R. Intrinsic functional connectivity as a tool for human connectomics: Theory, properties, and optimization. J Neurophysiol 2010;103(1): 297-321.

91. Bellgowan P, Bandettini P, van Gelderen P, Martin A, Bodurka J. Improved BOLD detection in the medial temporal region using parallel imaging and voxel volume reduction. Neuroimage 2006;29(4): 1244-1251.

92. Schmitt T, Rieger JW. Recommendations of choice of head coil and Prescan normalize filter depend on region of interest and task. Front Neurosci 2021;15:1-16.

93. Keil B, Blau J, Biber S, et al. A 64-channel 3T array coil for accelerated brain MRI. Magn Reson Med 2013;70(1):248-258.

94. Deshmane A, Gulani V, Griswold M, Seiberlich N. Parallel MR imaging. J Magn Reson Imaging 2012;36(1):55-72.

95. Schmidt CF, Degonda N, Luechinger R, Henke K, Boesiger P. Sensitivity-encoded (SENSE) echo planar fMRI at 3T in the medial temporal lobe. Neuroimage 2005;25(2):625-641.

96. Miller KL, Bartsch AJ, Smith SM. Simultaneous multi-slice imaging for resting-state fMRI. *MAGNETOM Flash*. Erlangen: Siemens Healthineers; 2015. p 70-77.

97. McDowell AR, Carmichael DW. Optimal repetition time reduction for single subject event-related functional magnetic resonance imaging. Magn Reson Med 2019;81(3):1890-1897.

98. Jahanian H, Holdsworth S, Christen T, et al. Advantages of short repetition time resting-state functional MRI enabled by simultaneous multislice imaging. J Neurosci Methods 2019;311:122-132.

99. Molloy EK, Meyerand ME, Birn RM. The influence of spatial resolution and smoothing on the detectability of resting-state and task fMRI. Neuroimage 2014;86:221-230.

100. Bollmann S, Barth M. New acquisition techniques and their prospects for the achievable resolution of fMRI. Prog Neurobiol 2021;207: 101936.

101. Lin A, Andronesi O, Bogner W, et al. Minimum reporting standards for in vivo magnetic resonance spectroscopy (MRSinMRS): Experts' consensus recommendations. NMR Biomed 2021;34(5):e4484.

102. Poldrack RA, Fletcher P, Henson R, Worsley K, Brett M, Nichols T. Guidelines for reporting an fMRI study. Neuroimage 2008;40(2): 409-414.

Chapter 4: Amygdala Subregional Functional Connectivity in Treatment Resistant Depression

---

The work in this chapter was undertaken to investigate the capabilities of the current, widely used 2D GRE-EPI sequence optimised for high resolution fMRI data acquisition as per the recommendations made in the scoping review in Chapter Three, with the aim of interrogating the functional connectivity (FC) of the amygdala at a subregional level rather than as a single structure. A strong case was made in Chapter One for the need to investigate the amygdala in Major Depressive Disorder (MDD) at a more granular level, by optimising our current imaging sequences. Treatment Resistant Depression (TRD) patients are a subset of Major Depressive Disorder (MDD) patients with potentially the most to gain from an increased understanding of amygdala dysfunction, hence the selection of this cohort for testing against a treatment-sensitive (TSD) cohort in this chapter.

The optimised sequence was deployed in these two depression cohorts to investigate whether FC alterations could distinguish between the two groups at a subregional amygdala level (rather than whole amygdala level, reported in almost 90% of the scoping review studies). This was the first published study to report FC differences between TRD and TSD using an optimised high resolution 2D version of a current 3T sequence, combined with a subregional analysis approach. The study also found that FC results differed when using a subregional versus whole amygdala approach, a finding about which there are only a handful of reports in the literature. With results showing that a subregional approach was more sensitive to FC alterations, this work has important implications for future studies of the amygdala.

This chapter is published in the Journal of Affective Disorders Reports

Journal of Affective Disorders Reports 21 (2025) 100932

Contents lists available at ScienceDirect

Journal of Affective Disorders Reports

journal homepage: www.sciencedirect.com/journal/journal-of-affective-disorders-reports

Research Paper

Amygdala subregional functional connectivity in treatment-resistant depression

Sheryl L. Foster [a,b,*], Ramon Landin-Romero [a,f], Sarah Lewis [a,c], Ana Rita Barreiros [d,e,h], Sophie Matis [f], Anthony Harris [d,e,g], Mayuresh S. Korgaonkar [a,e]

[a] Discipline of Medical Imaging Science, Sydney School of Health Sciences, Faculty of Medicine and Health, The University of Sydney, Sydney, NSW 2006, Australia
[b] Department of Radiology, Westmead Hospital, Darcy Rd, Westmead, NSW 2145, Australia
[c] School of Health Sciences, Western Sydney University, Locked Bag 1797, Penrith, NSW, 2751, Australia
[d] Westmead Clinical School, Faculty of Medicine and Health, The University of Sydney, Sydney, NSW 2006, Australia
[e] Brain Dynamics Centre, The Westmead Institute for Medical Research, 176 Hawkesbury Rd, Westmead, NSW, 2145, Australia
[f] Brain and Mind Centre, The University of Sydney, 94 Mallett St, Camperdown, NSW 2050, Australia
[g] Specialty of Psychiatry, Sydney Medical School, The University of Sydney, Sydney, NSW 2006, Australia
[h] The Black Dog Institute, Prince of Wales Hospital, Randwick, NSW 2031, Australia

ARTICLE INFO

Keywords:
Treatment-resistant depression
Amygdala
Subregions
Functional connectivity, high-resolution

ABSTRACT

Background: Treatment resistance impacts almost 50 % of depression patients, with amygdala dysfunction being widely implicated. fMRI studies have typically focussed on identifying whole rather than individual subregional amygdala functional connectivity but this approach, together with cohort heterogeneity, is likely contributing to inconsistent results. This study used high resolution 3T fMRI data to investigate subregional alterations that may differentiate treatment-resistant cohorts from healthy individuals and depressed patients who respond to treatment.

Methods: Resting-state fMRI data were obtained in 35 participants diagnosed with Treatment-Resistant Depression (TRD), 38 healthy control participants (HC), and 35 treatment-sensitive participants (TSD). Seed-based functional connectivity analyses of three main subregions bilaterally (laterobasal, centromedial and superficial), as well as the whole amygdala, were performed and comparisons made between groups.

Results: We found connectivity differences in the right laterobasal amygdala subregion in TRD compared to both groups. TRD patients displayed hypoconnectivity to the right fusiform gyrus relative to HC whereas hyperconnectivity to the left inferior frontal gyrus relative to TSD was identified. No connectivity differences were found for the whole amygdala or any of the other subregions bilaterally.

Limitations: Modest sample size and cross-sectional study design are limitations. A causal relationship between functional connectivity alterations and treatment resistance cannot be established.

Conclusion: Altered connectivity of the right laterobasal subregion is a distinguishing feature of TRD. These alterations may underlie severe impairments in emotion processing and social functioning that are characteristic of TRD. These results emphasise the need for further investigation of the functional role of the amygdala subregions in depression.

1. Introduction

Of all patients diagnosed with Major Depressive Disorder, only around half will adequately respond to initial treatments based on antidepressant medications and targeted psychological interventions. These patients are considered Treatment-Sensitive (TSD) (Malhi et al., 2021; Scott et al., 2023). Approximately 30 % of depression patients exhibit a lack of adequate response to initial pharmacotherapy plus at least one other pharmaceutical or alternative equivalent treatment and are diagnosed with treatment-resistant depression (TRD) (Ionescu et al.,

* Corresponding author.
E-mail addresses: sheryl.foster@sydney.edu.au (S.L. Foster), ramon.landin-romero@sydney.edu.au (R. Landin-Romero), sarah.lewis@westernsydney.edu.au (S. Lewis), ana.barreiros@sydney.edu.au (A.R. Barreiros), sophie.matis@sydney.edu.au (S. Matis), anthony.harris@sydney.edu.au (A. Harris), m.korgaonkar@sydney.edu.au (M.S. Korgaonkar).

https://doi.org/10.1016/j.jadr.2025.100932
Received 2 September 2024; Received in revised form 29 April 2025; Accepted 17 May 2025
Available online 18 May 2025

2015; Voineskos et al., 2020). However, this figure could be as high as 55 %, as it is well-recognised that the lack of a universal definition contributes to widely variable estimates of prevalence across treatment settings (McIntyre et al., 2023).

The neural mechanisms that distinguish TRD from TSD remain unclear and current diagnostic methods, predicated on a combination of patient self-reporting and monitoring of symptoms, are clearly suboptimal. Improved outcomes for TRD patients depend on further advancements in diagnosis rather than multiple trials of treatments which are ineffective for many patients (Malhi et al., 2019; McIntyre et al., 2023). Increasing access to clinical research Magnetic Resonance Imaging (MRI) systems has meant that advanced neuroimaging techniques such as functional MRI (fMRI) are now well-established in Major Depressive Disorder (MDD) research (Kotoula et al., 2023) and concerted efforts have been made to review and synthesize the network and functional connectivity findings that have been generated, particularly in relation to the brain in its resting state. A meta-analysis of 32 fMRI studies by Sundermann and colleagues points to patterns of both hyperconnectivity and hypoconnectivity of midline cortical structures involving the posterior Default Mode Network and the Anterior Cingulate Cortex in MDD compared to healthy controls (HC) (Sundermann et al., 2014), and a recent study by Machaj and colleagues also reported intra-network hypoconnectivity in the Visual Network and inter-network hyperconnectivity between the Visual Network and the Salience and Dorsal Attention networks in drug-resistant depression compared to HC (Machaj et al., 2024). Kaiser and colleagues reported connectivity alterations in networks responsible for both emotion and attention regulation, noting hypoconnectivity between the Medial Prefrontal Cortex and the amygdala in a meta-analysis of 25 publications (Kaiser et al., 2015). In their highly-cited work, Drysdale et al. combined fMRI data from multiple studies to show that depressive symptoms could be categorised into two well-defined groupings of primary connectivity features; i) frontostriatal and orbitofrontal, and ii) limbic (principally the amygdala) (Drysdale et al., 2017). Interestingly, in their recent meta-analyses of over 4000 fMRI publications relating to depressed vs HC groups, Wang and colleagues listed the top ten brain regions displaying significant connectivity variations between groups, of which the amygdala was number one (Wang et al., 2024). The amygdala, a key region in the brain's emotion processing network, plays a significant role in treatment-resistant depression (Bakoyiannis, 2023). This region is crucial to study due to its involvement in affective symptoms of depression, such as sustained negative affect and difficulties in experiencing positive affect. Aberrant emotion reactivity and regulation, which are central to the pathology of depression, have been linked to dysfunction in the amygdala (Runia et al., 2023). Neurobiological models of depression emphasize the importance of the frontolimbic network, which includes the amygdala, in emotion dysregulation (Mayberg, 1997). As highlighted in a meta-analysis, neuroimaging studies have consistently shown that the amygdala exhibits heightened responsivity to negative stimuli in individuals with depression compared to healthy controls (Hamilton et al., 2012). These findings suggest that the amygdala's dysregulated activity contributes to the persistence of depressive symptoms and previous studies focusing on amygdala circuitry have clearly demonstrated the potential of fMRI to enhance our understanding of treatment responsiveness and remission in depressed cohorts (Goldstein-Piekarski et al., 2016; Williams et al., 2015).

Recent studies in TRD cohorts have utilised fMRI to focus on response to newer treatments such as ketamine, psilocybin and Transcranial Magnetic Stimulation therapies and neurofeedback strategies with promising results (Compère et al., 2024; Gill et al., 2022; Nair et al., 2024; Tu et al., 2025; Yun and Kim, 2024). Although the focus of our literature review is on resting-state studies reporting amygdala FC in TRD vs HC, it is interesting to note several recent task-based publications reporting positive treatment effects. A mini-review exploring the effects of ketamine on emotion regulation and cognition across fMRI studies in MDD and TRD cohorts noted its 'normalising' influence on the Anterior Cingulate Cortex and the amygdala (Ramezani et al., 2025). Similarly, Runia and colleagues reported an anti-depressant effect of DBS generated by Deep Brain Stimulation to the ventral limb of the internal capsule, a procedure which appeared to normalise amygdala responsivity, offering potential therapeutic avenues for TRD (Runia et al., 2023). Therefore, investigating the functional connectivity of the amygdala is essential to understanding its role in TRD and developing targeted treatments.

Despite the substantial body of work relating to fMRI in depression, there is limited literature focussing on TRD, especially in relation to resting-state FC variations compared to HC. Inconsistent findings have been outlined in two comprehensive meta-analyses reporting altered activation and connectivity of the amygdala during both task and resting state fMRI (rs-fMRI) studies and as noted by the authors, this is potentially due to diversity in acquisition and analysis techniques (Grehl et al., 2023; Kotoula et al., 2023). Incongruent fMRI task-based findings can be attributed to variations in fundamental task design across studies, whereas the rs-fMRI technique is easily replicated and should allow a more accurate comparison of findings across cohorts by analysing FC patterns during rest. However, reported findings of rs-fMRI FC patterns focusing on the amygdala in TRD have also been inconsistent. Of the few FC studies comparing TRD with HC there are reports of both hypoconnectivity (Ge et al., 2019; Lui et al., 2011; Wang et al., 2017) and hyperconnectivity (Siegel et al., 2021) of the amygdala with other brain regions. Similarly, in two studies comparing FC in TRD and TSD, one reported amygdala hypoconnectivity in TRD relative to TSD (Lui et al., 2011) whilst the other found no significant differences between cohorts (Zhang et al., 2022).

A further contributing factor to results inconsistency is that the majority of studies comparing amygdala FC in TRD vs HC cohorts have considered the amygdala as a single entity during data analyses, rather than a functionally diverse group of nuclei (Chen et al., 2020; Ge et al., 2019; Lui et al., 2011; Siegel et al., 2021; Vasavada et al., 2021; Wu et al., 2011). Previous animal and human work has shown that the amygdala is not a simple homogenous structure; it is composed of nine functionally different groups of nuclei which are further grouped into three primary subregions, the laterobasal (LB), centromedial (CM), and superficial (SF) based on histological features and patterns of structural and functional connectivity (Fig. 1) (Amunts et al., 2005; Bzdok et al., 2013; Kedo et al., 2018; Solano-Castiella et al., 2010). As well as being functionally diverse, the amygdala subregions also display asymmetric or lateralised connectivity (Ball et al., 2007; Bzdok et al., 2013; Kedo et al., 2018; Roy et al., 2009; Zhang et al., 2018). Acknowledging the need for greater accuracy in investigating and reporting subregional FC findings, parcellation techniques using high resolution 7 Tesla data have been developed (Eickhoff et al., 2005). The integration of probabilistic cytoarchitectonic maps into software analysis packages has enabled researchers to define separate standardised subregional regions-of-interest (ROIs) (Huang et al., 2024). This has facilitated more accurate reporting of localised FC alterations at a subregional rather than whole amygdala level.

However, there is yet another confounder potentially contributing to the inconsistency of FC results. Spatial resolution of fMRI acquisition protocols has remained largely unchanged, meaning the potential benefits of high-resolution fMRI data in imaging the subregions are predominantly unrealised (Foster et al., 2023; Olman and Yacoub, 2011). This is reflected in the handful of FC investigations of amygdala subregions in TRD to date that are primarily based on what is now considered standard (20–50 mm^3) and lower (> 50 mm^3) resolution data, likely contributing to the conflicting results being reported (Wang et al., 2017; Yuan et al., 2023; Zhang et al., 2022). Paradoxically, several TRD studies have acquired high-resolution data (< 20 mm^3) but reported FC alterations based on the whole amygdala rather than the subregions (Nakamura et al., 2021; Vasavada et al., 2021) (Olman and Yacoub, 2011). While there has been one previous high-resolution

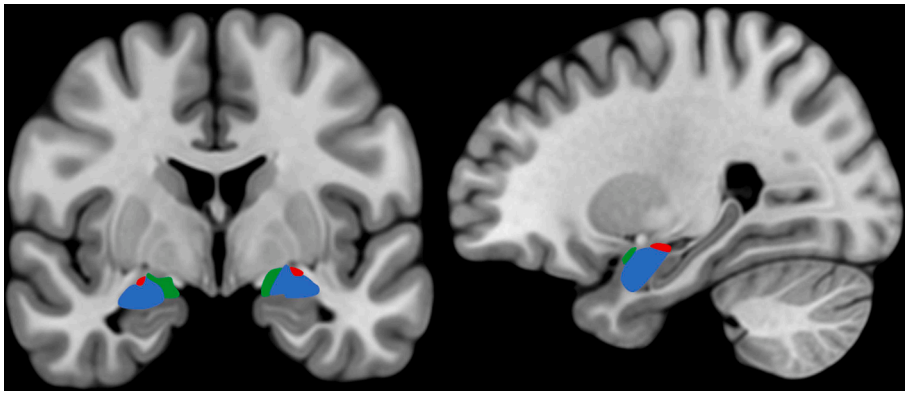

Fig. 1. T1-weighted coronal (left), and sagittal (right) MR images depicting location of the amygdala and three main subregions. Superficial (SF = green), laterobasal (LB = blue) and centromedial (CM = red).

subregional amygdala study in TRD vs HC that reported left SF hypoconnectivity (Batail et al., 2023), no previous study has evaluated subregional connectivity differences between TRD and TSD using high-resolution data. Given the limited understanding of the role of the amygdala subregions in TRD and the inconsistencies in results and imaging methods to date, there is clearly a need for further investigation.

The primary aim of this work was to build on current FC findings by using high-resolution fMRI data and subregional ROI analyses to examine alterations in resting-state FC of the amygdala in a TRD cohort compared with HC, with a secondary aim of comparing TRD and TSD cohorts. Conceptually, this technically advanced yet practical approach was designed to achieve a 'baseline' for subregional FC variations in TRD compared with HC as a step towards resolving inconsistency in results across studies. Based on previous studies, it was hypothesized that hypoconnectivity of the amygdala subregions would distinguish TRD from HC. We also hypothesized that amygdala subregional connectivity would differ between TRD and TSD. Further, as there are few reports of FC findings using both subregional ROIs and whole amygdala ROIs in the same cohorts, our third aim was to compare findings using both whole amygdala and subregional analysis methods.

2. Methods and materials

2.1. Participants

Thirty-nine TRD patients, thirty-five TSD patients and thirty-eight healthy controls (HC) totalling 112 participants aged between 18 and 65 years were recruited for the study. Referencing the Structured Clinical Interview for the DSM-5 (SCID-5), all TRD and TSD participants met DSM-5 criteria for primary diagnosis of Major Depressive Disorder (APA, 2013). Symptom severity was characterized by a 17-item Hamilton Depression Rating Scale (HAMD-21) (Hamilton, 1960). TRD was defined as the presence of unremitting moderate to severe symptoms in patients who had undergone at least two trials of six weeks duration of adequate dosage of antidepressant medication of different pharmacological classes and a HAMD-21 score of 16 and above. TSD was defined as at least two weeks of symptom remission and a HAMD-21 score of nine and below. Healthy controls had no previous history of psychiatric illnesses as assessed using the SCID-5. Exclusion criteria included inability to provide consent, lack of proficiency in English language, current diagnosis of eating disorder or other psychiatric disorder, substance dependence for past three months, pregnancy, prior history of or current neurological disorder, prior brain injury, Electroconvulsive Therapy (ECT) or Transcranial Magnetic Stimulation in previous 6-month period, or contraindications for MRI. Further details relating to the cohorts can be found in a previous publication (Barreiros et al., 2022). Ethics approval for the research protocol was obtained from Western Sydney Local Health District Human Research Ethics Committee and written consent was obtained from all participants. Imaging studies were undertaken at Westmead Hospital Radiology Department, Sydney, Australia.

2.2. Data acquisition

All imaging data were acquired on a 3 Tesla Siemens Prisma MRI system in conjunction with VE11C software (Siemens Medical Solutions, Germany) and a 64-channel head/neck array RF coil for signal reception. Participants were instructed to remain still and awake whilst viewing a fixation cross projected onto a coil-mounted screen during 8 min of resting-state data acquisition. Imaging parameters for the functional 2D T2*-weighted GRE-EPI sequence were as follows: Repetition time (TR) = 1500 ms; Echo time (TE) = 33 ms; Field-of-view (FOV) = 255 mm; Matrix = 104 × 104; Flip angle (FA) = 85°; Phase encoding direction = A to P; Total acceleration = 6 (MB 3); 320 vol; 60 interleaved axial-oblique slices at 2.5 mm thick (0 mm gap) parallel to the AC-PC line were acquired covering the whole brain with an isotropic voxel size of 2.5 mm^3.

A 3D T1-weighted gradient echo sequence was also acquired to provide a high-resolution structural scan for use in the pre-processing workflow for normalisation. Imaging parameters were as follows: Repetition time (TR) = 2400 ms; Echo time (TE) = 2.21 ms; Field-of-view (FOV) = 256 mm; Matrix = 288 × 288; Flip angle (FA) = 8°; Phase encoding direction = A to P; Acceleration (GRAPPA) = 2; 192 sagittal slices at 0.9 mm thick parallel to the interhemispheric fissure were acquired covering the whole brain with an isotropic voxel size of 0.9 mm^3.

2.3. Imaging data analyses

Whole-brain voxel-wise analyses were performed using a combination of Matlab R2022b (The MathWorks Inc. Natick, Massachusetts), SPM12 (Wellcome Trust Centre for Neuroimaging, London, UK) and CONN functional connectivity toolbox v22b (http://www.nitrc.org/projects/conn/). Preprocessing of anatomical and functional images was performed using the CONN modular preprocessing pipeline (Nieto-Castanon, 2020b). In brief, the data underwent realignment, unwarping, coregistration and resampling for motion correction and magnetic susceptibility interactions. Outliers were excluded and a BOLD reference image was created for each subject. Data were then normalised into standard Montreal Neurological Institute space and segmented into grey matter, white matter and cerebrospinal fluid, then resampled to isotropic 2 mm voxels. As the functional data were acquired at high resolution, smoothing with a Gaussian kernel of 6 mm full width half maximum (FWHM) was undertaken in order to maximise SNR whilst minimising spatial shift that can occur in small structures when larger

FWHM values are employed (Blazejewska et al., 2019). Denoising was performed using a standard pipeline including regression of potential confounders (Nieto-Castanon, 2020a), followed by bandpass filtering (0.01–0.1 Hz). Data was assessed for head motion and outliers were detected using the Assessment of Repetitive Tasks (ART)-based scrubbing technique in CONN. Outliers were defined as having greater than 0.9 mm framewise displacement, resulting in data from four TRD participants being identified as having unacceptable levels of head motion and excluded from further analysis, leaving a total of 108 datasets. A full description of the analysis methods is located in the Supplementary Information.

First-level analyses were based on a priori selection of ROIs. Six amygdala subregional masks or ROIs were extracted from The JuBrain Anatomy Toolbox (Eickhoff et al., 2005). These ROIs, left and right centromedial (CM), laterobasal (LB) and superficial (SF) (Fig. 1) were created using cytoarchitectonically-defined probabilistic maps from the JuBrain Cytoarchitectonic Atlas (Amunts et al., 2005). A further two whole amygdala ROIs constructed from a combination of the three subregional masks (left and right) were also extracted for the comparison analysis. These were used as seed regions in CONN to explore whole-brain voxel-wise FC and to determine FC strength represented by Fisher's z transform of the correlation coefficients from a weighted General Linear Model. This was computed by averaging the time course of all voxels in each seed ROI and correlating with the time course of every other voxel in the brain. Correlation coefficients were used in the group level analyses, performed using a General Linear Model. TRD and HC groups were compared using two-sample *t*-tests, followed by comparison of TRD and TSD groups. Statistical parametric maps were generated, and results were thresholded using a combination of cluster-forming $p < 0.001$ voxel-level threshold and a familywise corrected False Discovery Rate correction of p-FDR < 0.05 cluster-size threshold to control the proportion of false positive findings in significant results (Chumbley et al., 2010). Additionally, mean beta FC estimates were extracted from significant clusters identified in the primary analysis to further explore in post-hoc secondary analyses.

2.4. Analyses of demographic and clinical factors

Comparison of all three groups was performed for age (one-way ANOVA) and gender (chi square test). Patient groups were also compared for clinical measures including depression severity (HAMD-21), quality of life (SOFAS), age at first depressive episode, length of time on antidepressant medications (independent sample *t*-tests) and history of ECT and suicidality (chi square tests). To further explore variances in neural measures between TRD and TSD and to confirm that these were not driven by clinical differences between the patient groups, a univariate GLM ANOVA was used to explore the effect of group (fixed factor) controlling for co-variates of age at first depressive episode, length of time on antidepressant medications, quality of life and HAMD-21 scores.

For the TRD group, the same clinical variables were also tested for potential correlations with FC values. Independent samples *t*-tests were undertaken to compare FC variances between those patients with and without a history of suicidal ideation, suicide attempts and ECT treatment.

All statistical analyses were undertaken using SPSS software version 29 (IBM-SPSS, 2012). All statistical tests were corrected for multiple comparisons and effects considered significant at $p < 0.05$.

3. Results

3.1. Demographic and clinical characteristics

Demographic and clinical characteristics data relating to the cohort are shown in Table 1. All groups were comparable for age and gender; as expected, the depressive profile of the TRD group was significantly worse in comparison with the TSD group. The TRD group exhibited greater severity of depressive symptoms, poorer functioning and a higher number of suicide attempts. Results for both group analyses are summarised in Table 2.

3.2. Functional connectivity analyses - healthy controls vs TRD

Significant connectivity differences between groups were identified

Table 2
Summary of group results from functional connectivity analyses.

Seed region & groups	Brain region	Voxels in Cluster	Peak MNI coordinates			T-value	p FDR
			x	y	z		
Right LB HC > TRD	Right fusiform gyrus Right cerebellar crus 1 Right inferior temporal gyrus	95	48	−62	−20	5.49	p 0.023
Right LB TRD > TSD	Left Inferior frontal gyrus (pars opercularis & pars triangularis)	138	−48	18	16	5.24	p 0.003

Note: Results shown are those surviving multiple comparison corrections (cluster-level threshold of $P_{FDR} < 0.05$) and voxel-level threshold of p-uncorrected < 0.001.
Abbreviations: TRD –Treatment-Resistant Depression; HC–Healthy Controls; TSD – Treatment-Sensitive Depression; LB – Laterobasal.

Table 1
Demographic and clinical characteristics of all study participants.

	TRD (35)	TSD (35)	HC (38)	F/t/X^2	sig
Demographics					
Age, Mean ± SD [Min-Max]	42.3 ± 14.1 [18.1–64.3]	37.2 ± 11.0 [20.0–57.4]	47.1 ± 14.3 [18.9–66.0]	n.s.	n.s.
Gender (M), N (%)	14 (40)	17 (48.6)	17 (44.7)	n.s.	n.s.
Clinical Profile					
Age of onset, Mean ± SD [Min-Max]	26.97 ± 13.13 [8–53]	21.66 ± 9.26 [8–50]	n.a.	n.s.	n.s.
HAMD-21 score, Mean ± SD [Min-Max]	25.23 ± 6.46 [16–41]	4.18 ± 3.10 [0–9]	n.a.	15.819	<0.001
SOFAS score, Mean ± SD [Min-Max]	73.91 ± 16.18 [40–100]	89.58 ± 5.47 [78–95]	n.a.	−5.275	<0.001
History of ECT, N (%)	10 (28.6)	0 (0)	n.a.	11.667	0.001
History of Suicidal Ideation, N (%)	28 (80)	26 (74.3)	n.a.	n.s.	n.s.
History of Suicidal Attempt, N (%)	19 (54.3)	5 (14.3)	n.a.	13.938	<0.001
Time on ADM (yrs), Mean ± SD [Min-Max]	4.44 ± 3.71 [0.17–12]	4.18 ± 4.16 [0.12–17]	n.a	n.s	n.s.

Abbreviations: n.a. – not applicable, n.s. – not significant; SD – Standard Deviation; M – male; HAMD-21 – Hamilton Depression Rating Scale, 21 items.
SOFAS – Social and Occupational Functioning Assessment Scale; ECT – Electroconvulsive Therapy; ADM – Antidepressant Medication; N – total number.

between the right LB and a right-sided cluster centred on the fusiform gyrus, with hypoconnectivity in the TRD group relative to HC (Fig. 2). There were no FC group differences seen for any other subregion bilaterally.

No FC group differences were identified for the left or right whole amygdala ROI. However, at a less conservative threshold (uncorrected initial voxel threshold of $p < 0.005$ with a p cluster corrected FDR threshold of 0.05) two clusters including parts of the hippocampus, cingulate gyrus, precuneus cortex and vermis, showed decreased FC with the right amygdala in the TRD group relative to HC.

3.3. Functional connectivity analyses – TRD vs TSD

Significant connectivity group differences were identified between the right LB and the left inferior frontal gyrus with hyperconnectivity in TRD relative to TSD (Fig. 3). As observed in the previous analysis, there were no FC group differences seen for any of the other subregions bilaterally or for the left or right whole amygdala ROI, even at the less conservative threshold (uncorrected initial voxel threshold of $p < 0.005$ with a p cluster corrected FDR threshold of 0.05).

3.4. Functional connectivity analyses—HC vs TSD

No significant differences in FC between the amygdala subregions to any other brain regions were identified between the HC and TSD groups.

3.5. Correlations between FC and clinical and demographic measures

Post hoc analyses were conducted by running a univariate GLM ANOVA to evaluate the potential of age at first episode, length of time on antidepressant medications, HAMD-21 and SOFAS scores to be contributing factors to the group differences in FC measures identified between TRD and TSD. After controlling for clinical measures, there was still a significant effect of group ($F(1,44) = 4.58$, $p = 0.038$), that is, there were no significant effects of these clinical measures on the FC differences identified between the right LB and the cluster in the left inferior frontal gyrus. In the TRD cohort, no significant effects were identified in testing for correlations with FC values using three clinical variables; patients with and without a history of suicidal ideation, suicide attempts and history of ECT.

4. Discussion

This study utilised high-resolution fMRI data to examine patterns of subregional amygdala functional connectivity in TRD relative to healthy individuals (HC) and depressed patients who respond to treatments (TSD). As hypothesised, altered connectivity was identified in both group comparisons. Firstly, a pattern of hypoconnectivity was identified between the right amygdala LB subregion and the right fusiform gyrus in TRD relative to HC. Secondly, hyperconnectivity was found between the right amygdala LB and the left inferior frontal gyrus in the TRD cohort relative to TSD. These findings suggest that altered FC of the right LB subregion is a distinguishing feature of TRD.

These findings contribute to the limited work done so far in understanding the role of the amygdala and its subregions in TRD. This study highlighted that FC alterations of the right LB subregion are likely implicated in TRD. In comparison to HC, FC of the right LB was significantly decreased in TRD whereas it was significantly increased relative to TSD. To our knowledge, there are nine previous studies reporting amygdala resting state FC in TRD compared to HC, and only two comparing TRD and TSD. Based on a search of the literature, this study is the first to use both high resolution data and subregional ROIs to more accurately locate and report FC alterations in the amygdala subregions in a TRD cohort compared to TSD and only the second to compare TRD and HC cohorts.

The findings of the present study did not replicate previous findings in TRD relative to HC. Three of the six studies using whole amygdala ROIs reported hypoconnectivity of the right amygdala but to different brain regions (Chen et al., 2020; Ge et al., 2019; Vasavada et al., 2021). Another reported amygdala hyperconnectivity to the Default Mode Network (Siegel et al., 2021), and two found no significant amygdala FC differences (Lui et al., 2011; Wu et al., 2011). For the whole amygdala, we found differences between TRD and HC only at a less conservative threshold, with a pattern of hypoconnectivity for TRD to regions of the Default Mode Network, hippocampus and cerebellum. Of the three studies utilising subregional ROIs, two found left-sided hypoconnectivity of the SF, one to the left fusiform face area (Wang et al., 2017) and another to the left prefrontal cortex (Batail et al., 2023). The third study reported both hypoconnectivity of the right SF as well as hyperconnectivity of the right CM in their TRD cohort relative to HC (Zhang et al., 2022). Our study did not identify any connectivity

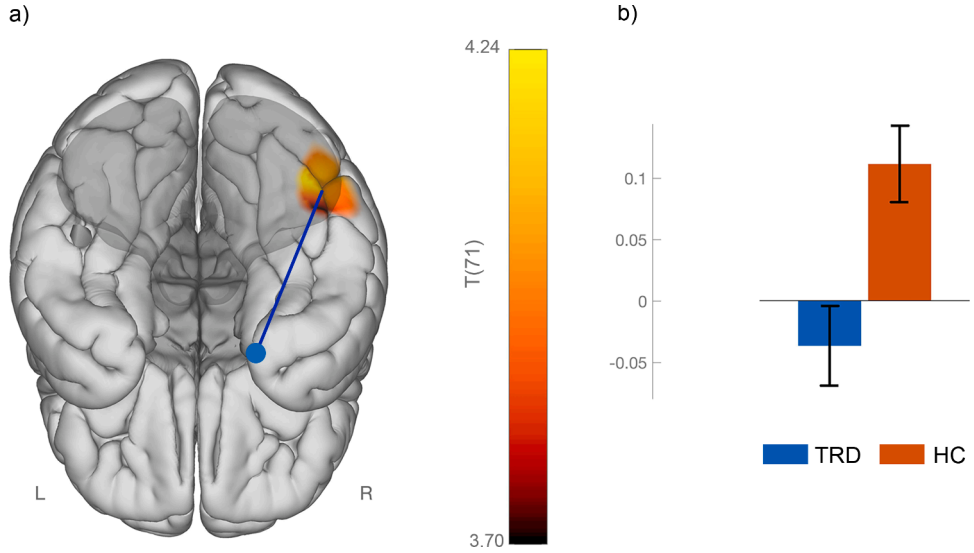

Fig. 2. Functional connectivity (FC) differences between Treatment-Resistant Depression (TRD) and Healthy Control (HC) groups. a) significant cluster centred in the right fusiform gyrus (inferior view) showed altered connectivity between right laterobasal (LB) amygdala subregion, with HC > TRD. b) mean FC of the right LB and right fusiform gyrus for TRD and HC groups. The colour scale bar represents the strength of the t-statistic. The mean FC on b) represents beta values of FC between the two regions (95 % CI). Results corrected for multiple comparisons at cluster-level threshold of $P_{FDR} < 0.05$ and voxel-level threshold of p-uncorrected < 0.001.

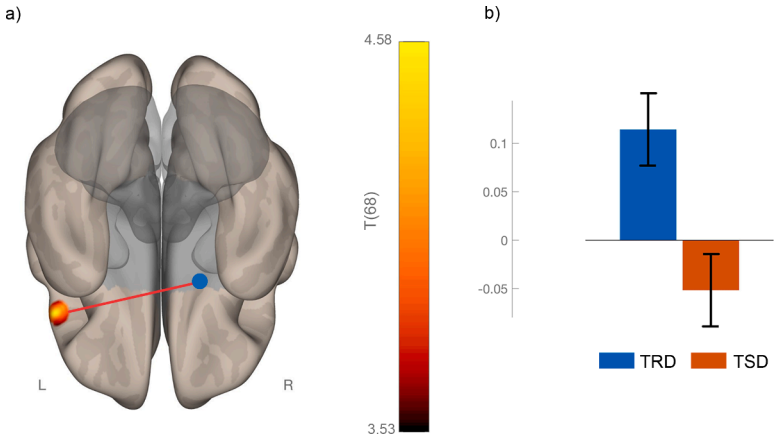

Fig. 3. Functional connectivity (FC) differences between Treatment-Resistant Depression (TRD) and Treatment-Sensitive Depression (TSD) groups. a) significant cluster in the left inferior frontal gyrus (inferior view) showed altered connectivity between right laterobasal (LB) amygdala subregion, with TRD > TSD. b) mean FC of the right LB and left inferior frontal gyrus for TRD and TSD groups. The colour scale bar represents the strength of the t-statistic. The mean FC on b) represents beta values of FC between the two regions (95 % CI). Results corrected for multiple comparisons at cluster-level threshold of P_{FDR} <0.05 and voxel-level threshold of p-uncorrected < 0.001.

differences related to the CM and SF subregions. During our review, it became evident that very little work has been done in directly comparing amygdala subregional FC in TRD and TSD cohorts. Two previous studies identified in the literature had conflicting results that were also inconsistent with those of the present study. Significantly decreased connectivity between the left amygdala and left anterior cingulate cortex in TRD relative to TSD was identified in a study using low resolution data and whole amygdala ROIs (Lui et al., 2011) whereas no FC differences were identified in a study using standard resolution data and both whole and subregional ROI methods (Zhang et al., 2022). Our study also found no significant FC differences using whole amygdala ROIs in TRD relative to TSD.

Interestingly, within this small group of nine previous studies that have compared amygdala FC in TRD vs HC, cohort heterogeneity was evident. Underscoring the confounding nature of this issue, significant FC differences have also been shown within a TRD cohort in which a comparison was made between Anxious Depression and Non-anxious Depression subgroups (Yuan et al., 2023). Although the present study did not assess anxiety as a confounding factor, heterogeneity was evident within the TRD cohort with 29 % reporting exposure to ECT. Additionally, medication status varied broadly, with the length of time on medication ranging from 62 days to 12 years. Given reports of inflammatory marker levels decreasing with ECT (Hestad et al., 2003) together with findings of a large meta-analysis reporting that antidepressant medications may decrease peripheral inflammatory markers that have been shown to be increased in depression (Köhler et al., 2018), the wide variation in medication timeframes and ECT history in our cohort has potentially contributed to inconsistent results. In essence, the lack of congruency in FC findings across all these TRD studies is a hallmark that may be attributed not only to differences in acquisition and analysis methods but may be a reflection of the broad heterogeneity within and across TRD cohorts, supporting the premise that patients diagnosed with TRD may have little in common other than their lack of treatment response and providing a potential explanation for inconsistent study results as well as the limited success of current treatment regimens (Malhi et al., 2019).

The connectivity findings in the present study are interesting given what we know so far about the functional role of the LB subregion in the context of psychiatric disorders. Previous work has shown that the LB is involved in fear conditioning and regulates visual and auditory sensory input (Bzdok et al., 2013; Roy et al., 2009; Shen et al., 2019; Yang and Wang, 2017). It also acts as a connectivity hub and, as proposed by Pessoa, has an overarching "What is it?" function, meaning that it acts a decision-maker in relation to incoming information, particularly in terms of stimulus value (Pessoa, 2010). This subregion has also been shown to play a role in anxiety, social stress and negative regulation of social behaviour (Felix-Ortiz and Tye, 2014; Yang and Wang, 2017).

The amygdala and fusiform gyrus are linked structurally by the inferior longitudinal fasciculus and a relationship between the two has been established in previous task-based fMRI studies, supporting the role of both structures in facial perception (Chan et al., 2009; Edmiston et al., 2024; Frank et al., 2019; Müller-Bardorff et al., 2018). In particular, the right fusiform gyrus has been shown to be the primary contributor to visual processing including facial recognition and face perception (Ocklenburg and Güntürkün, 2018; Rangarajan et al., 2014; Zhang et al., 2016). Bidirectional communication between the right amygdala and right fusiform gyrus has been demonstrated, increasing in line with facial discrimination task load, in support of Pessoa's "What is it?" hypothesis (Herrington et al., 2011; Pessoa, 2010). Interplay between the amygdala and the right fusiform gyrus has also been demonstrated in studies investigating depression using task-based fMRI (Chan et al., 2009; Sacu et al., 2023). Our findings are in line with a previous study that also reported decreased amygdala-fusiform FC in TRD relative to HC at baseline that subsequently increased after ECT treatment, although their findings were left-sided rather than right-sided (Wang et al., 2017). Our results of right LB amygdala hypoconnectivity with visual processing regions in TRD relative to HC parallel those in task-based studies that are suggestive of impaired bottom-up emotion processing of visual stimuli in the right amygdala (Ochsner et al., 2009; Ramasubbu et al., 2014). Given the known relevance of impaired facial processing in depressive symptoms, these findings may be indicative of a lesser known function of the amygdala-fusiform circuitry that could potentially be negatively impacting general social functioning in TRD cohorts (Akinci et al., 2022; Demenescu et al., 2010; Kupferberg and Hasler, 2023; Monferrer et al., 2023; Rutter et al., 2020).

The second key finding in TRD was hyperconnectivity of the right LB with the left inferior frontal gyrus compared to TSD. Part of the medial prefrontal cortex, the inferior frontal gyrus is implicated in several functions including semantic processing and social cognition. In particular, the left inferior frontal gyrus is thought to be responsive to the cognitive demands required during the execution of social tasks (Diveica et al., 2023) and also acts as a hub in the brain's emotional circuitry (Li et al., 2021a). Several previous studies using Amplitude of Low-Frequency Fluctuation and Regional Homogeneity analyses have demonstrated abnormal functional activity in the left inferior frontal gyrus in TRD relative to non-refractory Major Depressive Disorder, pinpointing this area as a potential differentiator between these cohorts (Guo et al., 2012; Sun et al., 2022; Wu et al., 2011).

Previous work has linked aberrant amygdala connectivity and suicide attempts, with FC alterations of the right amygdala being a differentiator of suicidal behaviour (Huang et al., 2020; Kang et al., 2017; Stumps et al., 2021). Another study in veterans showed that right amygdala connectivity alterations were indicative of recent suicide attempts (Jagger-Rickels et al., 2023). Our TRD and TSD cohorts displayed a significant difference in number of suicide attempts (54 % vs 14 %, $p < 0.001$), potentially reflected in our findings of right LB hyperconnectivity in TRD. Additionally, a direct relationship between severity of depression symptoms and strength of right amygdala FC has been reported; this is in alignment with our findings, noting HAMD-21 scores were significantly higher in the TRD cohort compared to TSD ($p < 0.001$) (Quidé et al., 2023). Although the present study did not focus on anxiety as a comorbid condition, it is likely that a proportion of both TRD and TSD cohorts experienced coexisting symptoms, particularly in the context of published comorbidity figures of over 70 % for depression and anxiety (Almeida-Filho et al., 2007). Previous work has shown that comorbidity in depression patients infers less likelihood of remission and greater likelihood of recurrence (Choi et al., 2020; Vittengl et al., 2019). Further, the top-down influence exerted on the amygdala by the medial prefrontal cortex is thought to be undermined by a range of chronic stressors causing structural amygdala neuronal remodelling and abnormal amygdala activation resulting in emotional disturbances (Liu et al., 2020; Zhang et al., 2021). The LB subregion is particularly implicated in relation to social stress and anxiety due to its composition of mainly excitatory neurons (Shen et al., 2019; Yang and Wang, 2017) (Zhang et al., 2021). Previous work found decreased volumes in the right lateral nucleus of the right LB subregion in MDD and an inverse relationship between right LB volume and severity of depression and anxiety (Tesen et al., 2022). It is interesting to note that another study showed bilateral LB hypoconnectivity compared to HC, but only in the subgroup of MDD patients with anxiety, so it is feasible that our findings of right LB hypoconnectivity compared to HC may be reflection of anxiety as a comorbid condition in our TRD cohort (Li et al., 2021b).

There is growing evidence in human studies that the pathophysiology of depression and anxiety disorders may, in part, be related to stress-induced neuroinflammation promoting regional changes in brain function, structure and volume (Han and Ham, 2021; Milaneschi et al., 2021; Risbrough et al., 2022; Slavich and Irwin, 2014). Decreased connectivity between the right amygdala and ventromedial prefrontal cortex in depression patients has pointed to inflammation, evidence by increased levels of C-reactive proteins (Mehta et al., 2018). Interestingly, around 25 % of depression patients exhibit neuroinflammatory markers associated with treatment resistance and have poorer prognoses than those without inflammation (Hassamal, 2023). The case for further work investigating inflammatory markers and amygdala FC of the subregions in TRD cohorts is compelling.

Aside from cohort heterogeneity in TRD, there are also several potential technical explanations for lack of congruent FC findings across studies. There is considerable diversity in both data analyses and acquisition protocols, particularly in relation to the spatial resolution of fMRI data (Foster et al., 2023; Kotoula et al., 2023; Miola et al., 2023). The divergent findings in this study may reflect the use of high spatial resolution data acquired with voxel volumes of 15.6 mm^3 combined with subregional amygdala ROIs for data analyses. Of the eight previous TRD rs-fMRI studies identified, four reported whole amygdala findings using low resolution data (above 50 mm^3) whilst one used standard resolution data. Of the three studies reporting subregional findings, two used standard and only one used high-resolution data (Batail et al., 2023). Although larger voxels result in inherently higher signal-to-noise ratios, their use can be disadvantageous when imaging the amygdala. Due to the amygdala location deep in the temporal lobe near the sphenoid sinuses, intravoxel dephasing can occur during data acquisition, detrimentally affecting signal-to-noise ratio levels. Additionally, its position abutting the Basal Vein of Rosenthal, together with the diminutive size of the subregions, can result in confounding signals and partial volume effects which reduce signal accuracy and compromise the ability to resolve the very small subregional structures (Boubela et al., 2015; Olman and Yacoub, 2011).

Further, the use of whole amygdala ROIs during data analyses may potentially confound findings. Zhang and colleagues reported both hypoconnectivity of the right SF and hyperconnectivity of the right CM in TRD compared with HC; however, their subregional results were not replicated in repeat analyses using a right whole amygdala ROI (Zhang et al., 2022). This was also the case in the present study, where the significant right LB subregional findings were unable to be replicated using the right whole amygdala ROI. These results support the premise that the common practice of considering the amygdala as a single structure may produce erroneous results, in part due to the potential for averaging of positive and negative subregional signals which are unable to be accurately interpreted using whole amygdala ROIs (Roy et al., 2009; Zhang et al., 2018).

The potential for measurement errors to confound findings is amplified when interrogating FC of very small structures such as the amygdala subregions with large voxels; however, these errors can be minimised whilst simultaneously maximising contrast-to-noise ratio by employing protocols with image resolution appropriate to the size of the structures being imaged (Blazejewska et al., 2019; Yoo et al., 2001). Similarly, data analysis methods using subregional ROI masks can aid in teasing out more accurately the individual FC contributions to other brain regions. Although probabilistic cytoarchitectonic maps of the amygdala subregions are now freely available, not all researchers employ this method which has the potential to introduce a level of standardisation and accuracy in localising significant clusters anatomically (Eickhoff et al., 2005). Further, tailoring the data preprocessing steps to take into account the acquired spatial resolution, selected region-of-interest and method of controlling family-wise error (FWE) are all methods of minimising measurement error (Mikl et al., 2008).

5. Limitations and future work

There are several limitations to this study which may be overcome in future work. A causal relationship between treatment resistance and FC alterations cannot be implied due to the cross-sectional nature of the study. Severity of depression has the potential to be a confounding factor and, although the findings in this study held when controlling for depression severity in the TRD vs TSD comparison, resolving both these limitations in future work would necessitate a longitudinal approach in which depression patients are followed before and after TRD diagnosis. Additionally, as disparity in FC results is characteristic across the limited number of published TRD studies, replication of the current study results using fMRI data with similar or higher resolution, for example at 7T, would strengthen both the current findings and the case for acquisition of higher resolution fMRI data and a subregional amygdala ROI analysis approach in future studies. A further limitation was that this study did not specifically evaluate anxiety as a coexisting condition across cohorts, potentially confounding the results. Although previous work has shown that altered connectivity of the subregions is implicated in anxiety (Etkin et al., 2009; Yuan et al., 2016; Li et al., 2021a) any discussion on the role of anxiety based on the findings of this study are purely speculative. Future work could provide new insights into the role of anxiety as a potential contributor to symptom persistence in TRD.

An additional limitation from a technical perspective is that we used a high-resolution acquisition protocol coupled with data analysis of individual subregions, meaning the method on which our comparisons were based differed from all but one previous study of TRD. This introduces a lack of generalisability when comparing our findings across studies, and this issue has been raised again in a recent meta-analysis of TRD neuroimaging studies, in which the authors noted that heterogeneity in both clinical cohorts and study methodologies is a barrier to results generalisability (Miola et al., 2023). However, our methodology has harnessed the technical advancements in the field that are now

available to researchers who can build on this work using updated techniques. Harmonisation of acquisition protocols and analysis methods across studies and sites is a recognised method of promulgating generalisability (Yamashita et al., 2019) and this concept has been widely embraced by collaborative groups such as International Consortium for Brain Mapping and Enhanced Neuroimaging and Genetics through Meta-Analysis.

6. Conclusion

This study showed that altered connectivity of the right LB subregion was a distinguishing feature of TRD. While much of the work to date has focused on the whole amygdala, these results, obtained with high resolution data focusing on the amygdala subregions, emphasise the potential for improved techniques to advance our knowledge of the pathophysiological processes that underpin TRD. The study also provides a window into the highly specialised role of the right LB subregion and its complex interplay between different brain regions bilaterally. Review of the literature for this work revealed that heterogeneity - of cohorts, of data acquisition and of analysis techniques – is likely constraining our efforts to better understand the underlying neural mechanisms of TRD and future work may benefit from addressing these considerations.

CRediT authorship contribution statement

Sheryl L. Foster: Writing – review & editing, Writing – original draft, Visualization, Resources, Methodology, Investigation, Formal analysis, Data curation. **Ramon Landin-Romero:** Writing – review & editing, Supervision, Methodology, Formal analysis. **Sarah Lewis:** Writing – review & editing, Supervision, Conceptualization. **Ana Rita Barreiros:** Writing – review & editing, Resources, Methodology. **Sophie Matis:** Writing – review & editing, Methodology. **Anthony Harris:** Writing – review & editing, Resources, Project administration, Data curation, Conceptualization. **Mayuresh S. Korgaonkar:** Writing – review & editing, Supervision, Project administration, Funding acquisition, Conceptualization.

Declaration of competing interest

The authors declare the following financial interests/personal relationships which may be considered as potential competing interests:

Mayuresh Korgaonkar and Anthony Harris report that financial support was provided by Takeda Pharmaceutical Company Limited. All other authors declare that they have no known competing financial interests or personal relationships that could have appeared to influence the work reported in this paper.

Acknowledgement

This work was supported by The Westmead Charitable Trust Career Development Grant to Sheryl Foster.

Data availability

The data that support the findings of this study are available from the corresponding author upon reasonable request.

Role of Funding Source

This work was supported by Takeda Pharmaceutical Company Limited COCKPI-T (Co-Create Knowledge for Pharma Innovation with Takeda) Research Grant.

None of the Takeda members had any specific role in the design and execution of this clinical study.

Supplementary materials

Supplementary material associated with this article can be found, in the online version, at doi:10.1016/j.jadr.2025.100932.

References

Akinci, E., Wieser, M.O., Vanscheidt, S., Diop, S., Flasbeck, V., Akinci, B., Stiller, C., Juckel, G., Mavrogiorgou, P., 2022. Impairments of social interaction in depressive disorder. Psychiatry Investig. 19 (3), 178–189. https://doi.org/10.30773/pi.2021.0289.

Almeida-Filho, N., Lessa, I., Magalhães, L., Araúho, M.J., Aquino, E., de Jesus, M.J., 2007. Co-occurrence patterns of anxiety, depression and alcohol use disorders. Eur. Arch. Psychiatry Clin. Neurosci. 257 (7), 423–431. https://doi.org/10.1007/s00406-007-0752-0.

Amunts, K., Kedo, O., Kindler, M., Pieperhoff, P., Mohlberg, H., Shah, N.J., Habel, U., Schneider, F., Zilles, K., 2005. Cytoarchitectonic mapping of the human amygdala, hippocampal region and entorhinal cortex: intersubject variability and probability maps. Anat. Embryol 210 (5), 343–352. https://doi.org/10.1007/s00429-005-0025-5.

APA, A.P.A., 2013. Diagnostic and Statistical Manual of Mental Disorders. The American Psychiatric Association.

Ball, T., Rahm, B., Eickhoff, S.B., Schulze-Bonhage, A., Speck, O., Mutschler, I., 2007. Response properties of Human amygdala subregions: evidence based on functional MRI combined with probabilistic anatomical maps. PLoS One 2 (3), e307. https://doi.org/10.1371/journal.pone.0000307.

Bakoyiannis, I., 2023. Amygdala's role in treatment-resistant depression. Nat. Ment. Health 1 (5), 300. https://doi.org/10.1038/s44220-023-00069-1. -300.

Barreiros, A.R., Breukelaar, I., Mayur, P., Andepalli, J., Tomimatsu, Y., Funayama, K., Foster, S., Boyce, P., Malhi, G.S., Harris, A., Korgaonkar, M.S., 2022. Abnormal habenula functional connectivity characterizes treatment-resistant depression. Neuroimage Clin. 34, 102990. https://doi.org/10.1016/j.nicl.2022.102990.

Batail, J.-M., Xiao, X., Azeez, A., Tischler, C., Kratter, I.H., Bishop, J.H., Saggar, M., Williams, N.R., 2023. Network effects of stanford neuromodulation therapy (SNT) in treatment-resistant major depressive disorder: a randomized, controlled trial. Transl. Psychiatry 13 (1), 240. https://doi.org/10.1038/s41398-023-02537-9.

Blazejewska, A.I., Fischl, B., Wald, L.L., Polimeni, J.R., 2019. Intracortical smoothing of small-voxel fMRI data can provide increased detection power without spatial resolution losses compared to conventional large-voxel fMRI data. Neuroimage 189, 601–614. https://doi.org/10.1016/j.neuroimage.2019.01.054.

Boubela, R.N., Kalcher, K., Huf, W., Seidel, E.-M., Derntl, B., Pezawas, L., Našel, C., Moser, E., 2015. fMRI measurements of amygdala activation are confounded by stimulus correlated signal fluctuation in nearby veins draining distant brain regions. Sci. Rep. 5 (1), 10499. https://doi.org/10.1038/srep10499.

Bzdok, D., Laird, A.R., Zilles, K., Fox, P.T., Eickhoff, S.B., 2013. An investigation of the structural, connectional, and functional subspecialization in the human amygdala. Hum. Brain Mapp. 34 (12), 3247–3266. https://doi.org/10.1002/hbm.22138.

Chan, S.W.Y., Norbury, R., Goodwin, G.M., Harmer, C.J., 2009. Risk for depression and neural responses to fearful facial expressions of emotion. Br. J. Psychiatry 194 (2), 139–145. https://doi.org/10.1192/bjp.bp.107.047993.

Chen, M.-H., Chang, W.-C., Lin, W.-C., Tu, P.-C., Li, C.-T., Bai, Y.-M., Tsai, S.-J., Huang, W.-S., Su, T.-P., 2020. Functional dysconnectivity of frontal cortex to striatum predicts ketamine infusion response in treatment-resistant depression. Int. J. Neuropsychopharmacol. 23 (12), 791–798. https://doi.org/10.1093/ijnp/pyaa056.

Choi, K.W., Kim, Y.-K., Jeon, H.J., 2020. Comorbid anxiety and depression: clinical and conceptual consideration and transdiagnostic treatment. In: Kim, Y.-K. (Ed.), Anxiety Disorders: Rethinking and Understanding Recent Discoveries. Springer, Singapore, pp. 219–235. https://doi.org/10.1007/978-981-32-9705-0_14.

Chumbley, J., Worsley, K., Flandin, G., Friston, K., 2010. Topological FDR for neuroimaging. Neuroimage 49 (4), 3057–3064. https://doi.org/10.1016/j.neuroimage.2009.10.090.

Compère, L., Siegle, G.J., Lazzaro, S., Riley, E., Strege, M., Canovali, G., Barb, S., Huppert, T., Young, K., 2024. Amygdala real-time fMRI neurofeedback upregulation in treatment resistant depression: proof of concept and dose determination. Behav. Res. Ther. 176, 104523. https://doi.org/10.1016/j.brat.2024.104523.

Demenescu, L.R., Kortekaas, R., den Boer, J.A., Aleman, A., 2010. Impaired attribution of emotion to facial expressions in anxiety and major depression. PLoS One 5 (12), e15058. https://doi.org/10.1371/journal.pone.0015058.

Diveica, V., Riedel, M.C., Salo, T., Laird, A.R., Jackson, R.L., Binney, R.J., 2023. Graded functional organization in the left inferior frontal gyrus: evidence from task-free and task-based functional connectivity. Cereb. Cortex 33 (23), 11384–11399. https://doi.org/10.1093/cercor/bhad373.

Drysdale, A.T., Grosenick, L., Downar, J., Dunlop, K., Mansouri, F., Meng, Y., Fetcho, R. N., Zebley, B., Oathes, D.J., Etkin, A., Schatzberg, A.F., Sudheimer, K., Keller, J., Mayberg, H.S., Gunning, F.M., Alexopoulos, G.S., Fox, M.D., Pascual-Leone, A., Voss, H.U., Liston, C., 2017. Resting-state connectivity biomarkers define neurophysiological subtypes of depression. Nat. Med. 23 (1), 28–38. https://doi.org/10.1038/nm.4246.

Edmiston, E.K., Chase, H.W., Jones, N., Nhan, T.J., Phillips, M.L., Fournier, J.C., 2024. Differential role of fusiform gyrus coupling in depressive and anxiety symptoms during emotion perception. Soc. Cogn. Affect. Neurosci. 19 (1). https://doi.org/10.1093/scan/nsae009.

Eickhoff, S.B., Stephan, K.E., Mohlberg, H., Grefkes, C., Fink, G.R., Amunts, K., Zilles, K., 2005. A new SPM toolbox for combining probabilistic cytoarchitectonic maps and functional imaging data. Neuroimage 25 (4), 1325–1335. https://doi.org/10.1016/j.neuroimage.2004.12.034.

Etkin, A., Prater, K.E., Schatzberg, A.F., Menon, V., Greicius, M.D., 2009. Disrupted amygdalar subregion functional connectivity and evidence of a compensatory network in generalized anxiety disorder. Arch. Gen. Psychiatry 66 (12), 1361–1372. https://doi.org/10.1001/archgenpsychiatry.2009.104.

Felix-Ortiz, A.C., Tye, K.M., 2014. Amygdala inputs to the ventral hippocampus bidirectionally modulate social behavior. J. Neurosci. 34 (2), 586–595. https://doi.org/10.1523/jneurosci.4257-13.2014.

Foster, S.L., Breukelaar, I.A., Ekanayake, K., Lewis, S., Korgaonkar, M.S., 2023. Functional Magnetic resonance imaging of the amygdala and subregions at 3 tesla: a scoping review. J. Magn. Reson. Imaging. https://doi.org/10.1002/jmri.28836.

Frank, D.W., Costa, V.D., Averbeck, B.B., Sabatinelli, D., 2019. Directional interconnectivity of the human amygdala, fusiform gyrus, and orbitofrontal cortex in emotional scene perception. J. Neurophysiol. 122 (4), 1530–1537. https://doi.org/10.1152/jn.00780.2018.

Ge, R., Torres, I., Brown, J.J., Gregory, E., McLellan, E., Downar, J.H., Blumberger, D.M., Daskalakis, Z.J., Lam, R.W., Vila-Rodriguez, F., 2019. Functional disconnectivity of the hippocampal network and neural correlates of memory impairment in treatment-resistant depression. J. Affect. Disord. 253, 248–256. https://doi.org/10.1016/j.jad.2019.04.096.

Gill, H., Puramat, P., Patel, P., Gill, B., Marks, C.A., Rodrigues, N.B., Castle, D., Cha, D.S., Mansur, R.B., Rosenblat, J.D., McIntyre, R.S., 2022. The effects of psilocybin in adults with major depressive disorder and the general population: findings from neuroimaging studies. Psychiatry Res. 313, 114577. https://doi.org/10.1016/j.psychres.2022.114577.

Goldstein-Piekarski, A.N., Korgaonkar, M.S., Green, E., Suppes, T., Schatzberg, A.F., Hastie, T., Nemeroff, C.B., Williams, L.M., 2016. Human amygdala engagement moderated by early life stress exposure is a biobehavioral target for predicting recovery on antidepressants. Proc. Natl. Acad. Sci. 113 (42), 11955–11960. https://doi.org/10.1073/pnas.1606671113.

Grehl, M.M., Hameed, S., Murrough, J.W., 2023. Brain features of treatment-resistant depression: a review of structural and functional connectivity Magnetic resonance imaging studies. Psychiatr. Clin. N. Am. 46 (2), 391–401. https://doi.org/10.1016/j.psc.2023.02.009.

Guo, W.-B., Liu, F., Xue, Z.-M., Xu, X.-J., Wu, R.-R., Ma, C.-Q., Wooderson, S.C., Tan, C.-L., Sun, X.-L., Chen, J.-D., Liu, Z.-N., Xiao, C.-Q., Chen, H.-F., Zhao, J.-P, 2012. Alterations of the amplitude of low-frequency fluctuations in treatment-resistant and treatment-response depression: a resting-state fMRI study. Prog. Neuro-Psychopharmacol. Biol. Psychiatry 37 (1), 153–160. https://doi.org/10.1016/j.pnpbp.2012.01.011.

Hamilton, J.P., Etkin, A., Furman, D.J., Lemus, M.G., Johnson, R.F., Gotlib, I.H., 2012. Functional neuroimaging of major depressive disorder: a meta-analysis and new integration of base line activation and neural response data. Am. J. Psychiatry 169 (7), 693–703. https://doi.org/10.1176/appi.ajp.2012.11071105.

Hamilton, M., 1960. A rating scale for depression. J. Neurol. Neurosurg. Psychiatry 23 (1), 56–62. https://doi.org/10.1136/jnnp.23.1.56.

Han, K.M., Ham, B.J., 2021. How inflammation affects the brain in depression: a review of functional and structural MRI studies. J. Clin. Neurol. 17 (4), 503–515. https://doi.org/10.3988/jcn.2021.17.4.503.

Hassamal, S., 2023. Chronic stress, neuroinflammation, and depression: an overview of pathophysiological mechanisms and emerging anti-inflammatories [Review]. Front. Psychiatry 14. https://doi.org/10.3389/fpsyt.2023.1130989.

Herrington, J.D., Taylor, J.M., Grupe, D.W., Curby, K.M., Schultz, R.T., 2011. Bidirectional communication between amygdala and fusiform gyrus during facial recognition. Neuroimage 56 (4), 2348–2355. https://doi.org/10.1016/j.neuroimage.2011.03.072.

Huang, M., Landin-Romero, R., Matis, S., Dalton, M.A., Piguet, O., 2024. Longitudinal volumetric changes in amygdala subregions in frontotemporal dementia. J. Neurol. 271 (5), 2509–2520. https://doi.org/10.1007/s00415-023-12172-5.

Hestad, K.A., Tønseth, S., Støen, C.D., Ueland, T., Aukrust, P., 2003. Raised plasma levels of tumor necrosis factor α in patients with depression: normalization during electroconvulsive therapy. J. ECT. 19 (4).

Huang, X., Rootes-Murdy, K., Bastidas, D.M., Nee, D.E., Franklin, J.C., 2020. Brain differences associated with self-injurious thoughts and behaviors: a meta-analysis of neuroimaging studies. Sci. Rep. 10 (1), 2404. https://doi.org/10.1038/s41598-020-59490-6.

IBM-SPSS, 2012. IBM SPSS Statistics For Windows. IBM Corp, Armonk (NY). Version 21.

Ionescu, D.F., Rosenbaum, J.F., Alpert, J.E., 2015. Pharmacological approaches to the challenge of treatment-resistant depression. Dialogues. Clin. Neurosci. 17 (2), 111–126. https://doi.org/10.31887/DCNS.2015.17.2/dionescu.

Jagger-Rickels, A., Stumps, A., Rothlein, D., Evans, T., Lee, D., McGlinchey, R., DeGutis, J., Esterman, M., 2023. Aberrant connectivity in the right amygdala and right middle temporal gyrus before and after a suicide attempt: examining markers of suicide risk. J. Affect. Disord. 335, 24–35. https://doi.org/10.1016/j.jad.2023.04.061.

Kaiser, R.H., Andrews-Hanna, J.R., Wager, T.D., Pizzagalli, D.A., 2015. Large-scale network dysfunction in major depressive disorder: a meta-analysis of resting-State functional connectivity. JAMA Psychiatry 72 (6), 603–611. https://doi.org/10.1001/jamapsychiatry.2015.0071.

Kang, S.-G., Na, K.-S., Choi, J.-W., Kim, J.-H., Son, Y.-D., Lee, Y.J., 2017. Resting-state functional connectivity of the amygdala in suicide attempters with major depressive disorder. Prog. Neuro-Psychopharmacol. Biol. Psychiatry 77, 222–227. https://doi.org/10.1016/j.pnpbp.2017.04.029.

Kedo, O., Zilles, K., Palomero-Gallagher, N., Schleicher, A., Mohlberg, H., Bludau, S., Amunts, K., 2018. Receptor-driven, multimodal mapping of the human amygdala. Brain Struct. Funct. 223 (4), 1637–1666. https://doi.org/10.1007/s00429-017-1577-x.

Kotoula, V., Evans, J.W., Punturieri, C., Johnson, S.C., Zarate, C.A., 2023. Chapter 5 - functional MRI markers for treatment-resistant depression: insights and challenges. In: Li, C.-T., Cheng, C.-M. (Eds.), Progress in Brain Research, Progress in Brain Research, 278. Elsevier, pp. 117–148. https://doi.org/10.1016/bs.pbr.2023.04.001.

Köhler, C.A., Freitas, T.H., Stubbs, B., Maes, M., Solmi, M., Veronese, N., de Andrade, N. Q., Morris, G., Fernandes, B.S., Brunoni, A.R., Herrmann, N., Raison, C.L., Miller, B. J., Lanctôt, K.L., Carvalho, A.F., 2018. Peripheral alterations in cytokine and chemokine levels after antidepressant drug treatment for major depressive disorder: systematic review and meta-analysis. Mol. Neurobiol. 55 (5), 4195–4206. https://doi.org/10.1007/s12035-017-0632-1.

Kupferberg, A., Hasler, G., 2023. The social cost of depression: investigating the impact of impaired social emotion regulation, social cognition, and interpersonal behavior on social functioning. J. Affect. Disord. Rep. 14, 100631. https://doi.org/10.1016/j.jadr.2023.100631.

Li, B.-z., Cao, Y., Zhang, Y., Chen, Y., Gao, Y.-h., Peng, J.-x., Shao, Y.-c., Zhang, X., 2021a. Relation of decreased functional connectivity between left thalamus and left inferior frontal gyrus to emotion changes following acute sleep deprivation [Original Research]. Front. Neurol. 12. https://doi.org/10.3389/fneur.2021.642411.

Li, Y.Y., Ni, X.K., You, Y.F., Qing, Y.H., Wang, P.R., Yao, J.S., Ren, K.M., Zhang, L., Liu, Z. W., Song, T.J., Wang, J., Zang, Y.F., Shen, Y.D., Chen, W., 2021b. Common and specific alterations of amygdala subregions in major depressive disorder with and without anxiety: a combined structural and resting-State functional MRI study. Front. Hum. Neurosci. 15, 634113. https://doi.org/10.3389/fnhum.2021.634113.

Liu, W.-Z., Zhang, W.-H., Zheng, Z.-H., Zou, J.-X., Liu, X.-X., Huang, S.-H., You, W.-J., He, Y., Zhang, J.-Y., Wang, X.-D., Pan, B.-X., 2020. Identification of a prefrontal cortex-to-amygdala pathway for chronic stress-induced anxiety. Nat. Commun. 11 (1), 2221. https://doi.org/10.1038/s41467-020-15920-7.

Lui, S., Wu, Q., Qiu, L., Yang, X., Kuang, W., Chan, R.C.K., Huang, X., Kemp, G.J., Mechelli, A.a., Gong, Q., 2011. Resting-State functional connectivity in treatment-resistant depression. Am. J. Psychiatry 168 (6), 642–648. https://doi.org/10.1176/appi.ajp.2010.10101419.

Machaj, W., Podgórski, P., Maciaszek, J., Piotrowski, P., Szcześniak, D., Korbecki, A., Rymaszewska, J., Zimny, A., 2024. Evaluation of intra- and inter-network connectivity within major brain networks in drug-resistant depression using rs-fMRI. J. Clin. Med. 13 (18). https://doi.org/10.3390/jcm13185507.

Malhi, G.S., Bell, E., Bassett, D., Boyce, P., Bryant, R., Hazell, P., Hopwood, M., Lyndon, B., Mulder, R., Porter, R., Singh, A.B., Murray, G., 2021. The 2020 royal Australian and New Zealand college of psychiatrists clinical practice guidelines for mood disorders. Aust. N. Z. J. Psychiatry 55 (1), 7–117. https://doi.org/10.1177/0004867420979353.

Malhi, G.S., Das, P., Mannie, Z., Irwin, L., 2019. Treatment-resistant depression: problematic illness or a problem in our approach? Br. J. Psychiatry 214 (1), 1–3. https://doi.org/10.1192/bjp.2018.246.

Mayberg, H.S., 1997. Limbic-cortical dysregulation: a proposed model of depression. J. Neuropsychiatry Clin. Neurosci. 9 (3), 471–481. https://doi.org/10.1176/jnp.9.3.471.

McIntyre, R.S., Alsuwaidan, M., Baune, B.T., Berk, M., Demyttenaere, K., Goldberg, J.F., Gorwood, P., Ho, R., Kasper, S., Kennedy, S.H., Ly-Uson, J., Mansur, R.B., McAllister-Williams, R.H., Murrough, J.W., Nemeroff, C.B., Nierenberg, A.A., Rosenblat, J.D., Sanacora, G., Schatzberg, A.F., Maj, M., 2023. Treatment-resistant depression: definition, prevalence, detection, management, and investigational interventions. World Psychiatry 22 (3), 394–412. https://doi.org/10.1002/wps.21120.

Mehta, N.D., Haroon, E., Xu, X., Woolwine, B.J., Li, Z., Felger, J.C., 2018. Inflammation negatively correlates with amygdala-ventromedial prefrontal functional connectivity in association with anxiety in patients with depression: preliminary results. Brain Behav. Immun. 73, 725–730. https://doi.org/10.1016/j.bbi.2018.07.026.

Mikl, M., Mareček, R., Hluštík, P., Pavlicová, M., Drastich, A., Chlebus, P., Brázdil, M., Krupa, P., 2008. Effects of spatial smoothing on fMRI group inferences. Magn. Reson. ImAging 26 (4), 490–503. https://doi.org/10.1016/j.mri.2007.08.006.

Milaneschi, Y., Kappelmann, N., Ye, Z., Lamers, F., Moser, S., Jones, P.B., Burgess, S., Penninx, B.W.J.H., Khandaker, G.M., 2021. Association of inflammation with depression and anxiety: evidence for symptom-specificity and potential causality from UK Biobank and NESDA cohorts. Mol. Psychiatry 26 (12), 7393–7402. https://doi.org/10.1038/s41380-021-01188-w.

Miola, A., Meda, N., Perini, G., Sambataro, F., 2023. Structural and functional features of treatment-resistant depression: a systematic review and exploratory coordinate-based meta-analysis of neuroimaging studies. Psychiatry Clin. Neurosci. 77 (5), 252–263. https://doi.org/10.1111/pcn.13530.

Monferrer, M., García, A.S., Ricarte, J.J., Montes, M.J., Fernández-Caballero, A., Fernández-Sotos, P., 2023. Facial emotion recognition in patients with depression compared to healthy controls when using human avatars. Sci. Rep. 13 (1), 6007. https://doi.org/10.1038/s41598-023-31277-5.

Müller-Bardorff, M., Bruchmann, M., Mothes-Lasch, M., Zwitserlood, P., Schlossmacher, I., Hofmann, D., Miltner, W., Straube, T., 2018. Early brain responses to affective faces: a simultaneous EEG-fMRI study. Neuroimage 178, 660–667. https://doi.org/10.1016/j.neuroimage.2018.05.081.

Nair, A.U., Klimes-Dougan, B., Silamongkol, T., Başgöze, Z., Roediger, D.J., Mueller, B. A., Albott, C.S., Croarkin, P.E., Lim, K.O., Widge, A.S., Nahas, Z., Eberly, L.E., Cullen, K.R., Thai, M.E., 2024. Deep transcranial magnetic stimulation for adolescents with treatment-resistant depression: behavioral and neural correlates of clinical improvement. J. Affect. Disord. 372, 665–675. https://doi.org/10.1016/j.jad.2024.12.057.

Nakamura, T., Tomita, M., Horikawa, N., Ishibashi, M., Uematsu, K., Hiraki, T., Abe, T., Uchimura, N., 2021. Functional connectivity between the amygdala and subgenual cingulate gyrus predicts the antidepressant effects of ketamine in patients with treatment-resistant depression. Neuropsychopharmacol. Rep. 41 (2), 168–178. https://doi.org/10.1002/npr2.12165.

Nieto-Castanon, A., 2020a. FMRI denoising pipeline. Handbook of Functional Connectivity Magnetic Resonance Imaging methods in CONN. Hilbert Press, pp. 17–25. https://doi.org/10.56441/hilbertpress.2207.6599.

Nieto-Castanon, A., 2020b. FMRI minimal preprocessing pipeline. Handbook of Functional Connectivity Magnetic Resonance Imaging Methods in CONN. Hilbert Press, pp. 3–16. https://doi.org/10.56441/hilbertpress.2207.6599.

Ochsner, K.N., Ray, R.R., Hughes, B., McRae, K., Cooper, J.C., Weber, J., Gabrieli, J.D.E., Gross, J.J., 2009. Bottom-up and top-down processes in emotion generation:common and distinct neural mechanisms. Psychol. Sci. 20 (11), 1322–1331. https://doi.org/10.1111/j.1467-9280.2009.02459.x.

Ocklenburg, S., Güntürkün, O., 2018. Chapter 7 - Recognizing Yourself and Others—The Role of the Right Hemisphere for Face and Self Perception. In: Ocklenburg, S., Güntürkün, O. (Eds.), The Lateralized Brain. Academic Press, pp. 185–211. https://doi.org/10.1016/B978-0-12-803452-1.00007-2.

Olman, C.A., Yacoub, E., 2011. High-field FMRI for human applications: an overview of spatial resolution and signal specificity. Open. Neuroimag. J. 5, 74–89. https://doi.org/10.2174/1874440001105010074.

Pessoa, L., 2010. Emotion and cognition and the amygdala: from "what is it?" to "what's to be done? Neuropsychologia 48 (12), 3416–3429. https://doi.org/10.1016/j.neuropsychologia.2010.06.038.

Quidé, Y., Norman-Nott, N., Hesam-Shariati, N., McAuley, J.H., Gustin, S.M., 2023. Depressive symptoms moderate functional connectivity within the emotional brain in chronic pain. BJPsych. Open. 9 (3), e80. https://doi.org/10.1192/bjo.2023.61.

Ramasubbu, R., Konduru, N., Cortese, F., Bray, S., Gaxiola, I., Goodyear, B., 2014. Reduced intrinsic connectivity of amygdala in adults with major depressive disorder [Original Research]. Front. Psychiatry 5. https://doi.org/10.3389/fpsyt.2014.00017.

Ramezani, F., Mardani, P., Nemati, F., Cattarinussi, G., Sambataro, F., Schiena, G., Brambilla, P., Delvecchio, G., 2025. Effect of ketamine on task-based functional magnetic resonance imaging findings in major depressive disorder: a mini-review. J. Affect. Disord. 370, 181–189. https://doi.org/10.1016/j.jad.2024.10.118.

Rangarajan, V., Hermes, D., Foster, B.L., Weiner, K.S., Jacques, C., Grill-Spector, K., Parvizi, J., 2014. Electrical stimulation of the left and right Human fusiform gyrus causes different effects in conscious face perception. J. Neurosci. 34 (38), 12828. https://doi.org/10.1523/JNEUROSCI.0527-14.2014.

Risbrough, V.B., Vaughn, M.N., Friend, S.F., 2022. Role of inflammation in traumatic brain injury–Associated risk for neuropsychiatric disorders: state of the evidence and where do we go from here. Biol. Psychiatry 91 (5), 438–448. https://doi.org/10.1016/j.biopsych.2021.11.012.

Roy, A.K., Shehzad, Z., Margulies, D.S., Kelly, A.M.C., Uddin, L.Q., Gotimer, K., Biswal, B.B., Castellanos, F.X., Milham, M.P., 2009. Functional connectivity of the human amygdala using resting state fMRI. Neuroimage 45 (2), 614–626. https://doi.org/10.1016/j.neuroimage.2008.11.030.

Runia, N., Bergfeld, I.O., de Kwaasteniet, B.P., Luigjes, J., van Laarhoven, J., Notten, P., Beute, G., van den Munckhof, P., Schuurman, R., Denys, D., van Wingen, G.A., 2023. Deep brain stimulation normalizes amygdala responsivity in treatment-resistant depression. Mol. Psychiatry 28 (6), 2500–2507. https://doi.org/10.1038/s41380-023-02030-1.

Rutter, L.A., Passell, E., Scheuer, L., Germine, L., 2020. Depression severity is associated with impaired facial emotion processing in a large international sample. J. Affect. Disord. 275, 175–179. https://doi.org/10.1016/j.jad.2020.07.006.

Sacu, S., Wackerhagen, C., Erk, S., Romanczuk-Seiferth, N., Schwarz, K., Schweiger, J.I., Tost, H., Meyer-Lindenberg, A., Heinz, A., Razi, A., Walter, H., 2023. Effective connectivity during face processing in major depression - distinguishing markers of pathology, risk, and resilience. Psychol. Med. 53 (9), 4139–4151. https://doi.org/10.1017/s0033291722000824.

Scott, F., Hampsey, E., Gnanapragasam, S., Carter, B., Marwood, L., Taylor, R.W., Emre, C., Korotkova, L., Martín-Dombrowski, J., Cleare, A.J., Young, A.H., Strawbridge, R., 2023. Systematic review and meta-analysis of augmentation and combination treatments for early-stage treatment-resistant depression. J. Psychopharmacol. 37 (3), 268–278. https://doi.org/10.1177/02698811221104058.

Shen, C.-J., Zheng, D., Li, K.-X., Yang, J.-M., Pan, H.-Q., Yu, X.-D., Fu, J.-Y., Zhu, Y., Sun, Q.-X., Tang, M.-Y., Zhang, Y., Sun, P., Xie, Y., Duan, S., Hu, H., Li, X.-M., 2019. Cannabinoid CB1 receptors in the amygdalar cholecystokinin glutamatergic afferents to nucleus accumbens modulate depressive-like behavior. Nat. Med. 25 (2), 337–349. https://doi.org/10.1038/s41591-018-0299-9.

Siegel, J.S., Palanca, B.J.A., Ances, B.M., Kharasch, E.D., Schweiger, J.A., Yingling, M.D., Snyder, A.Z., Nicol, G.E., Lenze, E.J., Farber, N.B., 2021. Prolonged ketamine infusion modulates limbic connectivity and induces sustained remission of treatment-resistant depression. Psychopharmacology 238 (4), 1157–1169. https://doi.org/10.1007/s00213-021-05762-6.

Slavich, G.M., Irwin, M.R., 2014. From stress to inflammation and major depressive disorder: a social signal transduction theory of depression. Psychol. Bull. 140 (3), 774–815. https://doi.org/10.1037/a0035302.

Solano-Castiella, E., Anwander, A., Lohmann, G., Weiss, M., Docherty, C., Geyer, S., Reimer, E., Friederici, A.D., Turner, R., 2010. Diffusion tensor imaging segments the human amygdala in vivo. Neuroimage 49 (4), 2958–2965. https://doi.org/10.1016/j.neuroimage.2009.11.027.

Stumps, A., Jagger-Rickels, A., Rothlein, D., Amick, M., Park, H., Evans, T., Fortenbaugh, F.C., Fortier, C.B., Fonda, J.R., Lee, D., Milberg, W., McGlinchey, R., DeGutis, J., Esterman, M., 2021. Connectome-based functional connectivity markers of suicide attempt. J. Affect. Disord. 283, 430–440. https://doi.org/10.1016/j.jad.2020.11.061.

Sun, J., Ma, Y., Chen, L., Wang, Z., Guo, C., Luo, Y., Gao, D., Li, X., Xu, K., Hong, Y., Hou, X., Tian, J., Yu, X., Wang, H., Fang, J., Xiao, X., 2022. Altered brain function in treatment-resistant and non-treatment-resistant depression patients: a resting-State functional Magnetic resonance imaging study [Original Research]. Front. Psychiatry 13. https://doi.org/10.3389/fpsyt.2022.904139.

Sundermann, B., Olde lütke Beverborg, M., Pfleiderer, B., 2014. Toward literature-based feature selection for diagnostic classification: a meta-analysis of resting-state fMRI in depression [Original Research]. Front. Hum. Neurosci. 8. https://doi.org/10.3389/fnhum.2014.00692.

Tesen, H., Watanabe, K., Okamoto, N., Ikenouchi, A., Igata, R., Konishi, Y., Kakeda, S., Yoshimura, R., 2022. Volume of amygdala subregions and clinical manifestations in patients with first-episode, drug-naïve major depression [Original Research]. Front. Hum. Neurosci. 15. https://doi.org/10.3389/fnhum.2021.780884.

Tu, P.C., Chang, W.C., Su, T.P., Lin, W.C., Li, C.T., Bai, Y.M., Tsai, S.J., Chen, M.H., 2025. Thalamocortical functional connectivity and rapid antidepressant and antisuicidal effects of low-dose ketamine infusion among patients with treatment-resistant depression. Mol. Psychiatry 30 (1), 61–68. https://doi.org/10.1038/s41380-024-02640-3.

Vasavada, M.M., Loureiro, J., Kubicki, A., Sahib, A., Wade, B., Hellemann, G., Espinoza, R.T., Congdon, E., Narr, K.L., Leaver, A.M., 2021. Effects of serial ketamine infusions on corticolimbic functional connectivity in major depression. Biol. Psychiatry: Cogn. Neurosci. Neuroimaging 6 (7), 735–744. https://doi.org/10.1016/j.bpsc.2020.06.015.

Vittengl, J.R., Clark, L.A., Smits, J.A.J., Thase, M.E., Jarrett, R.B., 2019. Do comorbid social and other anxiety disorders predict outcomes during and after cognitive therapy for depression? J. Affect. Disord. 242, 150–158. https://doi.org/10.1016/j.jad.2018.08.053.

Voineskos, D., Daskalakis, Z.J., Blumberger, D.M., 2020. Management of treatment-resistant depression: challenges and strategies. Neuropsychiatr. Dis. Treat. 16, 221–234. https://doi.org/10.2147/ndt.S198774.

Wang, J., Wei, Q., Bai, T., Zhou, X., Sun, H., Becker, B., Tian, Y., Wang, K., Kendrick, K., 2017. Electroconvulsive therapy selectively enhanced feedforward connectivity from fusiform face area to amygdala in major depressive disorder. Soc. Cogn. Affect. Neurosci. 12 (12), 1983–1992. https://doi.org/10.1093/scan/nsx100.

Wang, X., Nie, X., Zhang, F., Wei, Y., Zeng, W., Zhang, Y., Lin, H., 2024. Functional magnetic resonance imaging of depression: a bibliometrics and meta-analysis. Ann. Gen. Psychiatry 23 (1), 39. https://doi.org/10.1186/s12991-024-00525-x.

Williams, L.M., Korgaonkar, M.S., Song, Y.C., Paton, R., Eagles, S., Goldstein-Piekarski, A., Grieve, S.M., Harris, A.W.F., Usherwood, T., Etkin, A., 2015. Amygdala reactivity to emotional faces in the prediction of general and medication-specific responses to antidepressant treatment in the randomized iSPOT-D trial. Neuropsychopharmacology 40 (10), 2398–2408. https://doi.org/10.1038/npp.2015.89.

Wu, Q.-Z., Li, D.-M., Kuang, W.-H., Zhang, T.-J., Lui, S., Huang, X.-Q., Chan, R.C.K., Kemp, G.J., Gong, Q.-Y., 2011. Abnormal regional spontaneous neural activity in treatment-refractory depression revealed by resting-state fMRI. Hum. Brain Mapp. 32 (8), 1290–1299. https://doi.org/10.1002/hbm.21108.

Yamashita, A., Yahata, N., Itahashi, T., Lisi, G., Yamada, T., Ichikawa, N., Takamura, M., Yoshihara, Y., Kunimatsu, A., Okada, N., Yamagata, H., Matsuo, K., Hashimoto, R., Okada, G., Sakai, Y., Morimoto, J., Narumoto, J., Shimada, Y., Kasai, K., Imamizu, H., 2019. Harmonization of resting-state functional MRI data across multiple imaging sites via the separation of site differences into sampling bias and measurement bias. PLoS. Biol. 17 (4), e3000042. https://doi.org/10.1371/journal.pbio.3000042.

Yang, Y., Wang, J.-Z., 2017. From structure to behavior in basolateral amygdala-hippocampus circuits [Mini Review]. Front. Neural Circuits 11 (86). https://doi.org/10.3389/fncir.2017.00086.

Yoo, S.-S., Guttmann, C.R.G., Panych, L.P., 2001. Multiresolution data acquisition and detection in Functional MRI. Neuroimage 14 (6), 1476–1485. https://doi.org/10.1006/nimg.2001.0945.

Yuan, M., Zhu, H., Qiu, C., Meng, Y., Zhang, Y., Shang, J., Nie, X., Ren, Z., Gong, Q., Zhang, W., 2016. Group cognitive behavioral therapy modulates the resting-state functional connectivity of amygdala-related network in patients with generalized social anxiety disorder. BMC Psychiatry 16 (1), 1–9. https://doi.org/10.1186/s12888-016-0904-8.

Yuan, S., Luo, X., Chen, X., Wang, M., Hu, Y., Zhou, Y., Ning, Y., Zhang, B., 2023. Functional connectivity differences in the amygdala are related to the antidepressant efficacy of ketamine in patients with anxious depression. J. Affect. Disord. 320, 29–36. https://doi.org/10.1016/j.jad.2022.09.125.

Yun, J.-Y., Kim, Y.-K., 2024. Neural correlates of treatment response to ketamine for treatment-resistant depression: a systematic review of MRI-based studies. Psychiatry Res. 340, 116092. https://doi.org/10.1016/j.psychres.2024.116092.

Zhang, S., Cui, J., Zhang, Z., Wang, Y., Liu, R., Chen, X., Feng, Y., Zhou, J., Zhou, Y., Wang, G., 2022. Functional connectivity of amygdala subregions predicts vulnerability to depression following the COVID-19 pandemic. J. Affect. Disord. 297, 421–429. https://doi.org/10.1016/j.jad.2021.09.107.

Zhang, W., Wang, J., Fan, L., Zhang, Y., Fox, P.T., Eickhoff, S.B., Yu, C., Jiang, T., 2016. Functional organization of the fusiform gyrus revealed with connectivity profiles. Hum. Brain Mapp. 37 (8), 3003–3016. https://doi.org/10.1002/hbm.23222.

Zhang, W.H., Zhang, J.Y., Holmes, A., Pan, B.X., 2021. Amygdala circuit substrates for stress adaptation and adversity. Biol. Psychiatry 89 (9), 847–856. https://doi.org/10.1016/j.biopsych.2020.12.026.

Zhang, X., Cheng, H., Zuo, Z., Zhou, K., Cong, F., Wang, B., Zhuo, Y., Chen, L., Xue, R., Fan, Y., 2018. Individualized functional parcellation of the Human amygdala using a semi-supervised clustering method: a 7T resting State fMRI study [Original Research]. Front. Neurosci. 12 (270). https://doi.org/10.3389/fnins.2018.00270.

Chapter 5: Subregional Amygdala Connectivity to Resting State Networks: 3T vs 7T

Although higher SNR is an inherent feature of 7T MRI systems compared to 3T systems, lack of access to 7T means that most clinical research is performed at 3T. However, previous work at 7T has demonstrated the spatial resolution benefits of imaging the amygdala, providing evidence of the heterogenous structure and function of its nine component subnuclei.

We have seen in previous chapters that much of the research done at 3T has reported findings based on the amygdala as a single structure. At 7T, it is possible to resolve the amygdala contributions at a subnuclei level with high resolution data with VV of $10mm^3$ and less; however, the available SNR at 3T has generally precluded the acquisition of data with equivalent levels of resolution. Consequently, the work in this chapter is based on the widely accepted collection of three subregions used in Chapter Four (Eickhoff et al., 2005).

This chapter reports a qualitative comparison referencing the findings of a study by Elvira and colleagues titled '*Contributions of human amygdala nuclei to resting-state networks'* (Elvira et al., 2022). Their work used gold standard high resolution 7T fMRI data acquired as part of the Human Connectome Project to demonstrate amygdala co-activation at a subnuclei level with three of the primarily cortical resting state networks. The aim of the study comprising this chapter was to investigate the feasibility of using data acquired with an existing high resolution 2D sequence (used in Chapter Four) and a novel higher resolution 3D sequence, both optimised for 3T, to interrogate functional connections between the amygdala subregions and defined resting state networks-of-interest with primarily cortical connections. Findings from the 2D and 3D sequences are discussed in relation to how closely the connections mirror the subnuclei 7T findings of Elvira and colleagues, with the 2D results most closely matching 7T findings.

This chapter demonstrates the capability of optimised high resolution 2D fMRI protocols to resolve individual functional connections of the amygdala at a subregional level to resting state networks compared to results obtained at 7T, the gold standard. The results of the study in this chapter support the implementation of optimised high resolution 2D sequences into fMRI research protocols more broadly as a means of improving spatial accuracy of FC findings in relation to the amygdala and its subregions at 3T, the most widely available clinical research field strength.

5.1 Introduction

The currency of MR imaging is signal-to-noise ratio (SNR) which theoretically scales linearly with field strength. The introduction of high-field 7 Tesla (7T) MRI systems for clinical research has provided researchers with opportunities to make use of the concomitant SNR advantages in several ways, depending on the imaging technique of choice. For structural studies, increased SNR has facilitated the acquisition of data with sub-mm isotropic resolution and increased spatial location accuracy, allowing in-vivo identification of the amygdala subnuclei (Brown et al., 2020; Ghanem et al., 2024). For fMRI studies, increased spatial and/or temporal resolution is possible, depending on individual study requirements; for those investigating very small structures such as the amygdala, spatial resolution is typically prioritised (Geissberger et al., 2020; Zhang et al., 2018). A further advantage for fMRI studies at higher field strengths is that susceptibility effects are also increased resulting in increased BOLD sensitivity (Ladd et al., 2018; McRobbie et al., 2017) and this combination of superior spatial specificity and contrast-to-noise ratio (CNR) is attractive for neuroimaging research.

Paradoxically, however, increased susceptibility effects at 7T are also simultaneously disadvantageous in terms of localised signal loss (Olman et al., 2009). Further disadvantages to be considered are increased Radiofrequency (RF) power deposition, referred to as Specific Absorption Rate (SAR), reported in watts per kilogram. Since SAR is dependent on the square of the main magnetic field strength, an fMRI sequence scanned at 7T theoretically generates a SAR value around 5.4 times higher than the same sequence acquired at 3T (Balchandani & Naidich, 2015). Practically speaking, staying within regulated SAR limits may involve compromises in the imaging sequence such as acquisition of fewer slices for a reduced coverage or lengthening repetition times to allow tissue cooling (Ladd et al., 2018). An additional consideration is that physiological side effects of exposure to high magnetic fields have also been reported, manifesting as nausea, drowsiness and transient episodes of metallic taste sensations (Cavin et al., 2007).

In relation to the amygdala, it is worth noting that terminology differences act as a confounder to literature searches. Some authors have used the term amygdala ‘subnuclei’ or ‘nuclei’ when referring to less granular ‘subregional’ parcellations in their fMRI studies at 3T (Engman et al., 2016; Hofmann & Straube, 2019; Rausch et al., 2016). Additionally, data from some 7T studies has been analysed at a subregional level rather than as an interrogation of the individual subnuclei, even with data at high spatial resolution levels of 1.3mm^3 (Huggins et al., 2021),

1.5mm isotropic (Zhang et al., 2018) and 1.7mm isotropic (Solano-Castiella et al., 2011) that could potentially distinguish the subnuclei. Several other studies used high resolution data ranging from 1.5mm^2 x 2mm (Geissberger et al., 2020; Pedersen et al., 2017) to 2mm isotropic (Ebneabbasi et al., 2021) to report findings on the amygdala as a single structure. Other studies have investigated amygdala activation by parcellating the amygdala into five (Robertson et al., 2022) and six subregions (Brown et al., 2020). Only two resting state studies were identified that parcellated the amygdala at the level of seven (Klein-Flügge et al., 2022) or more subnuclei, including the study that the work in this chapter references, which identified nine (Elvira et al., 2022) as depicted in Figure 5.1. It is noteworthy that both studies made use of the freely available high resolution 1.6mm^3 isotropic Human Connectome Project data acquired at 7T (Van Essen et al., 2012) rather than study-specific data acquisitions.

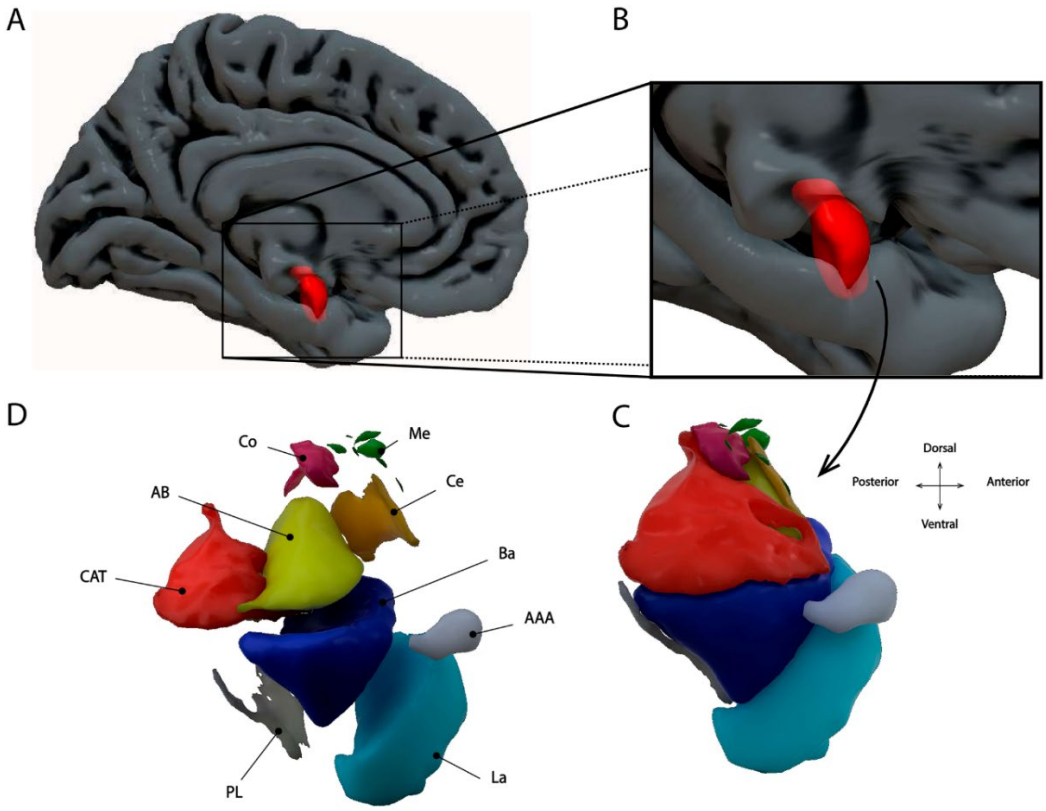

Figure 5.1: Location of amygdala in medial temporal lobe (A & B). Location of nine subnuclei within amygdala (C & D).

Note: Ce = Central; Me = Medial; AB = Accessory Basal; Ba = Basal; La = Lateral; PL = Paralaminar; AAA = Anterior Amygdaloid Area; Co = Cortical; CAT = CorticoAmygdaloid Transition (Elvira et al., 2022).

5.1.1 Spatial resolution requirements

Olman and Yacoub have contended that spatial resolution of the selected fMRI sequence should be driven by the research question; that is, different spatial scales are required depending on the brain regions under examination (Olman & Yacoub, 2011). Standard resolution data, defined as VV of 20-50mm^3 is adequate to examine varying neural responses in different regions of the cortex and can be acquired at 3T, whereas ultra-high resolution data (VV of 1mm^3 or less) is required to resolve the function of cortical columns and hypercolumns (Chaimow et al., 2018; Hendriks et al., 2020; Olman & Yacoub, 2011; Platt et al., 2021). Situated between these two categories is data designated as high resolution with VV of 1-20mm^3 (Olman & Yacoub, 2011). Data at this level of resolution is required to resolve neural signals in very close proximity to each other in cortical and subcortical regions (Olman & Yacoub, 2011) such as the amygdala (Geissberger et al., 2020; Sladky et al., 2018).

Continuous technological improvements in MRI scanner hardware and software have resulted in 3T systems that are now highly optimised to take advantage of available SNR for high resolution fMRI studies (Knudsen et al., 2023; Stirnberg et al., 2017). However, as outlined in the review in Chapter 3, many neuropsychiatric studies have relied on standard spatial resolution data which limits the ability to resolve fine-grained subregional activity (Bollmann & Barth, 2021; Foster et al., 2023). This approach is potentially hindering progress towards a more nuanced understanding of the individual roles of the subregions and their contributions to the heterogeneity and psychopathology of depression (Elliott et al., 2020; Li et al., 2021; Yatham, 2023).

Lack of access to 7T has meant that 3T is still the most commonly utilised field strength for clinical research. Although the concept of higher SNR at 7T is appealing, previous work has demonstrated the capability of 3T systems to provide sufficiently high levels of spatial resolution to image the amygdala at a subregional level (Balderston et al., 2015; Kwon et al., 2024; Labuschagne et al., 2024; Li et al., 2021). In the setting of limited access to 7T, as well as taking into account the associated safety issues (Okada et al., 2022) and increased susceptibility-related signal losses in the temporal lobes where the amygdala is located (Cramer et al., 2024; Ladd et al., 2018), 3T may be the preferred option. Implementation of optimised fMRI acquisition protocols at 3T may be an important step in expanding our knowledge of the functions of the individual subregions. Optimisation of spatial resolution is a simple yet

effective method towards achieving this goal (Bandettini, 2001), and one that can be easily implemented in clinical research settings by a specialist MRI radiographer.

5.2 Fundamentals of SNR and tSNR

SNR is defined as the ratio of global signal intensity to background noise and is typically measured on a single MR image as a method of assessing one aspect of image quality. Contributions to noise include thermal and physiological as well as scanner system elements. In fMRI, temporal or time-series SNR (tSNR) is measured by dividing the mean signal over the image volumes by the standard deviation along the time-series (Poser et al., 2010) and provides information on temporal noise properties that may affect the stability of SNR over the time-series (Murphy et al., 1993). It is not uncommon for both terms to be theoretically referred to as SNR in fMRI (Welvaert & Rosseel, 2013) but in practical terms, their values vary at different levels of spatial resolution due to mainly physiological noise contributions over time (Figure 5.2).

Accurate quantification of functional connectivity is dependent on adequate tSNR levels with which to spatially localise and measure low-frequency BOLD fluctuations (Golestani & Goodyear, 2011). Although the focus of this work is on spatial resolution and its relationship to tSNR, contrast-to-noise ratio (CNR) measures are also central to fMRI as the technique is reliant on BOLD contrast. CNR in resting state fMRI is a measure of the low frequency signal fluctuations compared to noise. Adequate CNR levels will ensure signals from different regions or voxels are distinguishable from each other and from the associated noise (Huettel et al., 2004; Narasimhan & Jacobs, 2002). As signal amplitudes are relatively low in resting state BOLD, tSNR and CNR levels are particularly sensitive to noise and increased levels of noise can negatively impact the accuracy of FC measures (Peer et al., 2016). The ideal imaging scenario in which tSNR and BOLD contrast are maximised whilst noise is minimised provides the best opportunity for optimal data acquisition and accurate FC measurements (Murphy et al., 2007; Welvaert & Rosseel, 2013). Although their results initially appear intuitively at odds, Bellgowan and colleagues have demonstrated that the use of smaller VV in the temporal lobes, the location of the amygdala and an area of high susceptibility, resulted in higher tSNR and CNR measurements. They attributed their findings to greater tissue homogeneity responsible for less intravoxel dephasing and signal loss (Bellgowan et al., 2006). Newton and colleagues also reported significant improvements in CNR with a higher spatial resolution acquisition

technique, noting the significant contribution of reduced levels of partial volume averaging to the results (Newton et al., 2012).

5.2.1 *Spatial resolution and voxel volumes (VV)*

Intuitively, 7T is a superior option for imaging at high spatial resolution in general. However, its inherent disadvantages mean it may not always be the best option, depending on the study endpoint (Okada et al., 2022). Spatial resolution (VV in mm^3) is a key parameter in protocol optimisation and, as we have seen, its selection should be based on the research question (Olman & Yacoub, 2011). Spatial resolution is intrinsically tied to SNR levels, as the two are directly proportional; thus, higher spatial resolution imaging requires smaller VVs which theoretically possess inherently lower SNR (Olman & Yacoub, 2011) as seen in Figure 5.2. In practice, however, when noise contributions are accounted for in time series data, tSNR values increase to a peak at smaller VV before plateauing, demonstrating that the use of larger VV add no further tSNR benefits whilst simultaneously reducing spatial resolution (Figure 5.2). As outlined in Chapter 2, the optimum slice thickness for functional imaging of the amygdala is 2 - 2.5mm^3 resulting in an isotropic VV of 8 - 15.6mm^3 (Robinson et al., 2004). Beyond this point there are marginal tSNR gains to be made (Figure 5.2 - right). As previously noted, smaller voxels reclaim SNR that may be lost due to phase error mismapping and partial voluming caused by tissue heterogeneity in larger voxels, both of which lead to increased noise levels, and this is more evident at increasing field strengths. As they are more likely to contain homogenous tissue, smaller voxels benefit from less intravoxel dephasing (Bandettini, 2002; Robinson et al., 2004) and they are also less likely to be affected by vascular signal from vessels such as the nearby basal vein of Rosenthal (Boubela et al., 2015).

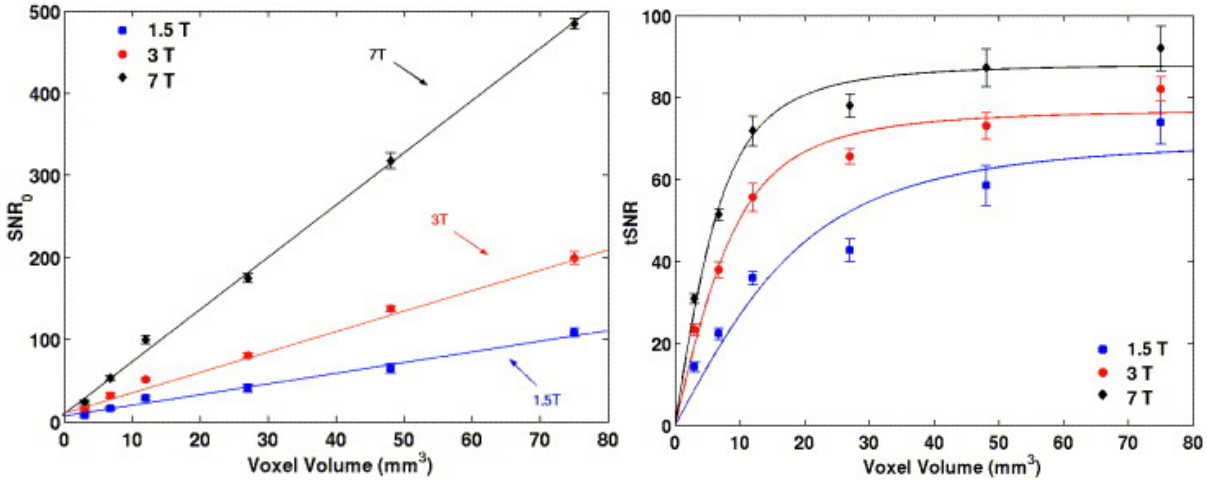

Figure 5.2: SNR (left) and tSNR (right) as a function of voxel volume with 2D acquisition at field strengths of 1.5T, 3T and 7T.

Note: SNR (left) scales linearly with field strength whereas tSNR (right) demonstrates diminishing tSNR returns with larger voxel volumes (Triantafyllou et al., 2005).

Overall tSNR reductions resulting from susceptibility-related field distortion, signal loss (Olman et al., 2009; Yang et al., 2012) and noise are observable at all three field strengths as depicted in Figure 5.2, but these issues are exacerbated at 7T (Viessmann & Polimeni, 2021). A further complication of higher field strength imaging is wavelength variation. At 3T the RF transmission wavelength in tissue is approximately 26cm (Bernstein et al., 2006) but this value is significantly shorter at 7T, being 11-12cm. As a result, RF inhomogeneity due to nonuniform RF transmission across tissues, together with alterations in tissue properties, also contribute to lower achievable tSNR levels in practice (Erturk et al., 2019; Pohmann et al., 2016). This is reflected in the comparative SNR and tSNR values at a VV of 20mm^3, the upper limit of high spatial resolution as previously defined. Interestingly, although 7T systems possesses over twice the theoretical SNR to 3T systems as seen in Figure 5.2 - left, at this level of spatial resolution the tSNR differential is significantly reduced, with a value of approximately 80 for 7T compared with 68 for 3T. Given the disadvantages of 7T related to physiological effects, RF wavelength tissue complications and increased SAR levels potentially limiting whole brain coverage required for resting state studies, 3T is potentially the more attractive option for functional connectivity studies probing the amygdala subregions.

5.3 Imaging the amygdala subregions at 3T

The 2D T2*-W GRE-EPI sequence is considered the gold standard and is widely used in clinical and research settings (Bollmann & Barth, 2021; Foster et al., 2023). The 3D GRE-EPI version, typically not in use outside research settings, has been shown to have significant advantages over the 2D sequence, including greater sensitivity for functional connectivity measures as well as higher spatial resolution capabilities and the potential for shorter acquisition times and potentially smaller sample sizes. This is largely due to inherently higher SNR levels resulting from the different k-space acquisition strategy, and this is more evident in the centrally located deep grey matter structures (Lutti et al., 2013; Stirnberg et al., 2017; Tijssen et al., 2011). Additionally, extrapolation of findings from previous work at 7T indicates that reduced levels of thermal SNR may also contribute to the superior performance of 3D sequences at 3T (Lutti et al., 2013). Taking into consideration the potential SNR gains in subcortical structures and the requirement for higher spatial resolution imaging to resolve the functional connections of the individual amygdala subregions, an investigation into the utility of a 3D sequence was warranted. A fuller discussion of the technical considerations of the 2D and 3D sequence comparison is located in Appendix D.

As noted, the optimum slice thickness to maximise SNR in fMRI investigations of the amygdala is between 2mm and 2.5mm (Robinson et al., 2004). The slice thickness of the previously optimised 2D sequence used in this study was 2.5mm, resulting in a voxel volume (VV) of 15.6mm^3. The 3D sequence, a works-in-progress sequence developed and provided by Siemens Healthineers (Erlangen, Germany), was optimised for this amygdala study; a slice thickness of 2mm provided a VV of 8mm^3, just over half that of the 2D sequence. Both sequences benefited from the use of isotropic voxels which have been shown to increase signal sampling accuracy (Mulder et al., 2019; Smith et al., 2013).

5.3.1 Study Aim

The primary aim of this pilot study was to assess the FC capabilities of two high-resolution GRE-EPI sequences, 2D (optimised in line with Chapter Three recommendations and also used in Chapter Four) and 3D, with different VV and acquisition strategies, optimised for use at 3T. The two sequences were assessed for their capability in identifying subregional amygdala functional connectivity with primarily cortical resting state networks. Results were compared to those reported by Elvira and colleagues (Elvira et al., 2022) who used a combination of 2D data and Independent Component Analysis, a data driven technique useful in exploratory

settings when there are no a priori assumptions (Rosazza et al., 2012). They investigated the functional connectivity contributions of individual amygdala subnuclei to resting-state networks utilising Human Connectome Project (HCP) data (Van Essen et al., 2012) acquired with a 2D GRE-EPI sequence at 7T (Elvira et al., 2022). These authors identified FC contributions of nine amygdala subnuclei to three of the seven resting state networks identified by Yeo and colleagues (Yeo et al., 2011). These networks (hereafter referred to collectively as networks-of-interest) were the Default Mode, Somatomotor and Ventral Attention networks (Elvira et al., 2022). Resting state networks are referred to by an alternate nomenclature in the analysis software used in this study; however, for ease of comparison, the Yeo nomenclature used by Elvira *et al.* is used in this work. Details of all Yeo and CONN toolbox nomenclatures are outlined in Table S1 in Appendix D.

For their 7T study, Elvira and colleagues parcellated the amygdala into nine subnuclei (Table 5.1) and reported individual subnuclei connections to the three networks-of-interest. They also calculated relative contributions of each of the subnuclei within the networks-of-interest. Table 5.1 lists the nine the individual subnuclei and their subregional groupings (CM, LB and SF). It also includes the individual subnuclei connections to networks-of-interest and rankings in order of contribution to each network-of-interest reported for each of the subnuclei in the 7T study. Although amygdala FC at a subnuclei level has been demonstrated using high quality, high resolution data with VV of $10mm^3$ and less at 7T, this has not been the case at 3T due to lower inherent SNR levels. Therefore, this study is based on the coarser parcellation of three subregions as previously defined (Eickhoff et al., 2005). The overarching aim of the study was to demonstrate that, in the absence of widespread access to gold standard 7T systems, researchers can use data from optimised 3T sequences to interrogate amygdala FC at a subregional level to primarily cortical resting state networks.

Table 5.1: Amygdala subregions used in 3T study; subnuclei used in 7T study; network-of-interest connections

3T Subregions	7T **Individual Subnuclei**	**Networks-of-interest Identified at 7T**
Centromedial (CM)	Central (Ce)	Default Mode (5) Ventral Attention (4)
	Medial (Me)	Default Mode (4)
Laterobasal (LB)	Accessory basal (AB)	Default Mode (2) Somatomotor (4)
	Basal (Ba Lateral (La) Paralaminar (PL)	Somatomotor (5) Nil Somatomotor (2)
Superficial (SF)	Anterior Amygdaloid Area (AAA)	Ventral Attention (2) Somatomotor (3)
	Cortical (Co)	Default Mode (1) Ventral Attention (1)
	CorticoAmygdaloid Transition (CAT)	Somatomotor (1) Ventral Attention (3) Default Mode (3)

Note: Yeo nomenclature used by Elvira & colleagues. Numbers refer to order of relative contributions of amygdaloid subnuclei to that network-of-interest as reported in 7T study. For example, two subnuclei located in the Superficial (SF) subregion were the primary contributors of functional connections to all three networks. These were Cortical nucleus for Default Mode Network & Ventral Attention Networks and Corticoamygdaloid Transition area for Somatomotor Network (labelled 1) (Elvira et al., 2022).

5.4 Materials and Methods

5.4.1 Participants

Ten healthy participants (5 males) aged 18 - 64 years (mean 35 years) took part in this pilot study. All participants were physically healthy and had no significant history of neurological disease, psychiatric disease, or head injury. Approval was obtained from Western Sydney Local Health District Ethics Committee and written informed consent was obtained from all participants. Imaging studies were undertaken at Westmead Hospital Radiology Department, Sydney, Australia.

5.4.2 Data acquisition

All imaging data were acquired on a 3 Tesla Siemens Prisma MRI system in conjunction with VE11C software (Siemens Healthineers, Erlangen, Germany). A 64-channel head/neck array RF coil was employed for signal reception. Participants viewed a fixation cross projected onto a coil-mounted screen whilst two sequences of resting-state data (2D and 3D) were acquired. Participants were instructed to remain still and awake. Imaging parameters for the functional 2D T2*-weighted GRE-EPI sequence were as follows: Repetition time (TR) = 1500ms; Echo time (TE) = 33ms; Field-of-view (FOV) = 255mm; Matrix = 104 x 104; Flip angle (FA) = 85°; Phase encoding direction = A to P; Total acceleration = 6 (MB 3); 320 volumes ; 60 interleaved axial-oblique slices at 2.5mm thick (0mm gap) parallel to the AC-PC line were acquired covering the whole brain with a VV of 15.6mm^3 in an acquisition time of 8 minutes 12 seconds.

Imaging parameters for the functional 3D T2*-weighted GRE-EPI sequence were as follows: Repetition time (TR) = 54ms (total = 2160ms); Echo time (TE) = 28ms; Field-of-view (FOV) = 224mm; Matrix = 112 x 112; Flip angle (FA) = 10°; Phase encoding direction = A to P; Total acceleration = 4; 220 volumes ; 80 ascending axial slices at 2mm thick (0mm gap) parallel to the AC-PC line were acquired covering the whole brain with a VV of 8mm^3 in an acquisition time of 8 minutes 11 seconds.

Both GRE-EPI sequences were tailored to result in equivalent acquisition times of just over 8 minutes by adjusting the total number of volumes. The total number of slices for each sequence was prefaced on the requirement for a whole number multiple of the slice acceleration factor of the individual sequence. Additionally, due to the location of the amygdala in an area known for increased magnetic susceptibility issues due to air/bone/tissue/interfaces, slice partial Fourier sampling was not engaged in the 3D sequence to avoid the potential for increased signal

losses (Stirnberg et al., 2017). The main magnetic field was shimmed once automatically prior to the first GRE-EPI acquisition to reduce variability in field homogeneity between sequences.

A high-resolution structural 3D T1-weighted magnetisation-prepared gradient echo sequence was also acquired with imaging parameters as follows: Repetition time (TR) = 2400ms; Echo time (TE) = 2.21ms; Inversion Time (TI) = 900ms; Field-of-view (FOV) = 256mm; Matrix = 288 x 288; Flip angle (FA) = 8°; Phase encoding direction = A to P; Acceleration (GRAPPA) = 2 ; 192 sagittal slices at 0.9mm thick parallel to the interhemispheric fissure were acquired covering the whole brain with a VV of $0.7mm^3$ in an acquisition time of 6 minutes 23 seconds.

5.4.3 *ROI selection, data preprocessing and analyses*

Functional connectivity was assessed with a seed-based connectivity Region-of-Interest (ROI-to-ROI) method. Analyses were based on a priori selection of ROIs. Six amygdala subregional masks or ROIs were extracted from The JuBrain Anatomy Toolbox (Eickhoff et al., 2005). Left and right centromedial (CM), laterobasal (LB) and superficial (SF) ROIs were created using cytoarchitectonically-defined probabilistic maps from the JuBrain Cytoarchitectonic Atlas (Amunts et al., 2005) and imported into the CONN toolbox for analyses.

Data analyses were performed using a combination of Matlab R2022b (The MathWorks Inc. Natick, Massachusetts), SPM12 (Wellcome Trust Centre for Neuroimaging, London, UK) and CONN functional connectivity toolbox v22b (http://www.nitrc.org/projects/conn/). Preprocessing of anatomical and functional images was performed using the CONN modular preprocessing pipeline (Nieto-Castanon, 2020b). Noting that spatial smoothing in ROI analyses has a negligible effect (Huettel et al., 2004) and is potentially detrimental for native high resolution data undergoing resting state analyses by reducing spatial specificity (Alakörkkö et al., 2017; Bollmann & Barth, 2021; Lindquist, 2008; Sladky et al., 2013) this step was removed from the preprocessing pipeline. Similarly, in line with findings showing that slice time correction is not required for high resolution data (Glasser et al., 2013; Wu et al., 2011) this step was also removed. The data underwent realignment, unwarping, co-registration and resampling for motion correction, and magnetic susceptibility interactions and a BOLD reference image was created for each subject. Data were then segmented into grey matter, white matter and cerebrospinal fluid and then normalised into standard Montreal Neurological Institute space. Functional data were denoised using a standard pipeline including regression of potential confounders (CompCor) from white matter, CSF and motion parameters (Nieto-Castanon, 2020a), followed by bandpass filtering (0.01-0.1 Hz). Data was assessed for head

motion using the Assessment of Repetitive Tasks (ART)-based scrubbing technique in CONN, with outliers being defined as having greater than 0.9mm framewise displacement. No participants were excluded based on less than 5% scans deemed as outliers.

ROI to ROI analyses were undertaken separately for the 2D and 3D sequences to characterise FC strengths between the six seed ROIs and the target network ROIs. As the study aim was to identify the presence of functional connections between a prescribed set of ROIs as per Elvira *et al*, a one sample t-test was used to test each individual subregional amygdala ROI seed (left and right LB, CM and SF) for significant correlations with each of the network ROIs (targets) in CONN using a Fisher-transformed bivariate correlation coefficient using a General Linear Model and calculated from the BOLD signal time series for each ROI pair. The target ROIs comprised the individual regions of each resting state network in CONN, including the networks-of-interest. Due to the small sample size in this pilot study, the results did not survive correction for multiple comparisons at a significance threshold of $p<0.05$ after controlling for false discovery rate; consequently, results displayed in Table 5.2 were thresholded at an uncorrected $p < 0.05$. Functional connectivity results of both sequences were collated for comparison.

5.5 Results

5.5.1 Network-of-interest to subregion connectivity – 2D sequence

The ROI-to-ROI analysis for the 2D sequence identified connections to all three networks-of-interest from five of the six subregions. In total, ten separate subregional connections to the three networks-of-interest were identified. For the Default Mode Network, four connections were identified: namely, with the right and left CM, left LB and left SF. For the Somatomotor network, two separate connections to the left LB were identified, potentially arising separately from the AB and Ba subnuclei. For the Ventral Attention network, four connections were also identified; with the left CM, right and left SF and left LB. Whilst Elvira and colleagues reported connections between this network and subnuclei in the CM and SF, their findings for the Ventral Attention network did not include any individual subnuclei that form the LB subregion.

5.5.2 Network-of-interest to subregion connectivity – 3D sequence

The ROI-to-ROI analysis for the 3D sequence identified overall fewer connections, with only two between networks-of-interest and subregions. One connection was identified between the Ventral Attention network and right SF, the only finding in alignment with those of Elvira and colleagues. A second connection between the Somatomotor network and left CM was also

identified; however, Elvira and colleagues did not report a connection between this network and any subnuclei in the CM, but rather to those subnuclei located in the LB and SF subregions. No Default Mode network connections were identified using the 3D sequence.

Functional connectivity results for network-of interest to amygdala subregions for 2D and 3D sequences are shown in Table 5.2 and Figure 5.3. Results for connections to other networks are shown in Appendix D (Table S3 for the 2D sequence and Table S4 for the 3D sequence). See Table S2 in Appendix D for comparison of Yeo and CONN network region nomenclature.

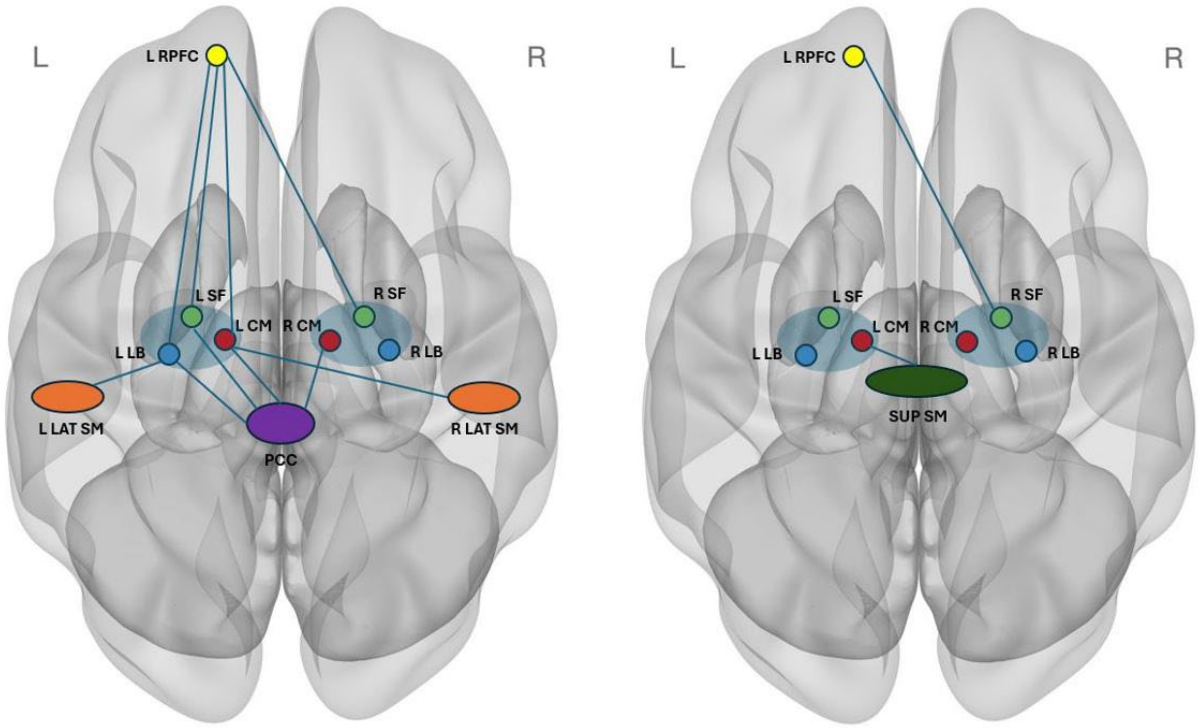

Figure 5.3: Amygdala subregional functional connectivity in healthy controls: 2D > 3D

Subregional amygdala regions-of-interest demonstrating stronger functional connections to other brain regions in 2D sequence (at left) compared to 3D sequence (at right). Neurological image orientation shown with left hemisphere on left and frontal lobes at the top.

CM = centromedial (red); LB = laterobasal (blue); SF = superficial (green); L RPFC = Left Rostral Prefrontal Cortex (yellow); L & R LAT SM = Left and right lateral sensorimotor (orange); PCC = Posterior Cingulate Cortex (purple); SUP SM = Superior Sensorimotor (dark green); Whole amygdala region (aqua ellipse).

Table 5.2: Resting-State Functional Connectivity results between networks-of-interest and amygdala subregions for 2D and 3D sequences

Subregion & sequence	Target Network-of-interest and region	T-stat	p-unc < 0.05	Results common to Elvira *et al*. (subnuclei level)
2D				
R_CM*	Default Mode - PCC	-3.27	0.010	DMN (Ce & Me)
L_CM*	Default Mode - PCC	-3.68	0.005	DMN (Ce & Me)
L_CM*	Ventral Att. - RPFC (L)	-2.48	0.034	Ventral Att. (Ce only)
L_LB*	Default Mode - PCC	-3.84	0.004	DMN (AB only)
L_LB*	Somatomotor - Lateral (R)	+2.76	0.022	Somatomotor (AB, Ba, PL)
L_LB#	Ventral Att. - RPFC (L)	-2.67	0.025	Ventral att. (#CM, SF)
L_LB*	Somatomotor - Lateral (L)	+2.28	0.048	Somatomotor (AB, Ba, PL)
R_SF*	^Ventral Att. - RPFC (L)	-2.30	0.047	Ventral att. (AAA, Co, CAT
L_SF*	Ventral Att. - RPFC (L)	-3.3	0.009	Ventral att. (AAA, Co, CAT)
L_SF*	Default Mode - PCC	-2.59	0.029	DMN (Co, CAT)
3D				
L_CM#	Somatomotor - Superior	-2.27	0.050	Somatomotor (#LB, SF)
R_SF*	^Ventral Att. - RPFC (L)	-2.85	0.019	Ventral att. (AAA, Co, CAT)

Note: 7T findings of Elvira et al. shown for comparison (Elvira et al., 2022).

Results did not survive multiple comparisons at $P_{FDR}<0.05$; shown at p-uncorrected < 0.05

^ *indicates same network connection in both 2D and 3D sequences*

+ *indicates positive correlation with network region*

***** *indicates subregions containing subnuclei connected with network-of-interest in this study that replicate findings of Elvira et al.*

 # indicates subregions containing subnuclei connected with network-of-interest in this study that differ from findings of Elvira et al.

5.6 Discussion

This study investigated the capability of two high resolution fMRI sequences optimised for use at 3T to identify functional connections between the amygdala subregions (CM, LB and SF) and resting state networks-of-interest, Default Mode, Ventral Attention and Somatomotor. FC results were compared to findings reported at 7T by Elvira and colleagues, who explored FC of nine amygdala subnuclei to networks-of-interest using a combination of 2D data and Independent Component Analysis, a data driven technique useful in exploratory settings when there are no a priori assumptions (Rosazza et al., 2012). The main findings of the study were that the performance of the 2D sequence was superior to that of the 3D sequence in identifying subregional amygdala connections to networks-of-interest. Whilst the 3D sequence identified only two subregional connections to network-of-interests, the 2D sequence identified ten separate connections from the three networks-of-interest to five of the six amygdala subregions. In comparison, the 7T study identified 14 connections between the networks-of-interest and eight of the nine amygdala subnuclei.

In considering the performance of the 2D 3T sequence in this pilot study compared to the results reported at 7T, it is noteworthy that the findings of Elvira and colleagues were identified using high resolution data (VV 4.1mm^3) acquired at 7T as part of the Human Connectome Project (Van Essen et al., 2012). Additionally, their analysis was performed using two 16-minute resting state data acquisitions per participant (Elvira et al., 2022) whereas the data acquired in this 3T study comprised of one 8-minute resting state acquisition per sequence with VV of 8mm^3 (3D) and 15.6mm^3 (2D). In such a setting, it may seem surprising that the findings of the 2D 3T sequence were relatively favourable in comparison to the 7T findings. Signal averaging by acquiring multiple volumes of data over longer acquisition times, in one or more runs, is a commonly used method of increasing SNR; however, previous work has shown that there is minimal benefit derived in using acquisition times of longer than six minutes to investigate FC strength of resting state networks including the Default Mode Network (Van Dijk et al., 2010).

Although they did not specify laterality in their findings, the authors did identify an effect of hemisphere, noting increased connectivity on the right, which was in contrast to the findings of the present study which identified more left-sided connections overall. Interestingly, Elvira *et al.* also reported that the amygdala subnuclei function in preferential configurations in their interactions with resting state networks, for example for the DMN, the relative contributions

from amygdala subnuclei in order were Cortical, Accessory Basal, CorticoAmygdaloid Transition, Medial and Central, with this combination representing contributions from all three subregions. Relative contributions of each of the amygdala subnuclei to the networks-of-interest in the 7T study are listed in Table 5.1. A more direct performance assessment between the 2D 3T and 7T findings is presented in Table 5.3, with left and right subregional findings grouped together for clarity in the following discussion.

Table 5.3: 2D 3T subregional amygdala functional connectivity findings compared to 7T subnuclei amygdala functional connectivity findings to networks-of-interest

Subnuclei **No laterality specified**	**Network-of-interest** **7T Elvira *et al.***	**Subregion** **Left or Right**	**Network-of-interest** **3T 2D**
Central (Ce)	DMN VAN	R Centromedial (CM)	DMN
Medial (Me)	DMN	L Centromedial (CM)	DMN VAN
Accessory basal (AB)	DMN Somatomotor	R Laterobasal (LB)	*Nil
Basal (Ba)	Somatomotor	L Laterobasal (LB)	DMN Somatomotor VAN Somatomotor
Lateral (La)	*Nil		
Paralaminar (PL)	Somatomotor		
Anterior Amygdaloid Area (AAA)	VAN Somatomotor		
Cortical (Co)	DMN VAN	R Superficial (SF)	VAN
CorticoAmygdaloid Transition (CAT)	Somatomotor VAN DMN	L Superficial (SF)	VAN DMN

Note: DMN = Default Mode Network; VAN = Ventral Attention Network; R = right; L = left

5.6.1 *Centromedial subregion*

For the CM subregion, the 2D 3T sequence identified three connections to two networks-of-interest, two of which were to the Default Mode Network. The 7T study also identified two connections between the Default Mode Network and the two subnuclei that make up the CM

subregion. Given that laterality was not specified, it is possible that the left and right CM connections identified in the 2D 3T analysis emerged from these individual subnuclei. Also, in line with the 7T findings, a connection between the Ventral Attention network and the CM was identified. The 7T study also reported a connection between the Ventral Attention network and one of the two CM subnuclei, the Ce; this may represent the connection shown in the 2D 3T analysis at a coarser level. In summary, of three network-of-interest connections reported at 7T between the two subnuclei that form the CM, the 2D 3T sequence also identified three.

5.6.2 *Laterobasal subregion*

The LB, the largest subregion by volume at around 80% of the whole amygdala structure, is comprised of four individual subnuclei (Roddy et al., 2021; Saygin et al., 2011). In the 7T study, four individual connections, one to the Default Mode Network and three to the Somatomotor network, were reported between three of the four subnuclei. Of these four network-of-interest connections, the 2D 3T sequence identified three. The 2D 3T sequence also identified four separate connections, lateralised to the left LB, three of which aligned with the findings of the 7T study. These included one connection to the Default Mode Network and two to the Somatomotor network. A fourth connection between the left LB and the Ventral Attention Network identified in the 2D 3T analysis was not reported in the 7T study. No connections were identified between any of the networks-of-interest and the right LB in the 2D 3T analysis. Similarly, no connections were identified to one of the LB subnuclei, the La, in the 7T study. In summary, of the four network-of-interest connections reported at 7T between the subnuclei that form the LB, the 2D 3T sequence identified three.

5.6.3 *Superficial subregion*

Incongruously, the SF subregion, although much smaller than the LB, appears to be the most heavily connected, with seven connections between its individual subnuclei to all three networks-of-interest identified in the 7T study. Connections between each of the three subnuclei comprising the SF subregion were reported to at least two networks-of-interest, with one subnucleus connecting to all three networks-of-interest. The 2D 3T sequence identified three connections from the SF to two of the three networks-of-interest, the Default Mode and Ventral Attention networks. In summary, of the seven network-of-interest connections reported at 7T between the three subnuclei that form the SF, the 2D 3T sequence identified three.

5.6.4 Subregions and individual subnuclei

Overall, the high resolution 2D 3T sequence showed promising capability in identifying amygdala connections to the networks-of-interest at a subregional level in comparison to subnuclei connections identified in the 7T study, notwithstanding the very small sample size. Scrutinising the connections of each subregion and comparing them to those of the individual subnuclei in Table 5.3, it is evident that the same three network-of-interest connections were identified for the CM subregion and its individual subnuclei (Ce and Me). As the CM is the smallest subregion by volume, at less than five percent of the whole amygdala (Roddy et al., 2021), this is a favourable result.

For the largest subregion, the LB, the 2D 3T sequence identified three of the same four connections identified at 7T between three of its four individual subnuclei (AB, Ba, PL) and networks-of-interest, as well as a fourth to the Ventral Attention network. The only individual subnucleus in the LB displaying no connections to the networks-of-interest at 7T was the La subnucleus.

A comparison of the SF subregion and its individual subnuclei showed that, of seven connections between the SF subnuclei (AAA, Co, CAT) and networks-of-interest at 7T, three were identified at a subregional level by the 2D 3T sequence, with connections between two subnuclei (AAA, CAT) and the Somatomotor network not identified. However, two of three connections to the Ventral Attention Network and one of two to the Default Mode Network were identified. Given that the volume of this subregion is only around 15 percent of the total amygdala volume at approximately 265mm^3 (Roddy et al., 2021) it may be difficult to spatially locate so many different signals arising from within such a small region at the level of resolution provided by the 2D 3T sequence that, although considered high-resolution, has VV of four times larger than the 7T data. This premise is supported by previous work demonstrating the capability of ultra-high resolution 7T fMRI data to differentiate multiple signals arising from various depths in the cortex where high resolution data is unable to resolve the signals individually (Polimeni & Wald, 2018). Intriguingly, the CM is approximately four times smaller than the SF, yet the same three individual network-of-interest connections were identified by the 2D 3T sequence as were reported at 7T, demonstrating the potential of the 2D sequence to spatially locate at least three individual connections within a small region. The location of the CM subregion superiorly in the amygdala may also have contributed to these

results; even though diminutive, positionally it benefits from a more homogeneous tissue environment, being distanced further from the skull base than the other subregions.

Negative correlations were identified between all subregions and networks in both 2D and 3D 3T sequences with the exception being two positively correlated connections between the left LB and Somatomotor networks in the 2D 3T sequence (Table 5.2). It has been suggested that global signal regression to reduce noise during data preprocessing is responsible for negatively correlated network findings (Murphy et al., 2009). However, the work of Chang and Glover identified negative correlations in the absence of this data preprocessing step (Chang & Glover, 2009). It has also been proposed that 'anti-correlations' are intrinsic to task-positive and task-negative network interactions and are representative of the participant's state of non-focused attention during resting state data acquisition (Fox et al., 2009; Greicius et al., 2003). Regarding the only positive correlations identified in the study, Kerestes and colleagues also reported significant positive correlations between the left LB and the Somatomotor network in their study (Kerestes et al., 2017) whilst Sylvester and colleagues reported mainly negative correlations between subregions and resting state networks (Sylvester et al., 2020). However, the results in this small pilot study did not reach significance and, as such, must be interpreted with caution.

Previous work comparing two similar 2D and 3D sequences to those in this study, but with identical spatial resolution of 2.4mm isotropic, reported overall higher functional connectivity values for the 3D sequence, noting its superiority in demonstrating connections to the Default Mode Network (Stirnberg et al., 2017). However, in this study the 2D sequence performance was superior in identifying multiple subregional connections not only to the Default Mode Network but to all three networks-of-interest. In contrast, the 3D sequence identified only two; however, the performance of the 3D sequence may have been impacted by physiological noise, which is known to be significantly more detrimental when employing a novel 3D k-space acquisition strategy (Triantafyllou et al., 2005). Additionally, data acquired in the temporal lobes, the location of the amygdala, is affected by physiological noise more so than other brain regions (Klein-Flügge et al., 2022). Previous work has shown the potential gains in tSNR by performing individual physiological noise regression in analyses of 3D datasets (Lutti et al., 2013; Stirnberg et al., 2017). Individual pulse and waveform data can be collected and recorded by means of a vendor-supplied respiratory belt fitted around the participant's chest and a pulse-oximeter device located on a finger. It was intended that physiological data capture capability would be available on the 3D sequence for the purposes of this study; however, due to technical

difficulties at the sequence compilation level it was unavailable for use during participant data acquisition.

Interestingly, as has been demonstrated in the work in Chapter Four, variations in amygdala connectivity results were again demonstrated in this study when comparing findings utilising a whole amygdala ROI versus three individual subregional ROIs. For the 2D 3T analysis, when the left whole amygdala was used as a single ROI, only three of eight network-of-interest connections previously identified with subregional ROIs were seen at p-unc < 0.05. They were Default Mode, Ventral Attention and Somatomotor. For the right whole amygdala, only one of two network-of-interest connections was identified, to the Default Mode Network.

A similar pattern was evident in the results for the 3D 3T analysis; when the left whole amygdala was used as a single ROI, the single network-of-interest connection previously identified at subregional level was no longer observable. However, for the right whole amygdala, the single network-of-interest connection to the Ventral Attention Network was retained. A potential explanation for these anomalous findings is that averaging of positive and negative discrete subregional signals occurs when the amygdala is considered as a single structure (Honey et al., 2009; Roy et al., 2009).

5.7 Limitations

There are a number of limitations to this study which may be overcome in future work, not the least that as a pilot, results did not reach significance after correction for multiple comparisons and thus are not generalisable due to the study being underpowered. A distinct limitation is that the spatial resolution of the two sequences differed, rendering head-to-head comparisons unviable; however, that was not the primary purpose of the study. Additionally, the amygdala subregional ROIs used in this study were based on cytoarchitectonic parcellations freely available in the SPM Anatomy Toolbox (Eickhoff et al., 2005) whereas Elvira et al. automatically segmented nine subnuclei for each individual participant using very high resolution T2-weighted images. Standardised ROIs have been shown to produce less accurate FC measures compared with individual segmentation (Sohn et al., 2015). Notwithstanding, the cytoarchitectonic derivation of the subregional amygdala ROIs in the SPM Anatomy Toolbox used in this study has been validated and is a method available to all researchers who value reproducibility, as the subregions, represented by maximum probability maps, are registered to standard MNI space. Conversely, tissue probability thresholds derived from automatic segmentation methods can differ between analysis platforms, rendering results non-comparable

across platforms and leading to inconsistent results and lack of reproducibility across studies utilising different software platforms (Tudorascu et al., 2016).

Variations in data preprocessing are also a limitation in terms of results comparisons across studies. As the data from both sequences was high resolution and the TR periods relatively short, slice timing correction and data smoothing were removed from the processing pipeline. As the native spatial resolution differed, this may have affected the results, and the data from both sequences may have benefited from smoothing with the same kernel width in order to match their spatiotemporal resolution for FC comparisons. Elvira *et al.* also used unsmoothed data in reporting their findings but employed individual subnuclei masks during analysis. As well as providing increased tSNR, data smoothing is an effective method of accounting for inter-subject anatomical variations (Bazeille et al., 2021; Wu et al., 2011). As subject-specific ROIs were not used in this study, data smoothing may have been beneficial; however, any such advantage needs to be considered through the prism of potential reductions in spatial specificity that accompany smoothing of native high resolution data (Alakörkkö et al., 2017; Bollmann & Barth, 2021).

The lack of physiological data correction, shown to have preferential data quality benefits, also likely constrained the performance of the 3D sequence and its deployment in future investigations of amygdala subregional FC is warranted. Lastly, although a discussion relating to echo times and their impact on BOLD sensitivity in different brain regions is outside the scope of this work, it should be noted that the echo times of the two sequences differed. Shorter echo times generally result in higher SNR due to less T2* dephasing prior to signal sampling (Krüger et al., 2001). Fundamentally, it could reasonably be expected that the 3D sequence with an echo time of 28ms would benefit in terms of SNR levels compared with the 2D sequence with a corresponding echo time of 33ms. However, there are other factors at play; echo times are optimal when maximum BOLD contrast is achieved, and this relates to differences in T2* signal decay and varies with field strength (Puckett et al., 2018). Further, the T2* values of cortical and subcortical brain regions differ and, as selection of TE value for fMRI data acquisition involves compromise between BOLD sensitivity, SNR and research question, it should be noted that this particular research question related to connectivity with cortical regions comprising three brain networks. As TE values between 30-35ms have been shown to be optimal for investigation of the cortex using a 2D sequence at 3T (Kang et al., 2023; Miletić et al., 2020), it is perhaps unsurprising that the 2D sequence with a TE of 33ms outperformed its 3D counterpart in this study.

5.8 Conclusion

The 2D GRE-EPI sequence optimised for high resolution acquisitions at 3T showed promise in accurate identification of amygdala subregional FC to resting state networks, highlighting the potentially underutilised capability of high spatial resolution fMRI at 3T. The performance of the 2D version was superior to that of the 3D version in most closely identifying functional connections between the amygdala subregions and the networks-of-interest in comparison to the subnuclei findings of Elvira *et al*. at 7T. In identifying ten of fourteen subnuclei connections at subregional level, particularly those three in the diminutive CM subregion, the 2D sequence demonstrated its potential in this small pilot study, and the strength of these results is highlighted when viewed from the perspective of the network connections, where the 2D sequence only missed one connection to the Somatomotor network from the SF subregion.

Given the increased spatial resolution and inherent tSNR advantages derived from its novel k-space acquisition strategy, the 3D sequence did not achieve the results that might have been expected. However, optimal performance requires the capture of individual physiological noise signals for regression during analysis, a feature that was unavailable at the time of data acquisition. Nevertheless, further investigation of its capabilities is warranted given that 2D sequences such as the one used are reliant on achieving relatively high levels of acceleration that require MR scanners with powerful gradient systems and sophisticated multi-array receiver coils. In contrast, the 3D sequence may have more translational value as it is less dependent on acceleration techniques requiring more powerful scanner and coil performance.

In conclusion, a high spatial resolution 2D GRE-EPI sequence optimised for 3T has demonstrated its capability and potential to identify amygdala functional connections at a subregional level and further work in larger cohorts is required to replicate and confirm these findings. Given the focus on increased understanding of the amygdala in relation to its role in depression, investigation at a subregional level rather than as a whole structure is a logical step to progressing our knowledge.

Acknowledgements

The authors would like to thank Dr Kieran O'Brien and Dr Jin Jin from Siemens Healthineers, ANZ, for provision of the 3D EPI-GRE Works-in-Progress acquisition sequence and assistance and advice regarding specific optimisations required for this work. Thanks also to Lucy Cartwright for SNR and MPV data comparisons and Simon Pullman for assistance with tables.

5.9 References

Alakörkkö, T., Saarimäki, H., Glerean, E., Saramäki, J., & Korhonen, O. (2017). Effects of spatial smoothing on functional brain networks. *Eur J Neurosci*, *46*(9), 2471-2480. https://doi.org/10.1111/ejn.13717

Balchandani, P., & Naidich, T. P. (2015). Ultra-High-Field MR Neuroimaging. *AJNR Am J Neuroradiol*, *36*(7), 1204-1215. https://doi.org/10.3174/ajnr.A4180

Balderston, N. L., Schultz, D. H., Hopkins, L., & Helmstetter, F. J. (2015). Functionally distinct amygdala subregions identified using DTI and high-resolution fMRI. *Soc Cogn Affect Neurosci*, *10*(12), 1615-1622. https://doi.org/10.1093/scan/nsv055

Bandettini, P. A. (2001). Selection of the optimal pulse sequence for functional MRI. In P. Jezzard, P. M. Matthews, & S. M. Smith (Eds.), *Functional Magnetic Resonance Imaging: An Introduction to Methods* (pp. 123–145). Oxford University Press. https://doi.org/10.1093/acprof:oso/9780192630711.003.0006

Bandettini, P. A. (2002). The spatial, temporal and interpretive limits of functional MRI In K. L. Davis, D. Charney, J. T. Coyle, & C. B. Nemeroff (Eds.), *Neuropsychopharmacology: The Fifth Generation of Progress : An Official Publication of the American College of Neuropsychopharmacology* (pp. 343-356). Lippincott Williams & Wilkins.

Bazeille, T., DuPre, E., Richard, H., Poline, J. B., & Thirion, B. (2021). An empirical evaluation of functional alignment using inter-subject decoding. *Neuroimage*, *245*, 118683. https://doi.org/10.1016/j.neuroimage.2021.118683

Bellgowan, P. S. F., Bandettini, P. A., van Gelderen, P., Martin, A., & Bodurka, J. (2006). Improved BOLD detection in the medial temporal region using parallel imaging and voxel volume reduction. *Neuroimage*, *29*(4), 1244-1251. https://doi.org/10.1016/j.neuroimage.2005.08.042

Bernstein, M. A., Huston III, J., & Ward, H. A. (2006). Imaging artifacts at 3.0T. *Journal of Magnetic Resonance Imaging*, *24*(4), 735-746. https://doi.org/10.1002/jmri.20698

Bollmann, S., & Barth, M. (2021). New acquisition techniques and their prospects for the achievable resolution of fMRI. *Prog Neurobiol*, *207*, 101936. https://doi.org/10.1016/j.pneurobio.2020.101936

Boubela, R. N., Kalcher, K., Huf, W., Seidel, E.-M., Derntl, B., Pezawas, L., Našel, C., & Moser, E. (2015). fMRI measurements of amygdala activation are confounded by stimulus correlated signal fluctuation in nearby veins draining distant brain regions. *Scientific Reports*, *5*(1), 10499. https://doi.org/10.1038/srep10499

Brown, S. S. G., Rutland, J. W., Verma, G., Feldman, R. E., Schneider, M., Delman, B. N., Murrough, J. M., & Balchandani, P. (2020). Ultra-High-Resolution Imaging of Amygdala Subnuclei Structural Connectivity in Major Depressive Disorder.

Biological Psychiatry: Cognitive Neuroscience and Neuroimaging, *5*(2), 184-193. https://doi.org/10.1016/j.bpsc.2019.07.010

Cavin, I. D., Glover, P. M., Bowtell, R. W., & Gowland, P. A. (2007). Thresholds for perceiving metallic taste at high magnetic field. *Journal of Magnetic Resonance Imaging*, *26*(5), 1357-1361. https://doi.org/10.1002/jmri.21153

Chaimow, D., Uğurbil, K., & Shmuel, A. (2018). Optimization of functional MRI for detection, decoding and high-resolution imaging of the response patterns of cortical columns. *Neuroimage*, *164*, 67-99. https://doi.org/10.1016/j.neuroimage.2017.04.011

Chang, C., & Glover, G. H. (2009). Effects of model-based physiological noise correction on default mode network anti-correlations and correlations. *Neuroimage*, *47*(4), 1448-1459. https://doi.org/10.1016/j.neuroimage.2009.05.012

Cramer, J., Ikuta, I., & Zhou, Y. (2024). How to Implement Clinical 7T MRI-Practical Considerations and Experience with Ultra-High-Field MRI. *Bioengineering (Basel)*, *11*(12). https://doi.org/10.3390/bioengineering11121228

Ebneabbasi, A., Mahdipour, M., Nejati, V., Li, M., Liebe, T., Colic, L., Leutritz, A. L., Vogel, M., Zarei, M., & Walter, M. (2021). Emotion processing and regulation in major depressive disorder: A 7T resting-state fMRI study. *Human Brain Mapping*, *42*(3), 797-810. https://doi.org/10.1002/hbm.25263

Eickhoff, S. B., Stephan, K. E., Mohlberg, H., Grefkes, C., Fink, G. R., Amunts, K., & Zilles, K. (2005). A new SPM toolbox for combining probabilistic cytoarchitectonic maps and functional imaging data. *Neuroimage*, *25*(4), 1325-1335. https://doi.org/10.1016/j.neuroimage.2004.12.034

Elliott, M. L., Knodt, A. R., Ireland, D., Morris, M. L., Poulton, R., Ramrakha, S., Sison, M. L., Moffitt, T. E., Caspi, A., & Hariri, A. R. (2020). What Is the Test-Retest Reliability of Common Task-Functional MRI Measures? New Empirical Evidence and a Meta-Analysis. *Psychological science*, *31*(7), 792-806. https://doi.org/10.1177/0956797620916786

Elvira, U. K. A., Seoane, S., Janssen, J., & Janssen, N. (2022). Contributions of human amygdala nuclei to resting-state networks. *PLOS ONE*, *17*(12), e0278962. https://doi.org/10.1371/journal.pone.0278962

Engman, J., Linnman, C., Van Dijk, K. R. A., & Milad, M. R. (2016). Amygdala subnuclei resting-state functional connectivity sex and estrogen differences. *Psychoneuroendocrinology*, *63*, 34-42. https://doi.org/10.1016/j.psyneuen.2015.09.012

Erturk, M. A., Li, X., Van de Moortele, P. F., Ugurbil, K., & Metzger, G. J. (2019). Evolution of UHF Body Imaging in the Human Torso at 7T: Technology, Applications, and Future Directions. *Top Magn Reson Imaging*, *28*(3), 101-124. https://doi.org/10.1097/rmr.0000000000000202

Foster, S. L., Breukelaar, I. A., Ekanayake, K., Lewis, S., & Korgaonkar, M. S. (2023). Functional Magnetic Resonance Imaging of the Amygdala and Subregions at 3 Tesla: A Scoping Review. *Journal of Magnetic Resonance Imaging*. https://doi.org/10.1002/jmri.28836

Fox, M. D., Zhang, D., Snyder, A. Z., & Raichle, M. E. (2009). The Global Signal and Observed Anticorrelated Resting State Brain Networks. *J Neurophysiol*, *101*(6), 3270-3283. https://doi.org/10.1152/jn.90777.2008

Geissberger, N., Tik, M., Sladky, R., Woletz, M., Schuler, A.-L., Willinger, D., & Windischberger, C. (2020). Reproducibility of amygdala activation in facial emotion processing at 7T. *Neuroimage*, *211*, 116585. https://doi.org/10.1016/j.neuroimage.2020.116585

Ghanem, K., Saltoun, K., Suvrathan, A., Draganski, B., & Bzdok, D. (2024). Longitudinal microstructural changes in 18 amygdala nuclei resonate with cortical circuits and phenomics. *Communications Biology*, *7*(1), 477. https://doi.org/10.1038/s42003-024-06187-5

Glasser, M. F., Sotiropoulos, S. N., Wilson, J. A., Coalson, T. S., Fischl, B., Andersson, J. L., Xu, J., Jbabdi, S., Webster, M., Polimeni, J. R., Van Essen, D. C., & Jenkinson, M. (2013). The minimal preprocessing pipelines for the Human Connectome Project. *Neuroimage*, *80*, 105-124. https://doi.org/10.1016/j.neuroimage.2013.04.127

Glover, G. H. (2011). Overview of functional magnetic resonance imaging. *Neurosurgery clinics of North America*, *22*(2), 133-vii. https://doi.org/10.1016/j.nec.2010.11.001

Golestani, A.-M., & Goodyear, B. G. (2011). A Resting-State Connectivity Metric Independent of Temporal Signal-to-Noise Ratio and Signal Amplitude. *Brain connectivity*, *1*(2), 159-167. https://doi.org/10.1089/brain.2011.0003

Greicius, M. D., Krasnow, B., Reiss, A. L., & Menon, V. (2003). Functional connectivity in the resting brain: a network analysis of the default mode hypothesis. *Proc Natl Acad Sci U S A*, *100*(1), 253-258. https://doi.org/10.1073/pnas.0135058100

Hendriks, A. D., D'Agata, F., Raimondo, L., Schakel, T., Geerts, L., Luijten, P. R., Klomp, D. W. J., & Petridou, N. (2020). Pushing functional MRI spatial and temporal resolution further: High-density receive arrays combined with shot-selective 2D CAIPIRINHA for 3D echo-planar imaging at 7 T. *NMR in Biomedicine*, *33*(5), e4281. https://doi.org/10.1002/nbm.4281

Hofmann, D., & Straube, T. (2019). Resting-state fMRI effective connectivity between the bed nucleus of the stria terminalis and amygdala nuclei. *Hum Brain Mapp*, *40*(9), 2723-2735. https://doi.org/10.1002/hbm.24555

Honey, C. J., Sporns, O., Cammoun, L., Gigandet, X., Thiran, J. P., Meuli, R., & Hagmann, P. (2009). Predicting human resting-state functional connectivity from structural

connectivity. *Proc Natl Acad Sci U S A*, *106*(6), 2035-2040. https://doi.org/10.1073/pnas.0811168106

Huettel, S. A., Song, A. W., & McCarthy, G. (2004). *Functional magnetic resonance imaging* (1st ed.). Sinauer Associates.

Huggins, A. A., Weis, C. N., Parisi, E. A., Bennett, K. P., Miskovic, V., & Larson, C. L. (2021). Neural substrates of human fear generalization: A 7T-fMRI investigation. *Neuroimage*, *239*, 118308. https://www.sciencedirect.com/science/article/pii/S105381192100584X?via%3Dihub

Kang, D., In, M.-H., Jo, H. J., Halverson, M. A., Meyer, N. K., Ahmed, Z., Gray, E. M., Madhavan, R., Foo, T. K., Fernandez, B., Black, D. F., Welker, K. M., Trzasko, J. D., Huston, J., Bernstein, M. A., & Shu, Y. (2023). Improved Resting-State Functional MRI Using Multi-Echo Echo-Planar Imaging on a Compact 3T MRI Scanner with High-Performance Gradients. *Sensors*, *23*(9), 4329.

Kerestes, R., Chase, H. W., Phillips, M. L., Ladouceur, C. D., & Eickhoff, S. B. (2017). Multimodal evaluation of the amygdala's functional connectivity. *Neuroimage*, *148*, 219-229. https://doi.org/10.1016/j.neuroimage.2016.12.023

Klein-Flügge, M. C., Jensen, D. E. A., Takagi, Y., Priestley, L., Verhagen, L., Smith, S. M., & Rushworth, M. F. S. (2022). Relationship between nuclei-specific amygdala connectivity and mental health dimensions in humans. *Nature Human Behaviour*, *6*(12), 1705-1722. https://doi.org/10.1038/s41562-022-01434-3

Knudsen, L., Bailey, C. J., Blicher, J. U., Yang, Y., Zhang, P., & Lund, T. E. (2023). Improved sensitivity and microvascular weighting of 3T laminar fMRI with GE-BOLD using NORDIC and phase regression. *Neuroimage*, *271*, 120011. https://doi.org/10.1016/j.neuroimage.2023.120011

Krüger, G., Kastrup, A., & Glover, G. H. (2001). Neuroimaging at 1.5 T and 3.0 T: Comparison of oxygenation-sensitive magnetic resonance imaging. *Magnetic Resonance in Medicine*, *45*(4), 595-604. https://doi.org/10.1002/mrm.1081

Kwon, H., Ha, M., Choi, S., Park, S., Jang, M., Kim, M., & Kwon, J. S. (2024). Resting-state functional connectivity of amygdala subregions across different symptom subtypes of obsessive–compulsive disorder patients. *NeuroImage: Clinical*, *43*, 103644. https://doi.org/10.1016/j.nicl.2024.103644

Labuschagne, I., Dominguez, J. F., Grace, S., Mizzi, S., Henry, J. D., Peters, C., Rabinak, C. A., Sinclair, E., Lorenzetti, V., Terrett, G., Rendell, P. G., Pedersen, M., Hocking, D. R., & Heinrichs, M. (2024). Specialization of amygdala subregions in emotion processing. *Human Brain Mapping*, *45*(5), e26673. https://doi.org/10.1002/hbm.26673

Ladd, M. E., Bachert, P., Meyerspeer, M., Moser, E., Nagel, A. M., Norris, D. G., Schmitter, S., Speck, O., Straub, S., & Zaiss, M. (2018). Pros and cons of ultra-high-field

MRI/MRS for human application. *Progress in Nuclear Magnetic Resonance Spectroscopy*, *109*, 1-50. https://doi.org/10.1016/j.pnmrs.2018.06.001

Li, Y. Y., Ni, X. K., You, Y. F., Qing, Y. H., Wang, P. R., Yao, J. S., Ren, K. M., Zhang, L., Liu, Z. W., Song, T. J., Wang, J., Zang, Y. F., Shen, Y. D., & Chen, W. (2021). Common and Specific Alterations of Amygdala Subregions in Major Depressive Disorder With and Without Anxiety: A Combined Structural and Resting-State Functional MRI Study. *Front Hum Neurosci*, *15*, 634113. https://doi.org/10.3389/fnhum.2021.634113

Lindquist, M. (2008). The Statistical Analysis of fMRI Data. *Statistical Science*, *23*(4), 439-464. https://doi.org/DOI: 10.1214/09-STS282

Lutti, A., Thomas, D. L., Hutton, C., & Weiskopf, N. (2013). High-resolution functional MRI at 3 T: 3D/2D echo-planar imaging with optimized physiological noise correction. *Magn Reson Med*, *69*(6), 1657-1664. https://doi.org/10.1002/mrm.24398

McRobbie, D. W., Moore, E. A., Graves, M. J., & Prince, M. R. (2017). *MRI from Picture to Proton* (3 ed.). Cambridge University Press. https://doi.org/DOI: 10.1017/9781107706958

Miletić, S., Bazin, P.-L., Weiskopf, N., van der Zwaag, W., Forstmann, B. U., & Trampel, R. (2020). fMRI protocol optimization for simultaneously studying small subcortical and cortical areas at 7 T. *Neuroimage*, *219*, 116992. https://doi.org/https://doi.org/10.1016/j.neuroimage.2020.116992

Mulder, M. J., Keuken, M. C., Bazin, P.-L., Alkemade, A., & Forstmann, B. U. (2019). Size and shape matter: The impact of voxel geometry on the identification of small nuclei. *PLOS ONE*, *14*(4), e0215382. https://doi.org/10.1371/journal.pone.0215382

Murphy, B. W., Carson, P. L., Ellis, J. H., Zhang, Y. T., Hyde, R. J., & Chenevert, T. L. (1993). Signal-to-noise measures for magnetic resonance imagers. *Magnetic Resonance Imaging*, *11*(3), 425-428. https://doi.org/10.1016/0730-725X(93)90076-P

Murphy, K., Birn, R. M., Handwerker, D. A., Jones, T. B., & Bandettini, P. A. (2009). The impact of global signal regression on resting state correlations: are anti-correlated networks introduced? *Neuroimage*, *44*(3), 893-905. https://doi.org/10.1016/j.neuroimage.2008.09.036

Murphy, K., Bodurka, J., & Bandettini, P. A. (2007). How long to scan? The relationship between fMRI temporal signal to noise ratio and necessary scan duration. *Neuroimage*, *34*(2), 565-574. https://doi.org/10.1016/j.neuroimage.2006.09.032

Narasimhan, P. T., & Jacobs, R. E. (2002). 16 - Neuroanatomical Micromagnetic Resonance Imaging. In A. W. Toga & J. C. Mazziotta (Eds.), *Brain Mapping: The Methods (Second Edition)* (pp. 399-426). Academic Press. https://doi.org/10.1016/B978-012693019-1/50018-6

Narsude, M., Gallichan, D., van der Zwaag, W., Gruetter, R., & Marques, J. P. (2016). Three-dimensional echo planar imaging with controlled aliasing: A sequence for high temporal resolution functional MRI. *Magnetic Resonance in Medicine*, *75*(6), 2350-2361. https://doi.org/10.1002/mrm.25835

Newton, A. T., Rogers, B. P., Gore, J. C., & Morgan, V. L. (2012). Improving measurement of functional connectivity through decreasing partial volume effects at 7 T. *Neuroimage*, *59*(3), 2511-2517. https://doi.org/10.1016/j.neuroimage.2011.08.096

Norris, D. G. (2015). Pulse Sequences for fMRI. In K. Uludag, K. Ugurbil, & L. Berliner (Eds.), *fMRI: From Nuclear Spins to Brain Functions* (pp. 131-162). Springer US. https://doi.org/10.1007/978-1-4899-7591-1_7

Okada, T., Akasaka, T., Thuy, D. H., & Isa, T. (2022). Safety for Human MR Scanners at 7T. *Magn Reson Med Sci*, *21*(4), 531-537. https://doi.org/10.2463/mrms.rev.2021-0063

Olman, C. A., Davachi, L., & Inati, S. (2009). Distortion and Signal Loss in Medial Temporal Lobe. *PLOS ONE*, *4*(12), e8160. https://doi.org/10.1371/journal.pone.0008160

Olman, C. A., & Yacoub, E. (2011). High-field FMRI for human applications: an overview of spatial resolution and signal specificity. *Open Neuroimag J*, *5*, 74-89. https://doi.org/10.2174/1874440001105010074

Pedersen, W. S., Muftuler, L. T., & Larson, C. L. (2017). Disentangling the effects of novelty, valence and trait anxiety in the bed nucleus of the stria terminalis, amygdala and hippocampus with high resolution 7T fMRI. *Neuroimage*, *156*, 293-301. https://doi.org/10.1016/j.neuroimage.2017.05.009

Peer, M., Abboud, S., Hertz, U., Amedi, A., & Arzy, S. (2016). Intensity-based masking: A tool to improve functional connectivity results of resting-state fMRI. *Human Brain Mapping*, *37*(7), 2407-2418. https://doi.org/10.1002/hbm.23182

Platt, T., Ladd, M. E., & Paech, D. (2021). 7 Tesla and Beyond: Advanced Methods and Clinical Applications in Magnetic Resonance Imaging. *Invest Radiol*, *56*(11), 705-725. https://doi.org/10.1097/rli.0000000000000820

Pohmann, R., Speck, O., & Scheffler, K. (2016). Signal-to-noise ratio and MR tissue parameters in human brain imaging at 3, 7, and 9.4 tesla using current receive coil arrays. *Magnetic Resonance in Medicine*, *75*(2), 801-809. https://doi.org/10.1002/mrm.25677

Polimeni, J. R., & Wald, L. L. (2018). Magnetic Resonance Imaging technology-bridging the gap between noninvasive human imaging and optical microscopy. *Curr Opin Neurobiol*, *50*, 250-260. https://doi.org/10.1016/j.conb.2018.04.026

Poser, B. A., Koopmans, P. J., Witzel, T., Wald, L. L., & Barth, M. (2010). Three dimensional echo-planar imaging at 7 Tesla. *Neuroimage*, *51*(1), 261-266. https://doi.org/10.1016/j.neuroimage.2010.01.108

Puckett, A. M., Bollmann, S., Poser, B. A., Palmer, J., Barth, M., & Cunnington, R. (2018). Using multi-echo simultaneous multi-slice (SMS) EPI to improve functional MRI of the subcortical nuclei of the basal ganglia at ultra-high field (7T). *Neuroimage*, *172*, 886-895. https://doi.org/10.1016/j.neuroimage.2017.12.005

Rausch, A., Zhang, W., Haak, K. V., Mennes, M., Hermans, E. J., van Oort, E., van Wingen, G., Beckmann, C. F., Buitelaar, J. K., & Groen, W. B. (2016). Altered functional connectivity of the amygdaloid input nuclei in adolescents and young adults with autism spectrum disorder: a resting state fMRI study. *Molecular autism*, *7*(1), 1-13. https://doi.org/10.1186/s13229-015-0060-x

Robertson, R. V., Crawford, L. S., Meylakh, N., Macey, P. M., Macefield, V. G., Keay, K. A., & Henderson, L. A. (2022). Regional hypothalamic, amygdala, and midbrain periaqueductal gray matter recruitment during acute pain in awake humans: A 7-Tesla functional magnetic resonance imaging study. *Neuroimage*, *259*, 119408.

Robinson, S., Windischberger, C., Rauscher, A., & Moser, E. (2004). Optimized 3 T EPI of the amygdalae. *Neuroimage*, *22*(1), 203-210. https://doi.org/10.1016/j.neuroimage.2003.12.048

Roddy, D., Kelly, J. R., Farrell, C., Doolin, K., Roman, E., Nasa, A., Frodl, T., Harkin, A., O'Mara, S., O'Hanlon, E., & O'Keane, V. (2021). Amygdala substructure volumes in Major Depressive Disorder. *Neuroimage Clin*, *31*, 102781. https://doi.org/10.1016/j.nicl.2021.102781

Rosazza, C., Minati, L., Ghielmetti, F., Mandelli, M. L., & Bruzzone, M. G. (2012). Functional Connectivity during Resting-State Functional MR Imaging: Study of the Correspondence between Independent Component Analysis and Region-of-Interest−Based Methods. *American Journal of Neuroradiology*, *33*(1), 180. https://doi.org/10.3174/ajnr.A2733

Roy, A. K., Shehzad, Z., Margulies, D. S., Kelly, A. M. C., Uddin, L. Q., Gotimer, K., Biswal, B. B., Castellanos, F. X., & Milham, M. P. (2009). Functional connectivity of the human amygdala using resting state fMRI. *Neuroimage*, *45*(2), 614-626. https://doi.org/10.1016/j.neuroimage.2008.11.030

Saygin, Z. M., Osher, D. E., Augustinack, J., Fischl, B., & Gabrieli, J. D. (2011). Connectivity-based segmentation of human amygdala nuclei using probabilistic tractography. *Neuroimage*, *56*(3), 1353-1361. https://doi.org/10.1016/j.neuroimage.2011.03.006

Sladky, R., Baldinger, P., Kranz, G. S., Tröstl, J., Höflich, A., Lanzenberger, R., Moser, E., & Windischberger, C. (2013). High-resolution functional MRI of the human amygdala at 7 T [Journal Article]. *Eur J Radiol*, *82*(5), 728-733. https://doi.org/10.1016/j.ejrad.2011.09.025

Sladky, R., Geissberger, N., Pfabigan, D. M., Kraus, C., Tik, M., Woletz, M., Paul, K., Vanicek, T., Auer, B., Kranz, G. S., Lamm, C., Lanzenberger, R., & Windischberger,

C. (2018). Unsmoothed functional MRI of the human amygdala and bed nucleus of the stria terminalis during processing of emotional faces. *Neuroimage*, *168*, 383-391. https://doi.org/10.1016/j.neuroimage.2016.12.024

Smith, S. M., Beckmann, C. F., Andersson, J., Auerbach, E. J., Bijsterbosch, J., Douaud, G., Duff, E., Feinberg, D. A., Griffanti, L., Harms, M. P., Kelly, M., Laumann, T., Miller, K. L., Moeller, S., Petersen, S., Power, J., Salimi-Khorshidi, G., Snyder, A. Z., Vu, A. T., . . . Glasser, M. F. (2013). Resting-state fMRI in the Human Connectome Project. *Neuroimage*, *80*, 144-168. https://doi.org/10.1016/j.neuroimage.2013.05.039

Sohn, W. S., Yoo, K., Lee, Y. B., Seo, S. W., Na, D. L., & Jeong, Y. (2015). Influence of ROI selection on resting state functional connectivity: an individualized approach for resting state fMRI analysis. *Front Neurosci*, *9*, 280. https://doi.org/10.3389/fnins.2015.00280

Solano-Castiella, E., Schäfer, A., Reimer, E., Türke, E., Pröger, T., Lohmann, G., Trampel, R., & Turner, R. (2011). Parcellation of human amygdala in vivo using ultra high field structural MRI. *Neuroimage*, *58*(3), 741-748. https://doi.org/10.1016/j.neuroimage.2011.06.047

Stirnberg, R., Huijbers, W., Brenner, D., Poser, B. A., Breteler, M., & Stöcker, T. (2017). Rapid whole-brain resting-state fMRI at 3 T: Efficiency-optimized three-dimensional EPI versus repetition time-matched simultaneous-multi-slice EPI. *Neuroimage*, *163*, 81-92. https://doi.org/10.1016/j.neuroimage.2017.08.031

Sylvester, C. M., Yu, Q., Srivastava, A. B., Marek, S., Zheng, A., Alexopoulos, D., Smyser, C. D., Shimony, J. S., Ortega, M., Dierker, D. L., Patel, G. H., Nelson, S. M., Gilmore, A. W., McDermott, K. B., Berg, J. J., Drysdale, A. T., Perino, M. T., Snyder, A. Z., Raut, R. V., . . . Dosenbach, N. U. F. (2020). Individual-specific functional connectivity of the amygdala: A substrate for precision psychiatry. *Proceedings of the National Academy of Sciences*, *117*(7), 3808-3818. https://doi.org/doi:10.1073/pnas.1910842117

Tijssen, R. H. N., Okell, T. W., & Miller, K. L. (2011). Real-time cardiac synchronization with fixed volume frame rate for reducing physiological instabilities in 3D FMRI. *Neuroimage*, *57*(4), 1364-1375. https://doi.org/10.1016/j.neuroimage.2011.05.070

Triantafyllou, C., Hoge, R. D., Krueger, G., Wiggins, C. J., Potthast, A., Wiggins, G. C., & Wald, L. L. (2005). Comparison of physiological noise at 1.5 T, 3 T and 7 T and optimization of fMRI acquisition parameters. *Neuroimage*, *26*(1), 243-250. https://doi.org/10.1016/j.neuroimage.2005.01.007

Tudorascu, D. L., Karim, H. T., Maronge, J. M., Alhilali, L., Fakhran, S., Aizenstein, H. J., Muschelli, J., & Crainiceanu, C. M. (2016). Reproducibility and Bias in Healthy Brain Segmentation: Comparison of Two Popular Neuroimaging Platforms [Original Research]. *Frontiers in Neuroscience*, *Volume 10 - 2016*. https://doi.org/10.3389/fnins.2016.00503

Van Dijk, K. R., Hedden, T., Venkataraman, A., Evans, K. C., Lazar, S. W., & Buckner, R. L. (2010). Intrinsic functional connectivity as a tool for human connectomics: theory, properties, and optimization. *J Neurophysiol*, *103*(1), 297-321. https://doi.org/10.1152/jn.00783.2009

Van Essen, D. C., Ugurbil, K., Auerbach, E., Barch, D., Behrens, T. E. J., Bucholz, R., Chang, A., Chen, L., Corbetta, M., Curtiss, S. W., Della Penna, S., Feinberg, D., Glasser, M. F., Harel, N., Heath, A. C., Larson-Prior, L., Marcus, D., Michalareas, G., Moeller, S., . . . Yacoub, E. (2012). The Human Connectome Project: A data acquisition perspective. *Neuroimage*, *62*(4), 2222-2231. https://doi.org/10.1016/j.neuroimage.2012.02.018

Viessmann, O., & Polimeni, J. R. (2021). High-resolution fMRI at 7 Tesla: challenges, promises and recent developments for individual-focused fMRI studies. *Curr Opin Behav Sci*, *40*, 96-104. https://doi.org/10.1016/j.cobeha.2021.01.011

Welvaert, M., & Rosseel, Y. (2013). On the Definition of Signal-To-Noise Ratio and Contrast-To-Noise Ratio for fMRI Data. *PLOS ONE*, *8*(11), e77089. https://doi.org/10.1371/journal.pone.0077089

Wu, C. W., Chen, C.-L., Liu, P.-Y., Chao, Y.-P., Biswal, B. B., & Lin, C.-P. (2011). Empirical Evaluations of Slice-Timing, Smoothing, and Normalization Effects in Seed-Based, Resting-State Functional Magnetic Resonance Imaging Analyses. *Brain connectivity*, *1*(5), 401-410. https://doi.org/10.1089/brain.2011.0018

Yang, X., Holmes, M. J., Newton, A. T., Morgan, V. L., & Landman, B. A. (2012). A comparison of distributional considerations with statistical analysis of resting state fMRI at 3T and 7T. Medical Imaging 2012: Image Processing,

Yatham, L. N. (2023). Biomarkers for clinical use in psychiatry: where are we and will we ever get there? *World Psychiatry*, *22*(2), 263-264. https://doi.org/10.1002/wps.21079

Yeo, B. T., Krienen, F. M., Sepulcre, J., Sabuncu, M. R., Lashkari, D., Hollinshead, M., Roffman, J. L., Smoller, J. W., Zöllei, L., Polimeni, J. R., Fischl, B., Liu, H., & Buckner, R. L. (2011). The organization of the human cerebral cortex estimated by intrinsic functional connectivity. *J Neurophysiol*, *106*(3), 1125-1165. https://doi.org/10.1152/jn.00338.2011

Zhang, X., Cheng, H., Zuo, Z., Zhou, K., Cong, F., Wang, B., Zhuo, Y., Chen, L., Xue, R., & Fan, Y. (2018). Individualized Functional Parcellation of the Human Amygdala Using a Semi-supervised Clustering Method: A 7T Resting State fMRI Study. *Frontiers in Neuroscience*, *12*(270). https://doi.org/10.3389/fnins.2018.00270

Chapter 6: Subregional Amygdala Functional Connectivity at 3T: Comparison of High-Resolution 2D and 3D Acquisitions

---

The work in this chapter follows on from Chapter Five by assessing the capabilities of the two sequences used in the previous chapter but with a focus on subcortical rather than cortical functional connections from the amygdala subregions. With the bulk of fMRI literature relating to cortical studies, there are few articles focusing on subcortical connectivity as this area of the brain is quite challenging to visualise.

The primary aim of this pilot study was to compare the subregional amygdala functional connectivity capabilities of the 2D and 3D high resolution sequences, with different voxel volumes and k-space acquisition strategies, in relation to other subcortical regions such as the brainstem and hippocampus that are traditionally not well-visualized with current techniques. The results of the study confirmed that the 3D sequence outperformed its 2D counterpart, with this result likely due to its novel k-space acquisition strategy and the significant signal-to-noise-advantage this accorded.

This is the first published study to directly compare the performance of high resolution 2D and 3D fMRI data acquired at 3T in identifying subregional amygdala functional connections to deep subcortical structures such as the brainstem, hippocampus and contralateral amygdala.

This chapter is published in the Journal of Neuroimaging

Journal of Neuroimaging

WILEY

CLINICAL INVESTIGATIVE STUDY OPEN ACCESS

Subregional Amygdala Functional Connectivity at 3T: Comparison of High-Resolution 2D and 3D fMRI Acquisitions

Sheryl L. Foster[1,2] | Ramon Landin-Romero[1,3] | Sarah Lewis[1,4] | Mayuresh S. Korgaonkar[1,5,6]

[1]Discipline of Medical Imaging Science, Sydney School of Health Sciences, Faculty of Medicine and Health, The University of Sydney, Sydney, New South Wales, Australia | [2]Department of Radiology, Westmead Hospital, Westmead, New South Wales, Australia | [3]Brain and Mind Centre, The University of Sydney, Camperdown, New South Wales, Australia | [4]School of Health Sciences, Western Sydney University, Penrith, New South Wales, Australia | [5]Westmead Clinical School, Faculty of Medicine and Health, The University of Sydney, Sydney, New South Wales, Australia | [6]Brain Dynamics Centre, The Westmead Institute For Medical Research, Westmead, New South Wales, Australia

Correspondence: Sheryl L. Foster (sheryl.foster@sydney.edu.au)

Received: 23 August 2025 | **Revised:** 6 November 2025 | **Accepted:** 10 November 2025

Keywords: 3T | amygdala subregions | functional connectivity | high resolution

ABSTRACT

Background and Purpose: Amygdala dysfunction is implicated in major depressive disorder. Despite wide acknowledgement of its heterogeneity, the amygdala is predominantly considered as a single entity and functional connectivity investigations have reported findings using standard or low spatial resolution functional MRI data. This study compared the capabilities of two high spatial resolution acquisition strategies, the gold standard 2D and a novel 3D, in identifying amygdala functional connectivity to other brain regions at a subregional level.

Methods: Resting state fMRI data were acquired at 3T in 10 healthy controls using both versions of a Gradient-Echo Echo Planar Imaging (GRE-EPI) sequence. Whole brain voxel-wise functional connectivity measures were calculated using the whole amygdala and six subregional seed regions-of-interest; left and right basolateral, centromedial and superficial.

Results: The 3D data identified multiple stronger bilateral connections between both centromedial subregions, most notably to subcortical structures including brainstem and hippocampus, as well as intra-amygdala subregional connections. The 2D data displayed stronger connections to several cortical regions. Whole amygdala and subregional FC results differed.

Conclusions: This study identified underutilized capability in current fMRI acquisition techniques at 3T. 2D GRE-EPI sequences optimized for high spatial resolution with voxel volumes of 15.6 mm^3 capably demonstrate functional connectivity patterns of the amygdala at a subregional level, allowing interrogation of heterogeneous amygdala function at a more granular level. The novel 3D acquisition with voxel volumes of 8 mm^3 showed promise in outperforming its 2D counterpart in identifying amygdala subregional connections to other subcortical structures that are traditionally difficult to image well.

1 | Introduction

The amygdala is a small subcortical structure forming part of the limbic system and its dysfunction is known to contribute to maladaptive emotion processing characteristic of neuropsychiatric conditions including major depressive disorder (MDD) [1, 2]. It has been the focus of numerous functional magnetic resonance imaging (fMRI) studies since the 1990s when 1.5 Tesla (T) MRI systems became widely available [3]. Although cutting-edge at that time, 1.5T systems produced data

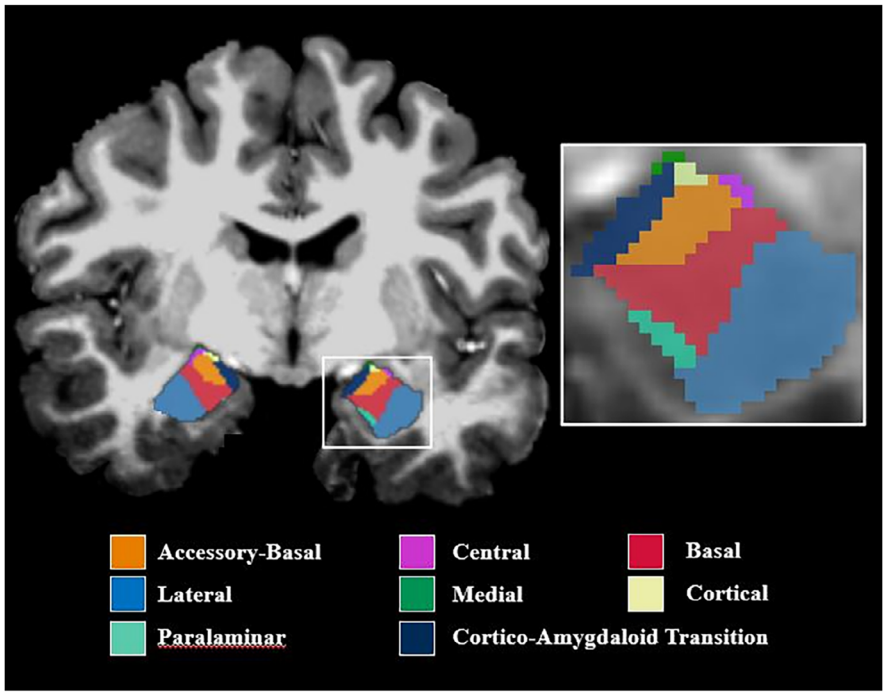

FIGURE 1 | T1-weighted coronal image acquired at 7T depicting the location of the amygdala subnuclei. Anterior amygdaloid area (part of superficial subregion) not visible.

that is now considered low spatial resolution, with the amygdala being considered as a single entity in reported findings [4–9]. However, it is now widely acknowledged that the amygdala is not a homogenous structure, being composed of multiple nuclei with diverse functional connections to multiple brain regions [10, 11], including traditionally difficult-to-image areas such as the brainstem and cerebellum [12]. Interrogating the amygdala at a more granular level requires much higher spatial resolution imaging than has traditionally been the norm [13], primarily due to the higher temporal resolution requirements of fMRI and the inverse nature of the relationship between the two [14].

Signal-to-noise resolution (SNR) is key to high temporal and spatial resolution imaging and scales linearly with field strength [15]. SNR in fMRI studies is technically a measure of temporal SNR (tSNR) averaged across all the images in the time-series, although the two terms tend to be used interchangeably [16]. Spatial resolution is referenced as voxel volume (VV) in mm^3 and has an intrinsic relationship with SNR, as the two are directly proportional [15]. High spatial resolution imaging (defined as VV of $< 20mm^3$) requires small VVs which theoretically possess lower SNR [17]. Whilst it may seem counterintuitive, there are potential SNR benefits to be recouped by employing an acquisition sequence with smaller voxels, particularly in relation to deep central structures such as the amygdala, located adjacent to the skull base and air-filled cavities [18]. Field distortion issues are prevalent at air/bone /tissue interfaces and magnetic susceptibility-related signal dropout results from protons effectively precessing at different frequencies, thus reducing overall SNR [19, 20]. Smaller voxels containing homogenous tissues suffer fewer signal losses related to phase errors, partial volume effects and intravoxel dephasing that typically occur in larger voxels [14, 21].

TABLE 1 | Three amygdala subregions and their individual subnuclei [23].

Centromedial	Laterobasal	Superficial
Central	Accessory basal	Anterior amygdaloid area
Medial	Basal	Cortical
	Lateral	Cortico amygdaloid transition
	Paralaminar	

Ultra-high-field 7T studies optimized for acquisition of very high spatial resolution have reported functional connectivity (FC) patterns of up to nine individual subnuclei (Figure 1) [22–24], whilst others have defined three primary subregions, the centromedial (CM), laterobasal (LB), and superficial (SF), each composed of individual subnuclei (Table 1) [25, 26].

Although 7T systems theoretically possess more than twice the SNR levels of 3T systems, in practice there are several factors that collectively reduce its inherent SNR advantages over 3T, including tissue property alterations, radiofrequency-field inhomogeneity, and susceptibility-related signal losses [27]. In addition, lack of access to 7T means that 3T is the most widely used field strength for clinical research [28, 29]. Consequently, 3T is an excellent compromise, particularly when considering advancements in radiofrequency (RF) coil design and acceleration techniques that have facilitated high spatial resolution fMRI data [17, 30].

Whilst a handful of studies have reported FC from the amygdala to other brain regions at the subregional level using high spatial resolution data acquired at 3T [1, 31–33] numerous studies continue to report findings based on the amygdala as

a single structure with standard or low spatial resolution data [34–39].

fMRI investigations of the amygdala have traditionally been task-based, with paradigms that are currently in use focusing on the amygdala as a single structure [40, 41]. This is due, in part, to the lack of suitably developed tasks or paradigms to activate specific subregions given that functional contributions of individual subregions remain poorly understood [31, 42]. An alternative technique, resting state fMRI (rs-fMRI) has become a mainstay for researchers investigating neural function [43, 44]. Unconstrained by task demands and specificity, this technique can provide a "baseline" of FC for true comparisons of functional organization across cohorts [45] and allow interrogation of amygdala subregional FC differences reflective of their underlying heterogeneity.

The 2D T2*-W GRE-EPI sequence is the workhorse of fMRI; it has high Blood Oxygen Level Dependent (BOLD) sensitivity at 3T, high temporal and spatial resolution capabilities and is widely employed [30, 46–48]. A novel 3D version of this sequence has been shown to possess key advantages over its 2D counterpart; that is, inherently higher temporal resolution and SNR capabilities resulting from an alternate k-space acquisition strategy, allowing use of smaller voxels [49]. SNR in the 3D version has been shown to be higher in central brain regions, the location of deep subcortical structures such as the amygdala, whereas SNR in the 2D version is typically reduced with greater distance from RF coil arrays [49–52]. Consequently, the 3D version shows potential for improved performance in resolving FC of the individual amygdala subregions to other subcortical structures at 3T.

The primary aim of this pilot study was to compare the subregional amygdala FC capabilities of these two high resolution GRE-EPI sequences with different VVs and acquisition strategies, particularly in relation to other central and subcortical locations such as the brainstem and hippocampus that are traditionally not well-visualized [12]. Based on previous work demonstrating the benefits of smaller voxels together with central SNR advantages previously outlined, we hypothesized that the novel 3D sequence would outperform the traditional 2D sequence in demonstrating functional connections between the amygdala subregions and other subcortical brain regions. Both sequences were optimized for use at 3T, with 2D VV being 15.6 mm^3 and 3D VV being 8 mm^3.

2 | Methods

2.1 | Participants

Ten healthy participants (five males) aged 18–64 years (mean 35 years) took part in this study. All participants were physically healthy with no significant history of neurological or psychiatric illness, or head injury. Approval was obtained from Western Sydney Local Health District Human Research Ethics Committee and written informed consent was obtained from all participants. Imaging studies were undertaken at Westmead Hospital Radiology Department, Sydney, Australia.

2.2 | Data Acquisition

Image data were acquired on a 3 Tesla Siemens Prisma MRI system running VE11C software (Siemens Healthineers, Erlangen, Germany) together with a 64-channel head/neck array RF coil. Participants were instructed to remain very still whilst focusing on a fixation cross projected onto a coil-mounted screen during acquisition of the 2D and 3D versions of the resting-state sequence.

Imaging parameters for the 2D T2*-weighted GRE-EPI sequence were as follows: Repetition time (TR) = 1500 ms; Echo time (TE) = 33 ms; Field-of-view (FOV) = 255 mm; Matrix = 104 × 104; Flip angle (FA) = 85°; Phase encoding direction = A to P; Total acceleration = 6 (MB 3); volumes = 320. Sixty interleaved axial-oblique slices at 2.5 mm thick (0 mm gap) parallel to the AC-PC line were acquired covering the whole brain with an isotropic voxel size of 2.5 mm (VV = 15.6 mm^3) in an acquisition time of 8 min and 12 s.

Imaging parameters for the 3D T2*-weighted GRE-EPI sequence were as follows: TR = 2160 ms; TE = 28 ms; FOV = 224 mm; Matrix = 112 × 112; FA = 10°; Phase encoding direction = A to P; Total acceleration = 4; volumes = 220. Eighty ascending axial slices at 2 mm thick (0 mm gap) parallel to the AC-PC line were acquired covering the whole brain with an isotropic voxel size of 2 mm (VV = 8 mm^3) in an acquisition time of 8 min and 11 s.

Due to the inherent differences in k-space acquisition strategies, the TR values differed between the two sequences; therefore the total number of volumes required (320 for the 2D sequence and 220 for the 3D sequence) was calculated to result in equivalent acquisition times of just over 8 min. The total number of slices for each sequence was prefaced on the requirement for whole brain coverage and a whole number multiple of the slice acceleration factor of the individual sequence [49]. In addition, due to the location of the amygdala in an area known for increased magnetic susceptibility issues due to air/bone/tissue/interfaces, slice partial Fourier sampling was not engaged in the 3D sequence to avoid the potential for increased signal losses [49]. The main magnetic field was shimmed once automatically prior to the first GRE-EPI acquisition to reduce variability in field homogeneity between sequences [49, 53].

A further 3D T1-weighted magnetization-prepared gradient echo sequence was acquired to provide high-resolution structural data with imaging parameters as follows: TR = 2400 ms; TE = 2.21 ms; Inversion Time (TI) = 900 ms; FOV = 256 mm; Matrix = 288 × 288; FA = 8°; Phase encoding direction = A to P; Acceleration (GRAPPA) = 2; 192 sagittal slices at 0.9 mm thick parallel to the interhemispheric fissure were acquired covering the whole brain with an isotropic voxel size of 0.9 mm in an acquisition time of 6 min and 23 s.

2.3 | Data Analyses

The functional seed-based connectivity analysis was based on a priori selection of regions-of-interest (ROIs). To facilitate this, six amygdala subregional masks or ROIs created from cytoarchitectonically-defined probabilistic maps (Amunts et al. 2005) were extracted from The JuBrain Anatomy Toolbox

(Eickhoff et al. 2005) [54, 55]. The ROIs, left and right CM, LB, and SF, were uploaded into the CONN toolbox in preparation for whole-brain voxel-wise analyses, which were performed using a combination of Matlab R2022b (The MathWorks Inc. Natick, Massachusetts), SPM12 (Wellcome Trust Centre for Neuroimaging, London, UK) and CONN FC toolbox v22b (http://www.nitrc.org/projects/conn/).

Preprocessing of anatomical and functional images for both 2D and 3D acquisitions was performed concurrently using the CONN modular preprocessing pipeline (Nieto-Castanon 2020a) [56]. In line with findings showing that slice time correction [57, 58] and spatial smoothing [18, 30, 59, 60] are unnecessary and potentially detrimental for native high resolution data undergoing resting state analyses by reducing spatial specificity, both steps were removed from the preprocessing pipeline. The data underwent realignment, unwarping, co-registration, and resampling for motion correction and magnetic susceptibility interactions and a BOLD reference image was created for each subject. Data were then segmented into grey matter, white matter, and cerebrospinal fluid and then normalized into standard Montreal Neurological Institute space. Functional data were denoised using a standard pipeline including regression of potential confounders (CompCor) from white matter, cerebrospinal fluid and motion parameters (Nieto-Castanon 2020b), followed by bandpass filtering (0.01–0.1 Hz) [61]. Data was assessed for head motion using the Assessment of Repetitive Tasks (ART)-based scrubbing technique in CONN, with outliers being defined as having greater than 0.9 mm framewise displacement; however, no participants were excluded based on less than 5% scans deemed as outliers.

The six ROIs (left and right CM, LB, and SF) were then used as seed regions to explore whole-brain voxel-wise FC and to determine FC strength represented by Fisher's z transform of the correlation coefficients from a weighted General Linear Model. This was computed by averaging the time course of all voxels in each seed ROI and correlating with the time course of every other voxel in the brain. Correlation coefficients were used in the group level analyses, performed using a General Linear Model. The 2D and 3D sequences were compared voxel-wise to identify potential differences in FC strengths from individual subregional ROIs to all other parts of the brain using paired t-tests. Statistical parametric maps were generated and results thresholded using a combination of cluster-forming $p < 0.001$ voxel-level threshold and an FDR-corrected $p < 0.05$ cluster-size threshold (Chumbley et al. 2010) [62].

3 | Results

Results of the whole brain voxel-wise analyses and comparison between the 2D and 3D sequences are shown in Table 2. Compared to the 3D sequence, the 2D sequence demonstrated higher FC values between four subregions (right CM, LB and SF, and left CM), and three cortical regions, the right and left parahippocampal gyri and the right fusiform cortex (Figure 2). The 2D sequence did not identify any subcortical functional connections

In contrast, the 3D sequence demonstrated higher FC values than the 2D sequence between three subregions (left and right CM and right LB) and eight individual brain regions, the majority of which were subcortical, including bilateral amygdala, hippocampus and brainstem regions (Figure 3). Significantly higher connectivity to cortical regions was also identified between both the right and left CM subregions and the right fronto-orbital cortex as well as between the right LB subregion and right middle frontal gyrus.

In addition, the 3D acquisition displayed significantly higher bilateral intra-amygdala connectivity arising from both the left and right CM subregions. The left CM subregion connected with the right CM and LB subregions as well as the left LB and SF subregions. The right CM subregion connected with all three left-sided subregions as well as the right LB subregion. The subregional sites of the intra-amygdala connections identified from the right and left CM subregions were localized using their Montreal Neurological Institute coordinates in the JuBrain Anatomy Toolbox [63]. Subregional locations represented by amygdala coordinates are shown in brackets in Table 2.

Whole amygdala ROI results differed from the subregional results. Compared to the 3D sequence, the 2D sequence displayed stronger FC from the left amygdala to only two clusters, the left and right parahippocampal gyri ($p = 0.000012$ and $p = 0.000338$, respectively, FDR-corrected). No significantly higher connectivity values were noted for the 3D sequence relative to the 2D sequence for the whole amygdala ROIs.

4 | Discussion

This pilot study in a healthy control cohort compared the capabilities of two optimized versions of the T2*-Weighted GRE-EPI sequence at 3T, the gold standard 2D version in common use for fMRI acquisitions, and a novel 3D version. As hypothesized, the novel 3D sequence was superior in identifying functional connections between the amygdala subregions and other subcortical structures, including the brainstem and hippocampus, whilst the 2D sequence identified stronger cortical connections from four of the six individual amygdala subregions to three regions, the parahippocampal gyri bilaterally and the right fusiform cortex. Previous work has shown that the parahippocampal gyrus acts as a link between the temporal lobe memory system and the Default Mode Network [64]. FC findings between the CM and SF to the parahippocampal gyri were in alignment with those of those of Roy et al. [65] who reported connections between right CM and right parahippocampal gyrus and also between right SF and left parahippocampal gyrus in healthy controls using rs-fMRI data with VV of 27 mm^3. Our findings of stronger FC identified by the 2D sequence compared to 3D between right LB and right fusiform cortex are also in line with those of Herrington et al. in their investigation into facial recognition in healthy controls and, interestingly, hyperconnectivity between these two brain regions was noted by Foster et al. in healthy controls compared to a treatment-resistant depression cohort [33, 66].

In contrast, the 3D version outperformed the 2D sequence in demonstrating subcortical connections, notwithstanding the identification of three additional subregion-to-cortex connections. Of note was its capability in identifying bilateral brainstem connections from bilateral CM subregions. In a previous rs-fMRI study, Roy et al. reported the efferent role of the CM in connecting

TABLE 2 | Differences in functional connectivity strength between amygdala subregions and other brain regions: 2D versus 3D sequence comparison.

	Amygdala subregion	Connected brain region	Peak MNI coordinates *x*, *y*, *z*	Cluster size in voxels	*T*-stat/*p* value
2D > 3D	L_CM	Parahippocampal gyrus—L	−30, −4, −34	5	5.77/0.000269
		Parahippocampal gyrus—R	+20, −16, −28	7	7.37/0.000042
	R_CM	Parahippocampal gyrus—R	+22, −18, −28	8	5.97/0.000211
	R_LB	Fusiform cortex—R	+26, +0, −42	7	4.78/0.000997
	R_SF	Parahippocampal gyrus—R	+18, −2, −30	5	5.00/0.000742
3D > 2D	L_CM	Amygdala—L (CM, SF, LB)	−20, −8, −14	23	5.14/0.000613
		Amygdala— L (CM, LB)	−28, −4, −18	21	5.84/0.000248
		Amygdala—R (CM, LB)	+24, −4, −14	59	6.65/0.000093
	L_CM	Hippocampus—L	−30, −22, −14	14	7.68/0.000031
		Hippocampus—R	+30, −20, −14	13	6.98/0.000065
	L_CM	Fronto-orbital cortex—R	+36, +20, −18	11	5.6/0.000335
			+42, +22, −16	5	5.77/0.000271
	L_CM	Brainstem—L	−6, −18, −20	8	6.8/0.000078
		Brainstem—R	+6, −18, −20	8	5.46/0.000401
	R_CM	c (LB, CM)	−30, −2, −20	17	4.96/0.000777
		Amygdala—L (CM, LB, SF)	−22, −4, −16	10	5.06/0.000678
		Amygdala—L (CM, SF)	−16, −8, −14	7	5.54/0.000362
		Amygdala—R (CM, LB)	+24, −4, −14	38	5.39/0.000436
		Amygdala—R (CM)	+24, −12, −12	5	5.75/0.000276
	R_CM	Brainstem—L	−6, −20, −20	5	5.15/0.000603
		Brainstem—R	+8, −18, −20	7	5.56/0.000350
	R_CM	Hippocampus—L	−34, −20, −14	7	5.02/0.000723
		Hippocampus—R	−28, −22, −14	6	7.45/0.000039
			+32, −20, −16	5	6.10/0.000179
	R_CM	Fronto-orbital cortex—R	+38, +18, −18	5	5.54/0.000359
	R_LB	Middle frontal gyrus—R	+46, +14, +48	5	6.28/0.000145

Note: Subregional contributions to voxel clusters represented by amygdala Montreal Neurological Institute coordinates are shown in brackets. Minimum reported cluster size = 5 voxels. Results corrected for multiple comparisons at cluster-level threshold of $P_{FDR} < 0.05$ and voxel-level threshold of p uncorrected < 0.001. Abbreviations: CM = Centromedial; LB = Laterobasal; SF = Superficial; L = Left; R = Right.

with the brainstem and cerebellum bilaterally as well as cortical regions [65]. Their findings were in alignment with those of Labuschagne et al., whose results were suggestive of the CM's centralized output role or hub for behavioral responses [31]. The brainstem houses multiple structures with varied functions and previous work has shown that it is the central (Ce) rather than the medial (Me) nucleus that is the output region of the CM, acting as a pathway for modulation of autonomic responses such as cardiac and respiratory rate in periods of stress or heightened emotion [11, 67–69]. Tracer techniques in animal models have shown structural connections between the brainstem and the Ce subnucleus, outlining the neural circuitry involved in the startle response and fear conditioning [12, 67, 70]. A previous high resolution study combining data acquired at 3T and 7T also reported that, of all the subnuclei, the strongest connections to the brainstem originated from the Ce subnucleus, noting its role in fear response [24]. These authors also reported a strong predictive pattern related to sleep between the Ce subnucleus and several brainstem regions, with their results suggesting a relationship between increasing severity of sleep issues and increasing strength of FC between the Ce subnucleus and the brainstem. Taken together, these findings support the premise that the connections identified between the CM and brainstem in the present study may, in fact, be arising from the Ce subnucleus of the CM.

Investigation of brainstem FC imposes similar technical challenges as amygdala imaging; its individual subregional structures are small in size with a deep central location, thus achieving adequate SNR can be problematic [24]. In addition, data acquisition in the region of the brainstem is more susceptible to both respiratory and cardiac physiological noise, exacerbated by the flow of cerebrospinal fluid [71]. The use of the multiband acceleration technique, used in the 2D sequence, has also been shown to exacerbate motion issues in and around the brainstem [72], a potential reason for its lower sensitivity in identification of amygdala subregion-to-brainstem connections in the present study.

The ability to identify stronger amygdala subregion-to-hippocampus connections was also a notable feature of the 3D performance, with connections between both left and right CM subregions to bilateral hippocampal locations evident.

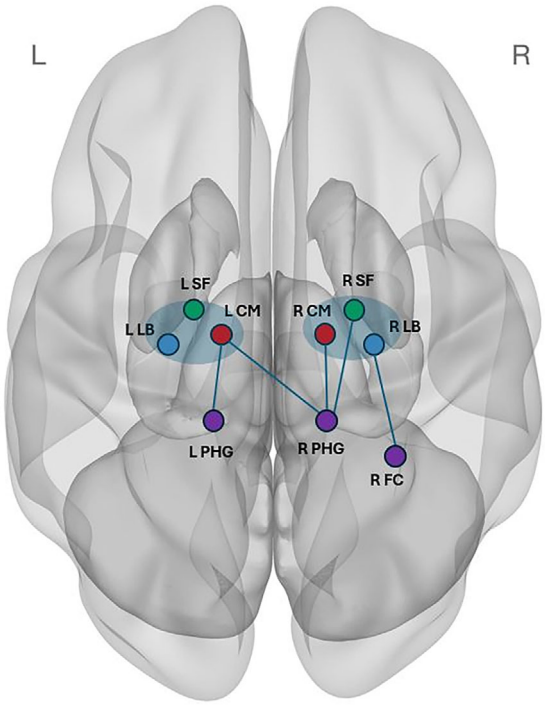

FIGURE 2 | Amygdala subregional functional connectivity in healthy controls: 2D > 3D. Subregional amygdala regions-of-interest demonstrating stronger functional connections to other brain regions (purple) in 2D sequence compared to 3D sequence. Neurological image orientation shown with left hemisphere on left and frontal lobes at the top. CM, centromedial (red); FC, fusiform cortex; L, Left; LB, laterobasal (blue); PHG, parahippocampal gyrus; R, Right; SF, superficial (green); Whole amygdala region (aqua ellipse).

As the amygdala is known to modulate emotion processing and memory retrieval, it has been suggested that emotional memories are enhanced by glucocorticoid hormonal effects via amygdala connections with the hippocampus [70, 73], and that intrinsic amygdala-hippocampal circuitry encodes fear memory [74]. In the context of prior animal work reporting input to the hippocampus from the Ba subnucleus and output from the hippocampus to the Ce, Ba, and La subnuclei [75], it is possible that our results were representative of a hippocampal connection to the Ce portion of the CM. Although there is limited high resolution work in humans reporting FC between the amygdala and hippocampus, this theory is supported by the findings of a 3T study investigating FC between resting state networks and two amygdala components, the bed nucleus of the stria terminalis and the central nucleus (Ce) [76]. These authors reported significant connectivity between the hippocampus and the Ce nucleus utilizing high resolution Human Connectome Project data with the same spatial resolution as our 3D data in a healthy control cohort.

A further noteworthy finding was the capability of the 3D sequence in identifying stronger intra-amygdala FC bilaterally relative to the 2D sequence. Both the left and right CM displayed connections to multiple clusters in the left and right amygdala, the subregional locations of which were defined using individual cluster coordinates. These findings are again in alignment with those of Berry et al. who reported connections from the Ce nucleus (part of CM) to both the SF and LB subregions, noting the key role of the LB in mediating incoming connections to the Ce nucleus which primarily functions as an output center [76, 77].

Extensive animal work has described intra-amygdala connections at a subnuclei level [11, 70, 73, 78, 79] but there is a dearth of literature relating to investigation of FC between the subnuclei or subregions in humans [80]. Whilst identification of intra-amygdala FC was not the primary purpose of this work, the results relating to multiple CM subregional connections are interesting in that context. A previous high resolution healthy control study (VV = 3.2 mm^3) performed at 4.7T investigating amygdala response and emotion processing reported connectivity between three groups of "subnuclei" [81]. They defined a CM subnuclei group (effectively the CM in the present study), a basal subnuclei group (defined as Ba, AB, and Co) and a lateral nucleus. For context, their basal subnuclei group and lateral nucleus form part of the LB subregion and Co forms part of the SF subregion in the present study. Not only were connections identified between their three subnuclei group, but differences in FC as well as sensitivity to emotional stimuli consisting of low, medium, and high emotional facial images were also reported. Interestingly, their CM group (our CM) was the most sensitive to negative emotional stimuli and displayed the highest BOLD response amplitude, potentially stemming from intrinsic behavioral and autonomic response regulation [81]. These high resolution imaging findings demonstrating multiple unilateral and bilateral intra-subregional connections from the CM subregion bilaterally, notably to the LB subregion, go some way towards supporting the theory of functional heterogeneity of the amygdala widely described in previous animal studies [73, 78].

Interestingly, the results of another 3T study investigating FC in generalized anxiety disorder compared with healthy controls were suggestive of subregional disorganization in their patient group between the BLA (LB minus the PL) and CMA (CM) based on antithetical connections from these two subregions to target regions; that is, the BLA connected to the CMA regions and vice versa [82]. Further, in support of the findings in the present study demonstrating multiple subcortical functional connections from bilateral CM subregions, Etkin et al. also reported a strong pattern of primarily subcortical CMA connectivity in both their healthy control cohorts, whilst BLA connectivity was found to be primarily cortical [82]. These results are a potential explanation for the FC differences demonstrated between our two sequences. The performances of the 2D and 3D versions was comparable, with very few differences in FC strength between cortical regions and the amygdala subregions whilst the 3D sequence performance was superior in demonstrating stronger subcortical connections with the CM subregion.

The 3D sequence in the present study also identified unilateral intra-subregional connectivity within both the left and right CM subregions, but in no other subregion. Only two studies were identified that reported intra-subregional FC findings. Etkin et al. reported significantly increased FC from the CM to both right and left CM compared to BLA in healthy controls [82] whilst Roy et al. reported significant FC in healthy controls within the right and left LB and the right and left SF but not the CM [83]. Animal work has demonstrated dense structural connections

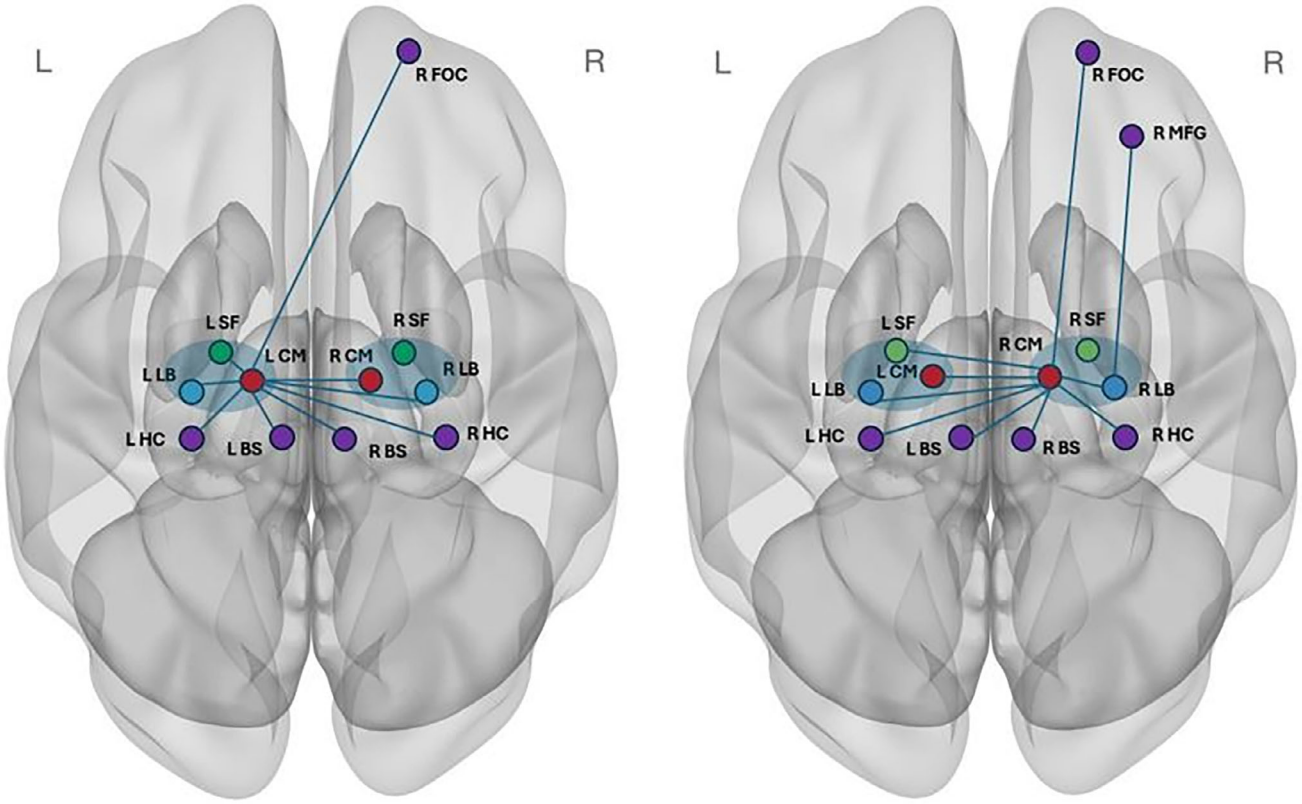

FIGURE 3 | Amygdala subregional functional connectivity in healthy controls: 3D > 2D. Left-sided (at left) and right-sided (at right) subregional amygdala regions-of-interest demonstrating stronger functional connections to other brain regions (purple) in 3D sequence compared to 2D sequence. Neurological image orientation shown with left hemisphere on left and frontal lobes at the top. BS, brainstem; CM, centromedial (red); FOC, fronto-orbital cortex; HC, hippocampus; L, Left; LB, laterobasal (blue); MFG, middle frontal gyrus; R, right; SF, superficial (green); whole amygdala region (aqua ellipse).

between Me and Ce subnuclei [84], as well as input and output connections between the Ce, Me, Ba, and La [75]. Further work using more fine-grained ROIs is needed to explore the potential of the sequence to identify individual subnuclei signals.

Lastly, an important finding was that results differed when using a whole amygdala analysis approach compared to the subregional approach, potentially a reflection of reduced sensitivity to individual subregional signals when using the whole amygdala for analysis. This finding has implications for future work interrogating the heterogeneous amygdala, supporting the notion that a more granular analysis methodology is required for increased accuracy.

Both versions of the GRE-EPI sequence used in this study are considered high resolution with VVs of 20 mm^3 or less [17]. Robinson et al. showed that a slice thickness of 2 mm to 2.5 mm is optimal for fMRI studies of the amygdala. Beyond this, there is an inverse relationship between slice thickness and SNR, driven primarily by intravoxel dephasing [21]. Consequently, for this study the slice thickness of the 2D sequence was selected at 2.5 mm whilst for the novel 3D version, the effective slice thickness was 2 mm. Both sequences were optimized to benefit from the use of isotropic voxels which have been shown to increase signal sampling accuracy [85, 86]. As the VV of the 2D sequence was almost twice that of the 3D version, SNR and tSNR levels of the 2D sequence are theoretically higher with all other parameters being equal [87]. However, the k-space data acquisition strategies of the two sequences differed markedly [49]. Aside from its high temporal resolution capabilities, the 3D volume excitation technique with 3D Fourier encoding typically results in relatively large tSNR gains over the 2D slice-by-slice acquisition method [88]. Previous work has shown that a similar 3D sequence to that used in this study outperformed its 2D counterpart in terms of tSNR, most notably in the center of the brain where tSNR values were twice as high in the 3D sequence [49]. With identical VV employed in both sequences, the authors attributed this finding to several technical facets; variations in T1 tissue contrast generated by the different acquisition strategies and preferential benefits of physiological noise correction for the 3D acquisition [49]. However, they also reported lower g-factor (noise amplification factor) values in the 3D acquisition due to lower acceleration requirements, noting that g-factor noise enhancement typically detracts from SNR centrally [49]. As the 2D sequence in the present study was more highly accelerated, it is likely that SNR in the 3D version benefited from a lower g-factor. Additional reductions in g-factor over conventional sampling patterns are achieved with the parallel imaging method known as Controlled Aliasing in Parallel Imaging Results in Higher Acceleration (CAIPIRINHA), a blipped and segmented k-space sampling pattern similar to that used in the 3D version [89].

Our results in demonstrating preferential subcortical connectivity are suggestive of a central tSNR advantage for the 3D version, despite its smaller VV, likely driven by its novel k-space sampling strategy. Aside from VV disparity between our sequences, there were several other aspects precluding a direct SNR comparison. The total volume TR of the 3D sequence was longer than that of its 2D counterpart and, in order to obtain the same total acquisition time of just over 8 min, fewer volumes were acquired. Variability in both these parameters is known to affect SNR levels [14]. However, using ImageJ version 1.52c and Microsoft Excel 2007 software, rudimentary SNR calculations across the imaging time series in the region of the amygdala showed a tSNR advantage of more than 250% for the 3D sequence over its 2D counterpart. Similarly for the 3D sequence, the Mean Pixel Value, a measure of the average signal in a voxel across the time series, averaged 90% of the 2D value despite the 3D voxels being approximately only half the volume. In the absence of a direct methodological comparison, these calculations support further investigation into the potential benefits of the 3D sequence for functional interrogation of central brain regions such as the amygdala in a larger cohort.

There are multiple limitations to be overcome in future studies of this nature. First, the sample size is very small and, despite being in keeping with cohort sizes in other similar studies [90], the work would benefit from being replicated in a much larger group. Although both sequences were high resolution, their spatial resolution values and acquisition strategies differed significantly, thus the results are not directly comparable. However, as the literature is suggestive of superior central SNR in similar 3D sequences, this study provided an opportunity to test the capabilities of the novel 3D version optimized for translation into a clinical research setting. From an analysis perspective, the use of standardized ROIs together with localization of subregions within clusters defined by MNI coordinates could lead to inaccuracies in the intra-amygdala FC findings. In addition, several data preprocessing steps were removed from the pipeline in line with current literature related to optimizing native high resolution data, and this may have had a disproportionate effect due to differences in VV between the two sequences. As study repeatability and reproducibility come under increased scrutiny, steps such as standardization of data processing [91] and use of validated analysis tools such as the JuBrain Anatomy Toolbox to reduce results variability have been recommended [63].

Although the current analysis approach included widely-used denoising procedures such as aCompCor [92] and temporal band-pass filtering [93], another limitation was the inability to capture individual physiological data for motion correction in the 3D sequence. Spatially correlated physiological noise may present as correlated signal fluctuations and an individualized approach is reportedly beneficial [94]; however, there are other considerations. Alterations in neuronal activity are known to be correlated with cardiac and respiratory signals and heart rate and breathing variability are associated with emotional arousal. This means that for studies interrogating the amygdala, with its role in emotion regulation, regression of these signals may result in removal of signals of interest [95].

Lastly, given that there is such wide variation in nomenclature relating to the amygdala subnuclei and subregions, it is a hazardous pastime attempting to compare findings across published studies. The requirement for some form of standardization will be key to advancements in this area now that systems have evolved to produce images with sufficient spatial resolution to interrogate the amygdala and its components at 3T, the field strength most widely used for clinical research.

Whilst the high resolution gold standard 2D GRE-EPI sequence performed well in investigation of amygdala subregional FC to cortical regions, it was outperformed by the novel 3D version in identifying subcortical FC. The SNR advantages of the 3D acquisition strategy make it an attractive option for researchers, given that current 2D sequences are reliant on achieving relatively high levels of acceleration that require MR scanners with powerful gradient systems and sophisticated multi-array receiver coils. In contrast, the novel 3D sequence may have more translational value, being less dependent on acceleration techniques requiring more powerful scanner and coil performance. Notwithstanding the issues of increased sensitivity to physiological motion [49], the argument to employ a high resolution 3D acquisition strategy for interrogation of intra-amygdala FC is compelling, particularly in view of the limited peer-reviewed literature available. The novel 3D sequence demonstrates great potential in identification of subcortical FC, notably intra-amygdala and brainstem FC alterations which may prove beneficial in differentiating neuropsychiatric cohorts with overlapping symptoms, thus advancing our understanding of the underlying neural mechanisms responsible for depression.

Acknowledgments

The authors would like to thank Dr. Kieran O'Brien and Dr. Jin Jin from Siemens Healthineers, ANZ, for facilitating use of the 3D EPI-GRE Works-in-Progress acquisition sequence and Dr. Jin Jin for assistance and advice regarding the specific optimizations required for this work. Additional thanks go to Dr. Elizabeth Haris for provision of Figure 1 and to Lucy Cartwright for tSNR and MPV calculations.

Funding

This work was supported by The Westmead Charitable Trust Career Development Grant to Sheryl Foster.

Conflicts of Interest

The authors declare no conflicts of interest.

References

1. J. Qiao, S. Tao, X. Wang, et al., "Brain Functional Abnormalities in the Amygdala Subregions Is Associated With Anxious Depression," *Journal of Affective Disorders* 276 (2020): 653–659.

2. S. C. Matthews, I. A. Strigo, A. N. Simmons, T. T. Yang, and M. P. Paulus, "Decreased Functional Coupling of the Amygdala and Supragenual Cingulate Is Related to Increased Depression in Unmedicated Individuals With Current Major Depressive Disorder," *Journal of Affective Disorders* 111, no. 1 (2008): 13–20.

3. R. Edelman, "The History of MR Imaging as Seen Through the Pages of Radiology," *supplement, Radiology* 273, no. 2S (2014): S181–S200.

4. W. D. S. Killgore, D. J. Casasanto, D. A. Yurgelun-Todd, J. A. Maldjian, and J. A. Detre, "Functional Activation of the Left Amygdala and

Hippocampus During Associative Encoding," *Neuroreport* 11, no. 10 (2000): 2259–2263.

5. T. Zalla, E. Koechlin, P. Pietrini, et al., "Differential Amygdala Responses to Winning and Losing: A Functional Magnetic Resonance Imaging Study in Humans," *European Journal of Neuroscience* 12, no. 5 (2000): 1764–1770.

6. P. J. Whalen, S. L. Rauch, N. L. Etcoff, S. C. McInerney, M. B. Lee, and M. A. Jenike, "Masked Presentations of Emotional Facial Expressions Modulate Amygdala Activity Without Explicit Knowledge," *Journal of Neuroscience* 18, no. 1 (1998): 411–418.

7. S. Posse, D. Fitzgerald, K. Gao, et al., "Real-Time fMRI of Temporolimbic Regions Detects Amygdala Activation During Single-Trial Self-Induced Sadness," *Neuroimage* 18, no. 3 (2003): 760–768.

8. H. C. Breiter, N. L. Etcoff, P. J. Whalen, et al., "Response and Habituation of the Human Amygdala During Visual Processing of Facial Expression," *Neuron* 17, no. 5 (1996): 875–887.

9. C. I. Wright, H. Fischer, P. J. Whalen, S. C. McInerney, L. M. Shin, and S. L. Rauch, "Differential Prefrontal Cortex and Amygdala Habituation to Repeatedly Presented Emotional Stimuli," *Neuroreport* 12, no. 2 (2001): 379–383.

10. Z. Saygin, D. Kliemann, J. Iglesias, et al., "High-Resolution Magnetic Resonance Imaging Reveals Nuclei of the Human Amygdala: Manual Segmentation to Automatic Atlas," *Neuroimage* 155 (2017): 370–382.

11. P. Sah, E. S. L. Faber, M. Lopez De Armentia, and J. Power, "The Amygdaloid Complex: Anatomy and Physiology," *Physiological Reviews* 83, no. 3 (2003): 803–834.

12. O. K. Harrison, X. Guell, M. C. Klein-Flügge, and R. L. Barry, "Structural and Resting State Functional Connectivity Beyond the Cortex," *Neuroimage* 240 (2021): 118379.

13. S. L. Foster, I. A. Breukelaar, K. Ekanayake, S. Lewis, and M. S. Korgaonkar, "Functional Magnetic Resonance Imaging of the Amygdala and Subregions at 3 Tesla: A Scoping Review," *Journal of Magnetic Resonance Imaging* 59, no. 2 (2024): 361–375.

14. P. Bandettini, "The Spatial, Temporal and Interpretive Limits of Functional MRI," in *Neuropsychopharmacology: The Fifth Generation of Progress* (Lippincott Williams & Wilkins, 2002), 343–356.

15. D. W. McRobbie, E. A. Moore, M. J. Graves, and M. R. Prince, *MRI From Picture to Proton*. 3rd ed. (Cambridge University Press, 2017).

16. B. Poser, P. Koopmans, T. Witzel, L. Wald, and M. Barth, "Three Dimensional Echo-Planar Imaging at 7 Tesla," *Neuroimage* 51, no. 1 (2010): 261–266.

17. C. Olman and E. Yacoub, "High-Field FMRI for Human Applications: An Overview of Spatial Resolution and Signal Specificity," *Open Neuroimaging Journal* 5 (2011): 74–89.

18. R. Sladky, P. Baldinger, G. S. Kranz, et al., "High-Resolution Functional MRI of the Human Amygdala at 7 T," *European Journal of Radiology* 82, no. 5 (2013): 728–733.

19. C. Olman, L. Davachi, and S. Inati, "Distortion and Signal Loss in Medial Temporal Lobe," *PLoS ONE* 4, no. 12 (2009): e8160.

20. X. Yang, M. J. Holmes, A. T. Newton, V. L. Morgan, and B. A. Landman, "A Comparison of Distributional Considerations With Statistical Analysis of Resting State fMRI at 3T and 7T," in *Medical Imaging 2012: Image Processing* (SPIE, 2012).

21. S. Robinson, C. Windischberger, A. Rauscher, and E. Moser, "Optimized 3 T EPI of the Amygdalae," *Neuroimage* 22, no. 1 (2004): 203–210.

22. S. Brown, J. W. Rutland, G. Verma, et al., "Ultra-High-Resolution Imaging of Amygdala Subnuclei Structural Connectivity in Major Depressive Disorder," *Biological Psychiatry: Cognitive Neuroscience and Neuroimaging* 5, no. 2 (2020): 184–193.

23. U. K. A. Elvira, S. Seoane, J. Janssen, and N. Janssen, "Contributions of Human Amygdala Nuclei to Resting-State Networks," *PLoS ONE* 17, no. 12 (2022): e0278962.

24. M. C. Klein-Flügge, D. E. A. Jensen, Y. Takagi, et al., "Relationship Between Nuclei-Specific Amygdala Connectivity and Mental Health Dimensions in Humans," *Nature Human Behaviour* 6, no. 12 (2022): 1705–1722.

25. E. M. Haris, R. A. Bryant, T. Williamson, and M. S. Korgaonkar, "Functional Connectivity of Amygdala Subnuclei in PTSD: A Narrative Review," *Molecular Psychiatry* 28, no. 9 (2023): 3581–3594.

26. A. A. Huggins, C. N. Weis, E. A. Parisi, K. P. Bennett, V. Miskovic, and C. L. Larson, "Neural Substrates of Human Fear Generalization: A 7T-fMRI Investigation," *Neuroimage* 239 (2021): 118308.

27. R. Pohmann, O. Speck, and K. Scheffler, "Signal-to-Noise Ratio and MR Tissue Parameters in Human Brain Imaging at 3, 7, and 9.4 Tesla Using Current Receive Coil Arrays," *Magnetic Resonance in Medicine* 75, no. 2 (2016): 801–809.

28. National Imaging Facility, "Instruments and Infrastructure," 2024, https://anif.org.au/what-we-do/our-capabilities/capabilities/.

29. X. Chen, L. Qu, Y. Xie, S. Ahmad, and P. Yap, "A Paired Dataset of T1- and T2-Weighted MRI at 3 Tesla and 7 Tesla," *Scientific Data* 10, no. 1 (2023): 489.

30. S. Bollmann and M. Barth, "New Acquisition Techniques and Their Prospects for the Achievable Resolution of fMRI," *Progress in Neurobiology* 207 (2021): 101936.

31. I. Labuschagne, J. F. Dominguez, S. Grace, et al., "Specialization of Amygdala Subregions in Emotion Processing," *Human Brain Mapping* 45, no. 5 (2024): e26673.

32. S. Zhang, J. Cui, Z. Zhang, et al., "Functional Connectivity of Amygdala Subregions Predicts Vulnerability to Depression Following the COVID-19 Pandemic," *Journal of Affective Disorders* 297 (2022): 421–429.

33. S. L. Foster, R. Landin-Romero, S. Lewis, et al., "Amygdala Subregional Functional Connectivity in Treatment-Resistant Depression," *Journal of Affective Disorders Reports* 21 (2025): 100932.

34. A. Domke, M. Hempel, C. Hartling, et al., "Functional Connectivity Changes Between Amygdala and Prefrontal Cortex After ECT Are Associated With Improvement in Distinct Depressive Symptoms," *European Archives of Psychiatry and Clinical Neuroscience* 273, no. 7 (2023): 1489–1499.

35. D. Stoliker, L. Novelli, F. X. Vollenweider, G. F. Egan, K. H. Preller, and A. Razi, "Neural Mechanisms of Resting-State Networks and the Amygdala Underlying the Cognitive and Emotional Effects of Psilocybin," *Biological Psychiatry* 96, no. 1 (2024): 57–66.

36. S. Yuan, X. Luo, X. Chen, et al., "Functional Connectivity Differences in the Amygdala Are Related to the Antidepressant Efficacy of Ketamine in Patients With Anxious Depression," *Journal of Affective Disorders* 320 (2023): 29–36.

37. T. Yang, B. Shen, A. Wu, et al., "Abnormal Functional Connectivity of the Amygdala in Mild Cognitive Impairment Patients With Depression Symptoms Revealed by Resting-State fMRI," *Frontiers in Psychiatry* 12 (2021): 533428.

38. C. Wackerhagen, I. M. Veer, S. Erk, et al., "Amygdala Functional Connectivity in Major Depression—Disentangling Markers of Pathology, Risk and Resilience," *Psychological Medicine* 50, no. 16 (2020): 2740–2750.

39. L. J. Mertens, M. B. Wall, L. Roseman, L. Demetriou, D. J. Nutt, and R. L. Carhart-Harris, "Therapeutic Mechanisms of Psilocybin: Changes in Amygdala and Prefrontal Functional Connectivity During Emotional Processing After Psilocybin for Treatment-Resistant Depression," *Journal of Psychopharmacology* 34, no. 2 (2020): 167–180.

40. J. P. Hamilton, A. Etkin, D. J. Furman, M. G. Lemus, R. F. Johnson, and I. H. Gotlib, "Functional Neuroimaging of Major Depressive Disorder: A Meta-Analysis and New Integration of Base Line Activation and Neural Response Data," *American Journal of Psychiatry* 169, no. 7 (2012): 693–703.

41. J. L. Robinson, A. R. Laird, D. C. Glahn, W. R. Lovallo, and P. T. Fox, "Metaanalytic Connectivity Modeling: Delineating the Functional

Connectivity of the Human Amygdala," *Human Brain Mapping* 31, no. 2 (2010): 173–184.

42. C. Hartling, S. Metz, C. Pehrs, et al., "Comparison of Four fMRI Paradigms Probing Emotion Processing," *Brain Sciences* 11, no. 5 (2021): 525.

43. B. Biswal, F. Zerrin Yetkin, V. M. Haughton, and J. S. Hyde, "Functional Connectivity in the Motor Cortex of Resting Human Brain Using Echo-Planar MRI," *Magnetic Resonance in Medicine* 34, no. 4 (1995): 537–541.

44. A. Snyder and M. Raichle, "A Brief History of the Resting State: The Washington University Perspective," *Neuroimage* 62, no. 2 (2012): 902–910.

45. K. J. Gorgolewski, N. Mendes, D. Wilfling, et al., "A High Resolution 7-Tesla Resting-State fMRI Test-Retest Dataset With Cognitive and Physiological Measures," *Scientific Data* 2, no. 1 (2015): 140054.

46. S. Foster, et al., "Functional Magnetic Resonance Imaging of the Amygdala and Subregions at 3 Tesla: A Scoping Review," *Journal of Magnetic Resonance Imaging* 59 (2023): 361–375.

47. G. Glover, "Overview of Functional Magnetic Resonance Imaging," *Neurosurgery Clinics of North America* 22, no. 2 (2011): 133–139.

48. D. G. Norris, "Pulse Sequences for fMRI," in *fMRI: From Nuclear Spins to Brain Functions*, ed. K. Uludag, K. Ugurbil, and L. Berliner (Springer, 2015), 131–162.

49. R. Stirnberg, W. Huijbers, D. Brenner, B. A. Poser, M. Breteler, and T. Stöcker, "Rapid Whole-Brain Resting-State fMRI at 3 T: Efficiency-Optimized Three-Dimensional EPI Versus Repetition Time-Matched Simultaneous-Multi-Slice EPI," *Neuroimage* 163 (2017): 81–92.

50. R. Tijssen, T. Okell, and K. Miller, "Real-Time Cardiac Synchronization With Fixed Volume Frame Rate for Reducing Physiological Instabilities in 3D FMRI," *Neuroimage* 57, no. 4 (2011): 1364–1375.

51. A. Lutti, D. L. Thomas, C. Hutton, and N. Weiskopf, "High-Resolution Functional MRI at 3 T: 3D/2D Echo-Planar Imaging With Optimized Physiological Noise Correction," *Magnetic Resonance in Medicine* 69, no. 6 (2013): 1657–1664.

52. B. Gruber, M. Froeling, T. Leiner, and D. W. Klomp, "RF Coils: A Practical Guide for Nonphysicists," *Journal of Magnetic Resonance Imaging* 48, no. 3 (2018): 590–604.

53. C. Juchem and R. de Graaf, "B(0) Magnetic Field Homogeneity and Shimming for In Vivo Magnetic Resonance Spectroscopy," *Analytical Biochemistry* 529 (2017): 17–29.

54. K. Amunts, O. Kedo, M. Kindler, et al., "Cytoarchitectonic Mapping of the Human Amygdala Hippocampal Region and Entorhinal Cortex: Intersubject Variability and Probability Maps," *Anatomy and Embryology* 210 no. 5 (2005): 343–352.

55. S. B. Eickhoff, K. E. Stephan, H. Mohlberg, et al., "A New Spm Toolbox for Combining Probabilistic Cytoarchitectonic Maps and Functional Imaging Data," *NeuroImage* 25 no. 4 (2005): 1325–1335.

56. A. Nieto-Castanon, "FMRI Minimal Preprocessing Pipeline, in Handbook of Functional Connectivity Magnetic Resonance Imaging Methods in CONN," Hilbert Press (2020a): 3–16.

57. C. W. Wu, C. Chen, P. Liu, Y. Chao, B. B. Biswal, and C. Lin, "Empirical Evaluations of Slice-Timing, Smoothing, and Normalization Effects in Seed-Based, Resting-State Functional Magnetic Resonance Imaging Analyses," *Brain Connectivity* 1, no. 5 (2011): 401–410.

58. M. F. Glasser, S. N. Sotiropoulos, J. A. Wilson, et al., "The Minimal Preprocessing Pipelines for the Human Connectome Project," *Neuroimage* 80 (2013): 105–124.

59. T. Alakörkkö, H. Saarimäki, E. Glerean, J. Saramäki, and O. Korhonen, "Effects of Spatial Smoothing on Functional Brain Networks," *European Journal of Neuroscience* 46, no. 9 (2017): 2471–2480.

60. M. Lindquist, "The Statistical Analysis of fMRI Data," *Statistical Science* 23, no. 4 (2008): 439–464.

61. A. Nieto-Castanon, "FMRI Denoising Pipeline, in Handbook of Functional Connectivity Magnetic Resonance Imaging Methods in CONN," Hilbert Press (2020b): 17–25.

62. J. Chumbley, K. Worsley, G. Flandin, and K. Friston, "Topological FDR for Neuroimaging," *Neuroimage* 49 no. 4 (2010): 3057–3064.

63. S. B. Eickhoff, K. E. Stephan, H. Mohlberg, et al., "A New SPM Toolbox for Combining Probabilistic Cytoarchitectonic Maps and Functional Imaging Data," *Neuroimage* 25, no. 4 (2005): 1325–1335.

64. A. M. Ward, A. P. Schultz, W. Huijbers, K. R. Van Dijk, T. Hedden, and R. A. Sperling, "The Parahippocampal Gyrus Links the Default-Mode Cortical Network With the Medial Temporal Lobe Memory System," *Human Brain Mapping* 35, no. 3 (2014): 1061–1073.

65. A. K. Roy, Z. Shehzad, D. S. Margulies, et al., "Functional Connectivity of the Human Amygdala Using Resting State fMRI," *Neuroimage* 45, no. 2 (2009): 614–626.

66. J. D. Herrington, J. M. Taylor, D. W. Grupe, K. M. Curby, and R. T. Schultz, "Bidirectional Communication Between Amygdala and Fusiform Gyrus During Facial Recognition," *Neuroimage* 56, no. 4 (2011): 2348–2355.

67. J. Price, "Comparative Aspects of Amygdala Connectivity," *Annals of the New York Academy of Sciences* 985, no. 1 (2003): 50–58.

68. B. S. Kapp, M. Gallagher, M. D. Underwood, C. L. McNall, and D. Whitehorn, "Cardiovascular Responses Elicited by Electrical Stimulation of the Amygdala Central Nucleus in the Rabbit," *Brain Research* 234, no. 2 (1982): 251–262.

69. M. Sawada, R. Adolphs, B. J. Dlouhy, et al., "Mapping Effective Connectivity of Human Amygdala Subdivisions With Intracranial Stimulation," *Nature Communications* 13, no. 1 (2022): 4909.

70. F. Olucha-Bordonau, L. Fortes-Marco, M. Otero-García, E. Lanuza, and F. Martínez-García, "Amygdala: Structure and Function," *Rat Nervous System*. 4th ed. (Academic Press, 2015), 441–490.

71. A. Mohamed, R. Kwiatek, P. Del Fante, V. D. Calhoun, J. Lagopoulos, and Z. Y. Shan, "Functional MRI of the Brainstem for Assessing Its Autonomic Functions: From Imaging Parameters and Analysis to Functional Atlas," *Journal of Magnetic Resonance Imaging* 60, no. 5 (2024): 1880–1891.

72. A. T. Vu, K. Jamison, M. F. Glasser, et al., "Tradeoffs in Pushing the Spatial Resolution of fMRI for the 7T Human Connectome Project," *Neuroimage* 154 (2017): 23–32.

73. J. LeDoux, "The Amygdala," *Current Biology* 17, no. 20 (2007): R868–R874.

74. W. Kim and J. Cho, "Encoding of Contextual Fear Memory in Hippocampal–Amygdala Circuit," *Nature Communications* 11, no. 1 (2020): 1382.

75. W. Zhang, J. Zhang, A. Holmes, and B. Pan, "Amygdala Circuit Substrates for Stress Adaptation and Adversity," *Biological Psychiatry* 89, no. 9 (2021): 847–856.

76. S. C. Berry, R. G. Wise, A. D. Lawrence, and T. M. Lancaster, "Extended-Amygdala Intrinsic Functional Connectivity Networks: A Population Study," *Human Brain Mapping* 42, no. 6 (2021): 1594–1616.

77. P. Janak and K. Tye, "From Circuits to Behaviour in the Amygdala," *Nature* 517, no. 7534 (2015): 284–292.

78. A. Pitkänen, V. Savander, and J. LeDoux, "Organization of Intra-Amygdaloid Circuitries in the Rat: An Emerging Framework for Understanding Functions of the Amygdala," *Trends in Neurosciences* 20, no. 11 (1997): 517–523.

79. A. McDonald, "Cortical Pathways to the Mammalian Amygdala," *Progress in Neurobiology* 55, no. 3 (1998): 257–332.

80. C. Kirstein, O. Güntürkün, and S. Ocklenburg, "Ultra-High Field Imaging of the Amygdala—A Narrative Review," *Neuroscience & Biobehavioral Reviews* 152 (2023): 105245.

81. S. Hrybouski, A. Aghamohammadi-Sereshki, C. R. Madan, et al., "Amygdala Subnuclei Response and Connectivity During Emotional Processing," *Neuroimage* 133 (2016): 98–110.

82. A. Etkin, K. E. Prater, A. F. Schatzberg, V. Menon, and M. D. Greicius, "Disrupted Amygdalar Subregion Functional Connectivity and Evidence of a Compensatory Network in Generalized Anxiety Disorder," *Archives of General Psychiatry* 66, no. 12 (2009): 1361–1372.

83. A. K. Roy, J. L. Fudge, C. Kelly, et al., "Intrinsic Functional Connectivity of Amygdala-Based Networks in Adolescent Generalized Anxiety Disorder," *Journal of the American Academy of Child & Adolescent Psychiatry* 52, no. 3 (2013): 290–299.

84. N. Canteras, R. Simerly, and L. Swanson, "Organization of Projections From the Medial Nucleus of the Amygdala: A PHAL Study in the Rat," *Journal of Comparative Neurology* 360, no. 2 (1995): 213–245.

85. M. J. Mulder, M. C. Keuken, P. Bazin, A. Alkemade, and B. U. Forstmann, "Size and Shape Matter: The Impact of Voxel Geometry on the Identification of Small Nuclei," *PLoS ONE* 14, no. 4 (2019): e0215382.

86. S. M. Smith, C. F. Beckmann, J. Andersson, et al., "Resting-State fMRI in the Human Connectome Project," *Neuroimage* 80 (2013): 144–168.

87. C. Triantafyllou, R. Hoge, G. Krueger, et al., "Comparison of Physiological Noise at 1.5 T, 3 T and 7 T and Optimization of fMRI Acquisition Parameters," *Neuroimage* 26, no. 1 (2005): 243–250.

88. N. N. Graedel, J. A. McNab, M. Chiew, and K. L. Miller, "Motion Correction for Functional MRI With Three-Dimensional Hybrid Radial-Cartesian EPI," *Magnetic Resonance in Medicine* 78, no. 2 (2017): 527–540.

89. K. Setsompop, B. A. Gagoski, J. R. Polimeni, T. Witzel, V. J. Wedeen, and L. L. Wald, "Blipped-Controlled Aliasing in Parallel Imaging for Simultaneous Multislice Echo Planar Imaging With Reduced G-Factor Penalty," *Magnetic Resonance in Medicine* 67, no. 5 (2012): 1210–1224.

90. D. Szucs and J. Ioannidis, "Sample Size Evolution in Neuroimaging Research: An Evaluation of Highly-Cited Studies (1990–2012) and of Latest Practices (2017–2018) in High-Impact Journals," *Neuroimage* 221 (2020): 117164.

91. L. M. Shah, J. A. Cramer, M. A. Ferguson, R. M. Birn, and J. S. Anderson, "Reliability and Reproducibility of Individual Differences in Functional Connectivity Acquired During Task and Resting State," *Brain and Behavior* 6, no. 5 (2016): e00456.

92. Y. Behzadi, K. Restom, J. Liau, and T. T. Liu, "A Component Based Noise Correction Method (CompCor) for BOLD and Perfusion Based fMRI," *Neuroimage* 37, no. 1 (2007): 90–101.

93. M. Hallquist, K. Hwang, and B. Luna, "The Nuisance of Nuisance Regression: Spectral Misspecification in a Common Approach to Resting-State fMRI Preprocessing Reintroduces Noise and Obscures Functional Connectivity," *Neuroimage* 82 (2013): 208–225.

94. O. Reynaud, J. Jorge, R. Gruetter, J. P. Marques, and W. van der Zwaag, "Influence of Physiological Noise on Accelerated 2D and 3D Resting State Functional MRI Data at 7 T," *Magnetic Resonance in Medicine* 78, no. 3 (2017): 888–896.

95. R. Birn, "The Role of Physiological Noise in Resting-State Functional Connectivity," *Neuroimage* 62, no. 2 (2012): 864–870.

Chapter 7: Overview of Findings, Discussion, and Future Work

7.1 Introduction

The overarching goal of this thesis was to investigate the potential of fMRI sequence optimisation, in the form of higher spatial resolution imaging, to improve our ability to discern functional connectivity (FC) patterns of the amygdala to other brain regions. The capability to demonstrate connectivity at a subregional level was investigated using a 3T MRI system, the most widely accessible field strength for clinical researchers.

The context for this work was that amygdala dysfunction is implicated in depression and there is broad acknowledgement that current clinical tools are suboptimal in diagnosis of this condition which is characterised by broad heterogeneity. Advancing our knowledge of the neural substrates underpinning depression is key to improving patient outcomes. The amygdala, the subject of extensive research, has been traditionally classified as a single structure; yet it is, in effect, a complex amalgamation of individual subnuclei. More than twenty years after the introduction of 3T systems for fMRI, there are well-documented inconsistencies in amygdala findings in both task-based and resting state studies in depression cohorts (Grehl et al., 2023; Kotoula et al., 2023). Where subjective clinical diagnostic measures are widely acknowledged as imprecise, objective imaging measures have shown significant potential to stratify depression subtypes, allowing for more targeted treatment regimes (Klein-Flügge et al., 2022). Central to this goal is the development of a more nuanced understanding of the role of the amygdala at a more granular level. Widely accessible 3T fMRI, with its recent advances in both hardware and software, is the technique with potential to reliably characterise amygdala FC at a subregional level, leading to advances in the field.

This thesis represents a body of work that has its genesis in the perceived limitations relating to spatial resolution of widely used protocols for fMRI studies interrogating the amygdala, as well as its treatment as a homogenous structure. This premise was subsequently supported by a formal scoping review quantifying the extent of the use of lower spatial resolution data. With the goal of advancing the field, two versions of an optimised high resolution acquisition sequences were introduced; firstly, the 2D gold standard sequence was employed to interrogate FC of the amygdala at a subregional level in depressed and healthy cohorts. Next, the capabilities of both 2D and 3D versions were scrutinised in relation to their potential to replicate, at a subregional level at 3T, amygdala subnuclei FC to resting state networks reported at 7T. Finally, as there has been little work reported in this area, the sequences were directly

compared to ascertain their abilities to identify subcortical connections to the amygdala subregions.

7.2 Overview of Thesis Findings

Chapter Three, in addressing the first aim, consisted of two sections: a formal scoping review protocol and the resultant comprehensive scoping review. The review was an integral step in surveying the current landscape in relation to 3T fMRI studies reporting amygdala findings. In documenting relevant imaging protocols in use globally, it provided an in-depth window into the technical side of research methodology and parameter selections. A primary driver for this review, aside from documenting the detail as a baseline, was to promote discussion about protocol choices and their impact on data quality and study outcomes.

The results of the scoping review were unexpected on several levels. Firstly, of 192 studies included in the review, less than 16% acquired high spatial resolution data in reporting amygdala-related findings, with only 11% reporting subregional findings. Further, of the twenty-one studies that did report subregional FC, only 19% used high resolution data, another 19% used low resolution data whilst the majority used standard resolution data. These results were interesting in the context of the SNR capabilities of 3T MRI systems in comparison to the 1.5T systems initially used for fMRI. It is possible that many of the studies reviewed were based on acquisition protocols that were initially developed for 1.5T systems; lack of collaboration with specialist imaging professionals may result in protocols not being updated by researchers in line with the evolution of technology. An alternate explanation is that researchers may be employing more general acquisition protocols developed for cortical fMRI studies without consideration of the need to tailor their protocol strategies to optimise for investigation of the deeper and smaller subcortical structures. Whatever the reasons, it appears that there have been missed opportunities to capitalise not only on the increased SNR at 3T, but the evolution of RF coil technology and acceleration techniques over the past twenty years.

Data reproducibility, particularly fMRI data, has become a hot topic in recent years for a number of reasons, with the two fundamental issues being variations in data acquisition and data analyses, leading Simmons and colleagues to coin the term ‘researcher degrees of freedom’ (Simmons et al., 2011). Increased access to 3T systems, whilst a positive development for advancement of neuroresearch generally, has enabled greater numbers of researchers to make their own acquisition protocol parameter decisions, effectively in silos. The results of this can

be seen in the broad data heterogeneity as demonstrated in this scoping review, rendering comparison of results across studies problematic. A further, well-documented issue is the abundance of highly cited yet low-powered studies (Szucs & Ioannidis, 2020). In parallel, a burgeoning interest in software development for analysis has led to methodological variations as groups have developed their own in-house methods, such as FMRIB Software Library, known as FSL, from the University of Oxford and CONN toolbox from Massachusetts Institute of Technology. The multiplicity of preprocessing and data analysis options within different software packages results in workflow variations that can impact results. An additional confounder is the lack of clarity in reporting important details such as the technique used for multiple-comparisons corrections. For those researchers with a focus on neuroimaging, highlighting these issues for discussion has been a significant step in moving towards more common ground (Poldrack et al., 2017).

In the interests of promoting protocol harmonisation, data reproducibility and improved reporting standards, two ancillary by-products were generated as part of the scoping review process in Chapter Three. In addition to documenting protocol variations across studies, the published review included a list of protocol recommendations for fMRI of the amygdala and its subregions based on best practice identified during the broad literature review. A data acquisition reporting checklist template for use by researchers was also included in the supplementary material; this was developed during the review process as it became evident that crucial elements of the data acquisition process were unreported in many publications, precluding meaningful comparisons across studies.

In summary, Chapter Three demonstrated that the majority of fMRI studies reporting amygdala findings had focused on the amygdala as a single entity using data with suboptimal spatial resolution for interrogation of subregional activation and functional connections. The review also revealed that, of the handful of studies reporting subregional findings, less than 20% used data with optimal high spatial resolution.

In addressing the second aim, the published study forming **Chapter Four** investigated FC patterns of the amygdala subregions based on high spatial resolution data. These data were acquired using the gold standard 2D GRE-EPI sequence previously optimised for resting state data acquisition in neuropsychiatric studies. This work aimed, firstly, to identify potential differences in FC of the amygdala subregions between a Treatment-Resistant Depression (TRD) cohort and healthy controls (HC) and secondly, between TRD and Treatment-Sensitive

Depression (TSD) cohorts. The results implicated the right laterobasal (LB) subregion as a differentiator of FC alterations between groups, with decreased FC in TRD relative to HC and increased FC in TRD relative to TSD. These findings are of note in the context of the composition of the LB which contains mainly excitatory neurons. LB dysfunction has been implicated in social stress and anxiety (Shen et al., 2019; Yang & Wang, 2017) and structural neuronal remodelling resulting from chronic stressors is thought to be responsible for amygdala dysfunction manifesting as emotional disturbances characteristic of depression (Liu et al., 2021; Zhang et al., 2021). Neuronal remodelling has been shown to result in volume loss and, with reports of an inverse relationship between symptom severity in depression and anxiety and right LB volume (Tesen et al., 2022), investigation of right LB volumes in the cohorts in this study may be a worthwhile undertaking in future work.

From a methodological perspective, the findings regarding the latter part of the second aim relating to FC differences between a subregional versus whole amygdala approach were surprisingly consequential. All FC data analyses were repeated, with the only difference being that the amygdala was considered as a single structure, requiring the whole amygdala to be defined as the region-of-interest (ROI) rather than utilising individual subregional ROIs. Interestingly, the significant subregional FC findings could not be replicated in either of the two group comparisons, and this was in alignment with one other study that also reported significant subregional FC variations, yet no whole amygdala FC variations (Zhang et al., 2022). These findings have wide implications for the field, particularly in the context of the results of the scoping review in Chapter Three, which showed that almost 90% of studies reported whole amygdala findings. It has been proposed that interpretation of amygdala FC patterns is open to error when the structure is considered as a single entity; positive and negative signals from individual subregions may be averaged in this scenario (Roy et al., 2009; Zhang et al., 2018). This work has demonstrated that, even in the setting of optimal high spatial resolution data acquisition, consideration of the amygdala as a single structure is likely contributing to incongruent results across studies.

In summary, the work in Chapter Four showed that, using high spatial resolution data acquired with an optimised 2D GRE-EPI sequence, FC alterations of the right LB were a distinguishing feature of TRD. As well as providing a general demonstration of the feasibility of using optimised high resolution protocols for fMRI data acquisition at 3T, this work also illustrated the value of a subregional approach to data analysis in terms of increased accuracy in

identifying individual subregional FC contributions, as these results were not replicated using a whole amygdala analysis approach.

To address the third aim, a novel higher resolution 3D sequence with an alternate k-space acquisition strategy and a voxel volume around half that of the 2D version was introduced in **Chapter Five**. In the pilot study forming this chapter. the capabilities of both sequences were assessed by investigating resting state network functional connections to the subregions in a cohort of healthy controls. Data from both versions of the sequence were qualitatively compared against FC results reported at 7T by Elvira and colleagues, who demonstrated FC patterns between eight of the nine amygdala subnuclei to three resting state networks-of-interest, including the Default Mode Network, in healthy controls (Elvira et al., 2022).

Consequently, it was notable that the optimised 2D version, in outperforming its 3D counterpart, achieved robust results by identifying ten functional connections to networks-of-interest compared with fourteen subnuclei connections in the gold standard 7T study. To highlight the strengths of these findings, when viewed from a network perspective the 2D 3T results replicated the 7T results at a subregional level in connections with the Ventral Attention and Default Mode networks and only missed one network connection for the Somatomotor network from the superficial (SF) subregion. To place these results squarely into context, they are particularly promising when considering the nature of the 7T data which was accessed from the Human Connectome Project; the spatial resolution was very high with VV of 4.1mm^3 and 32 minutes of resting state data were analysed for each participant compared with 8 minutes in each of the 2D and 3D sequences (Elvira et al., 2022). The demonstration of similar findings at a subregional level to those seen at a subnuclei level at 7T attested to the potential of this high resolution 3T approach, positioning it as a more accurate method compared to the commonly used combination of standard/low resolution data and whole amygdala analyses that had been identified in Chapter Three. However, our results were uncorrected in this small pilot study and replication in a much larger cohort, including patients, would be meaningful in view of the encouraging nature of these preliminary findings. Although the study participants were healthy individuals, the study design was based on identifying functional connections to regions with relevance in depression, such as the Default Mode Network, and thus transferable to patient cohort studies. The Default Mode Network is a key contributor to the pathophysiology of Major Depressive Disorder, with altered FC to brain regions, including the amygdala, being implicated (Chou et al., 2023; Li et al., 2013; Sambataro et al., 2014; Tozzi et

al., 2021; Young et al., 2018). Use of high resolution data acquired at 3T to successfully identify aberrant FC patterns seen at 7T is a compelling demonstration of underutilised capability, and one with potential to progress the field.

Much of the published fMRI work to date has been focused on the brain's cortical connectivity patterns with less of a focus on subcortical regions due to the difficulty in visualising the deep central locations well with traditional fMRI sequences (Harrison et al., 2021).

In addressing the fourth aim, **Chapter Six** highlights the potential of the 3D sequence, with its inherently higher SNR centrally due to an alternate k-space acquisition strategy (Afacan et al., 2012; Lutti et al., 2013; Stirnberg et al., 2017). In this study, a whole brain voxelwise analysis directly comparing data from the two sequences introduced in Chapter Five was undertaken and our hypothesis was supported by the results, which in this analysis, reached statistical significance; the novel 3D version proved superior in identifying stronger subcortical FC, demonstrated between the left and right centromedial subregions to bilateral areas in the brainstem and hippocampus. Interestingly, as was the case for the published study in Chapter Four, FC results differed when the amygdala was considered as a single structure rather than as individual subregions, adding further weight to the argument for widespread adoption of this subregional approach. A further notable finding was that of intra-amygdala connectivity, that is, connectivity between the subregions, including interhemispheric connectivity between both the left and right CM to multiple subregional clusters in the opposite hemisphere. Although these findings of intra-amygdala connectivity are in agreement with animal work (Pitkänen et al., 1997; Sah et al., 2003), the lack of published work in humans makes it challenging to ascertain whether further investigation of potentially aberrant intra-amygdala connectivity is warranted. However, the findings of two studies identified in a literature search indicate the possible significance of this avenue of imaging research. In reporting FC between all three subregions in healthy individuals, Hrybouski and colleagues found distinct subregional response patterns to negative emotional stimuli, with the highest sensitivity displayed by the centromedial subregion (Hrybouski et al., 2016). Additionally, Etkin and colleagues reported subregional disorganisation relating to the centromedial subregion and basolateral complex in a Generalised Anxiety Disorder cohort (Etkin et al., 2009). Given that the prevalence of comorbid anxiety in those diagnosed with Major Depressive Disorder is reportedly 45-67%, whilst 30-63% of patients diagnosed with anxiety have coincident symptoms of Major Depressive Disorder (Choi et al., 2020), further exploration of the functional relationships

between the amygdala subregions, in concert with their respective subcortical and cortical relationships, may further elucidate the neural underpinnings of both debilitating conditions.

7.3 General Discussion

Despite fMRI research investigations spanning almost three decades, the holy grail of biomarker identification at an individual level in mental health has not yet been attained. It is now accepted practice to classify physical disorders presenting with similar symptoms into cohorts for specialised treatment based on differences in laboratory and imaging findings (Insel et al., 2010). Yet in mental health disorders, including Major Depressive Disorder, diagnosis remains symptom-based despite widespread recognition that many symptoms are shared across conditions, and cohort heterogeneity is common within conditions (Malhi et al., 2021). Acknowledgement of the potential benefits of classification and stratification using a neuroscientific approach was the basis of the Research Domain Criteria (RDoC) project funded by the US National Institute of Mental Health. This project had its genesis in the perceived need for improved classification methods facilitated by the generation of '...a framework for research on pathophysiology, especially for genomics and neuroscience'. In defining mental health conditions as brain circuitry disorders, RDoC classification relies on objective tools such as functional neuroimaging and electrophysiology as well as genetic biomarkers (Insel et al., 2010).

Clearly there is desire to progress the field, so what is holding us back? In broad terms, the primary confounding issue spanning multiple aspects of this body of work based on imaging in depression appears to be 'heterogeneity'. As expected, heterogeneity was prevalent in relation to spatial resolution of fMRI data used to interrogate the amygdala, as presented in Chapter Three, with the issue being a primary driver for this work to be undertaken. Heterogeneity was also notable in study cohorts such as those reported in Chapter Four, and this challenge was noted in other studies reviewed during the course of this thesis work (Grehl et al., 2023; Kotoula et al., 2023; Yuan et al., 2023). Resting state analysis methods were also found to be quite variable (Azeez & Biswal, 2017) and a further, unanticipated source of heterogeneity was revealed in the nomenclature used to describe the amygdala and its components. Although the main theme of this thesis work relates to data quality of imaging in depression cohorts and has been addressed in depth, a brief review of the other confounding issues is justified

7.3.1 Cohort heterogeneity

Widely acknowledged as a potential confounder for individual patient treatment as well as a limitation to research study outcomes, MDD cohort heterogeneity is facing renewed attention. There are over 200 differing combinations of symptoms that meet the DSM criteria for MDD, and over 70% of patients are diagnosed with a comorbid condition (Buch & Liston, 2021; *Diagnostic and Statistical Manual of Mental Disorders*, 2022). In view of this, considerable effort has been invested in neuroimaging and genome studies to advance our knowledge of the neurobiological reasons for such heterogeneity amongst patient groups (Buch & Liston, 2021). A recent overarching meta-analysis showed that thousands of fMRI studies investigating depression have reported, among other findings, both hypoconnectivity and hyperconnectivity to a variety of brain regions including the amygdala in depressed cohorts compared with healthy controls (Wang et al., 2024). A noteworthy and very relevant finding of this review was that the most cited work since 2018 was that of Drysdale and colleagues who aimed to stratify a large depression cohort (Drysdale et al., 2017) by investigating potential FC biomarkers of neurophysiological subtypes, underscoring the level of interest in this avenue of imaging research (Wang et al., 2024). In fact, our group's previous work in MDD has pointed to intra-cohort stratification between treatment responders and non-responders which is suggestive of the theory that Treatment-Resistant Depression represents a distinct neurobiological subtype of depression (Barreiros et al., 2024; Rai et al., 2022). Also supportive of this hypothesis regarding cohort heterogeneity are the study findings outlined in Chapter Four that showed altered FC of the right LB subregion as a differentiator between treatment-resistant and treatment-sensitive depression cohorts (Foster et al., 2025).

As depression is a heritable condition, genome studies have been meta-analysed for increased power to investigate the neural basis of heterogeneity, resulting in identification of genetic risk variants exhibiting alterations in excitatory neurotransmitter function (Howard et al., 2019; Ripke et al., 2013; Wray et al., 2018). The laterobasal (LB) subregion, with its role being central to fear and anxiety regulation, has been implicated due to its composition of primarily excitatory glutamatergic neurons. The remaining proportion (around 20%) are Gamma-aminobutyric acid (GABA) inhibitory interneurons that act to modulate the excitatory neurons (Prager et al., 2016; Sah et al., 2003). Previous work points to an association between hyperexcitability of the LB and anxiety and depression via a mechanism of altered balance of inhibitory GABAergic to excitatory glutamatergic neurons (Fu & Tasker, 2024; Munshi et al.,

2023), an intriguing finding in the context of the results described in Chapter Four regarding FC of the right LB subregion differentiating between TRD and TSD cohorts. Our study did not focus on anxiety but, given its high comorbidity with depression (Choi et al., 2020), it is feasible that a proportion of both depression cohorts was affected. Although purely speculative, it is possible that the LB hyperconnectivity seen in the treatment-resistant cohort was driven by an imbalance between excitatory and inhibitory neurons, manifesting as hyperexcitability of the LB subregion.

All these considerations point to the fact that, to achieve better patient outcomes, we need more objective measures to diagnose depression patients within their broader heterogenous cohorts. The work in this thesis showed that FC alterations of the amygdala at a subregional level can distinguish between two different cohorts, those who are resistant to medication and those who respond. These findings highlight the fact that improved imaging data quality and updated analysis methods may augment our understanding of clinical heterogeneity in the context of depression and other neuropsychiatric conditions. The ability to utilise differences in FC metrics to stratify patient cohorts into subsets would serve to tip the scale away from the current practice of subjective symptoms-based diagnoses towards objective metrics-based stratification, a move that, as noted by Klein-Flügge and colleagues in their pivotal work referenced in Chapter One, is crucial to advancing the field.

7.3.2 Analysis methods

There are two primary computational methods of analysing BOLD data derived from resting state acquisitions; data-driven and model-driven, and whilst a deeper discussion is outside the scope of this work, a shallow dive further contextualises the issue of data heterogeneity. Model-driven approaches, including the seed-based correlation method used in the experimental studies in this thesis work, require a priori knowledge and selection of regions of interest (Rajamanickam, 2020). Although this method has been widely used, there is a range of alternative methods available to researchers (Li et al., 2023). Other model-driven methods that demonstrate temporal changes include multiple regression and GLM, whilst coherence is a frequency domain method focusing on spectral signal information. Data-driven methods are more numerous and include Independent Component Analysis, Principal Component Analysis and Regional Homogeneity, all of which demonstrate temporal changes, whereas Amplitude of low-frequency fluctuation methods are calculated in the frequency domain (Azeez & Biswal, 2017). This list goes some way towards illustrating the profusion of data analysis options for

data acquired with the resting state technique; whilst there is huge potential for incorporating different strategies into our experiments in the hope of revealing more nuanced metrics, the sheer volume of choices means that direct comparisons are not always easily achieved, and this can detract from the body of findings more broadly (Botvinik-Nezer et al., 2020; Germani et al., 2025).

Drilling down further, there are multiple data preprocessing steps that need to be completed prior to analysis. What are known in general terms as minimal preprocessing pipelines are available in software packages such as SPM, FSL and AFNI and, whilst the development of these platforms has gone some way towards introducing a level of standardisation, they still offer high levels of flexibility with little consensus; in fact, Poldrack and colleagues, in underscoring the scope of this issue, noted that the number of potential workflow combinations in FSL was over 69,000 (not a typo!) (Poldrack et al., 2017). Steps are taken to correct for various data anomalies including head motion during scanning, distortion stemming from field inhomogeneity, temporal effects of data acquisition and anatomical differences between subjects. These steps are broadly referred to as realignment, susceptibility distortion correction, slice timing correction and co-registration/normalisation. Data smoothing is usually performed to reduce effects of anatomical variability and can also boost SNR, and this is a parameter that can be varied according to researcher preference and study endpoint. As an example, smoothing has been shown to impact results of different analysis methods differentially (Nieto-Castanon, 2020; Wu et al., 2011) and is potentially detrimental to spatial specificity in native high resolution data; therefore, this step was removed from the analysis pipeline for 2D and 3D sequence data described in Chapters Five and Six. The next step, denoising, accounts for outlier data, physiological noise contributions and any residual effects of subject movement which are particularly problematic for resting state data analyses as they can introduce biases into functional connectivity measures (Poldrack et al., 2011). As a consequence, denoising strategies for resting state data vary compared to task-based data, tending towards the more conservative side (Wu et al., 2011).

Further opportunities for variation in methods are encountered when performing ROI analyses based on a priori selection of particular brain regions, as was the case in this work. Of the findings to come out of this thesis work, the one with potential for the most widespread impact is the finding that different FC results are achieved when considering the amygdala as a single entity, rather than as individual subregions. Previous work has shown both positive and

negative signal alterations arising from different subregions (Amunts et al., 2005; Roy et al., 2009) and from within individual subregions (Zhang et al., 2018). A whole amygdala ROI approach may result in signal averaging whereby these more nuanced results are lost, and this proved to be the case for the studies in Chapters Four and Six in which the subregional and whole amygdala FC results differed in the same cohorts. This was in alignment with the only other study identified that reported results using both methods (Zhang et al., 2022).

The subregional analysis method used in this thesis work was chosen based on its standardised nature, that is, the ROIs were cytoarchitectonically defined maps created in standard space and freely available (Eickhoff et al., 2005). Alternatives to the ROI method include use of locational knowledge from previous literature and seed coordinate identification from group data (Sohn et al., 2015). However, of the handful of studies reporting on amygdala subregions to date, most have used this same method as this work (Li et al., 2021; Michely et al., 2020; Qiu et al., 2018; Tang et al., 2019). This approach has advantages in accuracy over the traditional spherical ROI method which cannot account for irregularly shaped seed regions such as the subregions (Eickhoff et al., 2006). However, it may be less accurate in comparison to individualised amygdala segmentation of study data that can account for spatial variation between participants (Balderston et al., 2015). Nevertheless, this approach brings its own disadvantages; although reproducible within a single setting, it has the potential to introduce variability and bias between laboratories. Given reports of individualised segmentation results closely paralleling subregional locations derived from probabilistic tractography (Bach et al., 2011) and cytoarchitectonic parcellations (Amunts et al., 2005) the argument for using standardised ROIs is robust, particularly in a field striving for reproducibility.

An interesting example of the potential for results variability based on data acquisition and analysis differences is illustrated by drilling down to the basic methodologies of the following studies; in comparing MDD and HC cohorts, one study found no significant differences in FC between the amygdala and prefrontal cortex (Liu et al., 2023), whereas two other studies reported decreased FC between the two regions in MDD versus HC (Connolly et al., 2017; Dannlowski et al., 2009). In the first study by Liu and colleagues, the data comprised larger, standard resolution voxels of $47mm^3$ which was analysed in combination with amygdala ROIs parcellated from a single-subject dataset provided by the Montreal Neurological Institute, a method acknowledged to be less accurate than those based on cytoarchitectonic probabilistic maps (Tzourio-Mazoyer et al., 2002). Data in the other two studies differed, with data in the

study by Connolly and colleagues also standard resolution but with improved resolution due to smaller voxels of 27mm^3, whilst the study by Dannlowski and colleagues used high resolution data with voxels of 10.7mm^3. Additionally, these latter two studies both used reproducible ROI tools freely available in software toolboxes (WFU Pickatlas Tool (Maldjian et al., 2003) and SPM Anatomy Toolbox (Eickhoff et al., 2005) to define the amygdala location for analysis. Whilst the disparity in results between these studies may be attributable to a number of factors including cohort heterogeneity, it is also possible that suboptimal data quality and reduced accuracy in key parts of the analysis process have contributed.

It is well recognised that addressing issues of methodological variability is critical to advancing the field. Guidelines released by the Organisation for Human Brain Mapping in 2017 were designed to draw researchers' attention to the importance of transparency and reproducibility; these guidelines included checklists for best practice for conducting and reporting MRI studies (Poldrack et al., 2017). The introduction of preprocessing 'pipelines' such as that used in CONN toolbox (Whitfield-Gabrieli & Nieto-Castanon, 2012) and fMRIPrep (Esteban et al., 2019) go some way towards delivering software options that aim to facilitate reproducibility whilst encouraging transparency in workflows; this is accomplished via a 'glass box' approach of providing visual quality control reports and standard text for methodological details that can be included in publications (Esteban et al., 2019).

7.3.3 Amygdala nomenclature

In addition to the numerous other issues around heterogeneity, this thesis work provides a springboard for conversations around the plethora of options used in relation to amygdala nomenclature, and the potential for further confusion this engenders when it comes to comparing study results. The subregional naming convention used in this thesis was that proposed by Amunts and colleagues in 2005 in their cytoarchitectonic parcellation work based on probabilistic maps. In noting the requirement for 'reliable localisation' of functional imaging data as crucial to advancing the field of neuropsychiatry, the authors foreshadowed the growing need for accuracy, standardisation and reproducibility in data analysis and reporting (Amunts et al., 2005). They also recognised that the fast-paced evolution of MRI would result in systems equipped with higher spatial resolution capabilities sufficient to interrogate the amygdala and its functionally heterogenous subnuclei at a more granular level. Hence their release of region-of-interest probabilistic maps or seed regions based on the three subregions used in this thesis work: the centromedial, laterobasal and superficial. Whilst the use of these three subregional

maps and nomenclature have become increasingly adopted (Frühholz & Grandjean, 2013; Kwon et al., 2024; Li et al., 2021), some studies have excluded the superficial subregion (Liu et al., 2021; Qin et al., 2014), others have included a fourth subregion (Labuschagne et al., 2024; Tang et al., 2019), whilst others have reported four differently-named subregions (Entis et al., 2012). In some cases, the subregions are also referred to as clusters, with the terms ventral and dorsal (Gamer et al., 2010), as well as lateral (Morris et al., 2001) in use. To add to the complexity, some authors refer to subregions as subnuclei (Engman et al., 2016; Salman et al., 2024) whilst others refer to subnuclei as subregions (Jacob et al., 2022; Kim et al., 2021; Tesen et al., 2022), and finally, in one paper identified, the two terms were used interchangeably throughout (Hu et al., 2023).

This issue has broad repercussions, not the least that disparity in nomenclature increases the level of difficulty in comparing results across studies, and it is also not just limited to the amygdala. In their overarching appraisal of fMRI studies of the amygdala, Varkevisser and colleagues reported difficulties in comparisons of other brain regions across studies, notably in relation to defining brain regions anatomically versus functionally; they provide the example of the Anterior Cingulate Cortex in one study being labelled as medial Prefrontal Cortex and Orbitofrontal Cortex in other studies (Varkevisser et al., 2024).

7.4 Future Work - the big picture

Although there are still many unanswered questions about the causes of depression, it is important to acknowledge the substantial progress that has been made since the introduction of fMRI. Comprehensive meta-analyses have already shown group level alterations in brain networks in Major Depressive Disorder cohorts, with involvement in regions including the amygdala, dorsolateral prefrontal and anterior cingulate cortices, insula, hippocampus, thalamus and cerebellum (Miola et al., 2023; Tozzi et al., 2021). Focusing on high resolution data and large-scale collaborative efforts to increase statistical power, researchers are looking towards methods such as interrogation of neural dynamics and transitions between activity states to pave the way towards a better understanding of how behaviour is regulated on an individual level through network interactions between the amygdala, ventral tegmental area and neocortical regions (Spellman & Liston, 2020). To progress this network-level understanding, work has been undertaken in animal models to co-register high resolution BOLD fMRI data with high spatiotemporal resolution dynamic network information obtained

via mesoscopic calcium imaging; however, translation to human studies is still some way off (Kalin, 2020; Lake et al., 2019).

In the meantime, work in humans is ongoing, with attempts to identify the causes of disrupted brain networks in depression and how best to manage clinical symptoms of apparent dysregulation in various brain regions, including the amygdala. Novel treatments are being developed, with fMRI studies utilised to demonstrate underlying neurobiological effects in response to these treatments (Kalin, 2020), paralleling the more fundamental scientific approach to drug development in other neurological conditions such as Multiple Sclerosis, and raising the possibility of more timely clinical trial translation (Dichter et al., 2012). A meta-analysis of ketamine studies reported modulatory effects on the amygdala and anterior cingulate cortex, demonstrating its potential to 'normalise' hyperactive function in those regions linked to emotion dysregulation in depression, resulting in significant clinical improvements (Ramezani et al., 2025). Symptom improvement in a treatment-resistant cohort following deep brain stimulation of the internal capsule has also been shown, reportedly due to normalisation of amygdala responsiveness post treatment (Runia et al., 2023). Additionally, psilocybin, a serotonergic psychedelic compound, has shown promise as an alternative therapeutic, with fMRI being utilised to monitor underlying brain alterations potentially responsible for symptom improvement. A meta-analysis showed decreased amygdala activation in line with clinical symptom improvements in two Major Depressive Disorder cohort studies as well as changes in activation and FC in the amygdala and ventral medial prefrontal cortex in ten healthy control studies (Gill et al., 2022).

Whilst these novel studies are showing promising results for improved patient outcomes from quite different treatment options, it is interesting to note some key commonalities and relate them back to this thesis work. Of the twenty-one fMRI studies included in these two meta-analyses of ketamine and psilocybin treatments, only four used high resolution data (Loureiro et al., 2020; Loureiro et al., 2021; Murrough et al., 2015; Thai et al., 2020). Additionally, the focus still seems to be very much on the amygdala as a single structure, with none of the ten studies reporting amygdala results having considered its heterogenous nature in their findings. This raises the question as to whether disparity across study findings is related not only to cohort heterogeneity which, as we have seen, is a potentially a primary contributor, but to lack of spatial specificity in analysing amygdala signals.

Whilst current studies provide an indication of which brain regions possess altered connectivity with the whole amygdala in response to treatment, future work using high resolution imaging and a subregional amygdala analysis approach in treatment cohorts is needed for more accurate localisation of treatment-elicited signal alterations. This would allow greater specificity in reporting findings leading to improved congruency of results across studies. Additionally, as different treatments have their own specific mechanisms, there is potential to learn more about the biopathology underpinning MDD by differentiating which of the subregions and component subnuclei are involved in different therapy responses (Cui et al., 2024). To that end, Yuan and colleagues, in their investigation of ketamine infusions in an anxious depression cohort, reported FC alterations of the LB subregion as a prognostic indicator of treatment response, the first report of treatment efficacy at a subregional level (Yuan et al., 2023). Additionally, investigations into the treatment effects of psilocybin in depression and post-traumatic stress disorder also point to the LB subregion as being of primary significance in the manifestation of positive treatment response to psilocybin (Kelly et al., 2024; Tollenaar, 2025). These reports are interesting in the context of the findings in Chapter Four, which singled out FC alterations of the right LB as a differentiator between treatment resistance and response in our MDD cohort.

An additional avenue for future work is greater use of correlations between amygdala subregional volumes, FC findings and symptom severity. Morphologic alterations of the amygdala in MDD have been reported widely, with variables such as family history, illness duration and pharmacotherapy acknowledged as potential confounders (Hamilton et al., 2008). Work at 7T has demonstrated a significant relationship between depression severity in MDD and altered volumes of multiple amygdala subnuclei (Brown et al., 2019). A 3T study in an MDD cohort reported decreased volumes in the right LB subregion and an inverse relationship between right LB volume and severity of depression and anxiety symptoms (Tesen et al., 2022), whilst another, also in an MDD cohort, reported reduced volumes in the anterior amygdaloid area and lateral nucleus, part of the LB, compared to HC (Kim et al., 2021).

Combining measures derived from both structural and functional imaging as standard practice could shed further light on the neurobiology underpinning depression and other mental health conditions. There are multiple studies reporting on a single metric; for example, reduced left amygdala volumes in an MDD cohort compared to HC that were normalised after six infusions of ketamine (Zhou et al., 2020), and reductions in depressive symptoms that were positively

correlated with an increase in FC between the left amygdala and left medial Superior Frontal Gyrus in response to ketamine treatment in an MDD cohort (Liu et al., 2023). To gain a deeper understanding of the potential drivers of MDD in a female cohort, Yang and colleagues used a structural and functional data combination approach to show decreased FC between the right amygdala and putamen together with reduced bilateral putamen and right amygdala volumes, with the latter metric significantly correlated with anxiety scores (Yang et al., 2017). As fMRI studies typically acquire high resolution structural T1-weighted images as part of the study protocol, the addition of volume measurements would allow correlation of amygdala subnuclei volumes derived from the T1-weighted data together with either FC measures in resting state studies or activation metrics in task-based studies.

To take this approach a step further, preliminary work has been done in HC using structural diffusion tensor data to map projections from amygdala nuclei using probabilistic tractography that can be used as an alternative form of connectivity profile (Bach et al., 2011). A high resolution version of this 'connection density' technique has been adapted at 7T in an MDD cohort to show that three of the right-sided amygdala subnuclei (lateral, basal and central) display structural hyperconnectivity whilst the left medial subnucleus demonstrates hypoconnectivity compared to HC (Brown et al., 2020). Goetschius and colleagues have shown that interrogation of white matter connectivity between the amygdala and prefrontal cortex using this tractography methodology is viable at 3T by acquiring diffusion tensor data in a large cohort of adolescents (Goetschius et al., 2019). To further investigate this relationship and how it might modulate amygdala reactivity, they also acquired task fMRI data, with their novel results indicating that higher levels of white matter connectivity between the amygdala and prefrontal cortex were associated with diminished amygdala reactivity. A similar approach could be undertaken at 3T to further improve our understanding of the mechanistic and functional roles of the heterogeneous amygdala by interrogating amygdala white matter connectivity and reactivity at a subregional level.

This combination approach has been termed multimodal in the literature; it parallels use of the term 'multiparametric' in clinical MR imaging, a term most closely associated with prostate imaging which was introduced around the same time as the Prostate Imaging-Reporting and Data System known as PI-RADS (Barentsz et al., 2012). Multimodal studies utilising two or more types of data and analysis methods are few in MDD (Cui et al., 2024), but one recent article has demonstrated the promise of this approach. Li and colleagues have outlined a 'multi-

modal contrastive learning framework for the automatic diagnosis of MDD' (Li et al., 2024). Within this framework, they synthesized structural T1-weighted data to determine grey matter volumes, resting state fMRI data for functional connectivity measures and diffusion tensor data for fractional anisotropy measures, all acquired in a single cohort. Using publicly available MDD data as a training dataset, they generated a deep learning model whose diagnostic classification strength lay in the complementarity of the individual datasets.

This is the way forward. We now have MRI systems capable of providing the quality of data required, we have established machine learning as a vital tool in our clinical imaging environments (Pinto-Coelho, 2023) and we have an urgent need to move beyond diagnosis using patient-reported clinical symptomatology. Combining metrics from data acquired using different imaging techniques in a single session for a multimodal approach is achievable and the potential for progress has been highlighted by the development of collaborative consortia such as the International Consortium for Brain Mapping as well as Enhanced Neuroimaging and Genetics through Meta-Analysis (ENIGMA), with its added focus on genomics and machine learning.

Additionally, there is accumulating evidence of changes to brain structure and function in depressed patients relating to underlying stress-induced neuroinflammation (Han & Ham, 2021; Milaneschi et al., 2021; Risbrough et al., 2022; Slavich & Irwin, 2014). With inflammatory biomarkers such as C-reactive protein (CRP) known to be increased in a subset of depression patients, studies are being undertaken to evaluate potential underlying relationships with brain connectivity. One study has shown that increased levels of CRP are predictive of decreased FC between the amygdala and ventromedial prefrontal cortex in depression, and that this decreased FC was associated with increased symptoms of anxiety (Mehta et al., 2018). Interestingly, the regulatory roles of individual subnuclei to physiological and behavioural stressors has been shown to vary, resulting in localised structural remodelling which could potentially be quantified using high resolution T1-weighted data (Zhang et al., 2021). In a condition that continues to have an unclear aetiology, the standard addition of inflammatory marker measures to a multimodal investigative imaging framework for depression could provide further information to fill in the missing links in our knowledge (Cui et al., 2024).

7.5 Future Work – next steps

Several worthwhile avenues for follow-up have presented themselves as a result of this thesis work. As a first step, it would be of interest to perform volume measurements using the T1-weighted data acquired in the treatment-resistant and treatment-sensitive cohorts from the study reported in Chapter Four and compare those to the healthy controls. As there are few reports of subregional volume metrics in depressed cohorts (Tesen et al., 2022), this would be an interesting exercise, particularly in view of the potential to compare between refractory and non-refractory groups. Recent work has shown smaller subregional volumes in an anxious depression cohort that increased in size following electroconvulsive therapy, and these increased volumes were correlated with improved anxiety scores (Ishikawa et al., 2025). Normalisation of amygdala size has also been reported in a meta-analysis of depression patients treated with pharmacotherapy (Nolan et al., 2020), with these authors also noting the lack of published studies reporting subregional volume changes and attributing this to challenges relating to visualisation and definitions of the 'substructures' (yet another addition to the nomenclature!) Additionally, diffusion tensor metrics could be added to the FC and volume metrics; DTI data is often acquired in research protocols, as it is at our site, but not often correlated with FC measures. Consideration of all three measures together would provide a true multimodal approach and the potential for more meaningful translational findings.

Further work is also required to address questions around the use of pipelines for analysis of high resolution data, especially that acquired with a 3D k-space strategy, as there is currently expert advice but no consensus on whether some preprocessing steps should be excluded or altered, as noted for the data used in Chapters Five and Six. This data could be re-processed with alternate combinations of variables and compared for differences in results. Further to this, results from different levels of spatial smoothing need further investigation. Spatial specificity may be lost when native high resolution data are smoothed (Molloy et al., 2014); however, there are other benefits to smoothing, such as increases in SNR and reduction of inter-subject variability in group-level analyses, although the latter benefit can also be a disadvantage when considering inter-subject differences (Triana et al., 2020). It is well-recognised that high spatial and temporal resolution acquisitions can reduce tSNR and BOLD sensitivity; smoothing filters that can improve BOLD sensitivity while preserving spatial accuracy of activated clusters at an individual level have been developed to combat this issue. These techniques, including AWSOM (Adaptive-weight smoothing with optimized metrics) can preserve signal

from small clusters whilst avoiding false positive results (Ceja et al., 2024), and may prove to be particularly useful in analysis of ultrahigh resolution data acquired at 7T (Feinberg et al., 2023).

A similar 2D and 3D sequence comparison to that reported in a HC cohort but extended to MDD and HC cohorts would be interesting, particularly in light of the findings in Chapter Six showing enhanced subcortical FC capabilities of the 3D sequence compared to the 2D sequence. Pilot data has already been acquired for this experiment, but due to time constraints of the thesis, these results were not available for inclusion in this work.

In terms of technical comparisons, preliminary calculations demonstrated the tSNR advantages of the 3D acquisition strategy, outlined in the technical discussion in Appendix D. Estimates of tSNR levels for both 2D and 3D sequences were generated; although the simple methodology used does not provide technically accurate metrics for data acquired using undersampling methods such as parallel imaging (Kellman & McVeigh, 2005), it enabled a simple comparison between sequences. Strikingly, the average tSNR value over the amygdala ROI in the 3D sequence was 2.6 times higher than that of the 2D sequence. Whilst the result itself was not unexpected as there are multiple reports of notably higher tSNR levels in central brain regions with 3D acquisitions (Chen et al., 2023; Lutti et al., 2013; Stirnberg et al., 2017), the magnitude of the difference was surprising. Additional comparative data in the form of Mean Pixel Values (MPV) were derived from the amygdala ROIs in both sequences, representing the amount of signal in each voxel across the time series. Interestingly, although the 3D voxels were only half the volume, the average MPV in the region of the amygdala was 90% of that in the 2D voxels. This finding was attributed to reduced levels of intravoxel dephasing that are known to result from the use of smaller voxels as discussed in Chapter Two. The particularly strong performance of the 3D sequence in both metrics is likely due to two primary reasons. Firstly, the location of the region being measured is in close proximity to air, bone and brain tissue interfaces that traditionally amplify signal losses, but this was minimised using the smaller 3D voxels. This theory is supported by measurements made in a more homogenous region of peripheral brain tissue; results show the average MPV for the 3D sequence was 67% of the value derived from the 2D sequence. Secondly, the k-space acquisition strategy of the 3D sequence minimises thermal contributions to total noise (discussed in Chapter Five) and, in combination with the relatively high levels of signal per voxel, the 3D sequence has an overall tSNR advantage. This advantage is seen across the whole field-of-view, as demonstrated by

the peripheral tSNR value; although lower relative to the values centred over the amygdala, the peripheral tSNR value of the 3D sequence was 1.9 times higher than that of the 2D acquisition. (see Appendix D for ROI locations, tSNR methods and data).

Lastly, further investigation into the utility of the 3D acquisition sequence is needed, with the addition of physiological data capture for motion regression. Exploration of the enhanced sequence capability in identifying cortical level connections and core intrinsic brain networks is required to determine its value as a potential replacement for the current gold standard 2D sequence. Its inherent SNR and high resolution advantages, coupled with its apparent subcortical imaging strengths make the 3D sequence an attractive option, particularly for those sites whose 3T systems may not have high-end gradient capabilities.

7.6 Key Findings - opportunities for changes in practice identified by this work

1) As a result of the broad literature review performed in Chapter Three, practical hardware and protocol 'best practice' recommendations were published for use by sites acquiring fMRI data for interrogation of the amygdala.

2) A downloadable reporting template for hardware and parameter selections was also made available for researchers. The purpose of this template was to ensure that all required details of the data acquisition process are reported in publications to facilitate results comparisons and allow potential for study replication. These recommendations and reporting template initiatives align with the shift towards protocol harmonisation.

3) The work in Chapter Four has demonstrated that high spatial resolution data acquired at 3T with optimised currently available 2D sequences and analysis techniques are capable of identifying amygdala functional connectivity at a subregional level in depressed cohorts. There are few publications reporting on this approach, so there is still much to be learned about the clinical manifestations of altered connectivity of the individual subregions to other brain regions, even if identified. However, accurate identification is the first step, and this approach is easily implemented and could be widely adopted by other clinical research sites.

4) The work in Chapter Five has further illustrated the untapped potential of currently available techniques. The relative efficacy of the combined 2D high resolution acquisition/subregional analysis approach at 3T in identifying resting state network connections in comparison to the subnuclei results derived from 7T data was a

convincing display of underutilised capability. This a particularly notable finding in the setting of very limited access to 7T systems, yet wide availability of 3T systems for clinical research.

5) The capabilities of the novel higher resolution 3D sequence were highlighted in Chapter Six, particularly in relation to the enhanced tSNR centrally in the location of the amygdala. The comparative MPV measures from both datasets were a very effective demonstration of the benefits of smaller voxels in combatting intravoxel dephasing, underscoring the benefits to be derived from higher spatial resolution imaging in locations such as the amygdala. The overall tSNR measures also indicated the value of its acquisition strategy in reducing thermal noise. These traits suggest it should be the preferred option for investigation of subcortical FC as well as further investigations of intra-amygdala FC.

6) The work in Chapters Four and Six have highlighted an urgent need to move beyond whole amygdala analyses towards a more sensitive subregional approach in order to ensure that nuanced findings are being captured. This simple change has the potential to positively impact congruency of results across studies investigating the amygdala.

7) In general, the overarching results of this work point to the conclusion that sequence selection and optimisation should be driven by the research question, particularly in the context of amygdala dysfunction in depression. Spatial resolution choices should reflect the different spatial scales required, depending on the brain regions under examination; for example, whether cortical networks or subcortical regions are the primary focus. Similarly, choices regarding echo time and k-space acquisition strategies should reflect the research question, as these technical selections can be optimised for particular brain regions as noted in the technical discussion in Appendix D. Lastly, the importance of knowing what type of data analyses will be undertaken cannot be understated when selecting data acquisition methods, to ensure that data is fit for purpose.

7.7 Challenges and Limitations

7.7.1 General

A primary limitation of this work was the pilot sample size for the studies referenced in Chapters Five and Six. Uncorrected findings were reported in the ROI-to-ROI analyses used in Chapter Five and this experiment requires replication in a larger cohort to ensure validity of

the reported results. Similarly, although the results of the whole brain voxelwise analysis method used in Chapter Six were significant when corrected for multiple comparisons, it would also be valuable to replicate those findings in a larger cohort which included an MDD group.

7.7.2 Technical

There were a number of technical challenges encountered during the course of this thesis work which resulted in further limitations. Firstly, additional distortion correction was not applied during data analyses. The inherent design of the GRE-EPI sequence means the images are susceptible to signal inhomogeneity as well as geometric distortion in the phase encoding direction (Glover, 2011). Signal inhomogeneity at voxel level manifests as slight variations in resonant frequency, resulting in cumulative phase errors that are propagated along the phase encoding direction, traditionally anterior-to-posterior in fMRI. During reconstruction, these errors result in incorrect localisation of voxels, or mismapping (Olman et al., 2009). Of the techniques developed to mitigate image distortion, one common method known as reverse phase encoding involves acquiring several volumes of data in the opposite phase encoding direction, from posterior-to-anterior, and applying these data during analysis to correct opposing intensity and spatial distortions at voxel level (Hong et al., 2015; Morgan et al., 2004). However, both sequences in this work were high resolution with small voxel volumes which have been shown to reduce intra-voxel signal inhomogeneity (Robinson et al., 2004). Additionally, parallel imaging, an acceleration technique utilised in both sequences, has been shown to reduce image distortion significantly (Schmidt et al., 2005). Interestingly, in their handbook of fMRI data analysis, Poldrack and colleagues have noted that the best method of distortion correction is minimisation by use of an optimised data acquisition protocol (Poldrack et al., 2011).

A second limitation relates to the potential impact of physiological noise on the FC results of the novel 3D sequence. Although data were subjected to noise and motion correction aspects of the CONN toolbox data analysis pipeline, the acquisition strategy of the 3D sequence may increase its susceptibility to cardiac and respiratory motion compared to 2D acquisitions (Poser et al., 2010). These noise contributions have been shown to be mitigated by using high resolution small voxels (Triantafyllou et al., 2005) such as those used in both sequences. The methodology in the original thesis plan was to capture pulse and respiration data using pulse oximetry and a pneumatic belt which can then be modelled in the General Linear Model as nuisance regressors using methods such as RETROICOR, an image-based retrospective

correction method (Birn, 2012; Glover et al., 2000). However, due to technical issues at the sequence compilation level, the physiological data capture component was unable to be commissioned. Interestingly, it has been noted that, for brain regions in which neuronal effects may be induced by emotional responses resulting in elevated heart and respiratory rates, removal of physiological signals may result in removal of signals of interest (Birn, 2012). In the case of the amygdala with its role in emotion processing, use of this technique may prove to be counterproductive; however, these effects should be further explored by directly comparing physiologically corrected and uncorrected datasets.

A pitfall of traditionally low fMRI sampling rates is aliasing of cardiac and respiratory signals into the low frequency range approaching that of resting state BOLD signal fluctuations (< 0.1 Hz), potentially compromising the signal of interest and resulting in inaccurate FC measures (Glover et al., 2000). Acceleration methods such as the 2D multiband technique and the novel 3D k-space acquisition strategy used in this work provide a means to overcome this challenge by enabling significantly higher achievable sampling rates, with some studies reporting sub-second TR values as low as 350 ms (Jahanian et al., 2019). However, the impact of shorter TR values on SNR levels is well-established and in studies requiring high spatial resolution such as those in this thesis, temporal resolution compromises are required (Menon & Goodyear, 2001). In this setting, a perceived limitation of this work is the TR values used; 1500ms for the 2D sequence and 2160ms for the 3D version were used, selected to balance the requirement for speed, signal, spatial resolution and coverage. However, in an investigation of the effects of different sampling rates on resting state metrics, Huotari and colleagues showed minimal differences in FC measures using a range of TR values between 0.1 and 3 seconds (Huotari et al., 2019). Interestingly, they also noted maximal cardiorespiratory aliasing at TR values between 1 and 2 seconds in central brain regions. This is a potential explanation for why the 2D sequence with a TR value of 1.5 seconds, underperformed in subcortical regions in the whole brain voxelwise analysis compared to its 3D counterpart.

Motion artifacts more generally are a further limitation. Dealing with motion in fMRI is an important consideration, and preventing/mitigating patient motion during the data acquisition process is a fundamental pillar of MRI radiographer practice. Any residual patient motion in fMRI data is addressed at the data postprocessing stage with specialised software programmes identifying outlying data for removal from datasets prior to analysis. However, some of these strategies can result in fMRI signal discontinuity when motion-affected data is removed

(Balachandrasekaran et al., 2021). Researchers have continued to seek methods to improve motion correction strategies, including alternate k-space data acquisition methods (Glover & Lee, 1995) as well as the introduction of matrix and algorithmic corrections made during data postprocessing and analysis that are particularly useful in the setting of neonatal and foetal data acquisition (Balachandrasekaran et al., 2021).

7.8 Conclusion

The introduction of fMRI is arguably the most significant and impactful addition to the field of neuropsychiatry to date. However, the primary strength of the technique, choice, is also its Achilles heel. Variability in radiofrequency coil and sequence parameter selections, together with differences in analysis methods and terminology coalesce to form the meta-analyst's nightmare, data heterogeneity. This thesis work has explored data variability and its impact on amygdala FC measures with a focus on Major Depressive Disorder. Quantifying the paucity of studies acquiring high resolution data to report subregional amygdala findings was an important first step in highlighting a problem that had been either undetected or overlooked. Use of an optimised high spatial resolution 2D sequence to identify subregional FC differences between depression cohorts and healthy controls was a convincing demonstration of the underutilised capability of currently available imaging tools. The evidence of this was further substantiated by the noteworthy performance of the 2D sequence in the comparison with 7T findings, highlighting the missed opportunities for a more nuanced examination of the diverse functional connections of the amygdala. While further research is required to evaluate the full potential of the novel 3D acquisition approach, this early work showed its promise in revealing functional connections in traditionally challenging subcortical areas.

In the context of minimal discussion in the literature, the disparity in results derived from whole amygdala versus subregional analysis approaches in two different studies in this work should serve as a cautionary tale to researchers. In a field striving to better understand the neural correlates of depression, these results are a stark reminder that the amygdala urgently warrants consideration as a heterogenous structure and brings into question the accuracy of previously reported whole amygdala FC results.

The work presented in this thesis, whilst also highlighting new and innovative technology, has a primary underlying dominant theme, that of underutilised 3T capability. Although neuropsychiatry clinicians are increasingly looking to improve patient outcomes by moving

away from subjective clinical diagnoses towards more objective imaging-based disease stratification, it is clear that the strengths of our current repertoire of imaging tools for probing brain function in depression remain relatively untapped. The case for focusing on the amygdala as a heterogeneous collection of small subregions has been established, allowing the greatest likelihood of clinical translation of findings. In demonstrating the value that technical MRI specialists can bring to translational research collaborations, this work has shown that sequence optimisation, in the form of spatial resolution enhancements, is a simple but powerful technique that has the potential to advance the field in that direction.

7.9 References

Afacan, O., Hoge, W. S., Janoos, F., Brooks, D. H., & Morocz, I. A. (2012). Rapid full-brain fMRI with an accelerated multi shot 3D EPI sequence using both UNFOLD and GRAPPA. *Magnetic Resonance in Medicine*, *67*(5), 1266-1274. https://doi.org/10.1002/mrm.23106

Amunts, K., Kedo, O., Kindler, M., Pieperhoff, P., Mohlberg, H., Shah, N. J., Habel, U., Schneider, F., & Zilles, K. (2005). Cytoarchitectonic mapping of the human amygdala, hippocampal region and entorhinal cortex: intersubject variability and probability maps. *Anatomy and Embryology*, *210*(5), 343-352. https://doi.org/10.1007/s00429-005-0025-5

Azeez, A. K., & Biswal, B. B. (2017). A Review of Resting-State Analysis Methods. *Neuroimaging Clinics of North America*, *27*(4), 581-592. https://doi.org/10.1016/j.nic.2017.06.001

Bach, D. R., Behrens, T. E., Garrido, L., Weiskopf, N., & Dolan, R. J. (2011). Deep and Superficial Amygdala Nuclei Projections Revealed In Vivo by Probabilistic Tractography. *The Journal of Neuroscience*, *31*(2), 618. https://doi.org/10.1523/JNEUROSCI.2744-10.2011

Balachandrasekaran A, Cohen AL, Afacan O, Warfield SK, Gholipour A. Reducing the Effects of Motion Artifacts in fMRI: A Structured Matrix Completion Approach. IEEE Trans Med Imaging. 2022 Jan;41(1):172-185. doi: 10.1109/TMI.2021.3107829

Balderston, N. L., Schultz, D. H., Hopkins, L., & Helmstetter, F. J. (2015). Functionally distinct amygdala subregions identified using DTI and high-resolution fMRI. *Soc Cogn Affect Neurosci*, *10*(12), 1615-1622. https://doi.org/10.1093/scan/nsv055

Barentsz, J. O., Richenberg, J., Clements, R., Choyke, P., Verma, S., Villeirs, G., Rouviere, O., Logager, V., & Fütterer, J. J. (2012). ESUR prostate MR guidelines 2012. *Eur Radiol*, *22*(4), 746-757. https://doi.org/10.1007/s00330-011-2377-y

Barreiros, A. R., Breukelaar, I. A., Prentice, A., Mayur, P., Tomimatsu, Y., Funayama, K., Foster, S., Malhi, G. S., Arns, M., Harris, A., & Korgaonkar, M. S. (2024). Intra- and Inter-Network connectivity of the default mode network differentiates Treatment-Resistant depression from Treatment-Sensitive depression. *NeuroImage: Clinical*, *43*, 103656. https://doi.org/10.1016/j.nicl.2024.103656

Birn, R. M. (2012). The role of physiological noise in resting-state functional connectivity. *Neuroimage*, *62*(2), 864-870. https://doi.org/10.1016/j.neuroimage.2012.01.016

Botvinik-Nezer, R., Holzmeister, F., Camerer, C. F., Dreber, A., Huber, J., Johannesson, M., Kirchler, M., Iwanir, R., Mumford, J. A., Adcock, R. A., Avesani, P., Baczkowski, B. M., Bajracharya, A., Bakst, L., Ball, S., Barilari, M., Bault, N., Beaton, D., Beitner, J., . . . Schonberg, T. (2020). Variability in the analysis of a single neuroimaging dataset

by many teams. *Nature*, *582*(7810), 84-88. https://doi.org/10.1038/s41586-020-2314-9

Brown, S. S. G., Rutland, J. W., Verma, G., Feldman, R. E., Alper, J., Schneider, M., Delman, B. N., Murrough, J. M., & Balchandani, P. (2019). Structural MRI at 7T reveals amygdala nuclei and hippocampal subfield volumetric association with Major Depressive Disorder symptom severity. *Scientific Reports*, *9*(1), 10166. https://doi.org/10.1038/s41598-019-46687-7

Brown, S. S. G., Rutland, J. W., Verma, G., Feldman, R. E., Schneider, M., Delman, B. N., Murrough, J. M., & Balchandani, P. (2020). Ultra-High-Resolution Imaging of Amygdala Subnuclei Structural Connectivity in Major Depressive Disorder. *Biological Psychiatry: Cognitive Neuroscience and Neuroimaging*, *5*(2), 184-193. https://doi.org/10.1016/j.bpsc.2019.07.010

Buch, A. M., & Liston, C. (2021). Dissecting diagnostic heterogeneity in depression by integrating neuroimaging and genetics. *Neuropsychopharmacology*, *46*(1), 156-175. https://doi.org/10.1038/s41386-020-00789-3

Ceja, I. F. T., Gladytz, T., Starke, L., Tabelow, K., Niendorf, T., & Reimann, H. M. (2024). Precision fMRI and cluster-failure in the individual brain. *Hum Brain Mapp*, *45*(12), e26813. https://doi.org/10.1002/hbm.26813

Chen, X., Wu, W., & Chiew, M. (2023). Improving robustness of 3D multi-shot EPI by structured low-rank reconstruction of segmented CAIPI sampling for fMRI at 7T. *Neuroimage*, *267*, 119827. https://doi.org/10.1016/j.neuroimage.2022.119827

Choi, K. W., Kim, Y.-K., & Jeon, H. J. (2020). Comorbid Anxiety and Depression: Clinical and Conceptual Consideration and Transdiagnostic Treatment. In Y.-K. Kim (Ed.), *Anxiety Disorders: Rethinking and Understanding Recent Discoveries* (pp. 219-235). Springer Singapore. https://doi.org/10.1007/978-981-32-9705-0_14

Chou, T., Deckersbach, T., Dougherty, D. D., & Hooley, J. M. (2023). The default mode network and rumination in individuals at risk for depression. *Soc Cogn Affect Neurosci*, *18*(1). https://doi.org/10.1093/scan/nsad032

Connolly, C. G., Ho, T. C., Blom, E. H., LeWinn, K. Z., Sacchet, M. D., Tymofiyeva, O., Simmons, A. N., & Yang, T. T. (2017). Resting-state functional connectivity of the amygdala and longitudinal changes in depression severity in adolescent depression. *J Affect Disord*, *207*, 86-94. https://doi.org/10.1016/j.jad.2016.09.026

Cui, L., Li, S., Wang, S., Wu, X., Liu, Y., Yu, W., Wang, Y., Tang, Y., Xia, M., & Li, B. (2024). Major depressive disorder: hypothesis, mechanism, prevention and treatment. *Signal Transduction and Targeted Therapy*, *9*(1), 30. https://doi.org/10.1038/s41392-024-01738-y

Dannlowski, U., Ohrmann, P., Konrad, C., Domschke, K., Bauer, J., Kugel, H., Hohoff, C., Schöning, S., Kersting, A., Baune, B. T., Mortensen, L. S., Arolt, V., Zwitserlood, P.,

Deckert, J., Heindel, W., & Suslow, T. (2009). Reduced amygdala-prefrontal coupling in major depression: association with MAOA genotype and illness severity. *Int J Neuropsychopharmacol*, *12*(1), 11-22. https://doi.org/10.1017/s1461145708008973

Diagnostic and Statistical Manual of Mental Disorders. (2022). (5th ed., text rev ed.). American Psychiatric Association. https://doi.org/doi/book/10.1176/appi.books.9780890425787

Dichter, G. S., Sikich, L., Song, A., Voyvodic, J., & Bodfish, J. W. (2012). Functional neuroimaging of treatment effects in psychiatry: methodological challenges and recommendations. *Int J Neurosci*, *122*(9), 483-493. https://doi.org/10.3109/00207454.2012.678446

Drysdale, A. T., Grosenick, L., Downar, J., Dunlop, K., Mansouri, F., Meng, Y., Fetcho, R. N., Zebley, B., Oathes, D. J., Etkin, A., Schatzberg, A. F., Sudheimer, K., Keller, J., Mayberg, H. S., Gunning, F. M., Alexopoulos, G. S., Fox, M. D., Pascual-Leone, A., Voss, H. U., . . . Liston, C. (2017). Resting-state connectivity biomarkers define neurophysiological subtypes of depression. *Nature Medicine*, *23*(1), 28-38. https://doi.org/10.1038/nm.4246

Eickhoff, S. B., Heim, S., Zilles, K., & Amunts, K. (2006). Testing anatomically specified hypotheses in functional imaging using cytoarchitectonic maps. *Neuroimage*, *32*(2), 570-582. https://doi.org/10.1016/j.neuroimage.2006.04.204

Eickhoff, S. B., Stephan, K. E., Mohlberg, H., Grefkes, C., Fink, G. R., Amunts, K., & Zilles, K. (2005). A new SPM toolbox for combining probabilistic cytoarchitectonic maps and functional imaging data. *Neuroimage*, *25*(4), 1325-1335. https://doi.org/10.1016/j.neuroimage.2004.12.034

Elvira, U. K. A., Seoane, S., Janssen, J., & Janssen, N. (2022). Contributions of human amygdala nuclei to resting-state networks. *PLOS ONE*, *17*(12), e0278962. https://doi.org/10.1371/journal.pone.0278962

Engman, J., Linnman, C., Van Dijk, K. R. A., & Milad, M. R. (2016). Amygdala subnuclei resting-state functional connectivity sex and estrogen differences. *Psychoneuroendocrinology*, *63*, 34-42. https://doi.org/10.1016/j.psyneuen.2015.09.012

Entis, J. J., Doerga, P., Barrett, L. F., & Dickerson, B. C. (2012). A reliable protocol for the manual segmentation of the human amygdala and its subregions using ultra-high resolution MRI. *Neuroimage*, *60*(2), 1226-1235. https://doi.org/10.1016/j.neuroimage.2011.12.073

Esteban, O., Markiewicz, C. J., Blair, R. W., Moodie, C. A., Isik, A. I., Erramuzpe, A., Kent, J. D., Goncalves, M., DuPre, E., Snyder, M., Oya, H., Ghosh, S. S., Wright, J., Durnez, J., Poldrack, R. A., & Gorgolewski, K. J. (2019). fMRIPrep: a robust

preprocessing pipeline for functional MRI. *Nature Methods*, *16*(1), 111-116. https://doi.org/10.1038/s41592-018-0235-4

Etkin, A., Prater, K. E., Schatzberg, A. F., Menon, V., & Greicius, M. D. (2009). Disrupted amygdalar subregion functional connectivity and evidence of a compensatory network in generalized anxiety disorder. *Arch Gen Psychiatry*, *66*(12), 1361-1372. https://doi.org/10.1001/archgenpsychiatry.2009.104

Feinberg, D. A., Beckett, A. J. S., Vu, A. T., Stockmann, J., Huber, L., Ma, S., Ahn, S., Setsompop, K., Cao, X., Park, S., Liu, C., Wald, L. L., Polimeni, J. R., Mareyam, A., Gruber, B., Stirnberg, R., Liao, C., Yacoub, E., Davids, M., . . . Dietz, P. (2023). Next-generation MRI scanner designed for ultra-high-resolution human brain imaging at 7 Tesla. *Nature Methods*, *20*(12), 2048-2057. https://doi.org/10.1038/s41592-023-02068-7

Foster, S. L., Breukelaar, I. A., Ekanayake, K., Lewis, S., & Korgaonkar, M. S. (2023). Functional Magnetic Resonance Imaging of the Amygdala and Subregions at 3 Tesla: A Scoping Review. *Journal of Magnetic Resonance Imaging*. https://doi.org/10.1002/jmri.28836

Foster, S. L., Landin-Romero, R., Lewis, S., Barreiros, A. R., Matis, S., Harris, A., & Korgaonkar, M. S. (2025). Amygdala subregional functional connectivity in treatment-resistant depression. *Journal of Affective Disorders Reports*, *21*, 100932. https://doi.org/10.1016/j.jadr.2025.100932

Frühholz, S., & Grandjean, D. (2013). Amygdala subregions differentially respond and rapidly adapt to threatening voices. *Cortex*, *49*(5), 1394-1403. https://doi.org/10.1016/j.cortex.2012.08.003

Fu, X., & Tasker, J. G. (2024). Neuromodulation of inhibitory synaptic transmission in the basolateral amygdala during fear and anxiety [Review]. *Frontiers in Cellular Neuroscience*, *Volume 18 - 2024*. https://doi.org/10.3389/fncel.2024.1421617

Gamer, M., Zurowski, B., & Büchel, C. (2010). Different amygdala subregions mediate valence-related and attentional effects of oxytocin in humans. *Proceedings of the National Academy of Sciences*, *107*(20), 9400-9405. https://doi.org/10.1073/pnas.1000985107

Germani, E., Fromont, E., Maurel, P., & Maumet, C. (2025). HCP Multi-Pipeline: a derived dataset to investigate analytical variability in fMRI. *Scientific Data*, *12*(1), 940. https://doi.org/10.1038/s41597-025-05247-7

Gill, H., Puramat, P., Patel, P., Gill, B., Marks, C. A., Rodrigues, N. B., Castle, D., Cha, D. S., Mansur, R. B., Rosenblat, J. D., & McIntyre, R. S. (2022). The Effects of Psilocybin in Adults with Major Depressive Disorder and the General Population: Findings from Neuroimaging Studies. *Psychiatry Res*, *313*, 114577. https://doi.org/10.1016/j.psychres.2022.114577

Glover, G. H. (2011). Overview of functional magnetic resonance imaging. *Neurosurgery clinics of North America*, *22*(2), 133-vii. https://doi.org/10.1016/j.nec.2010.11.001

Glover, G.H. and Lee, A.T. (1995), Motion Artifacts in fMRI: Comparison of 2DFT with PR and Spiral Scan Methods. Magn. Reson. Med., 33: 624-635. https://doi.org/10.1002/mrm.1910330507

Glover, G. H., Li, T.-Q., & Ress, D. (2000). Image-based method for retrospective correction of physiological motion effects in fMRI: RETROICOR. *Magnetic Resonance in Medicine*, *44*(1), 162-167. https://doi.org/10.1002/1522-2594(200007)44:1<162::AID-MRM23>3.0.CO;2-E

Goetschius, L. G., Hein, T. C., Mattson, W. I., Lopez-Duran, N., Dotterer, H. L., Welsh, R. C., Mitchell, C., Hyde, L. W., & Monk, C. S. (2019). Amygdala-prefrontal cortex white matter tracts are widespread, variable and implicated in amygdala modulation in adolescents. *Neuroimage*, *191*, 278-291. https://doi.org/10.1016/j.neuroimage.2019.02.009

Grehl, M. M., Hameed, S., & Murrough, J. W. (2023). Brain Features of Treatment-Resistant Depression: A Review of Structural and Functional Connectivity Magnetic Resonance Imaging Studies. *Psychiatric Clinics of North America*, *46*(2), 391-401. https://doi.org/10.1016/j.psc.2023.02.009

Hamilton, J. P., Siemer, M., & Gotlib, I. H. (2008). Amygdala volume in major depressive disorder: a meta-analysis of magnetic resonance imaging studies. *Mol Psychiatry*, *13*(11), 993-1000. https://doi.org/10.1038/mp.2008.57

Han, K. M., & Ham, B. J. (2021). How Inflammation Affects the Brain in Depression: A Review of Functional and Structural MRI Studies. *J Clin Neurol*, *17*(4), 503-515. https://doi.org/10.3988/jcn.2021.17.4.503

Harrison, O. K., Guell, X., Klein-Flügge, M. C., & Barry, R. L. (2021). Structural and resting state functional connectivity beyond the cortex. *Neuroimage*, *240*, 118379. https://doi.org/10.1016/j.neuroimage.2021.118379

Hong, X., To, X. V., Teh, I., Soh, J. R., & Chuang, K.-H. (2015). Evaluation of EPI distortion correction methods for quantitative MRI of the brain at high magnetic field. *Magnetic Resonance Imaging*, *33*(9), 1098-1105. https://doi.org/10.1016/j.mri.2015.06.010

Howard, D. M., Adams, M. J., Clarke, T. K., Hafferty, J. D., Gibson, J., Shirali, M., Coleman, J. R. I., Hagenaars, S. P., Ward, J., Wigmore, E. M., Alloza, C., Shen, X., Barbu, M. C., Xu, E. Y., Whalley, H. C., Marioni, R. E., Porteous, D. J., Davies, G., Deary, I. J., . . . McIntosh, A. M. (2019). Genome-wide meta-analysis of depression identifies 102 independent variants and highlights the importance of the prefrontal brain regions. *Nat Neurosci*, *22*(3), 343-352. https://doi.org/10.1038/s41593-018-0326-7

Hrybouski, S., Aghamohammadi-Sereshki, A., Madan, C. R., Shafer, A. T., Baron, C. A., Seres, P., Beaulieu, C., Olsen, F., & Malykhin, N. V. (2016). Amygdala subnuclei response and connectivity during emotional processing. *Neuroimage*, *133*, 98-110. https://doi.org/10.1016/j.neuroimage.2016.02.056

Hu, H., Liu, F., Liu, L., Mei, Y., Xie, B., Shao, Y., & Qiao, Y. (2023). Smaller amygdala subnuclei volume in schizophrenia patients with violent behaviors. *Brain Imaging and Behavior*, *17*(1), 11-17. https://doi.org/10.1007/s11682-022-00736-4

Huotari, N., Raitamaa, L., Helakari, H., Kananen, J., Raatikainen, V., Rasila, A., Tuovinen, T., Kantola, J., Borchardt, V., Kiviniemi, V. J., & Korhonen, V. O. (2019). Sampling Rate Effects on Resting State fMRI Metrics [Original Research]. *Frontiers in Neuroscience*, *Volume 13 - 2019*. https://doi.org/10.3389/fnins.2019.00279

Insel, T., Cuthbert, B., Garvey, M., Heinssen, R., Pine, D. S., Quinn, K., Sanislow, C., & Wang, P. (2010). Research domain criteria (RDoC): toward a new classification framework for research on mental disorders. *Am J Psychiatry*, *167*(7), 748-751. https://doi.org/10.1176/appi.ajp.2010.09091379

Ishikawa, Y., Oishi, N., Kyuragi, Y., Hatakoshi, M., Hirano, J., Noda, T., Yoshihara, Y., Ito, Y., Miyata, J., Nemoto, K., Fujita, Y., Igarashi, H., Takahashi, K., Murakami, S., Kanno, H., Izumi, Y., Takamiya, A., Matsumoto, J., Kodaka, F., . . . Suwa, T. (2025). Electroconvulsive therapy-specific volume changes in nuclei of the amygdala and their relationship to long-term anxiety improvement in depression. *Molecular Psychiatry*, *30*(6), 2653-2664. https://doi.org/10.1038/s41380-024-02874-1

Jacob, Y., Morris, L. S., Verma, G., Rutter, S. B., Balchandani, P., & Murrough, J. W. (2022). Altered hippocampus and amygdala subregion connectome hierarchy in major depressive disorder. *Translational psychiatry*, *12*(1), 209. https://doi.org/10.1038/s41398-022-01976-0

Jahanian, H., Holdsworth, S., Christen, T., Wu, H., Zhu, K., Kerr, A. B., Middione, M. J., Dougherty, R. F., Moseley, M., & Zaharchuk, G. (2019). Advantages of short repetition time resting-state functional MRI enabled by simultaneous multi-slice imaging. *Journal of neuroscience methods*, *311*, 122-132. https://doi.org/10.1016/j.jneumeth.2018.09.033

Kalin, N. H. (2020). The Critical Relationship Between Anxiety and Depression. *American Journal of Psychiatry*, *177*(5), 365-367. https://doi.org/10.1176/appi.ajp.2020.20030305

Kellman, P., & McVeigh, E. R. (2005). Image reconstruction in SNR units: a general method for SNR measurement. *Magn Reson Med*, *54*(6), 1439-1447. https://doi.org/10.1002/mrm.20713

Kelly, T. J., Bonniwell, E. M., Mu, L., Liu, X., Hu, Y., Friedman, V., Yu, H., Su, W., McCorvy, J. D., & Liu, Q. S. (2024). Psilocybin analog 4-OH-DiPT enhances fear

extinction and GABAergic inhibition of principal neurons in the basolateral amygdala. *Neuropsychopharmacology*, *49*(5), 854-863. https://doi.org/10.1038/s41386-023-01744-8

Kim, H., Han, K.-M., Choi, K. W., Tae, W.-S., Kang, W., Kang, Y., Kim, A., & Ham, B.-J. (2021). Volumetric alterations in subregions of the amygdala in adults with major depressive disorder. *Journal of Affective Disorders*, *295*, 108-115. https://doi.org/10.1016/j.jad.2021.08.012

Klein-Flügge, M. C., Jensen, D. E. A., Takagi, Y., Priestley, L., Verhagen, L., Smith, S. M., & Rushworth, M. F. S. (2022). Relationship between nuclei-specific amygdala connectivity and mental health dimensions in humans. *Nature Human Behaviour*, *6*(12), 1705-1722. https://doi.org/10.1038/s41562-022-01434-3

Kotoula, V., Evans, J. W., Punturieri, C., Johnson, S. C., & Zarate, C. A. (2023). Chapter 5 - Functional MRI markers for treatment-resistant depression: Insights and challenges. In C.-T. Li & C.-M. Cheng (Eds.), *Progress in Brain Research* (Vol. 278, pp. 117-148). Elsevier. https://doi.org/10.1016/bs.pbr.2023.04.001

Kwon, H., Ha, M., Choi, S., Park, S., Jang, M., Kim, M., & Kwon, J. S. (2024). Resting-state functional connectivity of amygdala subregions across different symptom subtypes of obsessive–compulsive disorder patients. *NeuroImage: Clinical*, *43*, 103644. https://doi.org/10.1016/j.nicl.2024.103644

Labuschagne, I., Dominguez, J. F., Grace, S., Mizzi, S., Henry, J. D., Peters, C., Rabinak, C. A., Sinclair, E., Lorenzetti, V., Terrett, G., Rendell, P. G., Pedersen, M., Hocking, D. R., & Heinrichs, M. (2024). Specialization of amygdala subregions in emotion processing. *Human Brain Mapping*, *45*(5), e26673. https://doi.org/10.1002/hbm.26673

Lake, E. M., Ge, X., Shen, X., Herman, P., Hyder, F., Cardin, J. A., Higley, M. J., Scheinost, D., Papademetris, X., Crair, M. C., & Constable, R. T. (2019). Simultaneous mesoscopic Ca²⁺ imaging and fMRI: Neuroimaging spanning spatiotemporal scales. *bioRxiv*, 464305. https://doi.org/10.1101/464305

Li, B., Liu, L., Friston, K. J., Shen, H., Wang, L., Zeng, L.-L., & Hu, D. (2013). A Treatment-Resistant Default Mode Subnetwork in Major Depression. *Biological Psychiatry*, *74*(1), 48-54. https://doi.org/10.1016/j.biopsych.2012.11.007

Li, M. T., Sun, J. W., Zhan, L. L., Antwi, C. O., Lv, Y. T., Jia, X. Z., & Ren, J. (2023). The effect of seed location on functional connectivity: evidence from an image-based meta-analysis. *Front Neurosci*, *17*, 1120741. https://doi.org/10.3389/fnins.2023.1120741

Li, T., Guo, Y., Zhao, Z., Chen, M., Lin, Q., Hu, X., Yao, Z., & Hu, B. (2024). Automated Diagnosis of Major Depressive Disorder With Multi-Modal MRIs Based on

Contrastive Learning: A Few-Shot Study. *IEEE Trans Neural Syst Rehabil Eng*, *32*, 1566-1576. https://doi.org/10.1109/tnsre.2024.3380357

Li, Y. Y., Ni, X. K., You, Y. F., Qing, Y. H., Wang, P. R., Yao, J. S., Ren, K. M., Zhang, L., Liu, Z. W., Song, T. J., Wang, J., Zang, Y. F., Shen, Y. D., & Chen, W. (2021). Common and Specific Alterations of Amygdala Subregions in Major Depressive Disorder With and Without Anxiety: A Combined Structural and Resting-State Functional MRI Study. *Front Hum Neurosci*, *15*, 634113. https://doi.org/10.3389/fnhum.2021.634113

Liu, H., Wang, C., Lan, X., Li, W., Zhang, F., Fu, L., Ye, Y., Ning, Y., & Zhou, Y. (2023). Functional connectivity of the amygdala and the antidepressant and antisuicidal effects of repeated ketamine infusions in major depressive disorder. *Front Neurosci*, *17*, 1123797. https://doi.org/10.3389/fnins.2023.1123797

Liu, T., Ke, J., Qi, R., Zhang, L., Zhang, Z., Xu, Q., Zhong, Y., Lu, G., & Chen, F. (2021). Altered functional connectivity of the amygdala and its subregions in typhoon‐related post‐traumatic stress disorder. *Brain and Behavior*, *11*(1), e01952. https://doi.org/10.1002/brb3.1952

Loureiro, J. R. A., Leaver, A., Vasavada, M., Sahib, A. K., Kubicki, A., Joshi, S., Woods, R. P., Wade, B., Congdon, E., Espinoza, R., & Narr, K. L. (2020). Modulation of amygdala reactivity following rapidly acting interventions for major depression. *Human Brain Mapping*, *41*(7), 1699-1710. https://doi.org/10.1002/hbm.24895

Loureiro, J. R. A., Sahib, A. K., Vasavada, M., Leaver, A., Kubicki, A., Wade, B., Joshi, S., Hellemann, G., Congdon, E., Woods, R. P., Espinoza, R., & Narr, K. L. (2021). Ketamine's modulation of cerebro-cerebellar circuitry during response inhibition in major depression. *NeuroImage: Clinical*, *32*, 102792. https://doi.org/10.1016/j.nicl.2021.102792

Lutti, A., Thomas, D. L., Hutton, C., & Weiskopf, N. (2013). High-resolution functional MRI at 3 T: 3D/2D echo-planar imaging with optimized physiological noise correction. *Magn Reson Med*, *69*(6), 1657-1664. https://doi.org/10.1002/mrm.24398

Maldjian, J. A., Laurienti, P. J., Kraft, R. A., & Burdette, J. H. (2003). An automated method for neuroanatomic and cytoarchitectonic atlas-based interrogation of fMRI data sets. *Neuroimage*, *19*(3), 1233-1239. https://doi.org/10.1016/S1053-8119(03)00169-1

Malhi, G. S., Bell, E., Bassett, D., Boyce, P., Bryant, R., Hazell, P., Hopwood, M., Lyndon, B., Mulder, R., Porter, R., Singh, A. B., & Murray, G. (2021). The 2020 Royal Australian and New Zealand College of Psychiatrists clinical practice guidelines for mood disorders. *Australian & New Zealand Journal of Psychiatry*, *55*(1), 7-117. https://doi.org/10.1177/0004867420979353

Mehta, N. D., Haroon, E., Xu, X., Woolwine, B. J., Li, Z., & Felger, J. C. (2018). Inflammation negatively correlates with amygdala-ventromedial prefrontal functional

connectivity in association with anxiety in patients with depression: Preliminary results. *Brain, Behavior, and Immunity*, *73*, 725-730. https://doi.org/10.1016/j.bbi.2018.07.026

Menon, R. S., & Goodyear, B. G. (2001). Spatial and temporal resolution in fMRI. In P. Jezzard, P. M. Matthews, & S. M. Smith (Eds.), *Functional Magnetic Resonance Imaging: An Introduction to Methods* (pp. 146-158). Oxford University Press. https://doi.org/10.1093/acprof:oso/9780192630711.003.0007

Michely, J., Rigoli, F., Rutledge, R. B., Hauser, T. U., & Dolan, R. J. (2020). Distinct processing of aversive experience in amygdala subregions. *Biological Psychiatry: Cognitive Neuroscience and Neuroimaging*, *5*(3), 291-300. https://doi.org/10.1016/j.bpsc.2019.07.008

Milaneschi, Y., Kappelmann, N., Ye, Z., Lamers, F., Moser, S., Jones, P. B., Burgess, S., Penninx, B. W. J. H., & Khandaker, G. M. (2021). Association of inflammation with depression and anxiety: evidence for symptom-specificity and potential causality from UK Biobank and NESDA cohorts. *Molecular Psychiatry*, *26*(12), 7393-7402. https://doi.org/10.1038/s41380-021-01188-w

Miola, A., Meda, N., Perini, G., & Sambataro, F. (2023). Structural and functional features of treatment-resistant depression: A systematic review and exploratory coordinate-based meta-analysis of neuroimaging studies. *Psychiatry Clin Neurosci*, *77*(5), 252-263. https://doi.org/10.1111/pcn.13530

Molloy, E. K., Meyerand, M. E., & Birn, R. M. (2014). The influence of spatial resolution and smoothing on the detectability of resting-state and task fMRI. *Neuroimage*, *86*, 221-230. https://doi.org/10.1016/j.neuroimage.2013.09.001

Morgan, P. S., Bowtell, R. W., McIntyre, D. J. O., & Worthington, B. S. (2004). Correction of spatial distortion in EPI due to inhomogeneous static magnetic fields using the reversed gradient method. *Journal of Magnetic Resonance Imaging*, *19*(4), 499-507. https://doi.org/10.1002/jmri.20032

Morris, J. S., Buchel, C., & Dolan, R. J. (2001). Parallel neural responses in amygdala subregions and sensory cortex during implicit fear conditioning. *Neuroimage*, *13*(6 Pt 1), 1044-1052. https://doi.org/10.1006/nimg.2000.0721

Munshi, S., Albrechet-Souza, L., Dos-Santos, R. C., Stelly, C. E., Secci, M. E., Gilpin, N. W., & Tasker, J. G. (2023). Acute Ethanol Modulates Synaptic Inhibition in the Basolateral Amygdala via Rapid NLRP3 Inflammasome Activation and Regulates Anxiety-Like Behavior in Rats. *J Neurosci*, *43*(47), 7902-7912. https://doi.org/10.1523/jneurosci.1744-22.2023

Murrough, J. W., Collins, K. A., Fields, J., DeWilde, K. E., Phillips, M. L., Mathew, S. J., Wong, E., Tang, C. Y., Charney, D. S., & Iosifescu, D. V. (2015). Regulation of neural responses to emotion perception by ketamine in individuals with treatment-

resistant major depressive disorder. *Translational psychiatry*, *5*(2), e509-e509. https://doi.org/10.1038/tp.2015.10

Nieto-Castanon, A. (2020). FMRI minimal preprocessing pipeline. In *Handbook of functional connectivity Magnetic Resonance Imaging methods in CONN* (pp. 3-16). Hilbert Press. https://doi.org/10.56441/hilbertpress.2207.6599

Nolan, M., Roman, E., Nasa, A., Levins, K. J., O'Hanlon, E., O'Keane, V., & Willian Roddy, D. (2020). Hippocampal and Amygdalar Volume Changes in Major Depressive Disorder: A Targeted Review and Focus on Stress. *Chronic Stress*, *4*, 2470547020944553. https://doi.org/10.1177/2470547020944553

Olman, C. A., Davachi, L., & Inati, S. (2009). Distortion and Signal Loss in Medial Temporal Lobe. *PLOS ONE*, *4*(12), e8160. https://doi.org/10.1371/journal.pone.0008160

Pinto-Coelho, L. (2023). How Artificial Intelligence Is Shaping Medical Imaging Technology: A Survey of Innovations and Applications. *Bioengineering (Basel)*, *10*(12). https://doi.org/10.3390/bioengineering10121435

Pitkänen, A., Savander, V., & LeDoux, J. E. (1997). Organization of intra-amygdaloid circuitries in the rat: an emerging framework for understanding functions of the amygdala. *Trends in Neurosciences*, *20*(11), 517-523. https://doi.org/10.1016/S0166-2236(97)01125-9

Poldrack, R. A., Baker, C. I., Durnez, J., Gorgolewski, K. J., Matthews, P. M., Munafò, M. R., Nichols, T. E., Poline, J. B., Vul, E., & Yarkoni, T. (2017). Scanning the horizon: towards transparent and reproducible neuroimaging research. *Nat Rev Neurosci*, *18*(2), 115-126. https://doi.org/10.1038/nrn.2016.167

Poldrack, R. A., Mumford, J. A., & Nichols, T. E. (2011). *Handbook of Functional MRI Data Analysis*. Cambridge University Press. https://doi.org/DOI: 10.1017/CBO9780511895029

Poser, B. A., Koopmans, P. J., Witzel, T., Wald, L. L., & Barth, M. (2010). Three dimensional echo-planar imaging at 7 Tesla. *Neuroimage*, *51*(1), 261-266. https://doi.org/10.1016/j.neuroimage.2010.01.108

Prager, E. M., Bergstrom, H. C., Wynn, G. H., & Braga, M. F. (2016). The basolateral amygdala γ-aminobutyric acidergic system in health and disease. *J Neurosci Res*, *94*(6), 548-567. https://doi.org/10.1002/jnr.23690

Qin, S., Young, C. B., Duan, X., Chen, T., Supekar, K., & Menon, V. (2014). Amygdala Subregional Structure and Intrinsic Functional Connectivity Predicts Individual Differences in Anxiety During Early Childhood. *Biological Psychiatry*, *75*(11), 892-https://doi.org/10.1016/j.biopsych.2013.10.006

Qiu, L., Xia, M., Cheng, B., Yuan, L., Kuang, W., Bi, F., Ai, H., Gu, Z., Lui, S., Huang, X., He, Y., & Gong, Q. (2018). Abnormal dynamic functional connectivity of amygdalar

subregions in untreated patients with first-episode major depressive disorder. *J Psychiatry Neurosci*, *43*(4), 262-272. https://doi.org/10.1503/jpn.170112

Rai, S., Griffiths, K. R., Breukelaar, I. A., Barreiros, A. R., Boyce, P., Hazell, P., Foster, S. L., Malhi, G. S., Harris, A. W. F., & Korgaonkar, M. S. (2022). Common and differential neural mechanisms underlying mood disorders. *Bipolar Disorders*, *24*(8), 795-805. https://doi.org/10.1111/bdi.13248

Rajamanickam, K. (2020). A Mini Review on Different Methods of Functional-MRI Data Analysis. *Archives of Internal Medicine Research*, *3*, 44-60. https://www.fortunejournals.com/articles/a-mini-review-on-different-methods-of-functionalmri-data-analysis.html

Ramezani, F., Mardani, P., Nemati, F., Cattarinussi, G., Sambataro, F., Schiena, G., Brambilla, P., & Delvecchio, G. (2025). Effect of ketamine on task-based functional magnetic resonance imaging findings in major depressive disorder: A mini-review. *Journal of Affective Disorders*, *370*, 181-189. https://doi.org/10.1016/j.jad.2024.10.118

Ripke, S., Wray, N. R., Lewis, C. M., Hamilton, S. P., Weissman, M. M., Breen, G., Byrne, E. M., Blackwood, D. H., Boomsma, D. I., Cichon, S., Heath, A. C., Holsboer, F., Lucae, S., Madden, P. A., Martin, N. G., McGuffin, P., Muglia, P., Noethen, M. M., Penninx, B. P., . . . Sullivan, P. F. (2013). A mega-analysis of genome-wide association studies for major depressive disorder. *Mol Psychiatry*, *18*(4), 497-511. https://doi.org/10.1038/mp.2012.21

Risbrough, V. B., Vaughn, M. N., & Friend, S. F. (2022). Role of Inflammation in Traumatic Brain Injury–Associated Risk for Neuropsychiatric Disorders: State of the Evidence and Where Do We Go From Here. *Biological Psychiatry*, *91*(5), 438-448. https://doi.org/10.1016/j.biopsych.2021.11.012

Robinson, S., Windischberger, C., Rauscher, A., & Moser, E. (2004). Optimized 3 T EPI of the amygdalae. *Neuroimage*, *22*(1), 203-210. https://doi.org/10.1016/j.neuroimage.2003.12.048

Roy, A. K., Shehzad, Z., Margulies, D. S., Kelly, A. M. C., Uddin, L. Q., Gotimer, K., Biswal, B. B., Castellanos, F. X., & Milham, M. P. (2009). Functional connectivity of the human amygdala using resting state fMRI. *Neuroimage*, *45*(2), 614-626. https://doi.org/10.1016/j.neuroimage.2008.11.030

Runia, N., Bergfeld, I. O., de Kwaasteniet, B. P., Luigjes, J., van Laarhoven, J., Notten, P., Beute, G., van den Munckhof, P., Schuurman, R., Denys, D., & van Wingen, G. A. (2023). Deep brain stimulation normalizes amygdala responsivity in treatment-resistant depression. *Mol Psychiatry*, *28*(6), 2500-2507. https://doi.org/10.1038/s41380-023-02030-1

Sah, P., Faber, E. S. L., & Lopez De Armentia, M. P., J. (2003). The Amygdaloid Complex: Anatomy and Physiology. *Physiological Reviews*, *83*(3), 803-834. https://doi.org/10.1152/physrev.00002.2003

Salman, Y., Gérard, T., Huyghe, L., Colmant, L., Quenon, L., Malotaux, V., Ivanoiu, A., Lhommel, R., Dricot, L., & Hanseeuw, B. J. (2024). Amygdala atrophies in specific subnuclei in preclinical Alzheimer's disease. *Alzheimers Dement*, *20*(10), 7205-7219. https://doi.org/10.1002/alz.14235

Sambataro, F., Wolf, N. D., Pennuto, M., Vasic, N., & Wolf, R. C. (2014). Revisiting default mode network function in major depression: evidence for disrupted subsystem connectivity. *Psychol Med*, *44*(10), 2041-2051. https://doi.org/10.1017/s0033291713002596

Schmidt, C. F., Degonda, N., Luechinger, R., Henke, K., & Boesiger, P. (2005). Sensitivity-encoded (SENSE) echo planar fMRI at 3T in the medial temporal lobe. *Neuroimage*, *25*(2), 625-641. https://doi.org/10.1016/j.neuroimage.2004.12.002

Shen, C.-J., Zheng, D., Li, K.-X., Yang, J.-M., Pan, H.-Q., Yu, X.-D., Fu, J.-Y., Zhu, Y., Sun, Q.-X., Tang, M.-Y., Zhang, Y., Sun, P., Xie, Y., Duan, S., Hu, H., & Li, X.-M. (2019). Cannabinoid CB1 receptors in the amygdalar cholecystokinin glutamatergic afferents to nucleus accumbens modulate depressive-like behavior. *Nature Medicine*, *25*(2), 337-349. https://doi.org/10.1038/s41591-018-0299-9

Simmons, J. P., Nelson, L. D., & Simonsohn, U. (2011). False-Positive Psychology:Undisclosed Flexibility in Data Collection and Analysis Allows Presenting Anything as Significant. *Psychological science*, *22*(11), 1359-1366. https://doi.org/10.1177/0956797611417632

Slavich, G. M., & Irwin, M. R. (2014). From stress to inflammation and major depressive disorder: A social signal transduction theory of depression. *Psychological Bulletin*, *140*(3), 774-815. https://doi.org/10.1037/a0035302

Sohn, W. S., Yoo, K., Lee, Y. B., Seo, S. W., Na, D. L., & Jeong, Y. (2015). Influence of ROI selection on resting state functional connectivity: an individualized approach for resting state fMRI analysis. *Front Neurosci*, *9*, 280. https://doi.org/10.3389/fnins.2015.00280

Spellman, T., & Liston, C. (2020). Toward Circuit Mechanisms of Pathophysiology in Depression. *Am J Psychiatry*, *177*(5), 381-390. https://doi.org/10.1176/appi.ajp.2020.20030280

Stirnberg, R., Huijbers, W., Brenner, D., Poser, B. A., Breteler, M., & Stöcker, T. (2017). Rapid whole-brain resting-state fMRI at 3 T: Efficiency-optimized three-dimensional EPI versus repetition time-matched simultaneous-multi-slice EPI. *Neuroimage*, *163*, 81-92. https://doi.org/10.1016/j.neuroimage.2017.08.031

Szucs, D., & Ioannidis, J. P. A. (2020). Sample size evolution in neuroimaging research: An evaluation of highly-cited studies (1990–2012) and of latest practices (2017–2018) in high-impact journals. *Neuroimage*, *221*, 117164. https://doi.org/10.1016/j.neuroimage.2020.117164

Tang, S., Li, H., Lu, L., Wang, Y., Zhang, L., Hu, X., Bu, X., Hu, X., Gao, Y., Gong, Q., & Huang, X. (2019). Anomalous functional connectivity of amygdala subregional networks in major depressive disorder. *Depression and Anxiety*, *36*(8), 712-722. https://doi.org/10.1002/da.22901

Tesen, H., Watanabe, K., Okamoto, N., Ikenouchi, A., Igata, R., Konishi, Y., Kakeda, S., & Yoshimura, R. (2022). Volume of Amygdala Subregions and Clinical Manifestations in Patients With First-Episode, Drug-Naïve Major Depression [Original Research]. *Frontiers in Human Neuroscience*, *15*. https://doi.org/10.3389/fnhum.2021.780884

Thai, M., Başgöze, Z., Klimes-Dougan, B., Mueller, B. A., Fiecas, M., Lim, K. O., Albott, C. S., & Cullen, K. R. (2020). Neural and Behavioral Correlates of Clinical Improvement to Ketamine in Adolescents With Treatment Resistant Depression [Original Research]. *Front Psychiatry*, *Volume 11 - 2020*. https://doi.org/10.3389/fpsyt.2020.00820

Tollenaar, B. (2025). *Psilocybin's effect on depression by binding to serotonergic receptors in the basolateral amygdala* (Publication Number 45928) Utrecht University]. Utrecht. https://studenttheses.uu.nl/handle/20.500.12932/48967

Tozzi, L., Zhang, X., Chesnut, M., Holt-Gosselin, B., Ramirez, C. A., & Williams, L. M. (2021). Reduced functional connectivity of default mode network subsystems in depression: Meta-analytic evidence and relationship with trait rumination. *NeuroImage: Clinical*, *30*, 102570. https://doi.org/10.1016/j.nicl.2021.102570

Triana, A. M., Glerean, E., Saramäki, J., & Korhonen, O. (2020). Effects of spatial smoothing on group-level differences in functional brain networks. *Netw Neurosci*, *4*(3), 556-574. https://doi.org/10.1162/netn_a_00132

Triantafyllou, C., Hoge, R. D., Krueger, G., Wiggins, C. J., Potthast, A., Wiggins, G. C., & Wald, L. L. (2005). Comparison of physiological noise at 1.5 T, 3 T and 7 T and optimization of fMRI acquisition parameters. *Neuroimage*, *26*(1), 243-250. https://doi.org/10.1016/j.neuroimage.2005.01.007

Tzourio-Mazoyer, N., Landeau, B., Papathanassiou, D., Crivello, F., Etard, O., Delcroix, N., Mazoyer, B., & Joliot, M. (2002). Automated Anatomical Labeling of Activations in SPM Using a Macroscopic Anatomical Parcellation of the MNI MRI Single-Subject Brain. *Neuroimage*, *15*(1), 273-289. https://doi.org/10.1006/nimg.2001.0978

Varkevisser, T., Geuze, E., & van Honk, J. (2024). Amygdala fMRI—A Critical Appraisal of the Extant Literature. *Neuroscience Insights*, *19*, 26331055241270591. https://doi.org/10.1177/26331055241270591

Wang, X., Nie, X., Zhang, F., Wei, Y., Zeng, W., Zhang, Y., & Lin, H. (2024). Functional magnetic resonance imaging of depression: a bibliometrics and meta-analysis. *Annals of General Psychiatry*, *23*(1), 39. https://doi.org/10.1186/s12991-024-00525-x

Whitfield-Gabrieli, S., & Nieto-Castanon, A. (2012). Conn: a functional connectivity toolbox for correlated and anticorrelated brain networks. *Brain Connect*, *2*(3), 125-141. https://doi.org/10.1089/brain.2012.0073

Wray, N. R., Ripke, S., Mattheisen, M., Trzaskowski, M., Byrne, E. M., Abdellaoui, A., Adams, M. J., Agerbo, E., Air, T. M., Andlauer, T. M. F., Bacanu, S. A., Bækvad-Hansen, M., Beekman, A. F. T., Bigdeli, T. B., Binder, E. B., Blackwood, D. R. H., Bryois, J., Buttenschøn, H. N., Bybjerg-Grauholm, J., . . . Sullivan, P. F. (2018). Genome-wide association analyses identify 44 risk variants and refine the genetic architecture of major depression. *Nat Genet*, *50*(5), 668-681. https://doi.org/10.1038/s41588-018-0090-3

Wu, C. W., Chen, C.-L., Liu, P.-Y., Chao, Y.-P., Biswal, B. B., & Lin, C.-P. (2011). Empirical Evaluations of Slice-Timing, Smoothing, and Normalization Effects in Seed-Based, Resting-State Functional Magnetic Resonance Imaging Analyses. *Brain connectivity*, *1*(5), 401-410. https://doi.org/10.1089/brain.2011.0018

Yang, J., Yin, Y., Svob, C., Long, J., He, X., Zhang, Y., Xu, Z., Li, L., Liu, J., Dong, J., Zhang, Z., Wang, Z., & Yuan, Y. (2017). Amygdala Atrophy and Its Functional Disconnection with the Cortico-Striatal-Pallidal-Thalamic Circuit in Major Depressive Disorder in Females. *PLOS ONE*, *12*(1), e0168239. https://doi.org/10.1371/journal.pone.0168239

Yang, Y., & Wang, J.-Z. (2017). From Structure to Behavior in Basolateral Amygdala-Hippocampus Circuits [Mini Review]. *Frontiers in Neural Circuits*, *11*(86). https://doi.org/10.3389/fncir.2017.00086

Young, K. D., Siegle, G. J., Misaki, M., Zotev, V., Phillips, R., Drevets, W. C., & Bodurka, J. (2018). Altered task-based and resting-state amygdala functional connectivity following real-time fMRI amygdala neurofeedback training in major depressive disorder. *Neuroimage Clin*, *17*, 691-703. https://doi.org/10.1016/j.nicl.2017.12.004

Yuan, S., Luo, X., Chen, X., Wang, M., Hu, Y., Zhou, Y., Ning, Y., & Zhang, B. (2023). Functional connectivity differences in the amygdala are related to the antidepressant efficacy of ketamine in patients with anxious depression. *Journal of Affective Disorders*, *320*, 29-36. https://doi.org/10.1016/j.jad.2022.09.125

Zhang, S., Cui, J., Zhang, Z., Wang, Y., Liu, R., Chen, X., Feng, Y., Zhou, J., Zhou, Y., & Wang, G. (2022). Functional connectivity of amygdala subregions predicts vulnerability to depression following the COVID-19 pandemic. *J Affect Disord*, *297*, 421-429. https://doi.org/10.1016/j.jad.2021.09.107

Zhang, W. H., Zhang, J. Y., Holmes, A., & Pan, B. X. (2021). Amygdala Circuit Substrates for Stress Adaptation and Adversity. *Biol Psychiatry*, *89*(9), 847-856. https://doi.org/10.1016/j.biopsych.2020.12.026

Zhang, X., Cheng, H., Zuo, Z., Zhou, K., Cong, F., Wang, B., Zhuo, Y., Chen, L., Xue, R., & Fan, Y. (2018). Individualized Functional Parcellation of the Human Amygdala Using a Semi-supervised Clustering Method: A 7T Resting State fMRI Study [Original Research]. *Frontiers in Neuroscience*, *12*(270). https://doi.org/10.3389/fnins.2018.00270

Zhou, Y. L., Wu, F. C., Liu, W. J., Zheng, W., Wang, C. Y., Zhan, Y. N., Lan, X. F., & Ning, Y. P. (2020). Volumetric changes in subcortical structures following repeated ketamine treatment in patients with major depressive disorder: a longitudinal analysis. *Translational psychiatry*, *10*(1), 264. https://doi.org/10.1038/s41398-020-00945-9

APPENDICES

APPENDIX A – CHAPTER 1 SUPPLEMENTARY MATERIALS

Plain Language Synopsis

Depression affects one in twenty people globally and current diagnostic methods are based not on scientific methods, but on patient self-reporting of symptoms and observations of behaviour. Dysfunction of the amygdala, with its role in emotion processing, is widely implicated as a contributor to depression. Although very small in size, the amygdala is not a homogenous structure and is composed of functionally disparate subnuclei, grouped together into three distinct subregions; the basolateral (LB), the centromedial (CM) and the superficial (SF), each of which has differential functional connections to other parts of the brain.

Since its introduction into clinical and research centres in the 1980s, MRI has been deployed by researchers studying the amygdala in depression, initially to investigate amygdala volumes. Following the development of fMRI techniques in the 1990s, the amygdala became a focus for those hoping to not only demonstrate how its function may differ in depression, but also what that may mean for patients and for clinicians seeking satisfactory treatment options. Depending on the particular research question, either task-based methods to investigate amygdala activation or resting-state methods to map the brain's functional architecture can be performed, and often both methods are used complementarily. More recently, the focus of fMRI studies in depression has been on identification of potential biomarkers capable of differentiating patients who respond to treatment from those who are resistant to treatment (Williams et al., 2015). In this fMRI optimisation work at 3 Tesla, resting-state methods will be employed to investigate subregional amygdala FC, thus mitigating potential sources of variability that can be introduced in task-based studies.

Difficulties in spatially resolving small structures when SNR is limited, as is the case at 1.5T, has meant that the amygdala was primarily investigated as a single entity. With the advent of 3T systems, researchers encountered a choice in how to 'spend' the extra SNR as outlined below:

1. maintain current acquisition protocols with lower spatial resolution to investigate the **whole** amygdala whilst benefitting from improved Blood Oxygen Level Dependent (BOLD) contrast levels

2. maintain current acquisition protocols with lower spatial resolution to investigate the amygdala **subregions** whilst benefitting from improved Blood Oxygen Level Dependent (BOLD) contrast levels
3. **optimise** current acquisition protocols and benefit from **increased spatial resolution** to investigate the amygdala **subregions**

It is important to note several fundamental points here. Firstly, in the brain, high spatial resolution data is considered to be data with a voxel volume of $20mm^3$ or less. Secondly, whilst data acquisition strategies are the main consideration of this work, the data analysis process is integral and requires some explanation. For the type of analysis used in this work, (Seed Based Connectivity, explained more fully in Chapter Two), the region-of-interest (ROI) under investigation is isolated from other regions and the strength of connectivity to all other regions in the brain (positive or negative) is measured. Most studies have considered the amygdala as a single structure and utilised whole amygdala ROIs to report their findings. This method introduces a risk of positive and negative signal averaging which is avoided with the use of subregional ROIs.

An initial review of the literature relating to 3T fMRI studies reporting on amygdala activation and connectivity, the results of which were borne out by the scoping review forming Chapter Three, showed that most researchers chose Option One (together with whole amygdala ROIs for analysis), fewer chose Option Two and very few chose Option Three. It appeared that there was considerable inconsistency in results across studies investigating depression, particularly in those displaying treatment resistance, and this was borne out by the results of the literature review undertaken for the work outlined in Chapter Four.

In the field of clinical MRI, it is broadly accepted that imaging protocols providing enhanced data quality and higher spatial resolution are more diagnostically reliable, and the same principle is ostensibly true in a research setting. Optimised 3T acquisition protocols can improve data accuracy by better resolving the very small amygdala subregions and more accurately identifying their functional connections with other brain regions, potentially providing us with greater insights into the neural correlates of different depression subtypes. In summary, there may be potential for improvements in data acquisition on widely available 3T MRI systems that can be converted into higher spatial resolution imaging. Unlocking that potential may lead to greater insights into the function of the amygdala subregions and how subregional dysfunction may impact patients with depression.

APPENDIX B – CHAPTER 2 SUPPLEMENTARY MATERIALS

Table S1: Summary of Imaging Parameter Trade-Offs

Note: nc = no change

Increase in Parameters below	SNR	Resolution	Acquisition Time	Distance Covered	Max. no. of Slices
FOV	+	–	nc	nc	nc
NEX	+	nc	+	nc	nc
Slice Thickness	+	–	nc	+	nc
Gap	+	–	nc	+	nc
TR	+	nc	+	nc	+
TE	–	nc	nc	nc	–
Matrix Size	–	+	+	nc	nc
Bandwidth	–	nc	nc	nc	+
Field Strength	+	nc	nc	nc	nc

APPENDIX C – CHAPTER 3 SUPPLEMENTARY MATERIALS

Functional Magnetic Resonance Imaging of the Amygdala and Subregions at 3 Tesla: A Scoping Review Protocol

---

This review protocol was developed for the scoping review that forms Chapter Three. It was registered on the Open Science Framework as per recommendations regarding best practice from Cochrane and PRISMA Reporting Guidelines and subsequently published online as a preprint available to other researchers. Protocol registration aligns with the principles of transparency and reproducibility and, aside from the primary benefit of ensuring the review protocol and methodology for this study was appropriately developed beforehand, it has other scientific benefits such as the reduction of bias and unintentional duplication of research.

medRxiv
THE PREPRINT SERVER FOR HEALTH SCIENCES

RADIOLOGY AND IMAGING

Functional Magnetic Resonance Imaging of the amygdala and subregions at 3 Tesla: A scoping review protocol

Sheryl L. Foster [1 2 *], Isabella A. Breukelaar [3], Kanchana Ekanayake [4], Sarah Lewis [1] and Mayuresh S. Korgaonkar [3]

[1] *Sydney School of Health Sciences, Faculty of Medicine and Health, The University of Sydney, Sydney, NSW 2006, Australia*

[2] *Department of Radiology, Westmead Hospital, Westmead, NSW 2145, Australia*

[3] *Brain Dynamics Centre, The Westmead Institute for Medical Research, The University of Sydney, Westmead, NSW, Australia*

[4] *University Library, The University of Sydney, Sydney, NSW, 2006*

[*] Corresponding author; email: sheryl.foster{at}sydney.edu.au

medRxiv preprint DOI: https://doi.org/10.1101/2022.04.14.22273332

Posted: April 18, 2022, Version 1

Abstract

Background Functional Magnetic Resonance Imaging (fMRI) is a widely accepted and utilised method of investigating neural activation within the brain. There has been increasing awareness and understanding in the field of neuropsychology over the last 10-15 years that the amygdala plays an important role in many mental health conditions. Functional connectivity (FC) of the amygdala with other parts of the brain is well-documented in the literature; however the role of the amygdala and its reported connections is still not well understood and this can be attributed, in part, to its very small size. It is challenging to achieve adequate spatial resolution to visualise amygdala activation using 3T MRI systems that are in widespread use for this type of clinical research. Optimisation of protocols for improved data accuracy and reproducibility may potentially lead to standardisation and subsequent advancements in overall image quality in this field.

Methods The protocol for this scoping review was developed in line with the Preferred Reporting Items for Systematic reviews and Meta-Analyses extension for Scoping Reviews (PRISMA-ScR) and registered with the Open Science Framework (OSF). A literature search of five databases (Medline, Embase, Web of Science, Google Scholar and Scopus) will be undertaken using a refined search strategy; peer-reviewed publications identified as being relevant will then be imported into Covidence software for abstract screening and data extraction by two reviewers working independently. The quantitative findings will be tabulated to provide an

overview of the current methodologies for comparison. This will be accompanied by a narrative report summarising the extracted data in relation to the stated research questions.
Discussion The objective of this scoping review is to identify and map the range of existing protocols used in fMRI for imaging the activation and FC patterns of the amygdala at 3 Tesla. This will be achieved by collating and presenting quantitative data relating to protocol parameter choices as well as other qualitative aspects of the data acquisition process.

Registration Open Science Framework (OSF) – Registration type: OSF Pre-registration

Registration: https://osf.io/e3c28, DOI: 10.17605/OSF.IO/KW58P

Background

Functional Magnetic Resonance Imaging (fMRI) is a widely accepted and utilised method of investigating neural activation within the brain (**Glover, 2011**). fMRI has advanced our understanding of the structure and function of distinct brain regions as well as how these different regions may be working together (**Huettel, Song, & McCarthy, 2004**). Although it has long been recognised by neuroscientists that the amygdala is an intrinsic component of the emotion circuitry of the brain (**LeDoux, 2000**), there has been increasing awareness and understanding in the field of neuropsychology over the last 10-15 years that the amygdala plays an important role in many mental health conditions (**Leppänen, 2006**; **Schumann, Bauman, & Amaral, 2011**).

The amygdalae comprises a pair of almond-shaped structures located deep in the temporal lobes of the brain with each amygdala being only around 10-20mm^3 in size (**Amunts et al., 2005**). The brain has both structural and functional connections and investigation of the functional connectivity (FC) of the amygdala with other parts of the brain is well-documented in the literature; however the role of the amygdala and its reported connections is still not well understood (**Mohanty, Sethares, Nair, & Prabhakaran, 2020**) and this can be attributed, in part, to the very small size of the amygdala. Complicating matters further is that each amygdala is made up of three distinct subregions each with its own disparate connections to other parts of the brain (**Bzdok, Laird, Zilles, Fox, & Eickhoff, 2013**; **Nieuwenhuys, Voogd, & van Huijzen, 2008**).

Spatial resolution, the currency of MRI, is referenced on voxel volume and is a measure of pixel numbers in an imaging volume. The greater the number of pixels in a voxel, the higher the spatial resolution of an image; this is a requirement for very small structures such as the amygdala to be well-resolved. Although imaging with sufficiently high spatial resolution can be accomplished using high-field strength 7T systems that possess inherently higher signal-to-noise ratio (SNR), these systems are not widely available for clinical research (**Iranpour,**

Morrot, Claise, Jean, & Bonny, 2015) and it is more challenging to achieve adequate spatial resolution to visualise amygdala activation using the lower strength 3T MRI systems that are in widespread use for this type of clinical research (**Sladky et al., 2018**).

There is reported evidence that higher resolution imaging protocols can distinguish additional activation patterns and connections in many brain areas including the amygdala, and this has been demonstrated at both 3T and 7T (**Iranpour et al., 2015**; **Sladky et al., 2018**). Additionally, some authors have reported imaging of amygdala activation using coronal and sagittal acquisition planes rather than the standard axial plane at 3T in order to improve SNR by reducing through-plane signal dephasing (**Boubela et al., 2015**; **Kim, Somerville, Johnstone, Alexander, & Whalen, 2003**). There is also evidence that different designs in radiofrequency (RF) coils used for signal reception can have significant implications for SNR and achievable spatial resolution (**Gruber, Froeling, Leiner, & Klomp, 2018**). Taking stock of the protocols in common use for fMRI data acquisition of the amygdala at 3T is the first step in potential optimisation and standardisation of protocols for improved data accuracy, reproducibility and overall quality.

Study Rationale

Variability in imaging protocols, even at the same field strength, may result in significant disparity in data output and quality. In such a compact organ as the amygdala, this variability in protocols and data quality can have major implications for accurate reporting of activation and functional connections within the brain. To our knowledge, there is no apparent standardisation of fMRI protocols for imaging activation of the amygdala at 3T in the field of neuroimaging.

Study Objective

The scoping review has been chosen as a method of summarising and disseminating findings in relation to 3T fMRI protocols in use for studying activation and functional connectivity (FC) in the amygdala and its subregions. The review will provide evidence as to current practice and document protocol disparities across clinical research facilities worldwide. It will potentially provide evidence and context for recommending that standardised and refined fMRI protocols are developed for reliably imaging activation of the amygdala. Optimised fMRI protocols applied consistently across imaging groups could lead to increased replication of findings and a greater understanding of the role of the amygdala in mental health and other conditions.

Methodology

The protocol was developed in line with the Preferred Reporting Items for Systematic reviews and Meta-Analyses extension for Scoping Reviews (PRISMA-ScR)(**Tricco et al., 2018**) and registered with the Open Science Framework (OSF). The aim is to identify and chart specific

fMRI protocol parameters and data acquisition techniques from a range of studies across multiple sites and geographic locations, the results of which will provide a transparent summary of current protocols for comparison and review by fMRI researchers. As such, this review will not extend to an appraisal of study quality.

The scoping review will follow the five steps proposed in the methodological framework of Arksey and O'Malley as outlined below (**Arksey & O'Malley, 2005**).

i. identifying the research question

ii. identifying relevant studies

iii. selection of eligible studies

iv. charting the data

v. collating, summarising and reporting the results

Step 1: Identifying the research question

The review question was developed in line with PCC (Population, Concept, Context) elements as outlined in the JBI Manual for Evidence Synthesis (Aromatis & Munn, 2020).

- Population – amygdala and subregions
- Concept – fMRI protocols
- Context – 3T

The main research question addressed in the scoping review is "What is the current 3 Tesla functional MRI protocol in research use for imaging activation of the amygdala and its subregions?"

There are five research sub-questions:

i. What was the value of the spatial resolution achieved (in mm^3)

ii. What imaging plane was utilised?

iii. Was full brain coverage achieved?

iv. What was the sequence acquisition time?

v. What type of radiofrequency (RF) coil was utilised for signal reception?

Step 2: Identifying relevant studies

As per the recommendations of Peters and colleagues, the search strategy was developed using keywords based on the research question in partnership with co-authors (MK, SL, KE) (**Peters et al., 2020**). The latter co-author, an academic librarian, subsequently recommended appropriate and relevant databases in which to conduct the searches. An initial (more complex) search strategy was piloted together with the academic librarian, during which the electronic databases listed below were searched. The combination of databases selected was based on the findings of Bramer and colleagues who reported that the combination of the first four databases listed was optimal in systematic review literature searches with an overall recall rate of 98.3% (**Bramer, Rethlefsen, Kleijnen, & Franco, 2017**). Their recommendation of the addition of Scopus as a fifth database if the number of studies identified was low was also followed.

- Medline (M)
- Embase (E)
- Web of Science (WoS)
- Google Scholar (GS)
- Scopus (S)

The search strategy was then refined and simplified, following which it was retested on the Medline and Embase databases and results compared to those of the more complex strategy. As the simple search strategy (29M and 197E) identified more studies than the more complex strategy (16M and 118E), it was chosen for the review. Results of the electronic database searches will be presented in tabular format (**Table 1**).

Search Index	Date of Search	Electronic Database	Keywords Searched	Number of Studies Retrieved	Number of Studies Selected

Table 1:

Electronic Database Search Recording Table

Keywords or Medical Subject Headings (MeSH) terms for the search encompassed the following:

- Functional Magnetic Resonance Imaging OR functional MRI OR fMRI
- Amygdal* OR amygdal* nucleus
- Functional connect* OR FC (functional connectivity)
- 3 Tesla OR 3T

A hand search of the identified/selected references for inclusion will be performed to identify other potential studies that may have been missed. Any grey (unpublished) literature identified will be examined and its suitability assessed for inclusion.

Step 3: Selection of eligible studies

In accordance with the PCC framework outlined above, titles and abstracts will be screened for suitability. Further inclusion and exclusion criteria will also be applied in order to screen out irrelevant studies.

Inclusion Criteria

- Imaging performed at 3T only
- Studies including full fMRI parameter details for extraction in methodology section
- Clinical fMRI research protocols only – acceptable imaging times (exclude research studies seeking highest resolution possible at expense of translational value)

Exclusion criteria

- Animal studies
- Qualitative studies, reviews, and conference abstracts
- Full-text studies that could not be sourced for review

Valuable information regarding paediatric protocols may be identified for comparison in the review; therefore no age limits have been specified. Similarly, a decision was made not to filter out studies in other languages at the screening stage in the interests of inclusivity; it is important to examine current practices as globally as possible. It was also deemed unnecessary to exclude studies based on a year of publication as 3 Tesla MRI systems only became clinically available in the early 2000s.

The search strategy has been refined and the full database searches will be undertaken. Identified articles will be imported into Covidence software (Version 2745 34609193) (**Covidence, 2022**). Duplicates will be identified and cross checked prior to removal in readiness for the screening process. The title and abstract screening process will be conducted by two authors (SF and IB) during April and May, 2022, following which the same authors will perform full-text screening of the studies selected for inclusion. An academic librarian will assist in obtaining full-text articles not freely available and any unresolved differences of opinion between the two reviewers as to study eligibility will be resolved by a third reviewer and reported in the review.

The recommendations outlined in the Preferred Reporting Items for Systematic Reviews and Meta-Analyses Extension for Scoping Reviews (PRISMA-ScR) checklist (**Tricco et al., 2018**) will be followed and the search and screening strategy will be charted for reporting the results for publication (**Figure 1**).

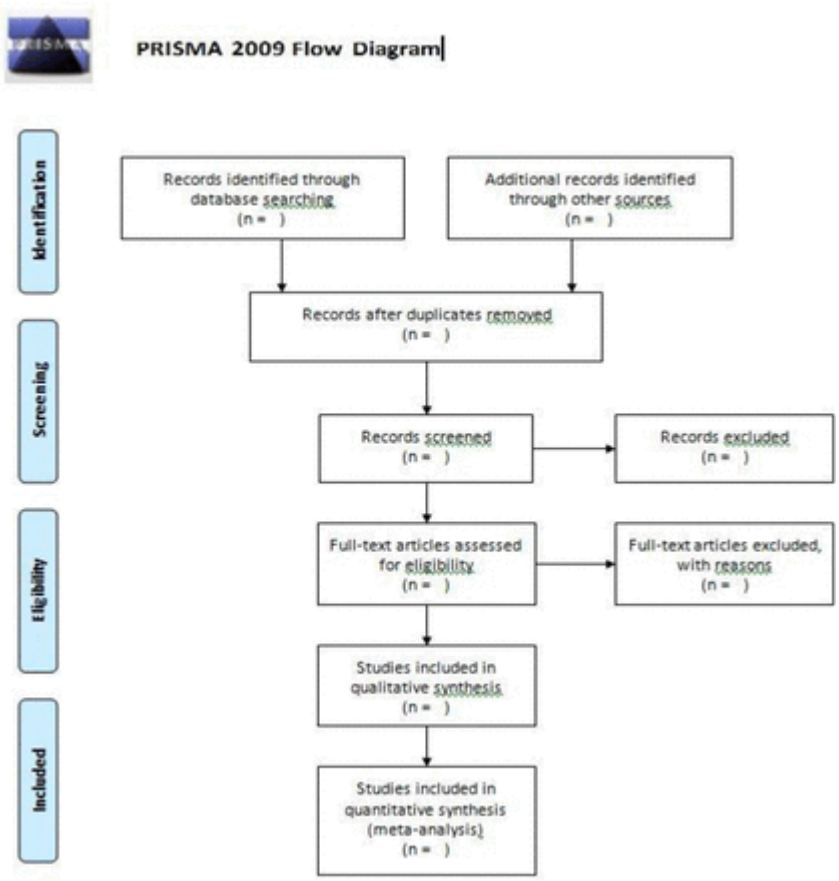

Figure 1:

PRISMA 2009 flow diagram (Moher, Liberati, Tetzlaff, Altman, & The, 2009)

Step 4: Charting the Data

In order to determine the variables for extraction a framework for charting and assessment of the data has been developed in line with the recommendations of Tricco and colleagues (**Tricco et al., 2018**). Prior to full data extraction, two reviewers will test the suitability of the charting framework on 10% of the included studies and discuss any revisions required prior to implementation. Following this process, the two reviewers, working independently to reduce the risk of bias, will use the final version of the data charting form to capture electronically the fields listed in **Table 2**.

Main Category	Description
Authors	
Title	
Journal	
Publication Year	
Type of Publication	specify whether website, journal, original research
Study Setting	specify the geographical area/healthcare or imaging setting
Study Population & Sample Size	specify age and health condition under investigation
Methodology (quantitative)	specify fMRI imaging parameters relating to spatial resolution (matrix size and slice thickness) and sequence acquisition time in minutes and seconds
Methodology (qualitative)	specify imaging plane, RF coil selection, brain coverage, sequence type
Offline Data Analysis Method	specify software programs used
Reported Outcomes	describe relevant study findings and any limitations

Table 2:

Data extraction framework

Step 5: Collating, summarising and reporting the results

The quantitative findings will be tabulated as a means of reporting an overview of the current methodologies for comparison. This will be accompanied by a narrative report summarising the extracted data in relation to the following outcomes; spatial resolution of the fMRI protocol in mm^3, plane of imaging, the type of RF coil employed and whether whole brain coverage was achieved. These results, reported together, will provide an accessible record of current practices in relation to the research question for the benefit of specialised fMRI researchers.

Discussion

The objective of this scoping review is to identify and map the range of existing protocols used in fMRI for imaging the activation and FC patterns of the amygdala at 3 Tesla; this will be achieved by collating and presenting quantitative data relating to protocol parameter choices as well as other qualitative aspects of the data acquisition process.

A preliminary limited review of the relevant literature has revealed a range of parameter selections in use in research protocols investigating the functional connectivity of the amygdala resulting in widely disparate spatial resolution values. To our knowledge this review will be the first to highlight these protocol inconsistencies in a structured and overarching manner and it likely has the potential to generate discussion and bring about review and advancement of practice in this highly specialised field.

A limitation of this review is that, due to its scoping nature, the quality of the data produced by the protocols identified will not be assessed; however the quantitative nature of the reported data together with the collated information regarding the qualitative data may prove to be a sound basis for discussion and further research built on the findings of this scoping review.

Data Availability

All data produced in the present work are contained in the manuscript

Authors' contributions

SF conceptualized the study and prepared the draft protocol under the supervision of MK and SL. SF, MK, SL and IB contributed to the development of the background, design of the study, and planned output of the research. KE advised on database selection and searches. SF and IB prepared the manuscript, and all authors reviewed, edited and approved the final manuscript for submission.

Funding

No funding was received for this study

Availability of data and materials

All data generated or analysed during this study will be included in the published scoping review manuscript

Ethics approval and consent to participate

Not applicable

Consent for publication

Not applicable

Competing Interests

The authors declare they have no competing interests

Abbreviations

fMRI

functional Magnetic Resonance Imaging;

3T

3 Tesla

RF coil

radiofrequency coil

PRISMA-ScR

Preferred Reporting Items for Systematic Reviews and Meta-Analyses Extension for Scoping Reviews

OSF

Open Science Framework

PCC

Population, Concept, Context

MeSH

Medical Subject Headings

FC

Functional Connectivity

References

Amunts, K., Kedo, O., Kindler, M., Pieperhoff, P., Mohlberg, H., Shah, N. J., … Zilles, K. (2005). Cytoarchitectonic mapping of the human amygdala, hippocampal region and entorhinal cortex: intersubject variability and probability maps. *Anatomy and Embryology*, **210**(5), 343–352. doi:10.1007/s00429-005-0025-5

Arksey, H., & O'Malley, L. (2005). Scoping studies: towards a methodological framework. *International Journal of Social Research Methodology*, **8**(1), 19–32. doi:10.1080/1364557032000119616

Boubela, R. N., Kalcher, K., Huf, W., Seidel, E.-M., Derntl, B., Pezawas, L., … Moser, E. (2015). fMRI measurements of amygdala activation are confounded by stimulus correlated signal fluctuation in nearby veins draining distant brain regions. *Scientific Reports*, **5**(1), 10499. doi:10.1038/srep10499

Bramer, W. M., Rethlefsen, M. L., Kleijnen, J., & Franco, O. H. (2017). Optimal database combinations for literature searches in systematic reviews: a prospective exploratory study. *Systematic reviews*, **6**(1), 245. doi:10.1186/s13643-017-0644-y

Bzdok, D., Laird, A. R., Zilles, K., Fox, P.T., & Eickhoff, S. B. (2013). An investigation of the structural, connectional, and functional subspecialization in the human amygdala. *Human Brain Mapping*, **34**(12), 3247–3266.

Covidence. (2022). *Covidence systematic review software*. from Veritas Health Innovation http://www.covidence.org

Glover, G. H. (2011). Overview of functional magnetic resonance imaging. *Neurosurgery clinics of North America*, **22**(2), 133–vii. doi:10.1016/j.nec.2010.11.001

Gruber, B., Froeling, M., Leiner, T., & Klomp, D. W. J. (2018). RF coils: A practical guide for nonphysicists. *Journal of magnetic resonance imaging : JMRI*, **48**(3), 590–604. doi:10.1002/jmri.26187

Huettel, S. A., Song, A. W., & McCarthy, G. (2004). *Functional magnetic resonance imaging (1st ed. ed.)*. Sunderland, Mass: Sinauer Associates.

Iranpour, J., Morrot, G., Claise, B., Jean, B., & Bonny, J.-M. (2015). Using high spatial resolution to improve BOLD fMRI detection at 3T. *PLoS ONE*, **10**(11), e0141358. doi:10.1371/journal.pone.0141358

Kim, H., Somerville, L. H., Johnstone, T., Alexander, A. L., & Whalen, P. J. (2003). Inverse amygdala and medial prefrontal cortex responses to surprised faces. *Neuroreport*, **14**(18), 2317–2322. doi:10.1097/00001756-200312190-00006

LeDoux, J. E. (2000). Emotion Circuits in the Brain. *Annual Review of Neuroscience*, **23**(1), 155–184. doi:10.1146/annurev.neuro.23.1.155

Leppänen, J. M. (2006). Emotional information processing in mood disorders: a review of behavioral and neuroimaging findings. *Current Opinion in Psychiatry*, **19**(1).

Mohanty, R., Sethares, W. A., Nair, V. A., & Prabhakaran, V. (2020). Rethinking Measures of Functional Connectivity via Feature Extraction. *Scientific Reports*, **10**(1), 1298. doi:10.1038/s41598-020-57915-w

Moher, D., Liberati, A., Tetzlaff, J., Altman, D. G., & The, P. G. (2009). Preferred Reporting Items for Systematic Reviews and Meta-Analyses: The PRISMA Statement. *PLOS Medicine*, **6**(7), e1000097. doi:10.1371/journal.pmed.1000097

Nieuwenhuys, R., Voogd, J., & van Huijzen, C. (2008). Telencephalon: amygdala and claustrum. *The human central nervous system*, 401–426.

Peters, M. D. J., Marnie, C., Tricco, A. C., Pollock, D., Munn, Z., Alexander, L., … Khalil, H. (2020). Updated methodological guidance for the conduct of scoping reviews. *JBI Evid Synth*, **18**(10), 2119–2126. doi:10.11124/jbies-20-00167

Schumann, C. M., Bauman, M. D., & Amaral, D. G. (2011). Abnormal structure or function of the amygdala is a common component of neurodevelopmental disorders. *Neuropsychologia*, **49**(4), 745–759. doi:10.1016/j.neuropsychologia.2010.09.028

Sladky, R., Geissberger, N., Pfabigan, D. M., Kraus, C., Tik, M., Woletz, M., … Windischberger, C. (2018). Unsmoothed functional MRI of the human amygdala and bed nucleus of the stria terminalis during processing of emotional faces. *NeuroImage*, **168**, 383–391.

Tricco, A. C., Lillie, E., Zarin, W., O'Brien, K. K., Colquhoun, H., Levac, D., … Straus, S. E. (2018). PRISMA Extension for Scoping Reviews (PRISMA-ScR): Checklist and Explanation. *Annals of Internal Medicine*, **169**(7), 467–473. doi:10.7326/M18-0850

APPENDIX D – CHAPTER 5 SUPPLEMENTARY MATERIALS

Table S2: Resting state network nomenclature & CONN toolbox network target regions

Resting state network nomenclature according to Yeo (left), CONN toolbox (centre). CONN toolbox network target regions (right) as shown in Results in Appendix D - Tables S3 and S4.

Yeo networks	CONN networks	Network regional target ROI names in CONN
^Default mode	Default mode	Posterior Cingulate Cortex (PCC), Left and Right Medial Prefrontal Cortex (MPFC L & R), Left and Right Lateral Parietal (LP L & R)
^Somatomotor	Sensorimotor	Left & Right Superior Left and Right Lateral
^Ventral attention	Salience	Left and Right Rostral Prefrontal Cortex (RPFC L & R) Left and Right Supramarginal Gyrus (SMG L & R) Anterior Cingulate Cortex (ACC) Left and Right Anterior Insula (Insula L & R)
Frontoparietal	Central Executive Frontoparietal*	Left and Right Posterior Parietal Cortex (PPC R & L) Left and Right Lateral Prefrontal Cortex (LPFC R & L)
Dorsal attention	Dorsal attention	Left and Right Frontal Eye Field (FEF L & R) Left and Right Intraparietal Sulcus (IPS L & R)
Visual	Visual	Medial Occipital Left and Right Lateral geniculate area (Lateral L & R)
Limbic*		Left and Right Temporal poles Left and right Ventral anterior temporal lobes Orbitofrontal Cortex
	Language*	Left and Right Inferior Frontal Gyrus (IFG L & R) Left and Right Posterior Superior Temporal Gyrus (pSTG L & R)
	Cerebellar*	Anterior Posterior

^ denotes network-of-interest

** denotes variation in network names between the two naming schemes*

Other network to subregion connectivity – 2D and 3D sequences

Although the focus of this work was on three networks-of-interest, results for connections to three other networks, Frontoparietal, Dorsal Attention and Visual, were also identified and recorded. For the 2D sequence, connections between regions of the Frontoparietal network and all six subregions were identified, with three connections from two subregions, the right LB and right SF, reaching significance at p-FDR < 0.05 despite the small sample size. Connections between the Dorsal Attention network and right SF, and between the Visual network and right CM were also identified. In total, 19 individual connections between these three other resting state networks and all six subregions were identified (Table S3).

For the 3D sequence, connections between regions of the Frontoparietal network and five of the six subregions were identified. Two connections between the Visual network and the right CM were identified, as well as six connections between the Dorsal Attention network and both right and left CM, and right and left SF. One result, Dorsal Attention Network to left CM, reached significance at p-FDR < 0.05 despite the small sample size. In total, 16 individual connections between the three other resting state networks and five of the six subregions were identified (Table S4).

Table S3: Resting-State ROI to ROI Functional Connectivity results for 2D sequence between amygdala subregions and other networks

Subregional ROI_2D	Target Network in CONN	T-statistic	p-unc < 0.05
Centromedial			
R_CM_2D	^Fronto Parietal.PPC (R)	-3.26	0.010
R_CM_2D	^Visual.Occipital	-3.2	0.011
R_CM_2D	Fronto Parietal.LPFC (R)	-3.09	0.013
R_CM_2D	Fronto Parietal.PPC (L)	-2.53	0.032
L_CM_2D	^Fronto Parietal.PPC (R)	-4.07	0.003
L_CM_2D	^Fronto Parietal.PPC (L)	-2.51	0.033
L_CM_2D	Fronto Parietal.LPFC (R)	-2.37	0.042
Laterobasal			
R_LB_2D	^Fronto Parietal.PPC (R)	-5.74	*0.000
R_LB_2D	Fronto Parietal.PPC (L)	-2.65	0.027
R_LB_2D	Fronto Parietal.LPFC (L)	-2.29	0.048
L_LB_2D	Fronto Parietal.PPC (R)	-3.03	0.014
Superficial			
R_SF_2D	^Fronto Parietal.LPFC (R)	-4.97	*0.001
R_SF_2D	^Fronto Parietal.LPFC (L)	-4.15	*0.002
R_SF_2D	Fronto Parietal.PPC (R)	-2.82	0.020
R_SF_2D	^Dorsal Attention.FEF (R)	-2.57	0.030
R_SF_2D	Dorsal Attention.IPS (L)	-2.46	0.036
L_SF_2D	^Fronto Parietal.LPFC (R)	-3.97	0.003
L_SF_2D	^Fronto Parietal.LPFC (L)	-3.44	0.007
L_SF_2D	Fronto Parietal.PPC (R)	-3.11	0.012

See Table S2 in Appendix D for network region nomenclature

^ *indicates same network connection with both 2D and 3D sequences*

* *indicates significant result corrected for multiple comparisons at p-FDR < 0.05*

Table S4: Resting-State ROI to ROI Functional Connectivity results for 3D sequence between amygdala subregions and other network regions

Subregional ROI_3D	Target Network in CONN	T-statistic	p-unc < 0.05
Centromedial			
R_CM_3D	Dorsal Attention.FEF (L)	-2.57	0.030
R_CM_3D	Visual.Medial	-2.47	0.036
R_CM_3D	^Visual.Occipital	-2.44	0.037
R_CM_3D	^Fronto Parietal.PPC (R)	-2.33	0.045
L_CM_3D	Dorsal Attention.FEF (L)	-4.88	*0.001
L_CM_3D	^Fronto Parietal.PPC (R)	-3.16	0.012
L_CM_3D	^Fronto Parietal.PPC (L)	-2.41	0.039
Laterobasal			
R_LB_3D	^Fronto Parietal.PPC (R)	-3.32	0.009
L_LB_3D	No results		
Superficial			
R_SF_3D	Dorsal Attention.IPS (L)	-3.62	0.006
R_SF_3D	Dorsal Attention.IPS (R)	-3.61	0.006
R_SF_3D	^Fronto Parietal.LPFC (R)	-3.36	0.008
R_SF_3D	^Dorsal Attention.FEF (R)	-3.14	0.012
R_SF_3D	^Fronto Parietal.LPFC (L)	-2.54	0.032
L_SF_3D	^Fronto Parietal.LPFC (L)	-4.14	0.003
L_SF_3D	Dorsal Attention.FEF (R)	-2.42	0.038
L_SF_3D	^Fronto Parietal.LPFC (R)	-2.41	0.039

See Table S2 in Appendix D for network region nomenclature

^ *indicates same network connection with both 2D and 3D sequences*

* *indicates significant result at p-FDR < 0.05*

Technical Considerations - 2D versus 3D sequences

A significant theoretical benefit of the 3D strategy is its inherently high temporal resolution which can potentially be converted into either shorter TRs to achieve more volume measurements or overall reduced acquisition times or, alternatively, higher spatial resolution whilst keeping the same TR (Poser et al., 2010). The latter option is a primary advantage of the 3D technique as, in practical terms, increased temporal resolution allows whole brain coverage with high through-plane resolution. As temporal and spatial resolution have an inverse relationship, high resolution 2D studies may require strategically selected coverage, depending on both the study primary end point and concomitant through-plane resolution requirements. In order to capture thin slices of the target area within a reasonable TR period, coverage may be limited, precluding subsequent evaluation of whole brain connectivity. Additionally, tissue contrast variations can be exacerbated due to slice profile imperfections that more commonly affect 2D acquisitions with thinner slices (Afacan et al., 2012). The single phase encoding direction and multiband acceleration required to achieve shorter TRs in the 2D sequence are replaced by a second phase encoding direction, effectively a slice encoding direction in the 3D sequence, which has the added SNR bonus of exciting the whole brain volume in one TR period, thereby negating slice profile issues (Afacan et al., 2012; Poser et al., 2010) .

A crucial element of its superior temporal resolution is the construction of the pulse sequence timing elements of the 3D sequence. Suppression or removal of fat signal is a requirement for fMRI studies due to the potential for lipid artifacts to degrade image quality (Seginer et al., 2021); however, the two different methods used accrue appreciably different time penalties. The 2D sequence relies on the Chemical Shift Selective technique which requires a separate RF pulse at the beginning of every TR period to selectively excite the fat protons, followed by a crusher gradient pulse to eliminate their signal contribution (Stirnberg et al., 2016). Aside from the SAR implications of multiple additional RF pulses, this combination can effectively occupy up to 20% of the TR period, during which no data acquisition occurs. The 3D sequence in this study has a different strategy to remove the fat signal; a rapid narrowband water excitation scheme employs a binomial 1 2 1 pulse triplet that selectively excites the water protons without the requirement for subsequent fat proton dephasing, resulting in less than 10% of the TR period being unavailable for data acquisition. Aside from SAR reductions and time savings, a further advantage over the 2D sequence is that SNR is not lost through the application of multiple fat suppression pulses (Stirnberg et al., 2017). If required, use of a faster bipolar 1 1 water excitation pulse can further reduce TR and subsequent acquisition time with

an added benefit of allowing shorter echo times; however, the trade-off is increased likelihood of suboptimal fat suppression at either end of the imaging volume (Siemens Healthineers Applications guide, WIP #1043A_v3).

Both sequences in this study also benefited from the use of acceleration to improve temporal resolution. The total acceleration factor for the 3D sequence was four compared with six for the 2D sequence. 2D acceleration was achieved using a combination of two methods: parallel imaging (acceleration factor of 2) and multiband or simultaneous multislice technique (acceleration factor of 3). The parallel imaging technique undersamples k-space in the phase encoding direction, and the time saving is predicated on the acceleration factor R; for example, in the case of R = 2, the scan time is effectively halved. However, the penalty is a reduction in SNR proportional to the square root of the acceleration factor multiplied by the geometry factor and can be calculated using the equation below where SNR_{PI} equates to the SNR of the image acquired with parallel imaging, SNR_0 is the SNR of the image had it been acquired without parallel imaging, g is the g-factor or coil geometry factor and R is the acceleration factor.

$$SNR_{PI} = \frac{SNR_0}{g\sqrt{R}}$$

The g-factor or noise amplification factor is spatially variant and determined by the coil geometry and sensitivity profiles of the receiver coil used for signal reception as well as the aliasing patterns in the resultant images (Breuer et al., 2009; Robson et al., 2008). G-factor noise enhancement is typically seen centrally in images where the likelihood of pixels aliasing together is higher (Figure S1), most notably in the setting of highly accelerated sequences (Todd et al., 2017).

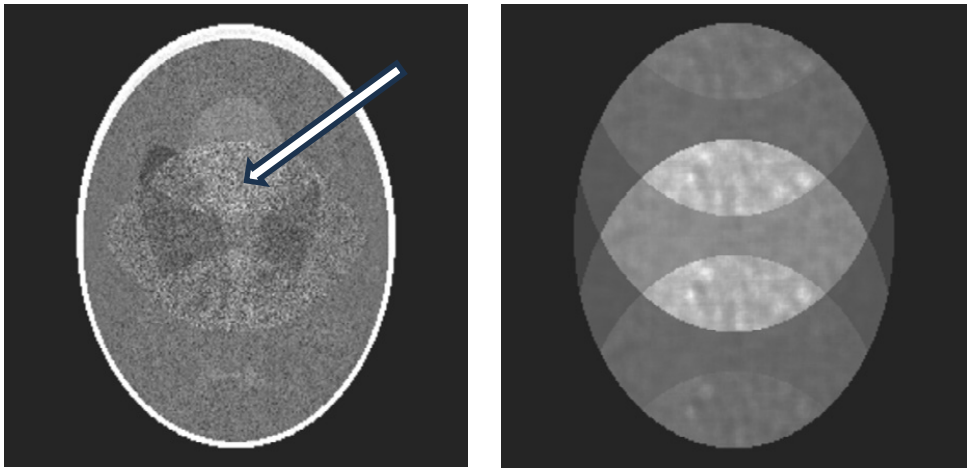

Figure S 1: Thermal noise and g-factor effects on SNR

Left: Low SNR reconstructed image (R=4); Right: g-factor map. Note low SNR area centrally on left (white arrow) in region of multiple overlapping pixels corresponding to higher g-factor regions. Adapted from (Cummings et al., 2022).

The g-factor also comes into play in terms of thermal noise contributions attributed to the subject in the scanner and the associated MR system electronics. Higher levels of parallel imaging tend to increase g-factor values and amplify thermal noise contributions, the value of which is dependent on field strength, TR and VV, with contributions greater at lower field strengths, shorter TR values and smaller VV (Triantafyllou et al., 2005; Vizioli et al., 2021). Extrapolations from data acquired at 7T have demonstrated that imaging with a high spatial resolution 3D GRE-EPI sequence at 3T has the potential for increased efficiency due to reductions in the thermal noise contribution, resulting in higher tSNR (Lutti et al., 2013). Several studies have reported higher tSNR values in 3D sequences compared to 2D sequences due to lower g-factor values associated with less acceleration (Lutti et al., 2013; Stirnberg et al., 2017) as well as the potential to share k-space undersampling between two phase encoding directions (Poser et al., 2010).

The second method of acceleration in the 2D sequence, the use of a multiband pulse to excite several slices simultaneously, allows an effective decrease in the TR value required to achieve thin slice whole brain coverage. Although the multiband technique does not inherently incur a SNR penalty, if the TR value is lower than the T1 of the tissues being imaged, SNR is effectively reduced as the tissues may not recover optimum levels of longitudinal magnetisation, resulting in a steady state with lower SNR and potentially altered tissue

contrast (Barth et al., 2016; Setsompop et al., 2012). Reconstruction artifacts such as residual aliasing and Nyquist-like ghosting from eddy currents generated by the rapidly switching gradients can also result from multiband use, especially at higher factors (Barth et al., 2016).

The inherently higher temporal resolution achieved by the 3D acquisition strategy precludes the need for excessive k-space undersampling which can notionally be performed in two planes as a means of acceleration to shorten the overall acquisition time. Although theoretically more time-efficient, the 3D acquisition strategy is more susceptible to motion than the 2D strategy due to the requirement for longer signal sampling times, that is, for a volume versus slice sampling; thus, the potential for greater motion effects in 3D acquisitions (Poser et al., 2010). Previous work has identified 3D sequences as being particularly susceptible to physiological motion, predominantly cardiac pulsations but also respiration, with increased potential for artifact generation due to motion and flow sensitivity (Afacan et al., 2012; Klein-Flügge et al., 2022; Tijssen et al., 2011).

In this setting, image acceleration in the form of parallel imaging can effectively decrease the 3D volume TR, a method that has been shown to reduce the impact of cardiac and respiratory physiological effects that manifest as signal fluctuations in the low frequency range (Stirnberg et al., 2017). Aliasing issues can arise at traditional TR values of around 3 seconds, as the sampling rate is too low to adequately differentiate these low frequency signals from the resting-state signals typically seen at < 0.1 Hz. A combination of shorter TR, noise regression and low-pass filtering can account for these unwanted signals (Narsude et al., 2016). Interestingly, in comparison to 2D data, physiological noise correction has been shown to enhance 3D data preferentially by increasing tSNR levels, with one study reporting higher FC values in the Default Mode, Motor and Visual networks with a 3D sequence (Stirnberg et al., 2017) and another reporting marked improvements in detection of six resting-state networks following physiological noise correction even at a relatively long TR of 3180ms (Narsude et al., 2016). In a comparison with a 2D GRE-EPI sequence with 1.5mm isotropic voxels, one study reported tSNR gains of more than 30% when using a 3D sequence combined with physiological noise correction during analysis (Lutti et al., 2013).

The 3D GRE-EPI sequence, a works-in-progress sequence provided by Siemens Healthineers (Erlangen, Germany) for the purposes of this study, was a segmented (multi-shot) sequence with “controlled aliasing in parallel imaging results in higher acceleration” or CAIPIRINHA acceleration (a 3D acceleration factor of 4 and a factor of one in the phase encoding direction

for a total acceleration of 4) and a reordering shift of 2. CAIPIRINHA blipped and segmented sampling patterns similar to that used in this sequence have been shown to achieve reductions in g-factor over conventional sampling patterns (Setsompop et al., 2012). The total or volume TR (2160ms) is calculated by the product of the number of partitions (40), the number of shots per partition (1), and the per-shot TR (54ms). As the overarching purpose of this study was to investigate high spatial resolution capabilities, the 3D sequence was tailored towards smaller VVs at the expense of temporal resolution for whole brain coverage; therefore, phase and slice Fourier reduction, another form of k-space undersampling designed to increase acquisition speed, were not employed. If necessary, further temporal resolution gains can be made in 3D acquisition strategies by employing variable echo train lengths, using an elliptical k-space mask and skipping acquisition of data points external to the mask (Stirnberg et al., 2014). In the setting of increased temporal performance of the 3D sequence, this may be an appealing option for studies wishing to maintain statistical power whilst reducing scan time, thus providing an opportunity for reductions in imaging costs or, alternatively, increases in cohort size.

Both versions of the GRE-EPI sequence in this study are considered high resolution with voxel volumes of 20mm^3 or less (Olman & Yacoub, 2011). The VV of the 2D sequence was almost twice that of the 3D sequence, therefore, with all other parameters being equal, SNR and tSNR levels are theoretically higher for the 2D sequence as shown in Chapter Five. Further, the volume TR was longer in the 3D sequence than the 2D sequence which had been previously optimised for clinical research. In practical terms, this resulted in fewer volumes acquired for the 3D sequence than the 2D sequence to obtain the same total acquisition time of just over 8 minutes. Theoretically, increased signal averaging also benefits tSNR levels in the 2D sequence. Nevertheless, the volume excitation technique coupled with 3D Fourier encoding strategy has been shown to provide relatively large tSNR gains over the 2D slice-by-slice acquisition method (Graedel et al., 2017). Previous work has shown that a similar 3D sequence to that used in this study outperformed its 2D counterpart in terms of tSNR, most notably in the centrally located white matter of the brain. They also reported increases of 1.5 times the tSNR levels in subcortical regions including the thalamus, caudate, putamen, hippocampus and amygdala, with the authors attributing these findings to several technical factors; a lower g-factor resulting from lower acceleration requirements, variations in T1 contrast generated by the different acquisition strategies and the implementation of physiological noise correction (Stirnberg et al., 2017).

Notwithstanding the potential for inaccuracy due to the differing VV and acquisition strategies in the 2D and 3D sequences used in this small pilot study, a rudimentary comparison revealed approximately 2.6 times more tSNR centrally in the approximate location of the amygdala in the 3D sequence compared to the 2D sequence, albeit the 3D VV was approximately half that of the 2D sequence. This result requires cautious interpretation for several reasons. Firstly, the simple method of tSNR calculation utilising ImageJ software (Schneider et al., 2012) lacked precision, favouring the 3D acquisition. Due to inherent differences in pixel sizes (in-plane resolution) the elliptical ROI used in the 3D calculation was slightly larger than that used in the 2D sequence (96mm^2 vs 84mm^2). Additionally, as the ROI was positioned very close to the skull base in order to replicate tSNR values in the actual amygdala location, the larger voxels of the 2D sequence may have suffered a greater degree of intra-voxel dephasing due to the heterogeneity of tissue types, such as air and bone, thereby reducing the detectable tSNR levels. However, the approximate figures produced by these basic calculations may potentially be a closer representation of the actual values than those calculated by averaging results across a range of subcortical regions. Structures such as the thalamus, caudate and putamen are more ideally located in terms of being less prone to susceptibility artifacts, resulting in more homogeneous voxels that should theoretically result in increased tSNR. Examples of ROI positions for tSNR calculations are located in Appendix D.

The temporal lobes, the location of the amygdala, are especially affected by physiological noise during data acquisition due to inherently longer signal sampling times (Klein-Flügge et al., 2022; Poser et al., 2010). As individual physiological noise regression was unable to be performed during data analysis, the anatomical component-based noise correction procedure (aCompCor) (Behzadi et al., 2007), part of the CONN default denoising pipeline that accounts for confounding noise components from white matter and cerebrospinal fluid, was used for noise correction in both 2D and 3D analyses. As there are multiple reports of superior findings using a 3D sequence combined with individual physiological data correction (Lutti et al., 2013; Reynaud et al., 2017; Stirnberg et al., 2017), it is reasonable to assume that the 3D sequence used in the present study may have underperformed in its absence. In fact, Klein-Flugge and colleagues investigated tSNR levels following data analysis with and without individual physiological noise correction in the amygdala and subsequently reported significant tSNR increases, noting that subcortical brain regions benefited most from this method of motion correction (Figure S2) (Klein-Flügge et al., 2022).

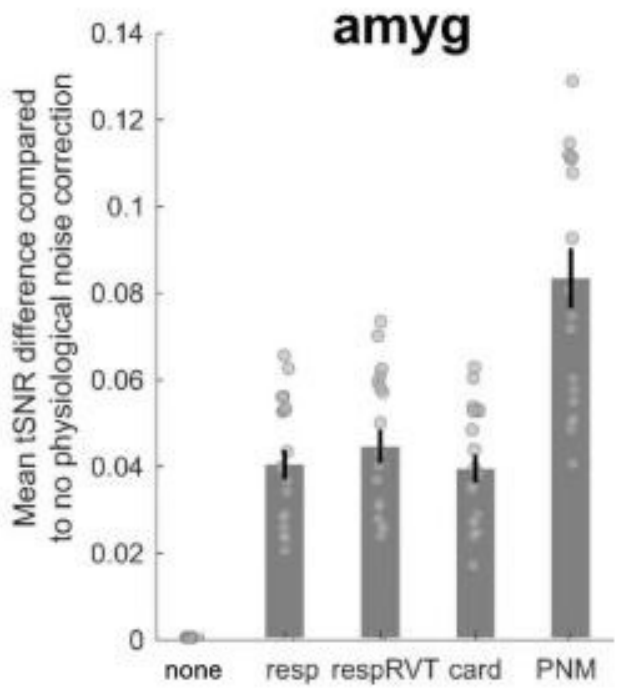

Figure S 2: Increases in tSNR in amygdala with physiological noise correction

Increases in tSNR in amygdala (amyg) relative to a baseline of no physiological noise correction (none), respiratory (resp), respiratory + respiratory volume (respRVT), cardiac (card) and a combination of all three (PNM). Adapted from (Klein-Flügge et al., 2022).

2D and 3D Study Results Variability Related to Technical Considerations

In relation to the work in this thesis, the variability in findings can be attributed to several technical factors. Firstly, making direct comparisons between the two sequences is problematic. As noted, the spatial resolution, although considered high for both these sequences acquired in the brain, was quite different. Secondly, the repetition times of the two sequences differed; ideally, the repetition times (TR) should be matched for sequence comparison. In our case, the TR of the 2D sequence was 1.5 seconds whereas the TR for the 3D sequence was 2.16 seconds. Maximal cardiorespiratory aliasing in central brain regions occurs at TR values of between 1 and 2 seconds, and this has been reported to affect data quality; hence, the TR value of the 2D sequence is a potential explanation for its poorer performance in the study in Chapter Six.

Additionally, as also noted, the alternate k-space acquisition strategy of the 3D sequence gives it a competitive SNR advantage over the 2D sequence, especially in deep central subcortical

brain regions. This drives the potential for even smaller voxels, noting that the spatial resolution of the 3D sequence was approximately twice as high as that of the 2D sequence; that is, the voxel volumes were approximately half (at $8mm^3$). This is likely responsible for the superior performance of the 3D sequence as discussed in Chapter Six.

It was interesting to note that the 2D outperformed the 3D in the study in Chapter Five, and this result was attributed to the longer echo time of the sequence optimised for cortical (rather than subcortical) connectivity. The TE of the 2D sequence was longer than that of the 3D sequence (33 milliseconds versus 28 milliseconds), reflecting its traditional role in investigating mainly cortical activation and connectivity. Echo times are optimal when maximum BOLD contrast is achieved, and this relates to differences in T2* signal decay and varies with field strength (Puckett et al., 2018). At 3T, selecting a TE value for fMRI data acquisition involves compromise between BOLD sensitivity and SNR loss; longer TE values can result in greater signal dephasing and lower SNR. Values between 30 and 35ms are typically used for 2D investigation of cortical activation and connectivity at 3T (Kang et al., 2023).

However, as the 3D sequence was optimised for interrogating the amygdala, a subcortical structure, its TE value was shorter at 28 ms. Previous studies have shown that some subcortical regions possess higher iron concentrations than cortical regions, manifesting as shorter T2* values. Similarly, these regions are affected by increased susceptibility issues due to their location adjacent to the skull base. Use of shorter echo times can counter the reduction in SNR that accompanies shorter T2* values, thus optimising BOLD sensitivity in these subcortical regions (Miletić et al. 2020).

Signal-to-noise ratio (SNR) and Mean Pixel Value (MPV) information – 2D vs 3D

Measurements of SNR across the time series (tSNR) for all ten participants were obtained in central and peripheral locations via ROI placement in the same position for all participants. For central SNR measurements, the first ROI was positioned over the region of the right amygdala whilst the second was located outside the image in the top corner of the field-of-view on the same side. See Figure S3 for examples of amygdala ROI placement for 2D and 3D sequences for central SNR measurements. For the peripheral SNR measurements, the first ROI was positioned in the right occipital region and the second was located outside the image as previously described. See Figure S4 for example of occipital ROI placement for peripheral SNR measurement and Figure S5 for examples of all ROI placements.

Measurements were obtained by dividing the mean signal firstly in the central amygdala ROI by the standard deviation of the noise within the second ROI using a correction factor of 1.53 to account for the non-Gaussian Rayleigh distribution of noise. This process was repeated using the second peripheral ROI. Due to different acquisition strategies resulting in different levels of spatial resolution, the ROI sizes differed. For the 2D sequence the elliptical ROI measured six pixels by three pixels and for the 3D sequence the ROI measured seven pixels by four pixels. The circular background ROIs had a diameter of 15 pixels for both datasets. The software used was ImageJ version 1.52c and data were analysed in Microsoft Excel.

Two outliers were noted in the central and peripheral SNR results. Datasets 2 and 3 recorded notably higher SNR levels than the other eight datasets. This was attributed to a radiofrequency coil element failure in the right anterior region of the head coil, which resulted in lower levels of noise in the area outside the field-of-view where the background ROI was positioned. This was confirmed during the regular weekly coil quality control check implemented at our site. Figures S6 and S7 represent SNR differences between the two sequences after excluding the two outliers.

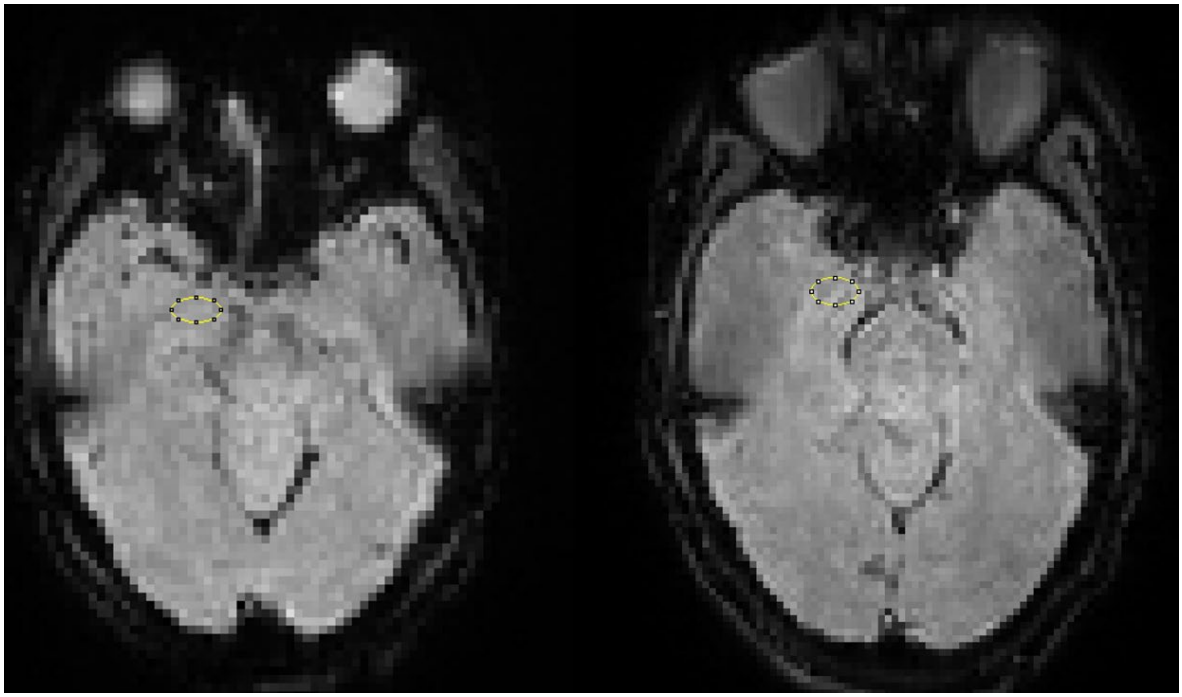

Figure S 3: ROI placements for central (amygdala) SNR and MPV calculations

Left: 2D sequence. Right: 3D sequence.

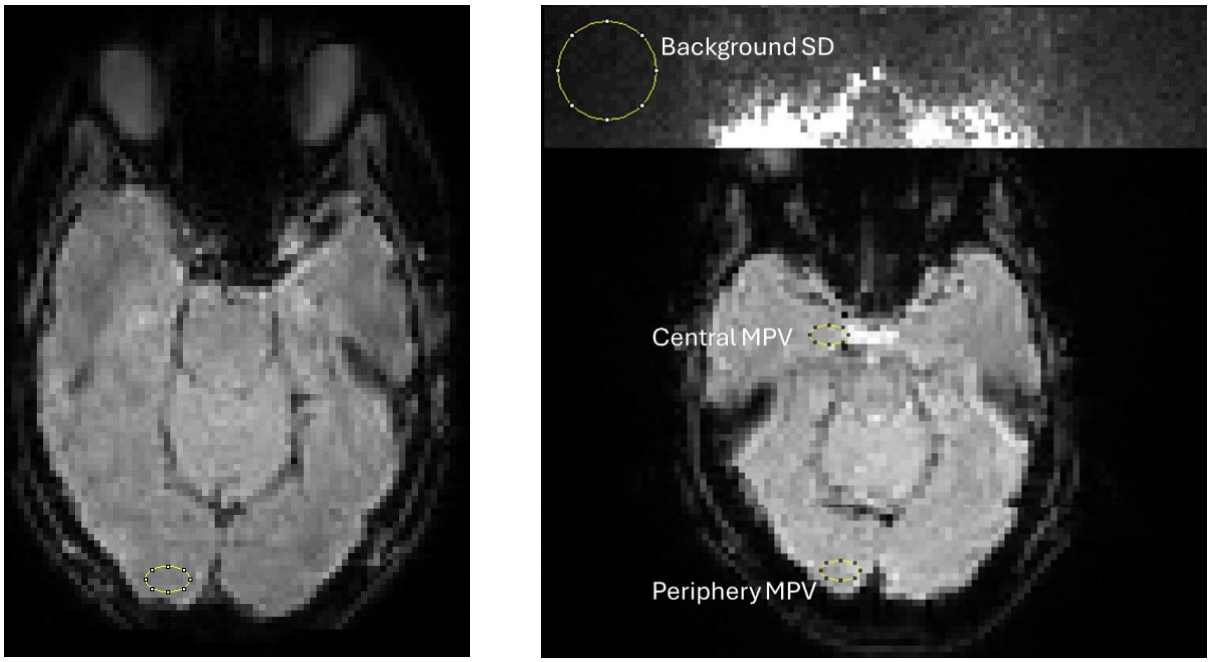

Figures S4 & S5: Examples of ROI placements for all SNR and MPV calculations

S4 (left): peripheral and S5 (right) all three ROI locations including background ROI

Figure S6: Central SNR values averaged over 8 datasets – 2D vs 3D

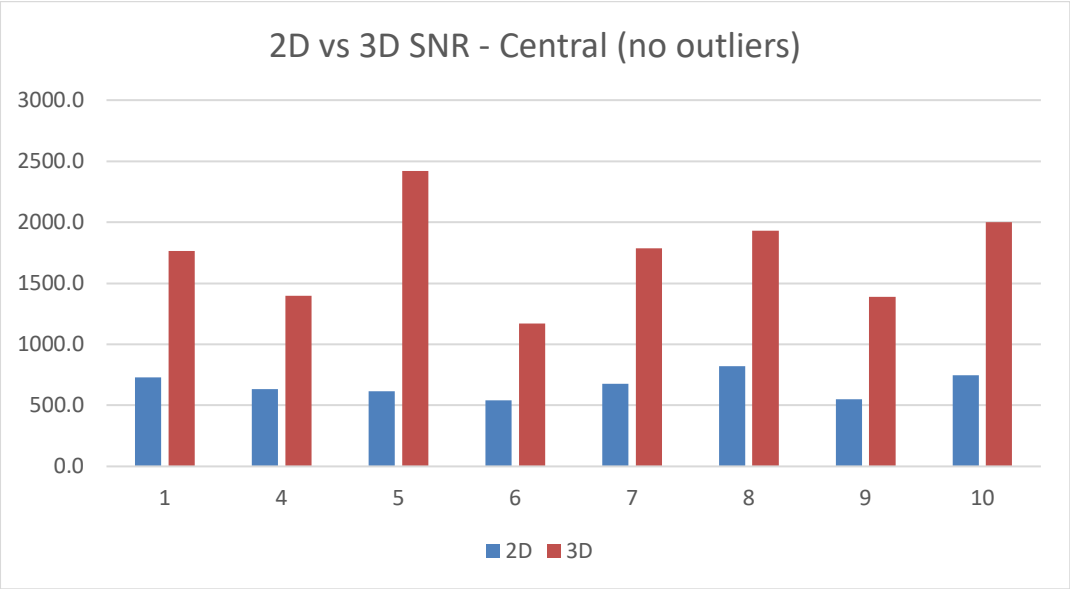

Note: Outliers excluded. Average SNR of 3D sequence up to 2.6 times higher centrally despite VV half that of 2D sequence. See technical discussion in Appendix D

Figure S7: Peripheral SNR values averaged over 8 datasets – 2D vs 3D

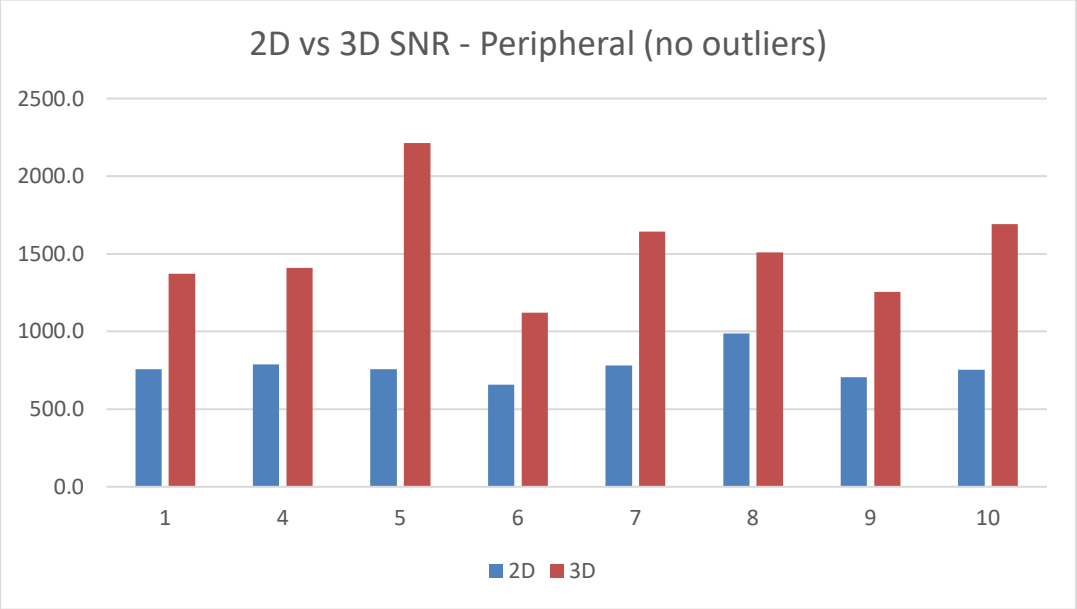

Note: Outliers excluded. Average SNR of 3D sequence up to 1.9 times higher peripherally despite VV half that of 2D sequence. See technical discussion in Appendix D

Mean Pixel Values (MPV) provide a measure of the mean signal intensity for each image in the time series. For MRI, the mean signal intensity is the average signal of the voxels in the region averaged over the time series. The MPVs within the ROIs as demonstrated in Figures S8 (central) and S9 (peripheral) show that, although the 3D VV is approximately only half that of the 2D VV, its average MPV across all datasets approaches 90% of the 2D values centrally and 67% of the 2D values peripherally. The benefits of smaller voxels in terms of improved signal due to fewer signal losses associated with larger voxels is discussed in Chapter Two.

Figure S8: Central Mean Pixel Values – 2D vs 3D

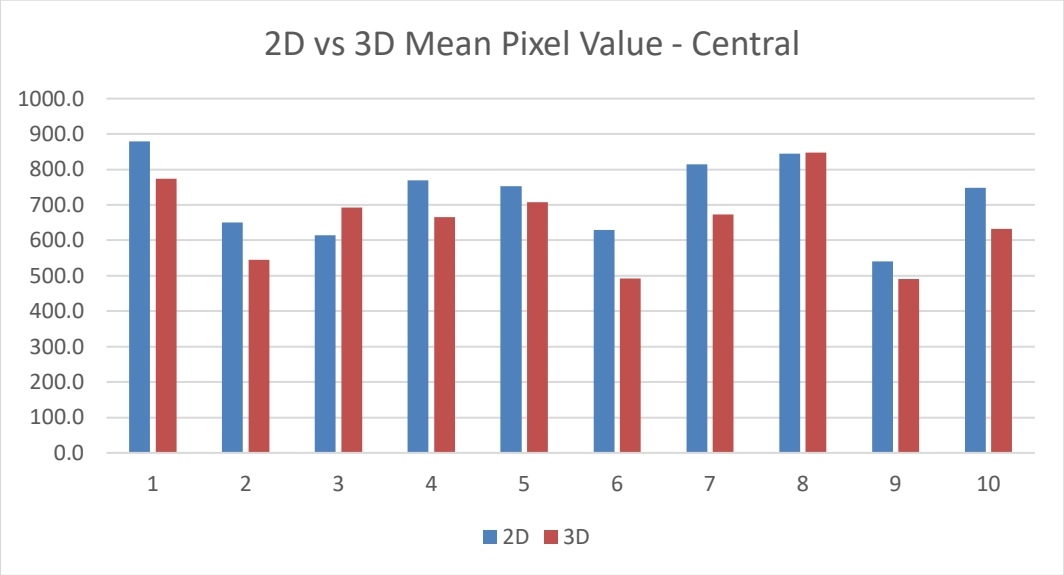

Figure S9: Peripheral Mean Pixel Values – 2D vs 3D

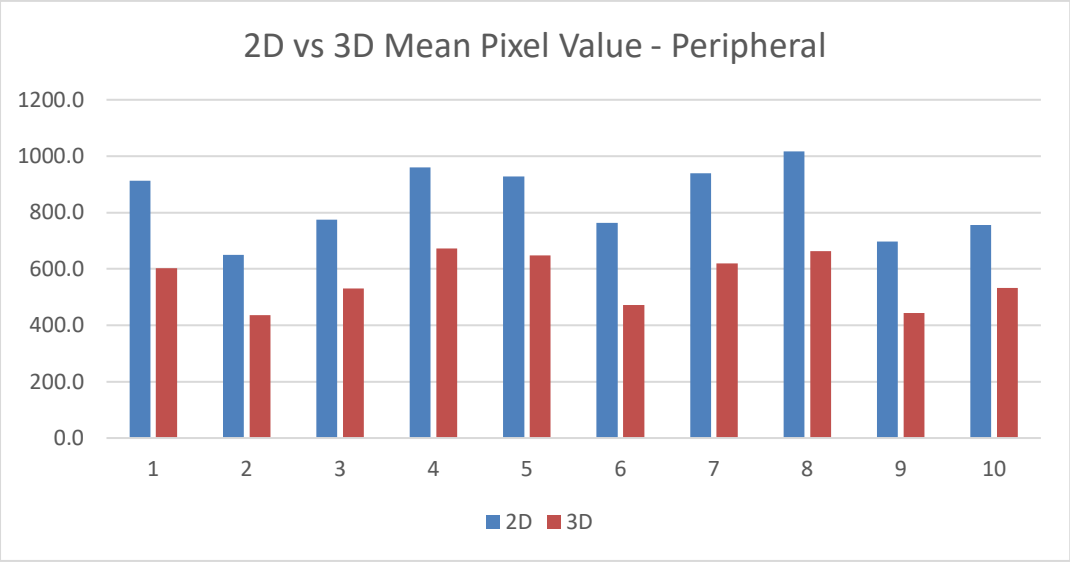

Note: Values representative of amount of signal per voxel measured over all images in the time series

Supplementary References

Afacan, O., Hoge, W. S., Janoos, F., Brooks, D. H., & Morocz, I. A. (2012). Rapid full-brain fMRI with an accelerated multi shot 3D EPI sequence using both UNFOLD and GRAPPA. *Magnetic Resonance in Medicine*, *67*(5), 1266-1274. https://doi.org/10.1002/mrm.23106

Barth, M., Breuer, F., Koopmans, P. J., Norris, D. G., & Poser, B. A. (2016). Simultaneous multislice (SMS) imaging techniques. *Magn Reson Med*, *75*(1), 63-81. https://doi.org/10.1002/mrm.25897

Behzadi, Y., Restom, K., Liau, J., & Liu, T. T. (2007). A component based noise correction method (CompCor) for BOLD and perfusion based fMRI. *Neuroimage*, *37*(1), 90-101. https://doi.org/10.1016/j.neuroimage.2007.04.042

Breuer, F. A., Kannengiesser, S. A., Blaimer, M., Seiberlich, N., Jakob, P. M., & Griswold, M. A. (2009). General formulation for quantitative G-factor calculation in GRAPPA reconstructions. *Magn Reson Med*, *62*(3), 739-746. https://doi.org/10.1002/mrm.22066

Cummings, E., Macdonald, J. A., & Seiberlich, N. (2022). Chapter 6 - Parallel Imaging. In M. Akçakaya, M. Doneva, & C. Prieto (Eds.), *Advances in Magnetic Resonance Technology and Applications* (Vol. 7, pp. 129-157). Academic Press. https://doi.org/10.1016/B978-0-12-822726-8.00016-6

Graedel, N. N., McNab, J. A., Chiew, M., & Miller, K. L. (2017). Motion correction for functional MRI with three-dimensional hybrid radial-Cartesian EPI. *Magnetic Resonance in Medicine*, *78*(2), 527-540. https://doi.org/10.1002/mrm.26390

Kang, D., In, M.-H., Jo, H. J., Halverson, M. A., Meyer, N. K., Ahmed, Z., Gray, E. M., Madhavan, R., Foo, T. K., Fernandez, B., Black, D. F., Welker, K. M., Trzasko, J. D., Huston, J., Bernstein, M. A., & Shu, Y. (2023). Improved Resting-State Functional MRI Using Multi-Echo Echo-Planar Imaging on a Compact 3T MRI Scanner with High-Performance Gradients. *Sensors*, *23*(9), 4329.

Klein-Flügge, M. C., Jensen, D. E. A., Takagi, Y., Priestley, L., Verhagen, L., Smith, S. M., & Rushworth, M. F. S. (2022). Relationship between nuclei-specific amygdala connectivity and mental health dimensions in humans. *Nature Human Behaviour*, *6*(12), 1705-1722. https://doi.org/10.1038/s41562-022-01434-3

Lutti, A., Thomas, D. L., Hutton, C., & Weiskopf, N. (2013). High-resolution functional MRI at 3 T: 3D/2D echo-planar imaging with optimized physiological noise correction. *Magn Reson Med*, *69*(6), 1657-1664. https://doi.org/10.1002/mrm.24398

Miletić, S., Bazin, P.-L., Weiskopf, N., van der Zwaag, W., Forstmann, B. U., & Trampel, R. (2020). fMRI protocol optimization for simultaneously studying small subcortical and

cortical areas at 7 T. *Neuroimage*, *219*, 116992. https://doi.org/https://doi.org/10.1016/j.neuroimage.2020.116992

Narsude, M., Gallichan, D., van der Zwaag, W., Gruetter, R., & Marques, J. P. (2016). Three-dimensional echo planar imaging with controlled aliasing: A sequence for high temporal resolution functional MRI. *Magnetic Resonance in Medicine*, *75*(6), 2350-2361. https://doi.org/10.1002/mrm.25835

Olman, C. A., & Yacoub, E. (2011). High-field FMRI for human applications: an overview of spatial resolution and signal specificity. *Open Neuroimag J*, *5*, 74-89. https://doi.org/10.2174/1874440001105010074

Poser, B. A., Koopmans, P. J., Witzel, T., Wald, L. L., & Barth, M. (2010). Three dimensional echo-planar imaging at 7 Tesla. *Neuroimage*, *51*(1), 261-266. https://doi.org/10.1016/j.neuroimage.2010.01.108

Puckett, A. M., Bollmann, S., Poser, B. A., Palmer, J., Barth, M., & Cunnington, R. (2018). Using multi-echo simultaneous multi-slice (SMS) EPI to improve functional MRI of the subcortical nuclei of the basal ganglia at ultra-high field (7T). *Neuroimage*, *172*, 886-895. https://doi.org/10.1016/j.neuroimage.2017.12.005

Reynaud, O., Jorge, J., Gruetter, R., Marques, J. P., & van der Zwaag, W. (2017). Influence of physiological noise on accelerated 2D and 3D resting state functional MRI data at 7 T. *Magnetic Resonance in Medicine*, *78*(3), 888-896. https://doi.org/10.1002/mrm.26823

Robson, P. M., Grant, A. K., Madhuranthakam, A. J., Lattanzi, R., Sodickson, D. K., & McKenzie, C. A. (2008). Comprehensive quantification of signal-to-noise ratio and g-factor for image-based and k-space-based parallel imaging reconstructions. *Magn Reson Med*, *60*(4), 895-907. https://doi.org/10.1002/mrm.21728

Schneider, C. A., Rasband, W. S., & Eliceiri, K. W. (2012). NIH Image to ImageJ: 25 years of image analysis. *Nature Methods*, *9*(7), 671-675. https://doi.org/10.1038/nmeth.2089

Seginer, A., Furman-Haran, E., Goldberg, I., & Schmidt, R. (2021). Reducing SAR in 7T brain fMRI by circumventing fat suppression while removing the lipid signal through a parallel acquisition approach. *Sci Rep*, *11*(1), 15371. https://doi.org/10.1038/s41598-021-94692-6

Setsompop, K., Gagoski, B. A., Polimeni, J. R., Witzel, T., Wedeen, V. J., & Wald, L. L. (2012). Blipped-controlled aliasing in parallel imaging for simultaneous multislice echo planar imaging with reduced g-factor penalty. *Magn Reson Med*, *67*(5), 1210-1224. https://doi.org/10.1002/mrm.23097

Stirnberg, R., Brenner, D., & Stöcker, T. (2014). Variable flip angles and echo train lengths in segmented 3d-EPI at 3 and 7 Tesla. Proc. Intl. Soc. Mag. Reson. Med,

Stirnberg, R., Brenner, D., Stöcker, T., & Shah, N. J. (2016). Rapid fat suppression for three-dimensional echo planar imaging with minimized specific absorption rate. *Magnetic Resonance in Medicine*, *76*(5), 1517-1523. https://doi.org/10.1002/mrm.26063

Stirnberg, R., Huijbers, W., Brenner, D., Poser, B. A., Breteler, M., & Stöcker, T. (2017). Rapid whole-brain resting-state fMRI at 3 T: Efficiency-optimized three-dimensional EPI versus repetition time-matched simultaneous-multi-slice EPI. *Neuroimage*, *163*, 81-92. https://doi.org/10.1016/j.neuroimage.2017.08.031

Tijssen, R. H. N., Okell, T. W., & Miller, K. L. (2011). Real-time cardiac synchronization with fixed volume frame rate for reducing physiological instabilities in 3D FMRI. *Neuroimage*, *57*(4), 1364-1375. https://doi.org/10.1016/j.neuroimage.2011.05.070

Todd, N., Josephs, O., Zeidman, P., Flandin, G., Moeller, S., & Weiskopf, N. (2017). Functional Sensitivity of 2D Simultaneous Multi-Slice Echo-Planar Imaging: Effects of Acceleration on g-factor and Physiological Noise. *Front Neurosci*, *11*, 158. https://doi.org/10.3389/fnins.2017.00158

Triantafyllou, C., Hoge, R. D., Krueger, G., Wiggins, C. J., Potthast, A., Wiggins, G. C., & Wald, L. L. (2005). Comparison of physiological noise at 1.5 T, 3 T and 7 T and optimization of fMRI acquisition parameters. *Neuroimage*, *26*(1), 243-250. https://doi.org/10.1016/j.neuroimage.2005.01.007

Vizioli, L., Moeller, S., Dowdle, L., Akçakaya, M., De Martino, F., Yacoub, E., & Uğurbil, K. (2021). Lowering the thermal noise barrier in functional brain mapping with magnetic resonance imaging. *Nature communications*, *12*(1), 5181. https://doi.org/10.1038/s41467-021-25431-8